Structure-Function Analysis of 11β-Hydroxysteroid Dehydrogenase

by

Alexander James Frank Lawson

A thesis submitted to
The University of Birmingham
for the degree of
DOCTOR OF PHILOSOPHY

School of Biosciences
The University of Birmingham
August 2010

Abstract

11β-hydroxysteroid dehydrogenase type 1 (11β-HSD1) is a key enzyme in the conversion of cortisone to the functional glucocorticoid hormone cortisol. This activation has been implicated in several human disorders, notably the metabolic syndrome where 11β-HSD1 has been identified as a novel target for potential therapeutic drugs. Crystal structures have revealed the presence of a pronounced hydrophobic surface patch lying on two helices at the C-terminus. The physiological significance of this region has been attributed to facilitating substrate access by allowing interactions with the endoplasmic reticulum membrane.

In order to initiate investigations into the potential interaction between 11β-HSD1 and membrane, hydrophobic residues in the C-terminal helices of human and guinea pig 11β-HSD1 were mutated to glutamic acid. One of these mutants, F278E, displayed greatly increased yields of soluble protein on expression in *E.coli* together with an increase in both monodispersity and activity. No change in structure was observed when compared to the previously reported wild-type structure.

Human F278E 11β-HSD1 enzyme was then used as a background to construct a hybrid dimer system to analyse novel heterozygous mutations in the *HSD11B1* gene (R137C and K187N) which are thought to give rise to cortisone reductase deficiency (CRD). Expression of the heterodimers in *E.coli* revealed that the negative effects of both mutations can extend to the normally-active WT partner, leading to a marked suppression of 11β-HSD1 activity, which could account for the phenotype observed in patients presenting with CRD.

Finally, a comparison of human WT and F278E 11β-HSD1 enzymes was used to probe the membrane association of 11β-HSD1. A combination of western blot analysis and fluorescence quenching experiments revealed that the binding of 11β-HSD1 to membrane is via both hydrophobic and electrostatic interactions.

Acknowledgements

Firstly, I would like to thank Dr Jon Ride for his patience, knowledge and guidance throughout this PhD. I must also show appreciation for our almost daily chats on football, music, guitars and computers. I would also like to thank Dr Elizabeth Walker for helping me to see the wider picture of the work, helping me to understand endocrinology and not blaming me too much when all the lab computers broke. I must also thank Dr Scott White, Dr Tim Dafforn and Dr Nick Davies for their contributions to this work (X-ray crystallography, analytical ultracentrifugation and excellent chit chat respectively).

On a personal level, I must thank my amazing girlfriend Anna, my family (Mum, Dad and Tom) and my friends for all the support. I know you'll all be glad not to hear me talk about 11β-HSD1 for a while. I would also like to thank my cats Ralphie and Molly for sitting next to me while I wrote up this PhD.

Finally, I would like to thank the MRC and the School of Biosciences for funding the work presented.

Table of Contents

List of Figures

Chapter 1.

List of Tables

Abbreviations

ACRD	Apparent Cortisone Reductase Deficiency
ACTH	Adrenocorticotropic Hormone
AME	Apparent Mineralocorticoid Excess
ASC	Adipose Stromal Cells
AUC	Analytical Ultracentrifugation
BCA	Bicinchoninic Acid
BSA	Bovine Serum Albumin
CBX	Carbenoxolone
CRD	Cortisone Reductase Deficiency
CVD	Cardiovascular Disease
CYP	Cytochrome P450 Monooxygenase
DNA	Deoxyribonucleic Acid
DPMG	1,2-dimyristoyl-sn-glycero-3-phosphoglycerol
E	Cortisone
EDTA	Ethylenediaminetetraacetic Acid
ER	Endoplasmic Reticulum
F	Cortisol
G6P	Glucose-6-phosphate
G6PDH	Glucose-6-phosphate Dehydrogenase
GC	Glucocorticoid
GR	Glucocorticoid Receptor
H6PDH	Hexose-6-phosphate Dehydrogenase
HEK	Human Embryonic Kidney
HPLC	High Performance Liquid Chromatography
HSD	Hydroxysteroid Dehydrogenase
IPTG	Isopropyl-β-D-thiogalactoside
MOPS	3-(N-morpholino)propanesulfonic acid
NAD(H)	Nicotinamide adenine dinucleotide
NADP(H)	Nicotinamide adenine dinucleotide phosphate
PAGE	Polyacrylamide Gel Electrophoresis
PBS	Phosphate Buffered Saline
PCR	Polymerase Chain Reaction
pdb	Protein Data Bank
SAT	Subcutaneous Adipose Tissue
SDS	Sodium Dodecyl Sulphate
SDR	Short Chain Dehydrogenase/Reductase
THE	Tetrahydrocortisone
THF	Tetrahydrocortisol
UV	Ultraviolet
VAT	Visceral Adipose Tissue

Chapter 1. General introduction

The inter-conversion between inactive glucocorticoids (cortisone in man and 11-dehydrocorticosterone in rodents) and hormonally active glucocorticoids (cortisol and corticosterone), is performed by the two isoforms of the enzyme 11β-hydroxysteroid dehydrogenase (Figure 1.1). The type 1 enzyme (11β-HSD1) is predominantly expressed in the liver (Lakshmi and Monder, 1988), brain (Seckl, 1997), pancreatic islets (Davani *et al.*, 2000) and adipose tissue (Bujalska *et al.*, 1997) with genome wide transcriptome analysis showing a small amount of 11β-HSD1 expression in most tissues (Shmueli *et al.*, 2003). 11β-HSD1 exhibits a predominant reductase activity *in vivo*, while the type 2 enzyme (11β-HSD2), which is expressed mainly in the kidney, acts predominantly as a dehydrogenase (Krozowski *et al.*, 1990). The two 11βHSD isoforms constitute an important 'pre-receptor' mechanism to regulate the physiological effects of active glucocorticoid (Draper and Stewart, 2005). However, before the importance of the 11βHSD proteins can be understood, the physiological importance of cortisol (a steroid hormone) must be explained.

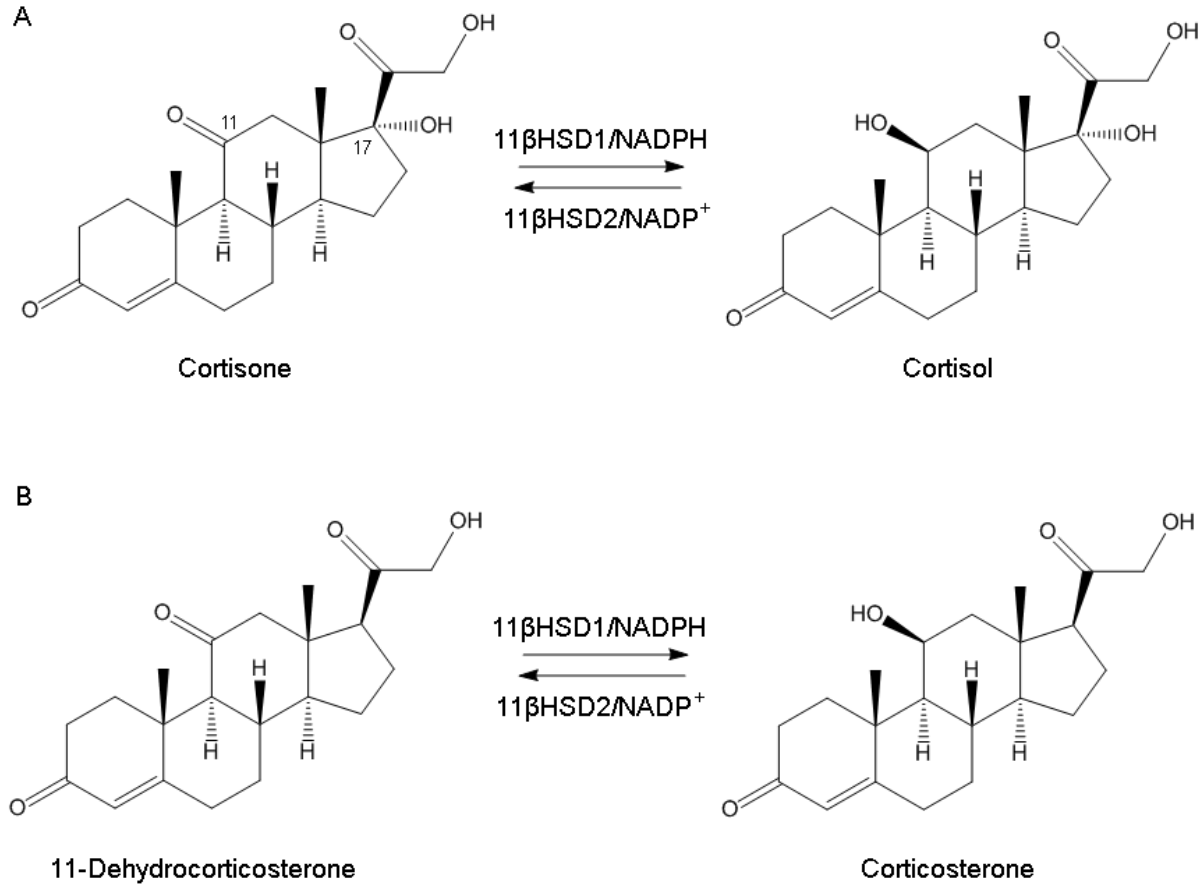

Figure 1.1. Inter-conversion of glucocorticoids in man (A) and rodents (B). In man, 11β-HSD1 converts inactive cortisone to active cortisol via reduction of the C-11 oxo-group. In rodents, 11β-HSD1 converts 11-dehydrocorticosterone into corticosterone. The inactivation of glucocorticoid, via the oxidation of the C-11 hydroxyl, is performed predominantly by the NAD^+ dependent 11β-HSD2. Figure produced using ChemDraw Ultra 7.0.

1.1. Hormones

The word ‘hormone’ (coined from the Greek word meaning ‘urge’) was first used in 1905 by Bayliss and Starling to describe the gastrointestinal molecule secretin. Hormones can be classed as molecules which are able to act as a chemical ‘messengers’ which are carried in the blood from their source (classicaly an endocrine gland) to a target cell, in which the hormone will trigger a specific effect. Hormones can be classified into 3 major groups: protein and polypeptide hormones, steroid hormones and a third group in which molecules can contain both amino and steroid groups. There are five main classes of steroid hormones: glucocorticoids, androgens, progestogens, mineralocorticoids and oestrogens. These hormones are synthesized in various locations around the body including the ovaries/gonads (progestogens, androgens and oestrogens), adrenal cortices (glucocorticoids, mineralocorticoids and androgens) and the skin (vitamin D metabolites) (Laycock, 1996). Steroid hormones regulate a wide range of functions in organisms. Mineralocorticoids, such as aldosterone, increase blood volume and pressure by causing the distal tubules of the kidney to increase the reabsorption of Na^+ and excretion of K^+. The sex hormones, androgens in males (e.g. testosterone) and oestrogens in females (e.g. oestrone), are mainly responsible for the development of secondary sex characteristics. In females, the main progestogen, progesterone, is involved with preparing the lining of the uterus for implantation of an ovum as well as being essential for the maintenance of pregnancy (Laycock, 1996). The vitamins A and D are also important lipid soluble signalling molecules, with a signalling role for vitamin E now described in addition to its classical role as an antioxidant. Vitamin D (cholecalciferol) is activated first in the liver, and then in the kidney to form 1,25 dihydroxycholecalciferol ($1,25(OH)_2D_3$) whose primary function is to promote the correct mineralization, growth and remodeling of bone via the regulation of the concentration of calcium and phosphate in the bloodstream (Laycock 1996). Vitamin A is located either in the retina of the eye as retinal, a

light absorbing molecule essential for low light and colour vision, or as the hormone retinoic acid which activates transcription of target genes via the retinoic acid receptors (RARs) or the retinoid 'X' receptors (RXRs) to mediate growth and development in children (Stryer *et al.,* 2001). Alpha-tocopherol, the active form of vitamin E, has recently been shown to upregulate genes involved with blood coagulation (christmas factor) and steroid metabolism (5α-steroid reductase type 1) implying a varied role for vitamin E as a hormone. (Rimbach *et al.*, 2010). Finally, glucocorticoids have a wide range of functions but are primarily concerned with the regulation of blood glucose and inflammation. For example, cortisol will increase blood glucose concentration via increasing gluconeogenesis in liver and lipolysis in the adipose, while antagonizing the action of insulin in peripheral tissues. As this review is concerned with the interconversion of the major glucocorticoid cortisol and its inactive 11-keto form, cortisone, the rest of this section will mainly address the synthesis and function of glucocorticoids. However, due to the involvement of 11β-HSD2 in the condition 'apparent mineralocorticoid excess' (AME, discussed later), reference will also be made to the synthesis of the major mineralocorticoid, aldosterone.

It is important to note that over the last 10 years, molecules which had no known signaling function have been shown to act as hormones. Bile acids, which have long been known to function as physiological detergents facilitating the absorption, transport and distribution of lipid soluble vitamins and dietry fats, have been shown to participate in a negative feedback pathway in which bile acid synthesis is inhibited when circulating levels are high (Chiang, 2002). This is achieved by activation of the farnesoid X receptor (FXR) by bile acids, which induces expression of small heterodimer partner (SHP), which in turn suppresses cholesterol 7 alpha-hydroxylase (CYP7A1, the enzyme responsible for the rate limiting step in bile acid synthesis) expression (Chiang, 2002).

1.1.1. Steroid hormone synthesis

Glucocorticoids, mineralocorticoids and adrenal androgens, are produced in the adrenal cortex of the adrenal gland. Adult humans possess two adrenal glands weighing approximately 5 grams with a size of around 30 x 50 x 10 mm. The adrenal gland is divided into three sections, the medulla, the cortex and the capsule (Figure 1.2). The medulla is composed primarily of chromaffin cells which are responsible for the production of the catecholamines such as adrenaline and noradrenalin (Ehrhart-Bornstein *et al.*, 1998). The adrenal capsule is a layer of connective tissue surrounding the adrenal cortex, responsible for maintenance of the shape and structure of the adrenal gland (Figure 1.2). The adrenal cortex is the largest section of the adrenal gland and is divided into 3 sections, each a distinct band of cells, which are enzymatically and histologically distinct (Figure 1.2). Each section contains different cytochrome P450 monooxygenase enzymes, which together with two dehydrogenase enzymes, are responsible for steroid hormone synthesis (Figure 1.3). The outer zona glomerulosa consists of poorly defined clusters of small, narrow cells which contain the CYP11B2 enzyme (aldosterone synthase) (Ghayee and Auchus, 2007, Bureik *et al.*, 2002, Ortiz de Montellano, 1995) and also lack the CYP17A1 (17-hydroxylase/17,20-lyase) enzyme responsible for 17α-hydroxylation of progesterone and pregnenolone (Ghayee and Auchus, 2007). These cells are therefore responsible for synthesis of the major mineralocorticoid, aldosterone. The middle layer, the zona fasciculata, makes up 75% of the adrenal cortex and contains both the CYP17A1 and also the CYP11B1 (11-hydroxylase) and is therefore responsible for the synthesis of cortisol and also some androgen precursors (Ghayee and Auchus, 2007, Bureik *et al.*, 2002). The innermost section of the adrenal gland is the zona reticularis and is responsible for the production of the adrenal androgens (Ghayee and Auchus, 2007).

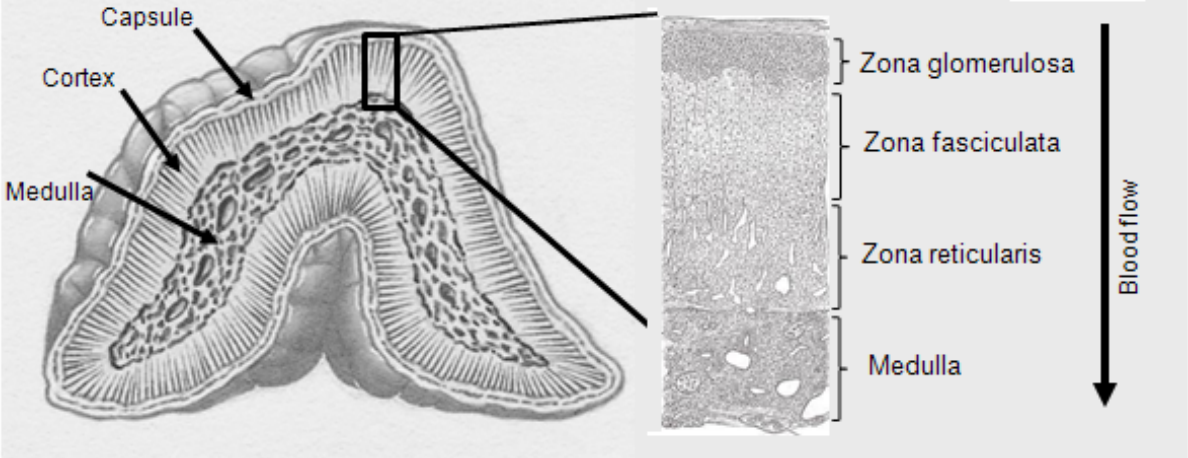

Figure 1.2 Corticosteroids are synthesized in the adrenal cortex of the adrenal gland. The three sections are enzymatically and histologically distinct. The outer zona glomerulosa is responsible for synthesis of the major mineralocorticoid aldosterone, with the middle zona fasciculata and inner zona reticularis responsible for the synthesis of glucocorticoid and androgens respectively. Image taken from Gray *et al.* (2000)

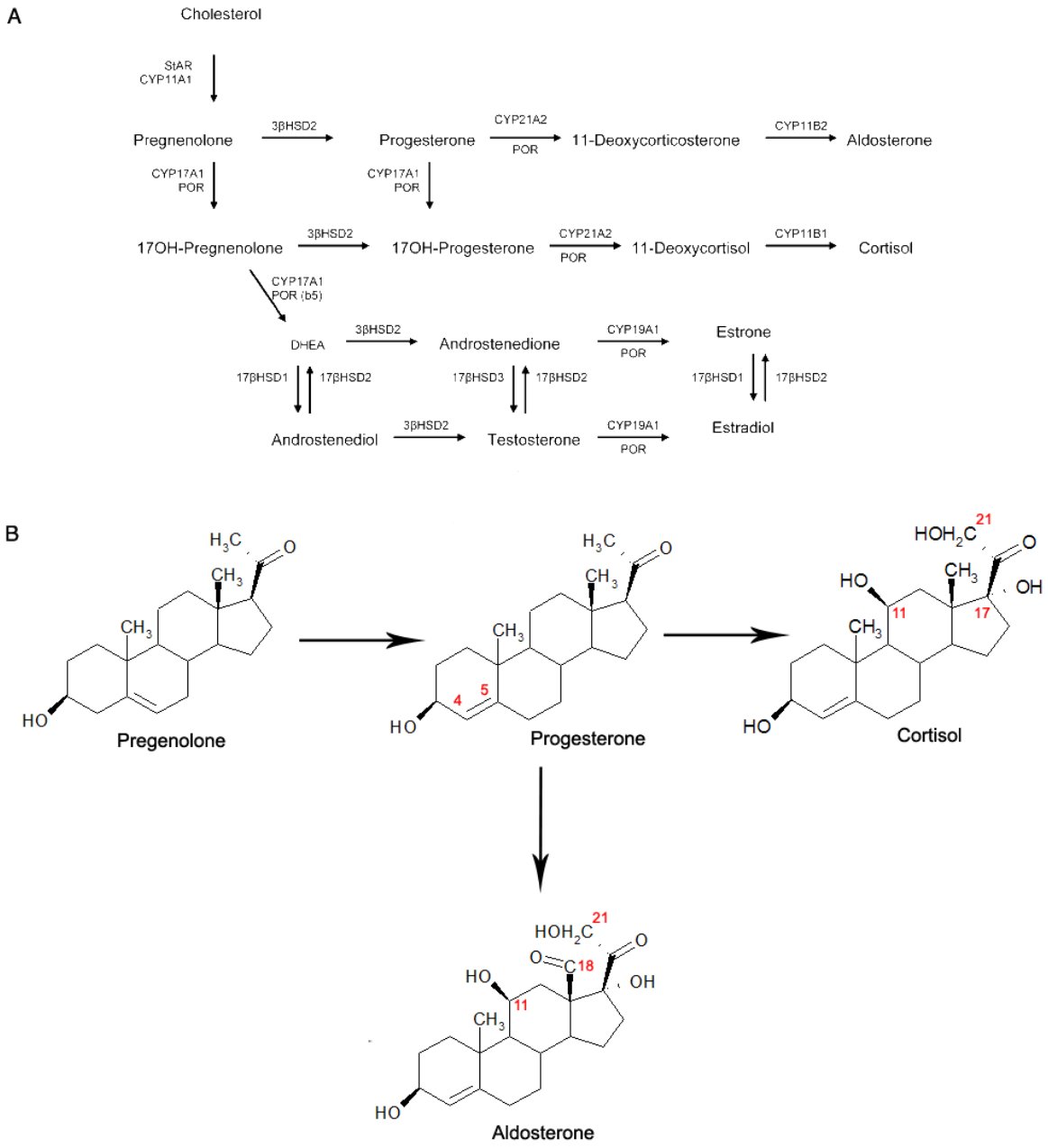

Figure 1.3. A - Common steroidogenic pathways and enzymes in humans. Also shown are the electron donor P450-oxidoreductase (POR) which is present in the ER, and mitochondrial steroidogenic acute regulatory protein (StAR). (Ghayee and Auchus, 2007)**.** B - Synthesis of the major mineralocorticoid, aldosterone and major glucocorticoid, cortisol. For simplicity, only active hormones and the prohormone are shown. Pregnenolone is converted to progesterone by 3βHSD, with 3 subsequent hydroxylation reactions in the 17, 21 and 11 positions yielding cortisol. These reactions are carried out by CYP17A1, CYP21A2 and CYP11B1 respectively. Progesterone is converted to aldosterone by 2 subsequent hydroxylation reactions in the 21 and 11 positions, followed by an oxidation of the C-18 angular methyl group to an aldehyde. These reactions are carried out by CYP21A2 and CYP11B2 respectively. Image adapted from Stryer *et al.* (2001).

All steroid hormones are produced from a common precursor, cholesterol (Figure 1.3 and Figure 1.4). In addition to its role in hormone biosynthesis, cholesterol is also involved in modulating membrane fluidity in animal cells and also in the production of bile salts. Cholesterol is present in most cells and can either be transported to the endocrine cell through the blood in complex with a lipoprotein or synthesized from acetyl CoA in a three stage process (Andersen and Dietschy, 1978). The structure of cholesterol is shown in Figure 1.4.

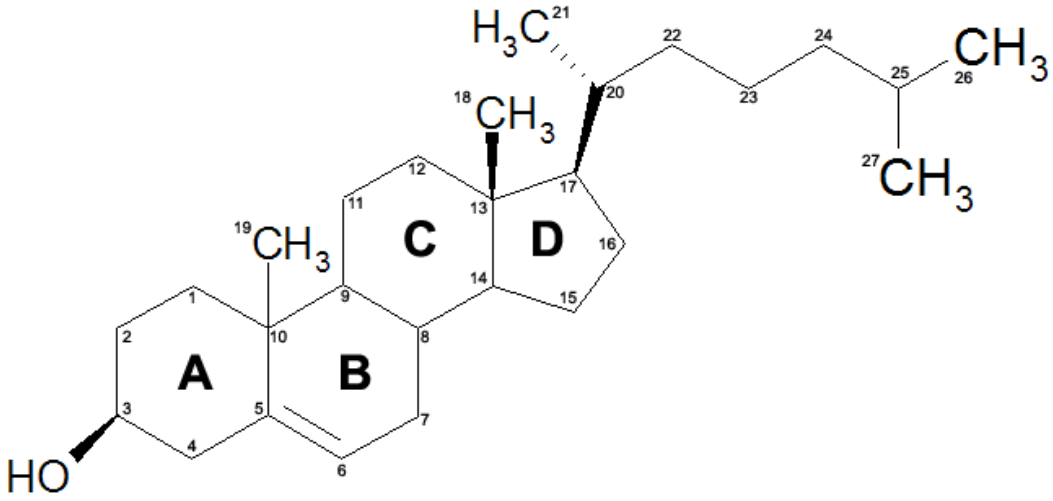

Figure 1.4. Cholesterol is the precursor to all steroid hormones. The numbering scheme for carbon atoms in cholesterol and other steroids is shown, along with the lettering scheme for the steroid rings. Adapted from Stryer *et al.* (2001).

Cholesterol is converted to the prohormone pregnenolone by the membrane bound mitochondrial CYP11A1, also known as P450scc. This rate limiting step in the production of steroid hormones (Chung *et al.*, 1986) involves 3 reactions which all take place in one CYP11A1 active site (Miller, 1988). The reactions of all cytochrome P450 enzymes are similar and can be summarized by:

$$R—H + O_2 + NADPH + H \rightarrow R—OH + H_2O + NADP^+ \qquad (1)$$

In order for both the C-20 and C-22 positions of cholesterol to become hydroxylated, this reaction must occur twice (Stryer, 2002). Following the 20α- and 22-hydroxylation reactions, the cholesterol side chain is cleaved to yield pregnenolone and isocaproic acid (Strauss, 1991).

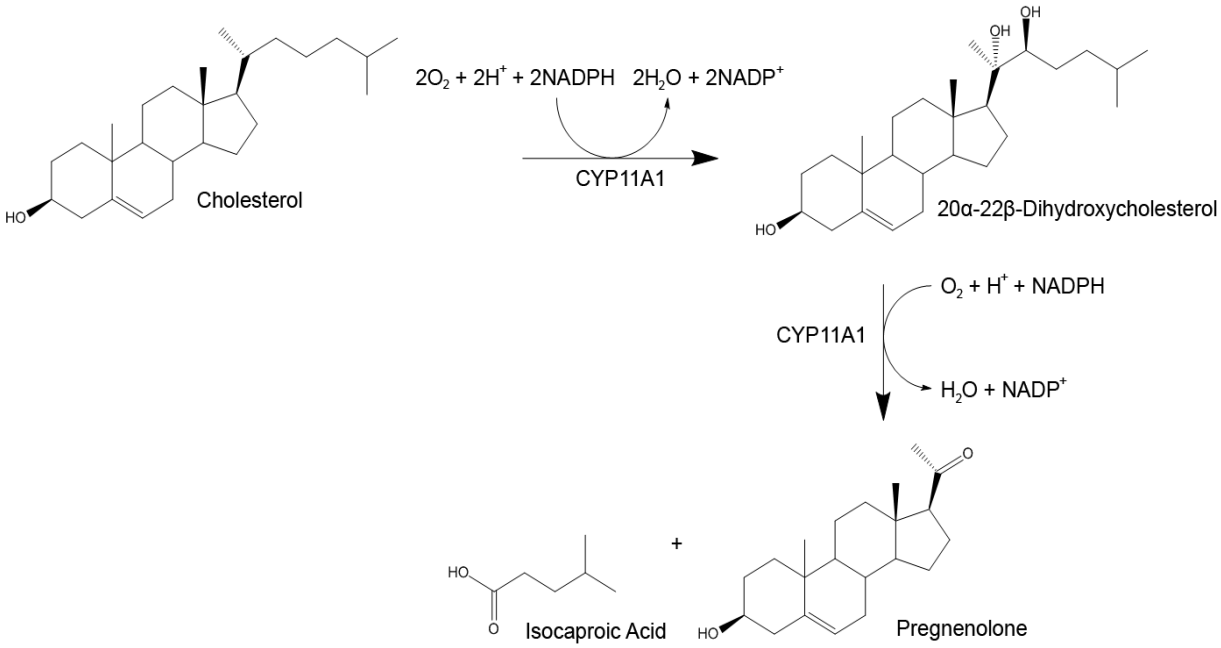

Figure 1.5. Pathway for the formation of the prohormone pregnenolone. Cholesterol is hydroxylated in both the C-20 and C-22 positions by the CYP11A1 enzyme (also known as cholesterol side-chain cleavage enzyme). The product, 20α, 22β-dihydroxycholesterol, is then cleaved to yield the prohormone pregnenolone and isocaproic acid. Image adapted from Stryer *et al.* (2001).

All steroid hormones are then produced from pregnenolone (Figures 1.3). Depending on the hormone being produced, pregnenolone can either be converted to 17-hydroxypregnenolone or progesterone. Progesterone is formed via the oxidation of the 3-hydroxyl group of pregnenolone to a 3-keto group, with the subsequent isomerisation of the Δ^5 double bond to a Δ^4 double bond. Both the 3β-hydroxysteroid dehydrogenation and isomerisation reactions are

carried out by the ER bound enzyme 3β-hydroxysteroid dehydrogenase (3βHSD2) (Ghayee and Auchus, 2007, Strauss, 1991). Interestingly, since 3βHSD2 belongs to the short chain dehydrogenase/reductase (SDR) superfamily of enzymes, it is the only enzyme in the adrenal pathway for corticosteroid synthesis which is not a member of the P450 family. Both pregnenolone and progesterone can undergo a 17α-hydroxylation reaction to form 17-hydroxypregnenolone or 17-hydroxyprogesterone respectively. This reaction is accomplished by the membrane bound, smooth ER enzyme CYP17A1 (Nakajin *et al.*, 1984) (Figure 1.3). A subsequent C17,20 carbon bond cleavage on 17-hydroxypregnenolone or 17-hydroxyprogesterone is also performed by CYP17A1. These give rise to dehydroepiandrosterone (DHEA) and androstenedione respectively. The hydroxylase and lyase activities are under separate hormonal control and as such, represent a branch point in hormone synthesis. If neither activity is present, the progesterone will go onto form the mineralocorticoid aldosterone (Figure 1.3). If the hydroxylase activity is present but lyase activity is absent, 17-hydroxyprogesterone will form the major glucocorticoid, cortisol. If both activities are present, the sex steroids will be produced (Figure 1.3) (Strauss, 1991). Due to the location of CYP17A1 in the ER, the electron donor for the hydroxylation reactions is different from the adrenodoxin reductase which is present in the mitochondria. The membrane bound cytochrome P450-oxidoreductase (POR) donates electrons to both CYP17A1 and CYP21A2 without the need for an iron/sulphur protein (Tamburini and Gibson, 1983).

The final common P450 involved in both glucocorticoid and mineralocorticoid synthesis is the CYP21A2. Located in the ER, CYP21A2 can use electrons donated by POR to hydroxylate both progesterone and 17-hydroxyprogesterone to yield deoxycorticosterone (DOC) and 11-deoxycortisol (Miller and Morel, 1989). In order for glucocorticoid production to proceed, CYP11B1 must be present. This membrane bound mitochondrial protein is expressed in high levels in the zona fasciculata of the adrenal cortex (Ghayee and Auchus, 2007, Erdmann *et al.*, 1995a, Erdmann *et al.*, 1995b) and is involved with the 11β-

hydroxylation of 11-deoxycortisol to yield the active glucocorticoid, cortisol (Figure 1.3). In contrast, expression of the CYP11B2 protein in the zona glomerulosa (Ghayee and Auchus, 2007, Miller, 1995) will yield the mineralocorticoid, aldosterone (Figure 1.3). This is achieved by two hydroxylation reactions at positions C11 and C18, followed by an oxidation at C18. 11β-hydroxylase, 18-hydroxylase and 18-oxidase activities are all performed by the CYP11B2 protein which, like CYP11B1, is located in the membrane of the mitochondria and as such, utilizes adrenodoxin and adrenodoxin reductase for electron donation.

1.1.2. Steroid hormone action

Due to the relatively hydrophobic nature of the steroid hormones, and their almost planar structure, they are able to diffuse freely through cell membranes. Once in the blood, most steroid hormones are bound to plasma proteins. These proteins both protect the hormone from being inactivated in the blood as well as ensuring that when the hormone reaches its target tissue, it is readily available. These transport proteins are usually globulins and can either have a high affinity for certain classes of hormone (e.g. transcortin in transport of cortisol) or be present in such high concentrations in the blood to allow a high capacity but low affinity binding (e.g. albumin). Unbound cortisol exerts effects via either genomic or non-genomic pathways. For genomic signalling, the primary targets of the steroid hormones are intracellular, with receptors located either in the cytosol or nucleus. Like estrogens and xenoestrogens, cortisol is also able to exert effects via a non-genomic pathway, although genomic signalling is thought to predominate (Losel *et al.*, 2003). Type 1 steroid receptors, which are responsible for the binding of sex hormones, glucocortoids and mineralocorticoids are situated in the cytosol and will move into the nucleus upon hormone binding (Jacobs and Lewis, 2002, Nicolaides *et al.*, 2009). Type 2 receptors, which are responsible for the binding of thyroid hormones and both vitamins A and D, are located in the nucleus (Swift *et al.*, 2008, Aranda *et al.*, 2009). Although each steroid hormone has a specific receptor, the domain

structure of these receptor proteins are similar. Each possess A/B regions which contain the components which activate transcription, and a highly conserved C region which functions as a DNA binding domain. A hinge region (D) links to a highly conserved E region which functions to bind steroid, activating the steroid receptor (Laycock, 1996). The glucocorticoid receptor (GR) will be discussed in more detail in Section 1.3.

1.2. Cortisol

As mentioned above, the corticosteroids are synthesized in the adrenal cortex from cholesterol utilizing four cytochrome P450 enzymes. Hence they have a common structure, the cyclopentanoperhydrophenanthrene nucleus. The corticosteroids can be separated into groups according to their primary effects: the mineralocorticoids (such as aldosterone) and the glucocorticoids (such as cortisol). Since the substrates of 11β-HSD1/11β-HSD2 system are the glucocorticoids, the rest of this section will concentrate on the release and subsequent activity of the major glucocorticoid in man, cortisol.

1.2.1. Systemic regulation of cortisol

The primary effect of cortisol, the major glucocorticoid in humans, is to regulate glucose metabolism and blood pressure in order to limit stress levels (Munck *et al.*, 1984). As a response to physical or psychological stress, corticotrophin releasing hormone (CRH) is secreted by the paraventricular nucleus (PVN) in the hypothalamus (Vale *et al.*, 1981). The CRH then acts synergistically with vasopressin (VP) in the anterior lobe of the pituitary gland to stimulate the production and subsequent secretion of the 39 amino acid adrenocorticotropic hormone (ACTH) (Millan *et al.*, 1987, Chen *et al.*, 1993, Guillemin and Rosenberg, 1955). Upon binding of ACTH to a G protein-coupled receptor on the adrenal cortex, an adenyl cyclase is activated causing a subsequent increase in cAMP levels. cAMP will then stimulate the conversion of cholesterol to pregnenolone, with subsequent production of cortisol (Holt and Hanley, 2007). Due to the wide array of physiological properties of cortisol (Table 1.1), the circulating levels of the glucocorticoid must be tightly controlled. Cortisol homeostasis is maintained by regulation of the hypothalamo-pituitary-adrenal (HPA) axis according to physical demands (Figure 1.6) (Cutler *et al.*, 1978). Increased concentrations of cortisol in the plasma exerts a negative feedback effect on both the hypothalamus and pituitary gland with

subsequent reductions in both CRH and VP secretion while also inhibiting production of ACTH (Matteri, 1995) (Figure 1.6).

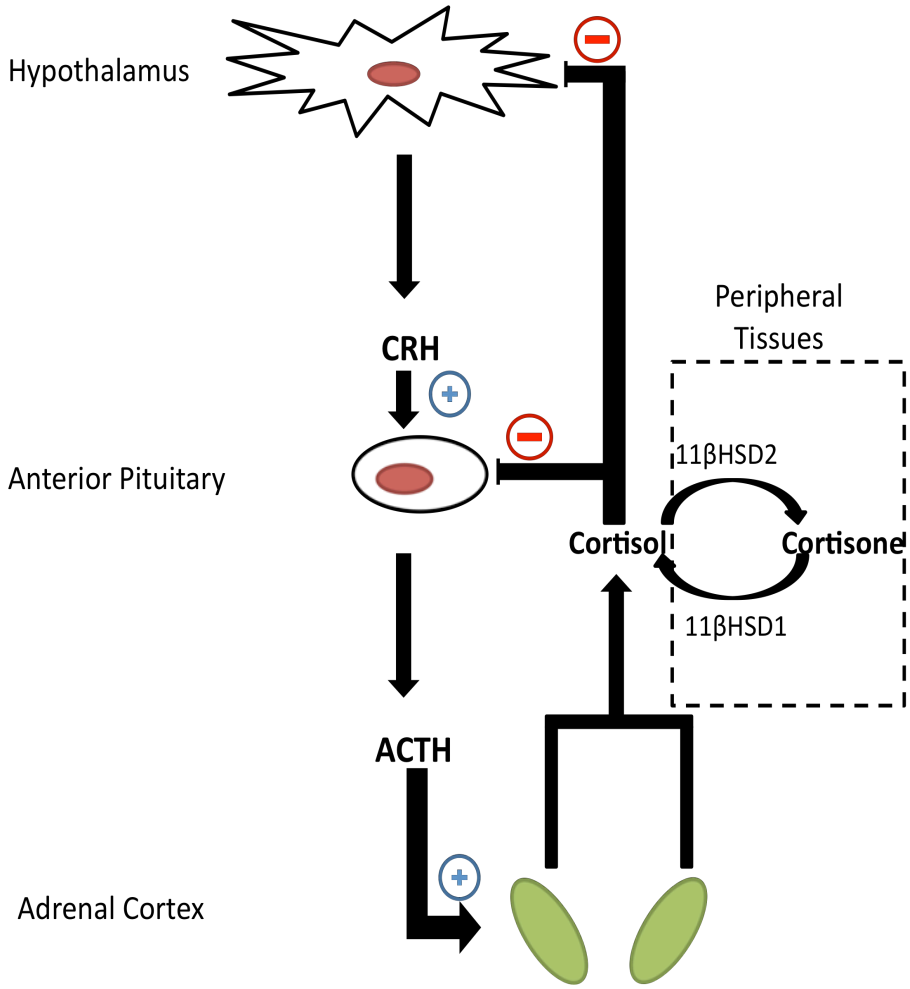

Figure 1.6. The hypothalamic-pituitary-adrenal (HPA) axis is a system to control cortisol homeostasis. In this system, an increase in circulating cortisol concentrations will cause a negative feedback effect on both the hypothalamus and the pituitary gland. This negative feedback will cause reductions in both CRH and VP secretion while also inhibiting the production of ACTH. The specific actions of 11β-HSD types 1 and 2 in peripheral tissues will be discussed in sections 1.3.2 and 1.3.1 respectively. Adapted from Holt and Hanley 2007.

1.2.2. Mechanism of action of cortisol

Unbound cortisol exerts effects via either genomic or non-genomic pathways. Genomic signalling is thought to predominate over the rapid, seconds to minutes non-genomic signalling although much controversy remain about the precise mechanisms and roles of non

genomic signalling (Losel *et al.*, 2003). Circulating cortisol is mostly bound (90%) to the cortisol binding globulin (CBG, also known as transcortin). However only the unbound cortisol is able to enter target cells via diffusion and exert an effect (Holt and Hanley, 2007). These effects are mediated by the 777 amino acid cytoplasmic glucocorticoid receptor (GR) (Hollenberg *et al.*, 1985). The human GR (hGR) is a member of the steroid/thyroid/retinoic acid nuclear receptor superfamily of transcription factor proteins, with alternative splicing of the hGR gene giving rise to two homologous isoforms, hGRα and hGRβ (Nicolaides *et al.*, 2009). While hGRα functions as a ligand-dependent transcription factor typical of steroid hormone receptors and will be discussed in more detail, hGRβ does not bind glucocorticoids (GC). Instead hGRβ has intrinsic, hGRα-independent, gene transcriptional activity and also exerts a dominant negative effect on the transcriptional activity of hGRα (Nicolaides *et al.*, 2009, Zhou and Cidlowski, 2005).

The domain structure of hGRα is typical of steroid hormone receptors, consisting of four distinct regions illustrated in Figure 1.7. The N-terminal domain (NTD, also known as the A/B region) contains the ligand-independent transactivation domain activation function (AF)-1, which interacts with various molecules necessary for transcription such as coactivators, chromatin modulators and basal transcription factors (Figure 1.7A) (Nicolaides *et al.*, 2009). The DNA binding domain (DBD) is the most conserved domain in the steroid receptor family and includes two zinc finger motifs, each containing a zinc atom tetrahedrally co-ordinated by four Cys residues. A small number of residues, known as the proximal (P)-box, in the first zinc finger are responsible for recognition of the glucocorticoid response elements (GRE) in the promoter region(s) of target genes. The second zinc finger contains a group of residues known as the distal (D)-box, which are responsible for the weak dimerisation interface of the DBD (Nicolaides *et al.*, 2009). The structurally flexible hinge region (HR) allows a single receptor dimer to interact with multiple, potentially different, GREs. Finally, the ligand-binding domain (LBD) binds glucocorticoid and also contains a second ligand-dependent

transactivation domain, AF-2. In addition, the LBD contains sequences for nuclear translocation, receptor dimerisation, heat shock protein association and interaction with cofactors (Nicolaides *et al.*, 2009).

When no glucocorticoid is present, hGRα resides in the cytoplasm as part of a hetero-oligomeric complex consisting of heat shock proteins (HSPs) 90, 70 and 50, in addition to the immunophillin FKBP51 (Nicolaides *et al.*, 2009, Pratt, 1993). HSP90 regulates both ligand binding and cytoplasmic retention by exposing the ligand binding site and masking the nuclear localization signals (NLS) 1 and 2 (Nicolaides *et al.*, 2009). Binding of glucocorticoid causes hGRα to undergo a conformational change that first results in dislocation of hGRα from the multiprotein complex, before the receptor is translocated into the nucleus where it forms a homodimer (Dahlman-Wright *et al.*, 1990, Dahlman-Wright *et al.*, 1992, Dahlman-Wright *et al.*, 1991, Oakley *et al.*, 1999). Once inside the nucleus, gene transcription is stimulated or suppressed by the dimerised GR interacting with a GRE on the target gene (Hayashi *et al.*, 2004) (Figure 1.7B). Ligand activated hGRα can also modulate gene expression independently of binding to GRE via direct protein-protein interaction with other transcription factors such as activator protein 1 (AP1), nuclear factor-κB (NFκB), p53 and signal transducers and activators of transcription (STATs) (Figure 1.8B) (Nicolaides *et al.*, 2009).

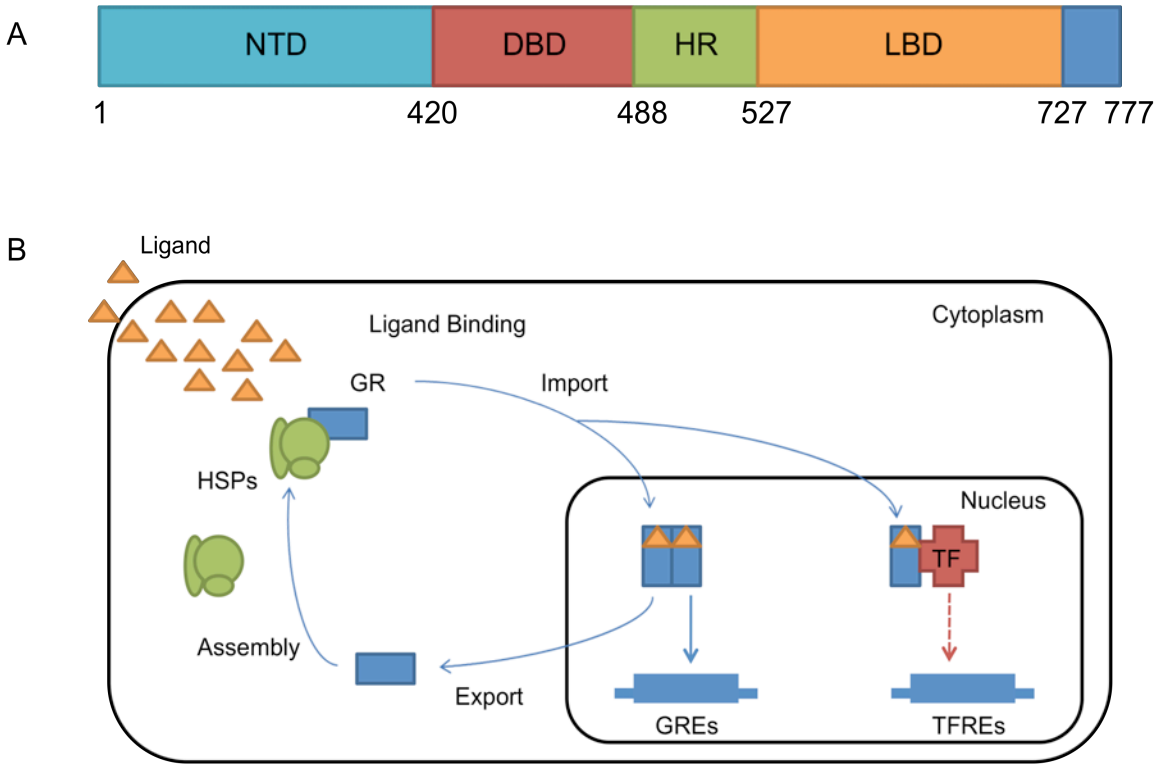

Figure 1.7. Domain structure (A) and nucleocytoplasmic shuffling (B) of the hGRα. A – The domain structure of hGRα is typical of steroid hormone receptors, consisting of four distinct regions known as the N-terminal domain (NTD), DNA binding domain (DBD), hinge region (HR) and the ligand-binding domain (LBD). B – In the absence of glucocorticoid, hGRα is present in the cytoplasm in complex with various heat shock proteins (HSPs). Upon ligand binding, hGRα is shuffled to the nucleus, dimerises and interacts with a GRE on the target gene. Alternatively, ligand activated hGRα can also modulate gene expression independently of binding to GRE via direct protein-protein interaction with other transcription factors (TF). GREs = glucocorticoid response elements, TFREs = transcription factor response elements. Image adapted from Nicolaides *et al.* (2009)

1.2.3. Physiological effects of cortisol

The primary effect of cortisol in humans is to regulate glucose metabolism and blood pressure in order to limit stress levels. A summary of some of the effects of cortisol are shown in Table 1.1. In terms of intermediary metabolism, the overall effect of cortisol is to raise circulating glucose via promoting gluconeogenesis, raising hepatic glucose output and inhibiting glucose uptake by muscle and fat. Cortisol is also able to stimulate gluconeogenesis indirectly via increasing amino acid uptake in hepatic tissues and by stimulating lipolysis in adipose tissue with a subsequent increase in the mobilization of fatty acids. The catabolic effect of cortisol on protein in skin, muscle and bone also contribute to an increase in circulating glucose via an

increase of circulating amino acids which will stimulate gluconeogenesis in the liver. An excess of cortisol would therefore lead to unusually high levels of circulating glucose. This, coupled with the detrimental effect of excessive cortisol on the serum lipid profile (an increase in both triglyceride and total cholesterol with an accompanied decrease in HDL cholesterol) and the permissive effect of cortisol on glucagon and epinephrine can lead to an 'insulin resistant' phenotype (Holt and Hanley, 2007). This is not true insulin resistance as although insulin is still able to exert its metabolic effect on the body, but greater insulin secretion is needed to achieve this effect. The metabolic complications of an excess of cortisol are discussed further in Section 1.4.

Effect	Description
Carbohydrate metabolism	Stimulates gluconeogenesis. Notably, cortisol activates PEPCK, the enzyme responsible for the rate-limiting step of gluconeogenesis. Antagonizes peripheral action of insulin on glucose uptake.
Protein metabolism	Amino acid uptake and protein synthesis inhibited in peripheral tissues and stimulated in hepatic tissues. Increased amount of amino acids in liver stimulates gluconeogenesis. Protein catabolic agent in muscle, skin and bone.
Lipid metabolism	Stimulates lipolysis in adipose tissue with subsequent increased mobilization of fatty acids. This can then stimulate gluconeogenesis in liver.
Apparent Mineralocorticoid Excess (AME)	Lack of 11β-HSD2 activity leading to an increase of cortisol binding to and activating mineralocorticoid receptors (discussed later).
Water metabolism	A high level of cortisol can increase the glomerular filtration (GFR) rate, resulting in increased water retention.
Cardiovascular Effect	Increases vascular tone via potentiating the vasoconstrictor effects of vasoactive molecules.
Growth	Excessive amounts can lead to impaired growth via inhibiting somatotrophin release and insulin-like growth factor I (IGF-I) synthesis.
Immune System	Negative feedback via IL-1 stimulation of hypothalamic and pituitary production of CRH and ACTH to stop excessive responsiveness of lymphocytes.
Stress response	Factors such as haemorrhage, severe trauma, acute hypoglycaemia and emotional stimuli cause a large increase in the concentration of cortisol and corticotrophin in the blood. Role is probably to induce metabolic and cardiovascular effects listed above.

Table 1.1. List of physiological effects of cortisol. PEPCK = Phosphoenolpyruvate kinase. Information taken from Laycock 2006.

1.2.4. Metabolism of cortisol

After exerting its actions, cortisol must be metabolised to remove the active glucocorticoid from circulation. Reduction of the C4-5 double bond, with a subsequent hydroxylation on the 3-oxo group by 5β- or 5α-reductase metabolises cortisol firstly to dihydrocortisol, then finally to 5β- or 5α-tetrahydrocortisol (5β- or 5α/allo-THF) where 5β-THF predominates in normal

physiology (Cope and Black, 1958). Cortisol can also be reduced on the 20-oxo group by 20α- or 20β-HSD to produce α- or β-cortols (Szymanski and Furfine, 1977, Shackleton, 1993). The THF and allo-THF can be conjugated to glucuronic acid and excreted in urine (Monder and Bradlow, 1980). It is worth noting here that cortisone is metabolised by the same pathways as cortisol.

1.3. 11β-hydroxysteroid dehydrogenase enzymes

In addition to the negative feedback control of circulating cortisol discussed previously, the level of cortisol can be controlled locally in certain tissues by the enzymes 11β-HSD1 and 11β-HSD2. These will be discussed in detail in the following sections.

1.3.1. 11β-hydroxysteroid dehydrogenase type 2 (11β-HSD2)

11β-HSD2 is a microsomally located, NAD^+-dependent dehydrogenase enzyme which belongs to the short chain dehydrogenase/reductase (SDR) superfamily of enzymes. *In vivo,* 11β-HSD2 converts the active glucocorticoid cortisol to inactive cortisone (Brown *et al.*, 1993, Stewart *et al.*, 1994) (Figure 1.8). However, when purified human kidney microsomes are incubated *in vitro* with an NADH regenerating system, some NADH-dependent 11-oxoreduction can be observed for 11β-HSD2 with both cortisone and dexamethasone (Diederich *et al.*, 1997, Obeyesekere *et al.*, 1997).

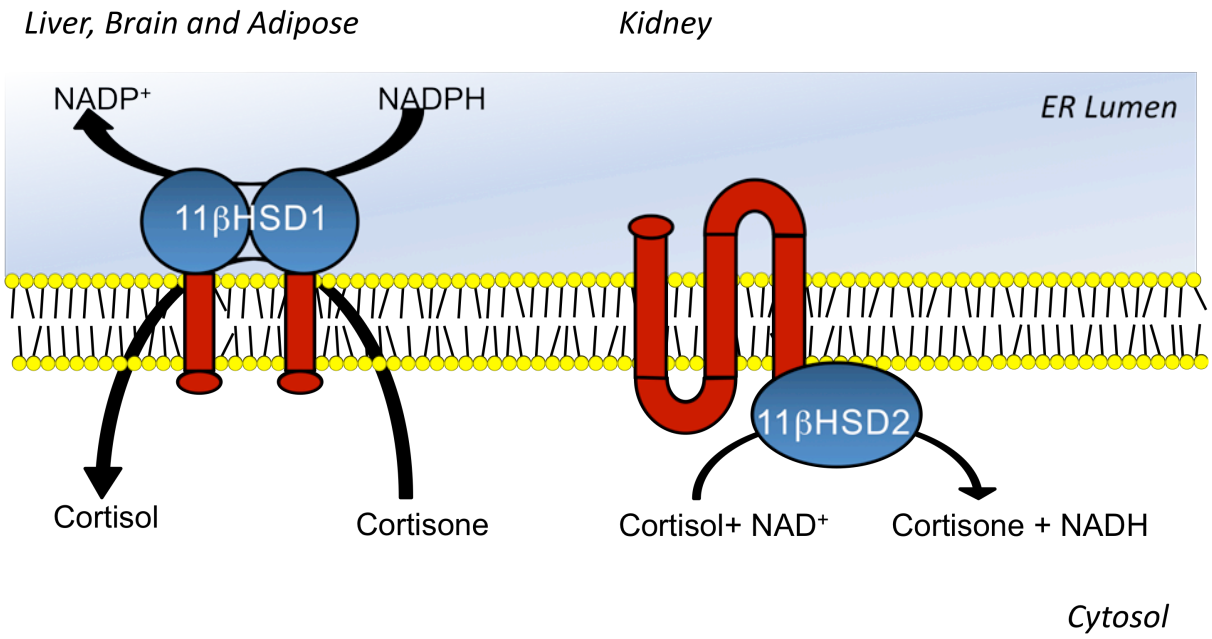

Figure 1.8. Diagrammatic representation of the 11β-HSD1 (left) and 11β-HSD2 (right) enzymes and their position in the cell. Note that 11β-HSD1 is expressed in liver, brain and adipose tissue, while 11β-HSD2 is expressed primarily in the kidney. The steroid conversions shown are those which predominate *in vivo*.

Cloning of 11β-HSD2 from a number of species including rat (Zhou *et al.*, 1995), rabbit (Naray-Fejes-Toth and Fejes-Toth, 1995), human (Albiston *et al.*, 1994), mouse (Condon *et al.*, 1997) and sheep (Agarwal *et al.*, 1994) has shown all orthologues to be around 400 amino acids in length with high conservation of the first 382 residues (>90% identity) (Li *et al.*, 1996). Although no high-resolution structures exist for 11β-HSD2, sequence comparisons with similar microsomal proteins have suggested a structure consisting of a luminal-orientated N-terminal pentapeptide followed by 3 transmembrane helices with a cytosolic, catalytic C-terminal domain (Obeyesekere *et al.*, 1997) (Figure 1.9). However, analysis of the 11β-HSD2 sequence using the TMHMM server (Krogh *et al.*, 2001) indicates that the probability of any transmembrane domains being present in 11β-HSD2 is low (Figure 1.9). Indeed, N-terminal truncation studies revealed that removal of the three putative transmembrane domains does not move the protein to the soluble fraction upon expression in Chinese hamster ovary cells (CHOP-4), suggesting the retention of 11β-HSD2 in the membrane is not solely due to this region (Obeyesekere *et al.*, 1997). This retention of protein in the insoluble fraction despite the removal of putative transmembrane domains has also been observed in the alcohol-inducible Cytochrome P450IIE1 (Larson *et al.*, 1991).

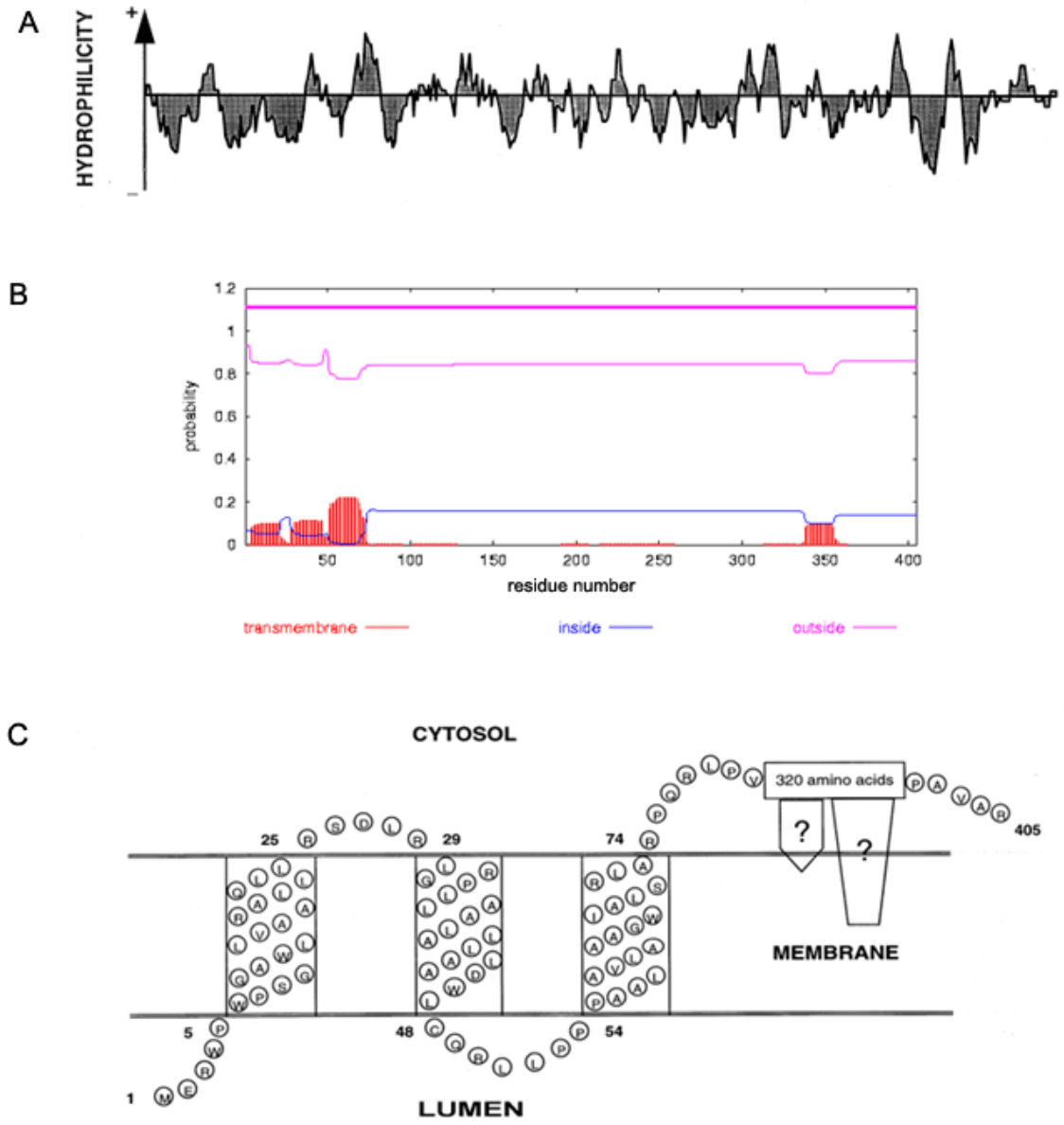

Figure 1.9. Analysis of the amino acid sequence of 11β-HSD2 indicates a potential membrane association. A – Hydrophobicity plot of 11β-HSD2. The three proposed transmembrane helices at the N-terminus can be clearly seen at the far left of the plot. B – Membrane protein topology prediction for 11β-HSD2 using the TMHMM method. In TMHMM, transmembrane domains would be represented by red, ca 20-residue wide peaks with a high probability score. Therefore, unlike the hydrophobicity plot (A), the TMHMM results suggest a low probability of any transmembrane domains. C – Model of putative 11β-HSD2 topology in the ER membrane. A and C taken from Obeyesekere *et al* (1997), B was produced using TMHMM (Krogh *et al.*, 2001).

Expression of 11β-HSD2 has been shown in a variety tissues including the kidney (Agarwal *et al.*, 1994, Albiston *et al.*, 1994, Stewart *et al.*, 1994) and colon (Whorwood *et al.*, 1994), which are rich in mineralocorticoid receptor (MR), as well as skin (Kenouch *et al.*, 1994),

ovary (Gomez-Sanchez *et al.*, 2009), placenta (Brown *et al.*, 1993, Lakshmi *et al.*, 1993) and salivary epithelial cells (Roland and Funder, 1996). The oligomerisation state of 11β-HSD2 has been seen to vary between tissues. Monomeric, active 11β-HSD2 with a size of approximately 40-kDa seems to be expressed in kidney, colon, adrenal and submandibular gland (Obeyesekere *et al.*, 1997, Smith *et al.*, 1997), whereas a dimeric, inactive and latent 11β-HSD2 with an approximate size of 80-kDa is expressed in the prostate and stomach (Smith *et al.*, 1997, Obeyesekere *et al.*, 1997). Both 40 and 80 kDa forms are expressed in the pancreas (Smith *et al.*, 1997, Obeyesekere *et al.*, 1997). Other groups have also shown 11β-HSD2 to exist as an inactive dimer (Gomez-Sanchez *et al.*, 2001), indicating that perhaps regulation of dimerisation could act as a mechanism for modulating enzyme activity. However, since the majority of SDRs are dimeric, with only the carbonyl reductases 1 & 3 known to exist as monomers (Oppermann, 2007), active, monomeric 11β-HSD2 is unlikely.

11β-HSD2 expression in MR-rich tissues is important as although the *in vivo* ligand for the MR is aldosterone, binding studies have shown that cortisol and corticosterone (the major rodent glucocorticoid) have a binding affinity for MR equal to that of aldosterone (0.5-1 nM) (Krozowski and Funder, 1983, Arriza *et al.*, 1988). Therefore the function of 11β-HSD2 in these tissues is to protect the MR from activation via cortisol/corticosterone. The importance of 11β-HSD2 in this respect came from the understanding of a disease condition known as apparent mineralocorticoid excess (AME).

AME is an autosomal recessive disease and is characterised by hypokalaemia and low-rennin, low-aldosterone hypertension. These symptoms have been attributed to a defective conversion of cortisol to cortisone in peripheral tissues caused by defective 11β-HSD2, resulting in illicit activation of the MR by cortisol (Stewart *et al.*, 1988). Due to reduced cortisol metabolism, the normal negative feedback system discussed previously decreases the rate of cortisol secretion, maintaining a normal level of circulating cortisol. This means that patients do not

present with Cushingoid features, the classic symptom of glucocorticoid excess (Stewart *et al.*, 1988).

Around 100 cases of AME have been reported to date, with sequence analysis showing mutations in each of the 5 exons of the 6.2kb *HSD11B2* gene, with most occurring on exons 3 & 4 (reviewed in Draper and Stewart 2005). Mutations in AME patients can either be due to amino acid substitutions, which are predicted to have deleterious effects on 11β-HSD2 structure, or be due to base changes which result in premature stop codons (Draper and Stewart, 2005).

Interestingly, the high expression of 11β-HSD2 in the placenta is thought to be a mechanism of preventing the high level of circulating maternal glucocorticoids predisposing the foetus to hypertension in adulthood (Benediktsson *et al.*, 1993).

1.3.2. 11β-hydroxysteroid dehydrogenase type I (11β-HSD1)

While 11β-HSD2 is expressed in mineralocorticoid target tissues (e.g. kidney), functioning to inactivate cortisol to cortisone, the isozyme 11β-HSD1 is expressed predominantly in glucocorticoid target tissues (e.g. liver and adipose) and converts the cortisone produced from the 11β-HSD2 reaction to active cortisol (Figure 1.8).

1.3.3. Primary structure of 11β-HSD1

11β-HSD1 is a microsomal (Ozols, 1995) 34 KDa integral membrane glycoprotein which is postulated to exist as a homodimer (Maser *et al.*, 2002), although some studies have suggested it may exist as a homotetramer under some conditions (Hosfield *et al.*, 2005). Although glycosylation has been postulated to be essential for structural stability (Filling *et al.*, 2001), it has been shown that 11β-HSD1 is active in its non-glycosylated form (Ozols, 1995, Blum *et al.*, 2000, Walker *et al.*, 2001b). 11β-HSD1 has an N-terminal membrane anchor (Mziaut *et al.*, 1999, Odermatt *et al.*, 1999), with a small portion of the extreme N-terminus of the enzyme being cytosolic. The C-terminal catalytic domain lies in the lumen of

the endoplasmic reticulum (Odermatt *et al.*, 1999, Walker *et al.*, 2001a) (Figure 1.9). 11β-HSD1 has been identified from a variety of species with primary sequences available for many of them. Species include human (Tannin *et al.*, 1991) (Genbank protein accession code: NP_005516), mouse (Rajan *et al.*, 1995, Oppermann *et al.*, 1995, Hult *et al.*, 2006) (NP_032314), guinea pig (Pu and Yang, 2000, Shafqat *et al.*, 2003) (NP_001166328), chicken (XP_417988), squirrel monkey (Moore *et al.*, 1993), pig (Klemcke *et al.*, 2003) (NP_999413), cow (Tetsuka *et al.*, 2003) (NP_001116504), sheep (Yang *et al.*, 1992) (NP_001009395), rhesus monkey (Magness *et al.*, 2005) (XP_001110531), rhesus macaque (Hult *et al.*, 2006), cat (Schipper *et al.*, 2004, Hult *et al.*, 2006), dog (NP_001005756), African clawed frog (NP_001079807), rabbit (Hult *et al.*, 2006), baboon (Pepe *et al.*, 2001), chimpanzee (Clark *et al.*, 2003) (XP_001168226) and rat (Nobel *et al.*, 2002) (NP_058776). An alignment comparing the amino acid sequences of the enzymes from some of these species is shown in Figure 1.10.

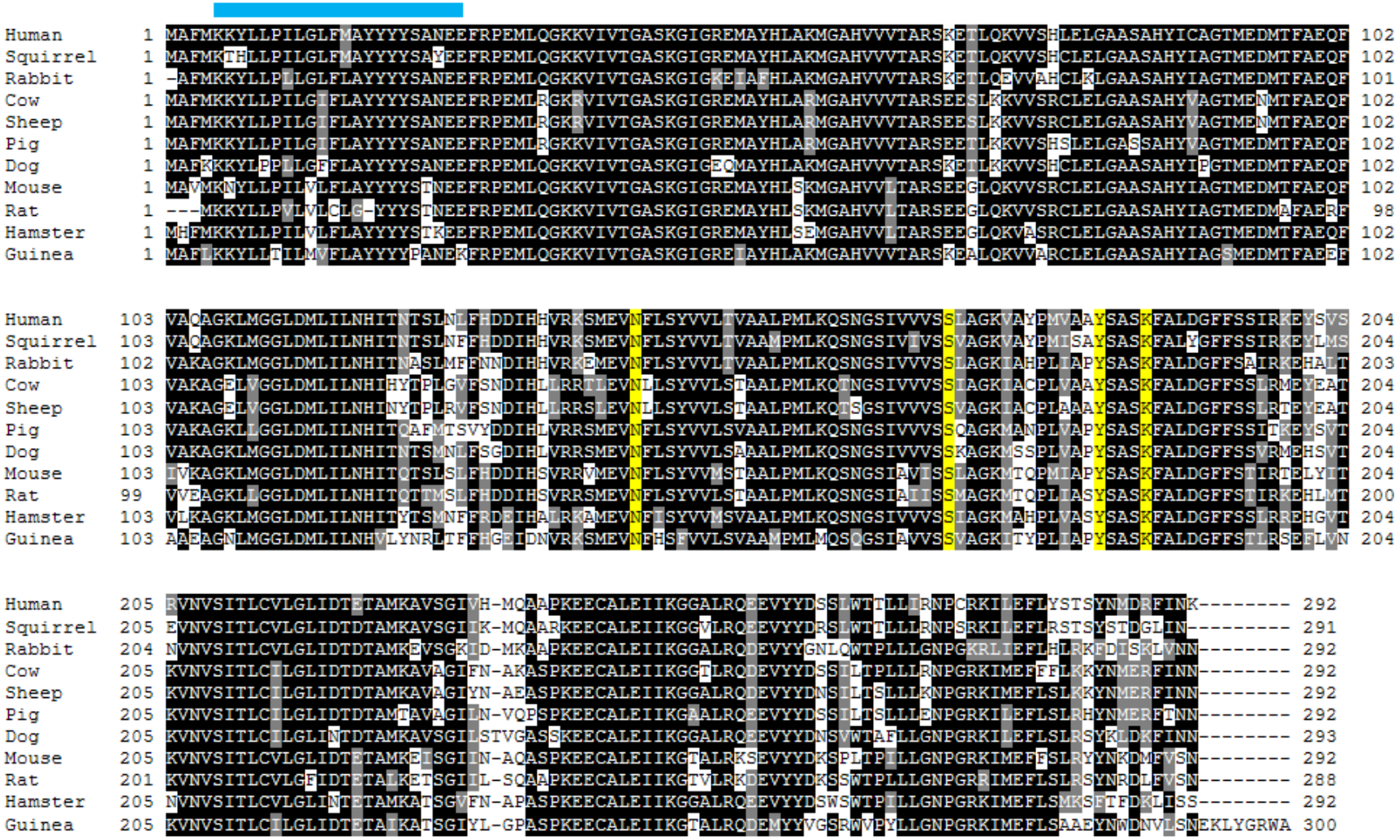

Figure 1.10. Multiple sequence alignment of the available amino acid sequences of 11β-HSD1 across 11 species. Conserved residues are shaded black with similar residues shaded gray. Active site residues of 11β-HSD1 are shaded yellow. Transmembrane region is represented by a light blue box. Squirrel=squirrel monkey. Diagram produced using ClustalW and Boxshade.

1.3.4. Kinetics and enzymology of 11β-HSD1

It has been calculated that all HSD catalysed reactions should favour the reduction of ketosteroid due to the thermodynamically favourable oxidation of NAD(P)H (~-30 kcal/mol) and a low free energy difference between ketosteroid and the corresponding hydroxysteroid (~1kcal/mol) (Sherbet *et al.*, 2007). It has been proven in a variety of studies that 11β-HSD1 displays a predominant reductase activity in intact cells (Bujalska *et al.*, 1997, Jamieson *et al.*, 1995) while 11β-HSD2 functions as a dehydrogenase (Brown *et al.*, 1993, Stewart *et al.*, 1994). This reductive activity *in vivo* of 11β-HSD1 can be partly attributed to the preference of 11β-HSD1 for the cofactor NADP(H) compared to 11β-HSD2, which utilizes NAD(H). Previous experiments using the analogous enzymes 17β-HSD1, which functions as a reductase, and 17β-HSD2, which function as a dehydrogenase, have shown that a single residue can alter the preference for cofactor, hence altering the reaction direction *in vivo*. Reductive HSDs contain a critical Arg residue (R38 in 17β-HSD1) which forms a salt bridge with the 2'-phosphate of NADP(H), distinguishing it from NAD(H) (Sherbet *et al.*, 2007). However, NAD(H) dependent HSDs lack this residue and contain a Asp residue in the preceding position, conferring electrostatic repulsion to the 2'phosphate (Sherbet *et al.*, 2007). Mutation studies have confirmed these observations, showing that mutation of the residue preceding Arg38 (L37) to Asp in 17β-HSD1 is enough to change cofactor preference from NADP(H) to NAD(H) and subsequently reverse directional preference to favour the dehydrogenase reaction (Khan *et al.*, 2004, Huang *et al.*, 2001). The reverse is also true, with a double mutant of the oxidative 3β-HSD1 (D36A + L37R) enough to change cofactor preference from NAD(H) to NADP(H) (Thomas *et al.*, 2003). The critical Arg residue seen in 17β-HSD1 is also present in 11β-HSD1 (R66) and although no high-resolution data exists for 11β-HSD2, one would expect an equivalent Asp residue to the one observed in 17β-HSD2 to be present. Therefore since large concentration gradients are present in cells due to

intermediary metabolism, with [NADPH] >> [$NADP^+$] and [NAD^+] >> [NADH] (Agarwal and Auchus, 2005), if each 11β-HSD isoform is restricted to one pair of cofactors, mass action will drive steroid flux for either hydroxysteroid oxidation (by NAD^+) or ketosteroid reduction (by NADPH) .

However, for 11β-HSD1 it appears that the factors governing directional preference are more complicated than in 17β-HSD1. 11β-HSD1 is present in the lumen of the ER, a relatively oxidative environment compared to the cytosol (Braakman *et al.*, 1992) in which $NADP^+$ might be expected to predominate over NADPH. It has frequently been observed that it is the dehydrogenase direction which predominates in purified preparations and cellular homogenates (Lakshmi and Monder, 1988). The apparent equilibrium constant (K_{app}) at pH 7.0 (shown by equation 2) for the NADPH-dependent conversion of cortisone to cortisol has been calculated to be 0.03 (Walker *et al.*, 2001a), showing the reaction equilibrium to be to the cortisone/NADPH side and therefore potentially explaining the tendency for the 11β-HSD1 reaction to proceed in the dehydrogenase direction *in vitro* (Figure 1.11).

$$K_{eq}[H^+] = [NADP^+][\text{cortisol}]/[NADPH][\text{cortisone}] \qquad (2)$$

However, if an NADPH-regenerating system is added to the *in vitro* assay (e.g. glucose-6-phosphate dehydrogenase plus glucose-6-phosphate), 11β-HSD1 is able to reduce cortisone to cortisol (Walker *et al.*, 2001a). It would therefore appear that the *in vivo* reductive activity of 11β-HSD1 requires a high NADPH/$NADP^+$ ratio for effective activity. This high luminal ratio of NADPH/$NADP^+$ is now known to be controlled by the microsomal enzyme hexose-6-phosphate dehydrogenase (H6PDH). This system is discussed in detail in Section 1.5.

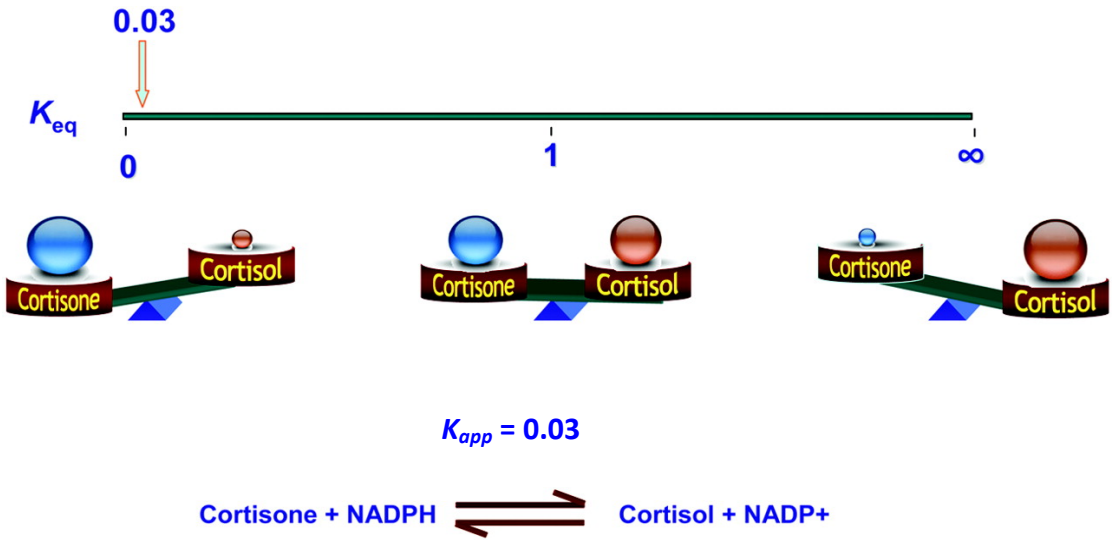

Figure 1.11. Diagrammatic representation of the apparent equilibrium constant, K_{app} (equivalent to K_{eq}[H+]) of 11β-HSD1 at pH 7.0. K_{app} is expressed as [NADP][cortisol]/[NADPH][cortisone] at equilibrium. Taken from Hewitt *et al.* 2005.

The 11β-HSD1 reaction follows a compulsory ordered ternary complex bi-bi mechanism (Castro *et al.*, 2007) using a catalytic tetrad of N-Y-S-K typical of SDRs (described in more detail in Section 1.7). In this ordered reaction, NADPH binds first at the active site, followed by cortisone. Cortisone is reduced to cortisol which leaves the active site followed by $NADP^+$ (Castro *et al.*, 2007). Interestingly, published Michaelis constants for 11β-HSD1 vary dramatically depending on method, species, substrate and authors. Some apparent K_m values for the steroid substrates of the human and rat enzymes are listed in Table 1.2. In terms of human 11β-HSD1, the discrepancies between Maser *et al.* (2002), Arampatzis *et al.* (2005) and the three groups which used bacterially produced recombinant protein can potentially be explained by the difference in how the protein was produced and subsequently assayed. Maser *et al.* (2002) utilized native protein purified from human liver and as such, the relatively high apparent K_m values, especially for cortisol, could perhaps reflect the purification procedure used to obtain 11β-HSD1. This could also potentially explain the observation of enzyme cooperativity which has not been observed elsewhere. The apparent

K_m values reported by Arampatzis *et al.* (2005) were assayed using lysed human embryonic kidney (HEK)-293 cells overexpressing 11β-HSD1. Using this system, the full length 11β-HSD1 protein should still be embedded in the microsomal membrane, with the lower apparent K_m values perhaps reflecting improved folding/stability of the protein in this environment (Table 1.2). An obvious disadvantage of this method is the impurity of the protein makes accurate estimation of protein amount, hence specific 11β-HSD1 activity, difficult.

However, the large differences between the three groups who used bacterially produced recombinant protein are harder to explain (Table 1.2). All the groups used the same *E.coli* system, BL21(DE3), expressing N-terminally truncated 11β-HSD1 containing residues 24–292 in a pET28 plasmid, with the resulting protein purified in a similar way (Castro *et al.*, 2007, Shafqat *et al.*, 2003, Walker *et al.*, 2001a). The only major difference in enzyme preparation is the removal of the His_6-tag by Castro *et al.*, which could potentially explain the low nanomolar apparent K_m values reported (Table 1.2). However, studies using heat shock protein HSC70, have shown that removal of His_6-tag does not effect enzyme activity (Amor-Mahjoub *et al.*, 2006) indicating that this is unlikely. The only other reported difference between these groups is the method of assay. Castro *et al.* (2007) include detergent and reducing agent in their assay, with steroid separation performed by high throughput liquid chromatography (HTLC). Walker *et al.* (2001) and Shafqat *et al.* (2003) do not include these additives with steroid separation performed by thin layer chromatography (TLC) and high performance liquid chromatography (HPLC) respectively. However, it seems unlikely that method of assay and steroid separation would cause such a large difference in apparent K_m values indicating that more studies are required to fully elucidate the accurate Michaelis constants for 11β-HSD1 produced using this recombinant system.

Species	K_m (μM)	k_{cat} (min^{-1})	Substrate	Assay method	Reference
Human	0.52 +/- 0.07	-	Cortisone	In cell (Lysed kidney cells)	(Arampatzis *et al.*, 2005)
Human (recombinant)	0.80 +/- 0.20 2.90 +/- 0.40	1.60 +/- 0.70 11.1 +/- 2.80	Cortisone Cortisol	*In vitro* (HIS-tagged)	(Shafqat *et al.*, 2003)
Human	13.9 +/- NA 41.3 +/- NA	- -	Cortisone Cortisol	*In vitro* (Purified from liver)	(Maser *et al.*, 2002)
Human (recombinant)	0.04 +/- 2.90	0.27 +/- 0.01	Cortisone	*In vitro* (HIS-tag removed)	(Castro *et al.*, 2007)
Human (recombinant)	9.50 +/- 0.90 1.40 +/- 0.60	- -	Cortisone Cortisol	*In vitro* (HIS-tagged)	(Walker *et al.*, 2001a)
Rat	1.83 +/- 0.06 17.3 +/- 2.24	- -	Corticosterone Cortisol	Purified from microsomes	(Lakshmi and Monder, 1988)
Rat	0.85 +/- 0.12	-	11-dehydrocorticosterone	In cell (Lysed kidney cells)	(Arampatzis *et al.*, 2005)
Human (recombinant)	14.4 +/- 1.70	0.21 +/- 0.01	NADPH	*In vitro* (HIS-tag removed)	(Castro *et al.*, 2007)

Table 1.2. Apparent K_m and k_{cat} values for steroid substrate calculated for 11β-HSD1 from rat and human. The equilibrium dissociation constant, K_ia, for the human enzyme was calculated to 147.5 (Castro *et al.*, 2007). Note particularly the large differences for the K_m values for the human protein. *In vitro* kinetic measurements of 11β-HSD1 with steroid were obtained using an excess of cofactor (i.e. >200μM**)** over enzyme.

It must be noted here that the glucocorticoid hormones are not the only substrate for 11β-HSD1. It has been shown that 11β-HSD1 can act as 7β-hydroxycholesterol dehydrogenase, or 7-keto-cholesterol reductase, inter-converting 7β-hydroxycholesterol and 7-ketocholesterol (Figure 1.12) (Schweizer *et al.*, 2004, Hult *et al.*, 2004). It has also been shown that 11β-HSD1 is able to interconvert 7α /7β-hydroxy-dehydroepiandrosterone (7α/7β-DHEA) and 7-

keto-dehydroepiandrosterone (7-keto-DHEA) (Figure 1.12) (Muller *et al.*, 2006). Furthermore, 11β-HSD1 is able to catalyse the epimerisation of the 5α-reduced 7-hydroxysteroids, 7α-hydroxy-epiandrosterone and 5α-androstane-3β,7α,17β–triol, to their 7β-hydroxy derivatives with the active site Ser-170 thought to produce a hemi-ketal species which allows reduction by NADPH (Hennebert *et al.*, 2009).

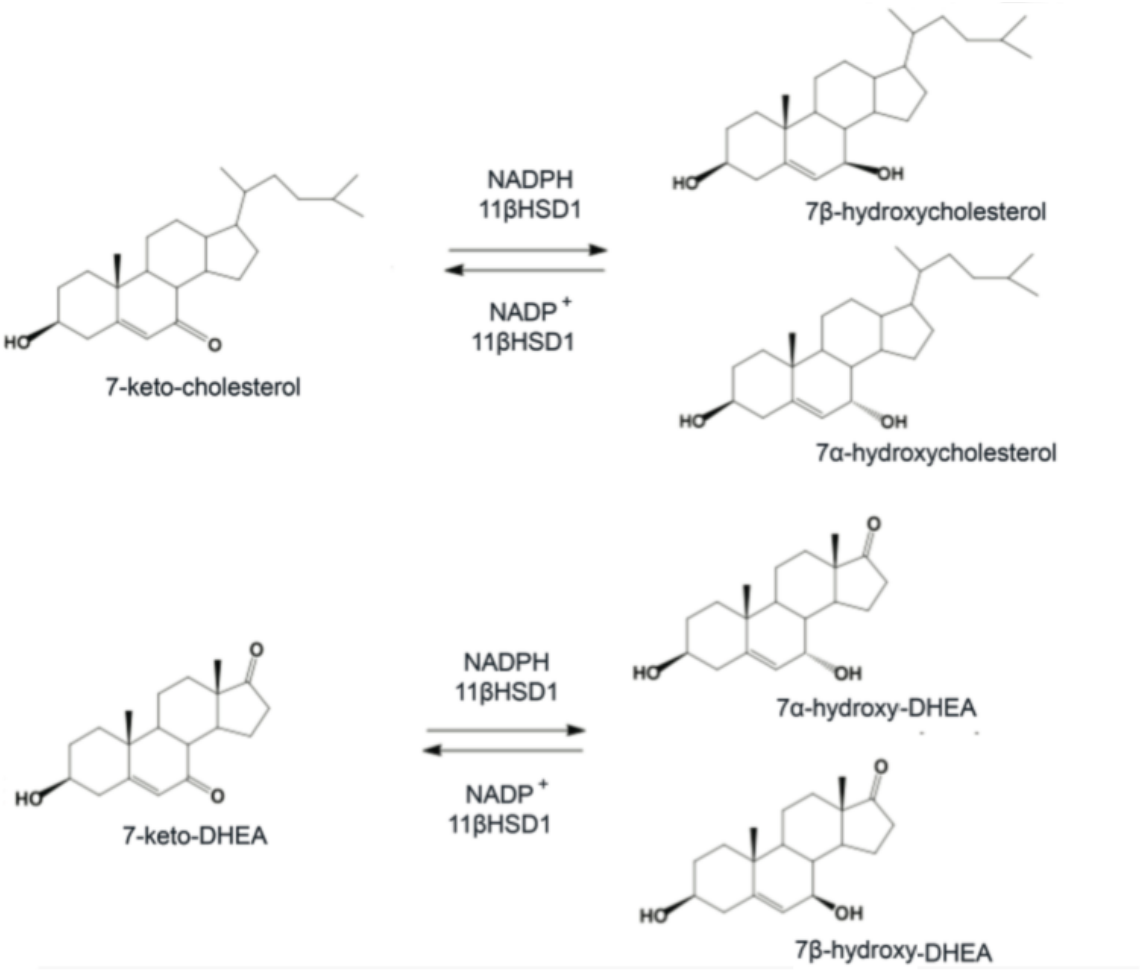

Figure 1.12. Alternative reactions catalyzed by 11β-HSD1.11β-HSD1 is able to convert the 7-keto forms of both dehydroepiandrosterone (7-keto-DHEA) and cholesterol (7-keto-cholesterol) to their respective 7α and 7β-hydroxylated metabolites. In both cases, there is a preference for the formation of 7β-hydroxylated metabolites over the 7α-hydroxylated species.

Interestingly, there seems to be a preference for the formation of 7β-metabolites from 7-keto substrates by 11β-HSD1. Modelling studies have suggested that 7β–hydroxy-DHEA and 7-keto-DHEA are able to bind to 11β-HSD1 in two conformations favourable to interact with nicotinamide ring and the catalytic tyrosine. One conformation has the D ring of the steroid oriented towards the centre of the protein (Figure 1.13A), while in the other conformation the steroid is essentially flipped, with the A ring oriented towards the centre of the protein (Figure 1.13B) (Nashev *et al.*, 2007). It can be seen in Figure 1.13B that this second conformation is not favoured for 7α–hydroxy-DHEA, perhaps explaining the preference for the formation of 7β-metabolites (Nashev *et al.*, 2007).

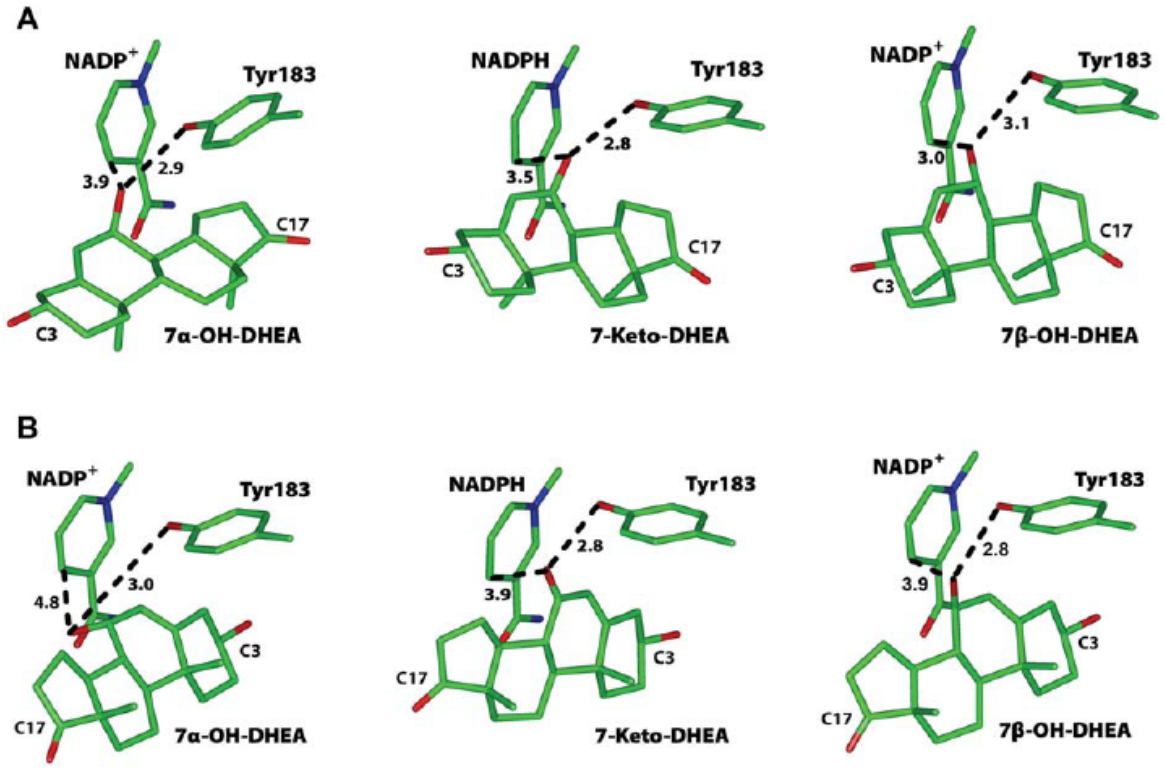

Figure 1.13. Modelling studies showing the theory to explain the preference for the formation of 7β-metabolites from 7-keto substrates by 11β-HSD1. A – The D ring of the steroid substrate is oriented towards the centre of the protein. B – The A ring of the steroid substrate is oriented towards the centre of the protein. The conformation of steroid in B is not sterically favoured for 7α–hydroxy-DHEA, perhaps explaining the preference for the formation of 7β-metabolites. Taken from Nashev *et al.* (2007).

1.4. 11β-HSD1 and the Metabolic Syndrome

Due to the wide array of physiological and cellular effects of cortisol (Table 1.1), variations in levels of the glucocorticoid can have profound effects on the health of an organism. There has been considerable interest recently in the possibility that glucocorticoid levels could have a pronounced influence on the 'metabolic syndrome', also referred to as syndrome X (Reaven, 1988) or insulin resistance syndrome. The metabolic syndrome refers to the tendency of certain risk factors for cardiovascular disease (CVD) to group together. These risk factors include insulin resistance, abnormal lipid and glucose metabolism, hypertension and central obesity (Draper and Stewart, 2005). Although some doubt has been expressed on the validity of this syndrome (Unwin, 2006), the epidemic increase in obesity accompanied by an equal rise in the metabolic complications of obesity would suggest the metabolic syndrome has considerable medical relevance (Eckel *et al.*, 2005). It also represents a useful reminder of the risk factors associated with a lack of physical activity and obesity.

The idea that an excess of cortisol could lead to the metabolic syndrome first came from studying sufferers of the hormonal disorder, Cushing's syndrome (Arnaldi *et al.*, 2003, Peeke and Chrousos, 1995). Nearly all patients who suffer from Cushing's syndrome are hypertensive with most showing some form of visceral obesity and up to 50% developing diabetes mellitus (Stewart, 2005). This is accompanied by the characteristic 'moon face' and fragile skin associated with the condition. The molecular pathogenesis of Cushing's syndrome, sometimes referred to as hypercortisolism, includes an increase in the level of circulating cortisol. This increase can come from a variety of sources. Firstly, glucocorticoids used as effective treatments for inflammatory diseases such as asthma, rheumatoid arthritis and lupus; or as immunosuppressive agents following transplant operations, can increase the level of circulating cortisol, leading to Cushing's syndrome (Whitworth *et al.*, 2005).

Alternatively, hypercortisolism can arise as a result of pituitary adenomas, adrenocortical carcinomas or small cell lung cancers which can increase the levels of glucocorticoid either by directly secreting the hormone or indirectly via ACTH secretion (Whitworth *et al.*, 2005).

However, Cushing's syndrome is a rare condition with an annual incidence rate of approximately 1-2 cases per million (Stewart, 2005). This together with the observations that circulating cortisol is often normal, if not reduced, in obesity indicates that a simple increase in circulating cortisol cannot explain obesity (Hautanen and Adlercreutz, 1993, Glass *et al.*, 1981, Dunkelman *et al.*, 1964, Migeon *et al.*, 1963, Streeten, 1993).

Since obesity could not be linked to a systemic increase in cortisol levels, investigation was directed at the regulation of cortisol at a tissue level. The first indication that a local excess of cortisol could cause deleterious effects on health came from the condition AME discussed previously. This condition is effectively caused by an excess of cortisol due to inactivity of the 11β-HSD2 enzyme, prompting some to call AME "Cushing's disease of the kidney" (Stewart, 2005). This led to the current idea that abnormal metabolism of cortisol by 11β-HSD1 in adipose and liver tissue could cause symptoms of the metabolic syndrome. This is illustrated in Figure 1.14. Interestingly, it has recently been shown that circulating 11β-HSD1 mRNA is decreased in obese patients, supporting the idea of tissue specific disregulation of 11β-HSD1 in obesity (Al Bakir *et al.*, 2008).

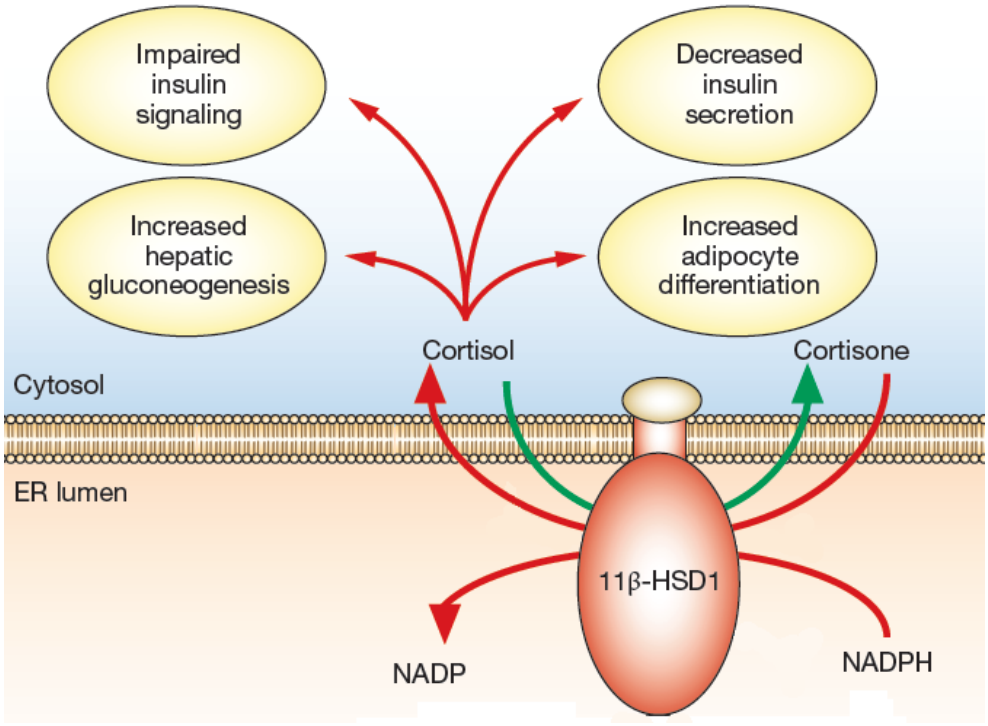

Figure 1.14. **The possible detrimental effects of production of cortisol by 11β-HSD1**. Evidence suggests that patients who present with obesity have down-regulated 11β-HSD1 in an attempt to control the deleterious effects of cortisol. It has also been shown that patients who present with type II diabetes are unable to down regulate 11β-HSD1. Red arrows represent the normal physiological reactions taking place in the liver and adipose tissue. A green arrow shows the $NADP^+$-dependent dehydrogenase reaction seen in some tissues. Adapted from Tomlinson & Stewart (2005).

In humans, adipose tissue is characterized as a specialized type of connective tissue consisting of lipid-laden cells known as adipocytes. Adipocytes are surrounded by connective tissue cells, known as adipose stromal cells (ASC), which consists of mainly macrophages, fibroblasts, pericytes and blood cells (Cryer, 1985). Mature adipocytes are known to develop from a specific line of connective tissue cells resembling fibroblasts known as preadipocytes (Cryer, 1985) which are present in the stromal-vascular fraction together with ASC. Due to the collagenase digestion method used to separate mature adipocytes from preadipocytes, it is not possible to separate the preadipocytes from the rest of the ASC, hence preadipocytes are also known as ASC. Adipose tissue can be stored in numerous locations

around the body and can be categorized by the location found; subcutaneous, perivascular, intermuscular, peritoneal (mesenteries and omentum), retro-peritoneal, synovial, mediastinal, retro-orbital, intraspinal and medullary (bone marrow) (Cryer, 1985). Despite the numerous locations in which adipose tissue is found, it is clear that symptoms of the metabolic syndrome correlate strongly with the amount of omental fat independently from total adiposity and the amount of subcutaneous abdominal fat (Despres *et al.*, 1989, Fujioka *et al.*, 1987).

At a cellular level, obesity is thought to be caused by a combination of preadipocyte differentiation and proliferation, and also hypertrophy of existing adipocytes (Yau *et al.*, 1995, Tomlinson and Stewart, 2001). Preadipocyte differentiation can be caused by cortisol (Hauner *et al.*, 1987). Furthermore, cortisone addition to omental preadipocytes expressing 11β-HSD1 has been shown cause differentiation to adipocytes (Bujalska *et al.*, 1999a) with subsequent studies showing that inhibition of 11β-HSD1 activity via depletion of luminal NADPH can block preadipocyte differentiation (Marcolongo *et al.*, 2008). Although 11β-HSD1 expression is low in preadipocytes, expression is greatly increased in the late stages of differentiation when induced by glucocorticoid (Bujalska *et al.*, 1999a). However, if 11β-HSD1 expression is blocked, glucocorticoid induced differentiation is inhibited, indicating the involvement of 11β-HSD1 in a positive feedback mechanism in which active glucocorticoid can induce 11β-HSD1 expression, which in turn leads to generation of more active glucocorticoid (Bujalska *et al.*, 1999a). The effect of cortisol on adipose tissue is not straightforward, as it has been shown that the glucocorticoid, modulated by 11β-HSD1, is able to inhibit human omental preadipocyte proliferation (Draper and Stewart, 2005). This is perhaps not unusual as it is known that cellular proliferation is generally inhibited by glucocorticoids (Laycock, 1996). It seems therefore that cortisol would have a twofold effect

on adipose tissue, both stimulating differentiation of preadipocytes while inhibiting proliferation.

An array of knockout, transgene and inhibitor studies on mice have gone some way to elucidate the role of 11β-HSD1 in the metabolic syndrome. Perhaps most importantly, it was found that 11β-HSD1 KO mice on a high fat diet were able to resist obesity (Masuzaki *et al.*, 2001) with other studies on the same mice showing improved insulin tolerance in the liver, glucose tolerance and improved lipid and lipoprotein profiles (Morton *et al.*, 2001). Further support of the role of 11β-HSD1 in obesity comes from transgenic experiments in which an 11β-HSD1 transgene, targeted to adipose tissue under the AP2 promoter enhancer, led to a sevenfold increase in 11β-HSD1 expression, a 15-30% increase in local active glucocorticoid and an obese phenotype (Masuzaki *et al.*, 2001). This was accompanied by marked hyperlipidemia, hyperglycaemia, hypertension and hyperinsulinaemia (Masuzaki *et al.*, 2003, Masuzaki *et al.*, 2001). No change in plasma cortisol levels was observed, due to a compensatory decrease in ACTH secretion. Similar experiments with another 11β-HSD1 transgene, this time targeted to the liver under the ApoE promoter, showed hepatic 11β-HSD1 overexpression gave marked insulin resistance, dyslipidaemia, hypertension and fat accumulation in the liver, but without an obese phenotype (Paterson *et al.*, 2004). Experiments on obese rodent models such as Zucker rats (Livingstone *et al.*, 2000) and *ob/ob* mice (Liu *et al.*, 2003), have shown disregulation of 11β-HSD1 at the tissue level, with expression reduced in the liver, but increased in adipose tissue. A study in which obese, hyperlipidaemic mice were able to reduce both weight gain and fasting insulin after administration of the 11β-HSD1 inhibitor carbenoxolone, via subcutaneous injection, supports the concept of 11β-HSD1 over-expression in obesity (Nuotio-Antar *et al.*, 2007).

In contrast somewhat to the studies on rodents, the involvement of 11β-HSD1 in obesity and type II diabetes in humans is not clear-cut. Many groups using the conventional method of

measuring 11β-HSD1 activity *in vivo*, via measuring the ratio of urinary metabolites of cortisol and cortisone (Figure 1.15, described in section 1.2.3), have seen inconsistent changes in 11β-HSD1 activity in both obese (Andrew *et al.*, 1998, Fraser *et al.*, 1999, Stewart *et al.*, 1999, Rask *et al.*, 2002, Klemcke *et al.*, 2003, Westerbacka *et al.*, 2003) and diabetic (Valsamakis *et al.*, 2004, Kerstens *et al.*, 2000, Andrews *et al.*, 2002) subjects. This is perhaps not surprising, as this ratio may be altered by the expression and activities of other enzymes, such as 11β-HSD2 and the 5α- and 5β-reductases that have been shown to differ in obesity (Sandeep *et al.*, 2005, Mussig *et al.*, 2008). The method is also insensitive to tissue specific changes in 11β-HSD1 expression and activity which could occur. This, however, has not stopped the technique being used, with a recent study showing 11β-HSD1 activity being reduced in obese boys (Wiegand *et al.*, 2007).

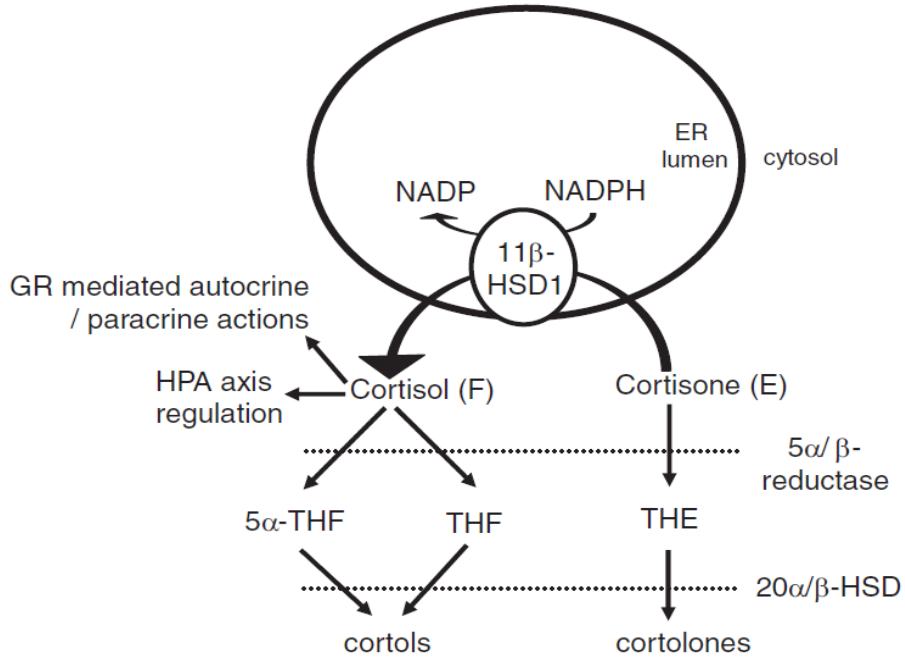

Figure 1.15. *In vivo* activity of 11β-HSD1 is conventionally measured by the ratio of urinary E to F metabolites. The metabolites of cortisone and cortisol generated by reactions catalysed by the 5α- and 5β-reductases and 20α- and 20β-HSD enzymes can be detected in the urine and serve as biomarkers of 11β-HSD1 activity. Impaired conversion of cortisone to cortisol is offset by changes to cortisol secretion by the HPA axis. THE = tetrahydrocortisone, THF = tetrahydrocortisol, allo-THF = allo-tetrahydrocortisol, HPA = hypothalamic-pituitary-adrenal. Adapted from Lavery *et al.* 2008.

In order to separate the tissue specific activities of 11β-HSD1, more exact methods must be used to elucidate the involvement of hepatic and adipose 11β-HSD1 in glucocorticoid regeneration and health. Studies to assess the activity of hepatic 11β-HSD1 using the measurement of cortisol in peripheral plasma following an oral dose of cortisone have found 11β-HSD1 activity in the liver to be reduced in obesity (Stewart *et al.*, 1999, Rask *et al.*, 2001, Valsamakis *et al.*, 2004, Westerbacka *et al.*, 2003). They also observed that this downregulation is not present in patients who also present with type II diabetes (Tomlinson and Stewart, 2005, Valsamakis *et al.*, 2004, Andrews *et al.*, 2002). It has been suggested that the decreased hepatic 11β-HSD1 activity represents a mechanism to protect the body from the deleterious effects of obesity by attempting to increase insulin sensitivity and decrease

hepatic glucose output. The inability of type II diabetes sufferers to downregulate hepatic 11β-HSD1 activity would lead hyperglycaemia, a potential increase in adiposity and decreased insulin sensitivity (Tomlinson and Stewart, 2005). It is also worth noting that the association between hepatic fat accumulation and hepatic overexpression of 11β-HSD1 which was seen in the transgenic mice was not observed in human subjects who presented with the most severe form of non-alcoholic fatty liver disease, non-alcoholic steatohepatitis (NASH) (Paterson *et al.*, 2004, Konopelska *et al.*, 2009).

The specific activity and expression of 11β-HSD1 has been investigated in both subcutaneous (SAT) and visceral (VAT) adipose tissue. This is an important distinction to make, as VAT releases large amounts of free fatty acids to the liver via the portal system and has long been regarded as having a greater number of glucocorticoid receptors (GR) than SAT (Bronnegard *et al.*, 1990). Therefore, an increased 11β-HSD1 activity in VAT could potentially have more deleterious effects on health than a similar increase in SAT would. However, recent work has suggested that VAT and SAT express a similar number of GR (Bujalska *et al.*, 2006). Many investigators have, using *in vitro* biopsies, shown marked increases in 11β-HSD1 mRNA and activity in the SAT of obese subjects when compared to lean (Rask *et al.*, 2002, Paulmyer-Lacroix *et al.*, 2002, Lindsay *et al.*, 2003, Wake *et al.*, 2003, Engeli *et al.*, 2004, Kannisto *et al.*, 2004). These increases are comparable to the increases seen in the transgenic mouse model (Masuzaki *et al.*, 2001). One group did not see any such increase (Tomlinson *et al.*, 2002), perhaps due to the method used to obtain the biopsies (Sandeep *et al.*, 2005).

A study by Sandeep *et al.* (2005) using an *in vivo* microdialysis technique, together with a 9,11,12,12-[$^{2}H_{4}$]cortisol tracer, showed increased 11β-HSD1 activity in SAT together with the previously documented decrease in 11β-HSD1 activity in the liver. This, together with the findings that the non-specific 11β-HSD1 inhibitor carbenoxolone will increase insulin sensitivity in both lean healthy (Walker *et al.*, 1995) and diabetic (Andrews *et al.*, 2003) men,

but not obese subjects (Sandeep *et al.*, 2005), supports the concept that a decrease in hepatic 11β-HSD1 may occur in obesity (Tomlinson and Stewart, 2005).

A more recent study (Desbriere *et al.*, 2006) has found elevated 11β-HSD1 mRNA in obese women in both VAT and SAT. This study was important as it was the first time in which elevated 11β-HSD1 mRNA was observed in VAT, with the amount of VAT in a patient being one of the major indicators of type II diabetes and obesity (Despres *et al.*, 1989, Fujioka *et al.*, 1987). This was followed by a study investigating the expression of 11β-HSD1 in VAT and SAT in both male and female patients presenting with obesity (Paulsen *et al.*, 2007). This study found that 11β-HSD1 mRNA expression, in both male and female obese patients, was increased in SAT compared to lean patients. However, expression of 11β-HSD1 was only increased in the VAT of obese women. This is interesting as when the level of 11β-HSD1 in lean men and women is compared in SAT, it can be seen that women have considerably less 11β-HSD1 expression than men. In obese subjects, the level of 11β-HSD1 expression is similar in both men and women. This sex specific difference, coupled with studies which show that increased levels of 11β-HSD1 in SAT correlate with metabolic disorders (Alberti *et al.*, 2007, Goedecke *et al.*, 2006), could potentially show that the upregulation of 11β-HSD1 in obesity may have a greater effect on women than men. This could go some way to explaining higher risk of CVD in women suffering from the metabolic syndrome (Paulsen *et al.*, 2007).

Interestingly, there is some evidence to suggest that 11β-HSD2 expression is increased in both the kidney and SAT in obese rodent models. A recent study (Mussig *et al.*, 2008), has shown 11β-HSD2 activity to be increased in the kidneys of 72 extremely obese human subjects. Although some groups have found no change in 11β-HSD2 activity (Stewart *et al.*, 1999), Mussig *et al.* (2008) argue that due to the high free plasma concentrations of cortisone, the inactive hormone can function as a rapidly available glucocorticoid which is activated to

cortisol in specific tissues such as the liver and adipose. Therefore, an increase in circulating free cortisone as a result of increased 11β-HSD2 activity, could indirectly lead to increased active hormone in adipose tissue, thereby enhancing that effect of increased 11β-HSD1 activity in the adipose tissue of obese subjects (Mussig *et al.*, 2008).

As has been mentioned previously in this text, in addition to hepatic and adipose expression, 11β-HSD1 is also expressed in pancreatic islet cells (Davani *et al.*, 2000). The beta cells of the pancreatic islets, which make up around 80% of islet cells, are responsible for the production of insulin, with glucocorticoids known to inhibit insulin secretion (Billaudel and Sutter, 1979, Pierluissi *et al.*, 1986, Lambillotte *et al.*, 1997). Interestingly, a recent report has shown that short term GC treatment will actually increase insulin section from islets, possibly priming the cells for a switch in GC response eventually resulting in glucose insensitivity and a decrease in insulin secretion (Hult *et al.*, 2009). In rodent models, glucose-stimulated insulin release (GSIR) was decreased in a dose dependent manner, when they were incubated with 11-dehydrocorticosterone, with the decrease reversed by addition of the 11β-HSD1 inhibitors carbenoxolone and BVT.2733 (Ortsater *et al.*, 2005, Davani *et al.*, 2000). This led to the idea that 11β-HSD1 was expressed in the insulin producing beta cells of the pancreatic islets. However, a recent study has shown via immunohistochemistry and immunofluorescence, that 11β-HSD1 co-localises with glucagon in the periphery of both human and murine islets (Swali *et al.*, 2008). This, coupled with the fact that no 11β-HSD1 co-localised with insulin, shows that 11β-HSD1 is localised exclusively in the alpha cells of pancreatic islets (Swali *et al.*, 2008). This implies that the relationship between generation of active glucocorticoid by 11β-HSD1 in islet cells and the decrease in GSIR may be more complicated than previously thought. Functional glucagon receptors can be found in human beta cells which are able to generate signals for GSIR. A recent study has shown the potent negative effect of glucocorticoids on both GSIR and glucagon secretion (Swali *et al.*, 2008).

The same study has also shown that the inhibitory properties of 11-dehydrocorticosterone on GSIR and glucagon secretion is dependent on 11β-HSD1 activating the inactive glucocorticoid to corticosterone (Swali *et al.*, 2008). Insulin secretion in beta cells can be stimulated by glucagon using both cAMP and protein kinase A dependent mechanisms (Gromada *et al.*, 1997), with glucagon receptor knockout mice having reduced GSIR when compared to WT mice (Sorensen *et al.*, 2006). This suggests that the generation of active glucocorticoid by 11β-HSD1 in alpha cells could impact on insulin secretion from beta cells by decreasing the secretion of glucagon, which would in turn decrease insulin secretion via the effects on the glucagon receptors on beta cells (Swali *et al.*, 2008).

1.4.1. Function and expression of 11β-HSD1 in other tissues

Recent research has indicated the involvement of 11β-HSD1 and 11β-HSD2 in the regulation of endothelial nitric oxide synthase (eNOS) expression and hence, a possible involvement of these enzymes in vascular function (Liu *et al.*, 2009). This was shown by the discovery of a previously unknown glucocorticoid response element (GRE) on the eNOS promoter region which, when in complex with cortisol bound to GR, serves to downregulate eNOS expression (Liu *et al.*, 2009). This is interesting as it is suggestive that suppression of eNOS may be involved with the pathology associated with the possible 11β-HSD1 overexpression in the metabolic syndrome or the 11β-HSD2 deficiency in AME.

Glucocorticoids play an important role in the function of the central nervous system (CNS) with known involvement in neurotransmission, neuronal division, cellular metabolism and survival (Woolley *et al.*, 1990, Swaab *et al.*, 2005, Landfield *et al.*, 1978). There is increasing evidence to suggest that an increase in GC can cause an impairment in cognitive function. Firstly, patients who suffer from Cushing's syndrome, in addition to the metabolic complications discussed earlier, can display cognitive and psychotic disorders (Swaab *et al.*,

2005). Secondly, the cognitive impairment due to ageing is associated with an increase in GC in rodents and humans (Meaney *et al.*, 1995). Finally, processes which maintain a lower level of GC through life, such as neonatal programming of tighter HPA control or adrenalectomy with low-dose GC replacement, have been shown to prevent the emergence of cognitive deficits which commonly occur with age (Meaney *et al.*, 1988, Landfield *et al.*, 1981). As previously mentioned, 11β-HSD1 is widely expressed in the brain, most notably in the cerebellum, hippocampus and neocortex, indicating involvement of the enzyme in memory and learning (Moisan *et al.*, 1990). Indeed, *in situ* hybridisation studies in the post mortem brain have confirmed the presence of 11β-HSD1 in these areas with 11β-HSD2 notably absent (Sandeep *et al.*, 2004). The presence of 11β-HSD1 in neuronal tissues leads to the question as to whether inhibition can be therapeutic in the treatment of cognitive impairment. The action of 11β-HSD1 to produce active GC, which are known to amplify the neuro-endangering process of excitory amino acid induced toxicity (Rajan *et al.*, 1996, Ajilore and Sapolsky, 1999) and the observation that aged 11β-HSD1$^{-/-}$ mice are able to resist the cognitive impairments seen in WT aged mice (Yau *et al.*, 2001) would suggest that 11β-HSD1 inhibition would be beneficial. In addition, a recent study has shown aging mice (18 months) overexpressing 11β-HSD1 in the forebrain display premature age associated cognitive decline in the absence of a increase in circulating cortisol (Holmes *et al.*, 2010). Studies have now shown that the non-specific 11βHSD inhibitor carbenoxolone is able to improve verbal fluency in healthy elderly men and verbal memory in patients with type 2 diabetes (Sandeep *et al.*, 2004). Improvements in cognitive function with 11β-HSD1 inhibition have also been shown in rodents (Dhingra *et al.*, 2004). However, due to the non-specific nature of inhibitor and KO studies, it is not currently known if the neuroprotective effects of 11β-HSD1 inhibition are secondary to the more well characterized metabolic and vascular effects of 11β-HSD1 inhibition (Wamil and Seckl, 2007).

In addition to a role for 11β-HSD1 in the pathogenesis of type II diabetes and obesity, it has been postulated that inhibition of 11β-HSD1 in the eye could lead to a novel therapeutic strategy against glaucoma. This can be explained by 11β-HSD1 expression in the rat (Stokes *et al.*, 2000), human (Stokes *et al.*, 2000, Rauz *et al.*, 2001) and rabbit eye (Onyimba *et al.*, 2006). A high amount of cortisol in this area can have profound effects on increasing intra-ocular pressure (Rauz *et al.*, 2001). Studies using the 11β-HSD1 inhibitor carbenoxolone have shown some success in reducing intraocular pressure in glaucoma sufferers (Rauz *et al.*, 2003, Rauz *et al.*, 2001).

1.4.2. Inhibitors of 11β-HSD1 activity

Although more research needs to be done to fully elucidate the role of 11β-HSD1 in obesity, it would seem that there is a clear relationship between an increase in 11β-HSD1 expression in adipose tissue, and obesity. It is also clear that there is a relationship between production of glucocorticoids by 11β-HSD1 and a decrease GSIR. Inhibitors which are selective for 11β-HSD1 could therefore be therapeutic for the treatment of both insulin resistance and obesity, with some success reported for various sulphonamides (Barf *et al.*, 2002, Alberts *et al.*, 2002, Alberts *et al.*, 2003, Neelamkavil *et al.*, 2009, Siu *et al.*, 2009, Sun *et al.*, 2009, Zhang *et al.*, 2009a, Xiang *et al.*, 2008, Tu *et al.*, 2008, Moreno-Diaz *et al.*, 2008), triazoles (Olson *et al.*, 2005, Tu *et al.*, 2008, Zhu *et al.*, 2008a, Zhu *et al.*, 2008b), spiro-carboxamides (Lepifre *et al.*, 2009), colletoic acid (Aoyagi *et al.*, 2008), sterenins (Ito-Kobayashi *et al.*, 2008), benzamides (Julian *et al.*, 2008), adamantanes (Rohde *et al.*, 2007, Su *et al.*, 2009) and thiazolones (Jean *et al.*, 2007, Caille *et al.*, 2009, Fotsch *et al.*, 2008). A selection of these inhibitors is shown in Figure 1.16. Various docking and crystallization studies suggest the above inhibitors function through binding to the 11β-HSD1 active site, although for most of the above the exact mode of inhibition is not known. Tu *et al.* (2008) have shown that while their sulphonamide compound (known as compound 1) shows simple substrate competitive

inhibition, their triazole inhibitor (compound 2) functions as a mixed inhibitor. Finally, a recent study has shown a stereo specific difference between the inhibitory properties of the two glycyrrhizin metabolites, 18α-glycyrrhetinic and 18β- glycyrrhetinic acid (18α-GA and 18β-GA) (Classen-Houben *et al.*, 2009). While both isomers were able to inhibit 11β-HSD1, only 18β-GA was able to inhibit 11β-HSD2, indicating that the olean scaffold, specifically structures similar to 18α-GA, may used in the development of selective 11β-HSD1 inhibitors (Classen-Houben *et al.*, 2009).

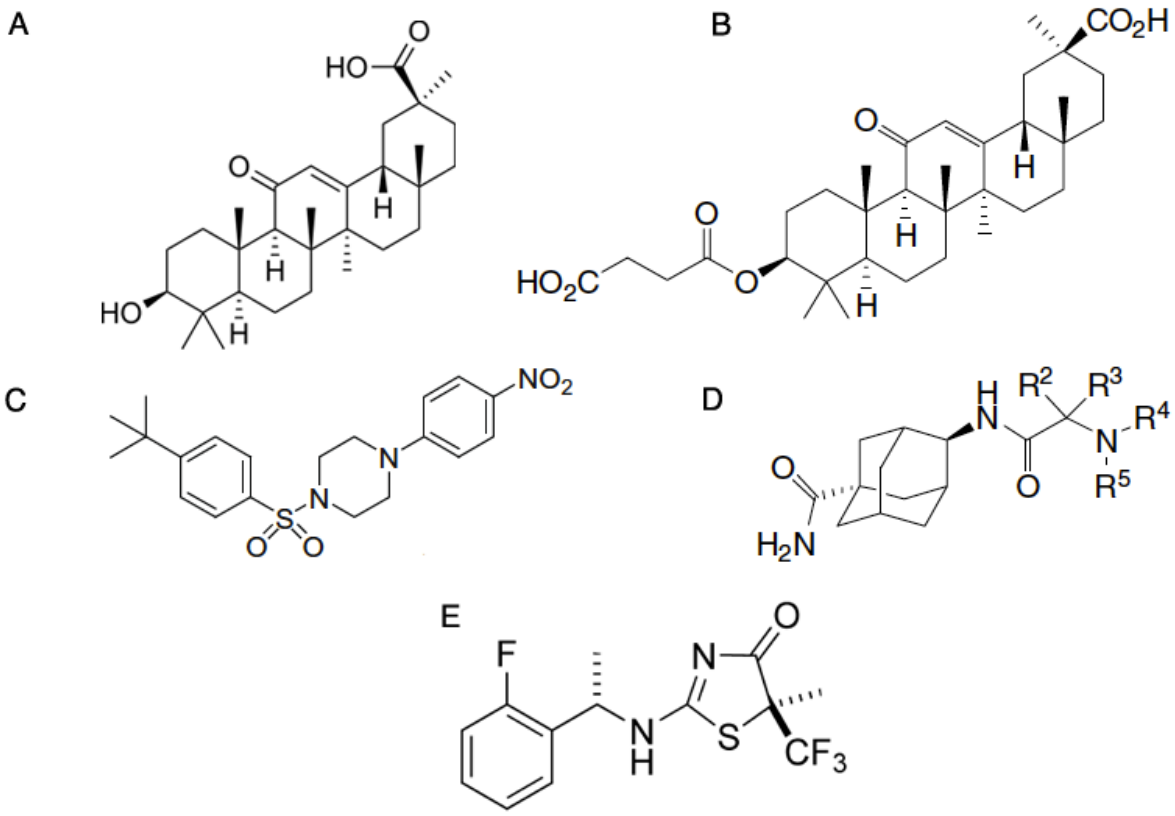

Figure 1.16. Some examples of the types of 11β-HSD1 inhibitors proposed for the treatment of the metabolic syndrome. Shown are the naturally occuring non-specific 11β-HSD1 inhibitor glycyrrhetinic acid (A) and its derivative, carbenoxolone (B). Also shown are the more specific, non-steroidal inhibitors such as an arylsulfonylpiperazine (C), an adamantane amide (D) and compound 2922 (a thiazolone, E).

Interestingly, the search for selective 11β-HSD1 inhibitors has not been purely via high throughput screens and structure based design. A recent study has shown that traditional antidiabetic medicines, such as extracts from *Eriobotrya japonica* (Rosaceae) and roasted *Coffea arabica* (coffee) beans, were able to selectively inhibit 11β-HSD1 activity in HEK-293 cells (Atanasov *et al.*, 2006, Gumy *et al.*, 2009).

1.5. Regulation of 11β-HSD1 activity via hexose-6-phosphate dehydrogenase

As mentioned previously, although 11β-HSD1 is known to display a predominant reductase activity in intact cells, it is the dehydrogenase direction which predominates in purified preparations and cellular homogenates. The equilibrium constant (at pH 7.0) for the conversion of cortisone to cortisol was calculated to be 0.03 (Walker *et al.*, 2001b), showing the reaction to favour cortisone and NADPH at equilibrium (Figure 1.11) and hence the tendency for the 11β-HSD1 reaction to proceed in the dehydrogenase direction *in vitro*. Since 11β-HSD1 acts as an ketoreductase *in vivo*, certain factors must be pushing the equilibrium towards cortisol and $NADP^+$. One of these factors appears to be the lumenal concentration of NADPH, or more specifically the ratio of NADPH to $NADP^+$, which is controlled by microsomal enzyme hexose-6-phosphate dehydrogenase (H6PDH).

The interest in the luminal ratio of NADPH/$NADP^+$ in relation to 11β-HSD1 was started by Agarwal *et al.* (1990), whose kinetic studies on purified, recombinant 11β-HSD1 from rat cDNA expressed in *Vaccinia* virus suggested that an important regulator of the reaction direction of 11β-HSD1 was the availability of cofactor (Agarwal *et al.*, 1990). In this system, addition of the cytosolic enzyme glucose-6-phosphate dehydrogenase (G6PDH), which converts $NADP^+$ to NADPH, increased reductase activity significantly. The potent effects of NADPH regeneration by G6PDH *in vitro* have since been demonstrated elsewhere (Bujalska *et al.*, 1999a) with *in vivo* studies also providing evidence that cofactor levels are an important regulator of 11β-HSD1 reaction direction (Ge *et al.*, 1997, Ferguson *et al.*, 1999, Bujalska *et al.*, 2002). However, due to the cytosolic location of G6PDH and the fact that pyridine nucleotides are generally believed not to cross cellular membranes, G6PDH is unlikely to perform this function *in vivo*. However a microsomal glucose dehydrogenase

exists (H6PDH) which is distinct from the cytosolic G6PDH (Beutler and Morrison, 1967). H6PDH is the first enzyme in the microsomal pentose phosphate pathway and has a broader substrate specificity than G6PDH, reducing not only the hexose-6-phosphates glucose-6-phosphate and galactose-6-phosphate, but also 2-deoxyglucose-6-phosphate and sugars such as glucose (Beutler and Morrison, 1967, Romanelli *et al.*, 1994). However, the physiological substrates are believed to be glucose-6-phosphate and $NADP^+$ (Kulkarni and Hodgson, 1982).

1.5.1. Structure and localization of H6PDH

The amino acid sequence for H6PDH was obtained for enzyme purified from rabbit liver microsomes (Ozols, 1993) and this allowed subsequent cloning and identification of the human and murine H6PDH cDNAs and genes (Mason *et al.*, 1999). Rabbit H6PDH is a 90-kDa protein, 763 amino acids in length with carbohydrate attached to both Asn-138 and Asn-263 (Ozols, 1993, Brands *et al.*, 1985). Although no transmembrane domain could be found, analysis of the amino acid sequence using SignalP clearly shows a the presence of a signal peptide, explaining the localization of H6PDH in the ER (Bendtsen *et al.*, 2004). Subsequent sequence comparisons between H6PDH and the enzymes of the cytosolic pentose phosphate pathway indicated that H6PDH had a high level of sequence similarity with not only G6PDH, but also with 6-phosphogluconolactonase (Hewitt *et al.*, 2005, Collard *et al.*, 1999). This suggested that H6PDH not only catalyzed the oxidation of glucose-6-phosphate but also the subsequent hydrolysis of 6-phosphogluconolactone (Figure 1.17). The bi-functional nature of H6PDH has subsequently been confirmed using purified native murine H6PDH (Mason *et al.*, 1999, Clarke and Mason, 2003). Although the bi-functional nature has not been proven for the human enzyme, a high level of sequence similarity between this enzyme and the murine form suggests that this is the case (Hewitt *et al.*, 2005).

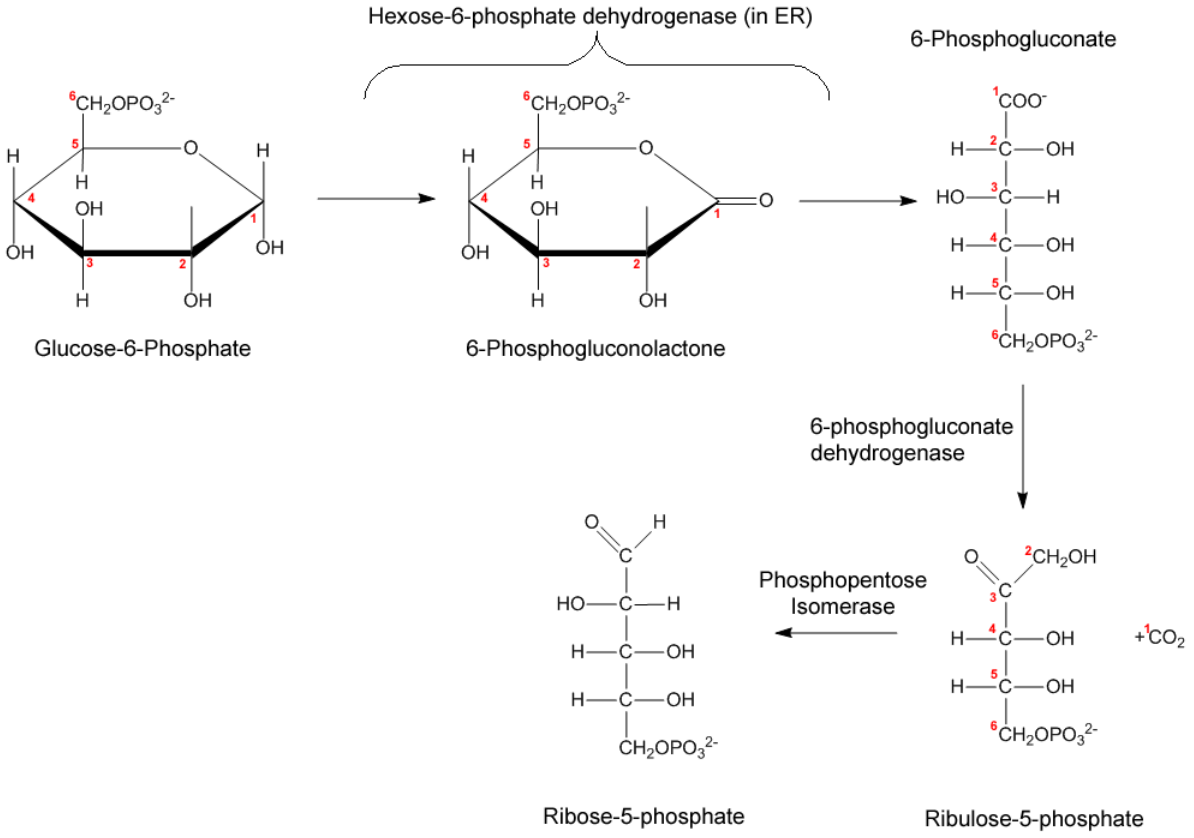

Figure 1.17. The oxidative stage of the pentose phosphate pathway in the cytosol. Also shown is the bi-functional nature of H6PDH in the ER. H6PDH can catalyze the first two steps of the microsomal pentose phosphate pathway. The N terminal domain oxidizes glucose-6-phosphate to 6-phosphogluconolactone, while the C terminal domain hydrolyses this product to 6-phosphogluconate.

Evidence for the role of H6PDH in NADPH regeneration, and therefore its role in promoting the reductase activity of 11β-HSD1, comes from a variety of *in vitro* and *in vivo* experiments. Firstly, a study by Atanasov *et al.* (2005) showed that expression of 11β-HSD1 in the ER lumen of human embryonic kidney (HEK)-293 or Chinese hamster ovary (Cho) cells showed it to have bidirectional activity, with a preference for the dehydrogenase direction (Atanasov *et al.*, 2004). However, a 5-fold increase in 11β-HSD1 reductase activity was seen when 11β-HSD1 was co-expressed with H6PDH. Co-expression also caused a 6-fold decrease in 11β-HSD1 dehydrogenase activity (Atanasov *et al.*, 2004). A second study by Bujalska *et al.*

(2005) supported these findings and showed in addition that the reductase activity of 11β-HSD1 was not affected by expression of the cytosolic G6PDH (Bujalska *et al.*, 2005). Finally, an *in vivo* study in mice demonstrated the potent activation of 11β-HSD1 reductase activity in intact hepatic microsomes by addition of the substrate for H6PDH, glucose-6-phosphate (Lavery *et al.*, 2006b). In the same study, it was shown that addition of glucose-6-phosphate to intact hepatic microsomes from a H6PDH KO mouse was unable to stimulate 11β-HSD1 reductase activity (Lavery *et al.*, 2006b), showing the requirement of H6PDH for 11β-HSD1 reductase activity. The potent effect of H6PDH on 11β-HSD1 activity is not just limited to the conversion of cortisone to cortisol, with 11β-HSD1 conversion of 7-keto-DHEA and 7-ketopregnenolone to their 7β-metabolites also dependent on the presence of H6PDH (Nashev *et al.*, 2007).

1.5.2. Direct interaction of H6PDH and 11β-HSD1

If estimates are to be believed, the ER lumen is an oxidative environment with a ratio of oxidized glutathione (GSSG) to reduced glutathione (GSH) of between 1 and 3 (Braakman *et al.*, 1992). Therefore, since it has been shown that efficient 11β-HSD1 reductase activity requires a 10-fold excess of NADPH over $NADP^+$ the ER lumen is either more reductive than thought or H6PDH and 11β-HSD1 interact in close proximity facilitating efficient 11β-HSD1 reductase activity (Dzyakanchuk *et al.*, 2009). A recent study has now shown via a combination of co-immunoprecipitation, Far-Western blotting and fluorescence resonance energy transfer (FRET) that 11β-HSD1 and H6PDH do interact directly in the ER lumen (Atanasov *et al.*, 2008). It was also shown that the 39 N-terminal amino acids of 11β-HSD1 were responsible for the direct interaction with H6PDH (Atanasov *et al.*, 2008). A further study using co-immunoprecipitation and purified recombinant protein has also demonstrated the direct interaction of H6PDH and 11β-HSD1 *in vitro* (Zhang *et al.*, 2009b). This protein-protein interaction between 11β-HSD1 and H6PDH is perhaps not surprising, as it provides a

direct coupling of intracellular glucose status, via glucose-6-phosphate, to glucose regulating hormones, such as cortisol. Due to the importance of H6PDH in conferring reductase activity to 11β-HSD1, it has been postulated that H6PDH could be a potential target of therapeutics aimed to decrease 11β-HSD1 activity (Atanasov *et al.*, 2008). This view has been given credence by studies which have demonstrated an adipose tissue specific increase in 11β-HSD1 and H6PDH expression both in obese rats (London *et al.*, 2007), and human patients who present with type 2 diabetes (Uckaya *et al.*, 2008).

1.5.3. Regulation of H6PDH activity

Just as levels of NADPH and cortisone regulate the activity of 11β-HSD1, the function of H6PDH is controlled via levels of its substrates, glucose-6-phosphate and $NADP^+$. Glucose-6-phosphate (G6P) is able to enter the ER via the glucose-6-phosphate transporter (G6PT) which transfers G6P from the cytosol to the lumen of the ER (Arion *et al.*, 1980a, Arion *et al.*, 1980b, Lange *et al.*, 1980) (Figure 1.19). It should be noted that another membrane bound enzyme, the glucose-6-phosphatase (G6Pase), competes with H6PDH for the G6P transferred into the ER (Foster *et al.*, 1997). It also interesting to note that both G6PT and G6Pase have been proposed as potential targets for the treatment of type II diabetes (Foster *et al.*, 1997). Interestingly, patients who present with glycogen storage disease type 1b, as a result of a deficiency in G6PT, display decreased 11β-HSD1 reductase activity, while those who present with glycogen storage disease type 1a with deficient G6Pase show increased 11β-HSD1 reductase activity (Walker *et al.*, 2007). Patients who present with glycogen storage disease type 1b are still able to reduce cortisone to cortisol to some extent, suggesting an alternative source for NADPH generation in the ER with some groups postulating that perhaps isocitrate dehydrogenase may carry out this role (Margittai and Banhegyi, 2008). However, the lack of signal peptide or a retention sequence makes in unclear how isocitrate dehydrogenase would

appear in the ER (Dzyakanchuk *et al.*, 2009). The microsomal G6PT-H6PDH-11β-HSD1 system is shown in Figure 1.18.

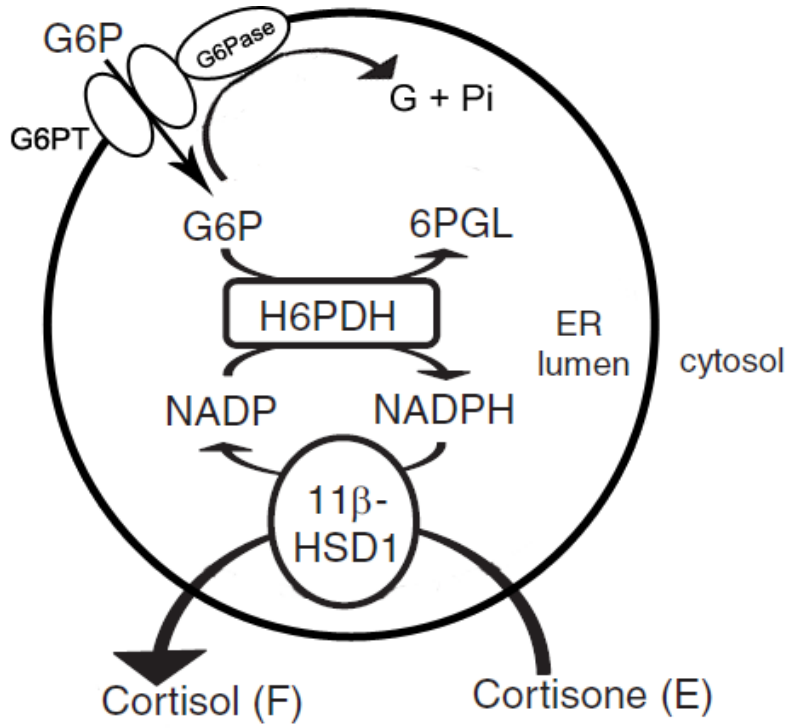

Figure 1.18. The G6PT-H6PDH-11β-HSD1 system in liver and adipose tissue. G6P enters the ER lumen via the specific G6PT and is converted to 6PGL via H6PDH, generating NADPH allowing 11β-HSD1 to convert cortisone to cortisol. 6PGL is further oxidized to 6-phosphogluconate by H6PDH. Also shown is the G6Pase, which competes for the G6P substrate. GP6 = glucose-6-phosphate, 6PGL = 6-phosphogluconolactone, G6PT = glucose-6-phosphate transporter, G = glucose, G6Pase = glucose-6-phosphatase. Adapted from Lavery *et al.* 2008.

1.6. 11β-HSD1, H6PDH and Cortisone Reductase Deficiency

In addition to the metabolic syndrome, diabetes and associated CVD, unusual activity of 11β-HSD1 is thought to be involved in a condition known as cortisone reductase deficiency (CRD). CRD is a disorder in which there is a failure to regenerate the active glucocorticoid cortisol (F) from cortisone (E) via 11β-HSD1 (Tomlinson *et al.*, 2004). A lack of cortisol regeneration stimulates ACTH-mediated adrenal hyperandrogenism (Figure 1.19), with males manifesting in adolescence with precocious pseudopuberty and females presenting in midlife with hirsuitism, oligoamenorrhoea, and infertility. Biochemically, CRD has been diagnosed through the assessment of urinary cortisol and cortisone metabolites, such as measuring the ratio of tetrahydrocortisol (THF) plus 5α-THF to tetrahydrocortisone (THE) (Figure 1.15). In CRD patients the ratio is typically lower than 0.1 (reference range 0.7–1.2) (Tomlinson *et al.*, 2004).

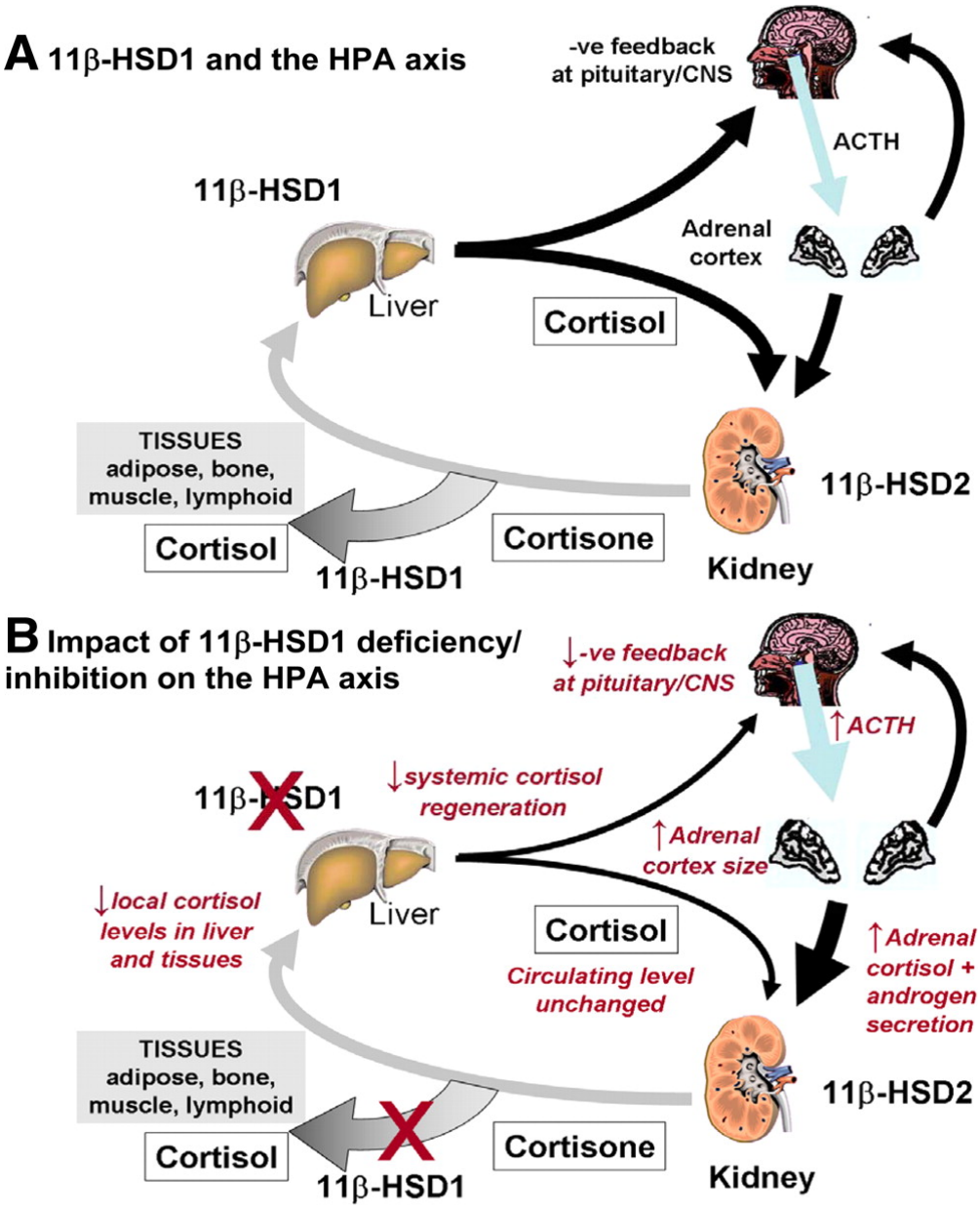

Figure 1.19. The possible involvement of 11β-HSD1 in the pathogenesis of CRD. A – Normal function of11β-HSD1 in the HPA axis. Cortisol is regenerated from cortisone in liver and peripheral tissues which contributes to the total amount of cortisol in circulation. B - Defective 11β-HSD1 activity would lead to a decrease in peripheral cortisol regeneration. Increased synthesis of ACTH ensures the maintenance of circulating cortisol via increased cortisol synthesis by the adrenal gland. This is at the expense of androgen excess. Taken from Cooper *et al.* 2009.

CRD was first described nearly 30 years ago (Taylor *et al.*, 1984) with patients unable to convert cortisone to cortisol due to a deficient 11βHSD activity. Until 2008, eleven individuals have been described (Taylor *et al.*, 1984, Savage, 1991, Nikkila *et al.*, 1993,

Phillipov *et al.*, 1996, Jamieson *et al.*, 1999, Nordenstrom *et al.*, 1999), with the *HSD11B1* gene of seven of the CRD kindreds analyzed. Although no functional mutations were found on the *HSD11B1* gene, analysis revealed an A insertion and a T-G substitution in intron 3 in some patients. This 83557A/83597T-G haplotype was seen to be associated with a 28-fold reduction in 11β-HSD1 mRNA in adipose tissue with complete loss of reductase activity indicating a potential biomarker for CRD. However, due to the heterozygous presence of this locus in 25% of normals and homozygous presence in 3% of normals, these mutations cannot account for the CRD phenotype (Draper and Stewart, 2005). It was also proposed that the A insertion in the *HSD11B1* gene, may act together with a R453Q mutation in the *H6PD* gene and that this might be a cause of CRD (Draper *et al.*, 2003). However, this theory has also been disproven (Smit *et al.*, 2006, Draper *et al.*, 2006, San Millan *et al.*, 2005, Lavery *et al.*, 2008). A more recent study has now revealed four novel homozygous mutations in the *H6PD* gene associated with defective 11β-HSD1 activity, all without mutations in the *HSD11B1* gene (Lavery *et al.*, 2008). The first of these (Case A in Figure 1.20) was a homozygous c.325delC mutation (i.e. the C at position 325 was deleted) on exon 2 which resulted in a frame shift, truncating H6PDH by 781 amino acids (Figure 1.20). The second (Case B in Figure 1.20) was a homozygous c.948C>G mutation in exon 4, which caused H6PDH to be truncated by 575 amino acids due to the introduction of a stop codon (Y316X) (Figure 1.20). Third, a homozygous c.1076G>A mutation in exon 5, resulting in G359 missense mutation (Case C in Figure 1.20). Finally, Case D was compound heterozygous for a maternally inherited c.1860ins29bp insertion mutation in exon 5 and a paternally inherited c960G>A mutation in exon 4. The c.1860ins29bp insertion mutation would generate both a frame shift and an in-frame stop codon, with the resulting H6PDH protein truncated by 268 amino acids (D620fsX3). The generation of a strong donor splice site consensus sequence from the c960G>A mutation results in two products. One in which mRNA is truncated by 54-

nucleotides with the resultant protein missing 18 amino acids, and another in which intron 4 is retained. (Figure 1.20). When expressed in HEK-293 cells, all mutant H6PDH proteins were inactive with a subsequent loss of 11β-HSD1 reductase activity within the cells (Lavery *et al.*, 2008). These mutations therefore result in apparent cortisol reductase deficiency (ACRD) as 11β-HSD1 reductase activity has been affected indirectly. Since it has been shown that H6PDH KO mice not only lose 11β-HSD1 reductase activity (Lavery *et al.*, 2006b), but show an increase in dehydrogenase activity, it has been postulated that ACRD patients (with defective H6PDH) would have a more severe biochemical phenotype than those with simple CRD (defective in 11β-HSD1). The mutations involved in CRD/ACRD are summarised in Table 1.3.

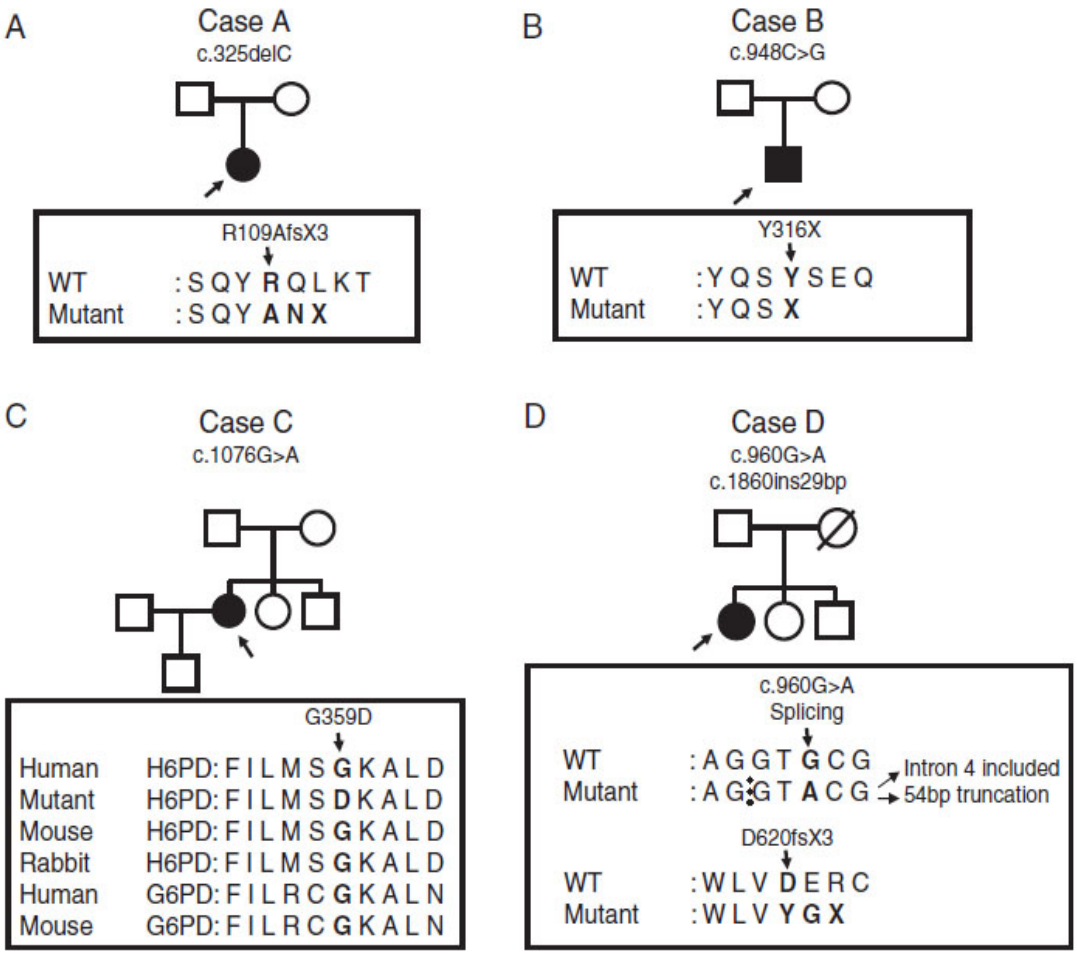

Figure 1.20. *H6PD* gene mutations which give rise to ACRD. Family pedigree and the alteration in both nucleotide and protein are shown. Mutations to the *H6PD* gene in cases A and B results in a severely truncated protein, while mutation to the *H6PD* gene in Case C causes a G359D missense mutation. Case 4 had a H6PDH protein which was truncated by 268 amino acids (D620fsX3) as a result of being heterozygous for a maternally inherited c.1860ins29bp mutation in exon 5 and a paternally inherited c.960G→A mutation in exon 4. All mutants, when expressed in HEK-293 cells, were inactive. Taken from Lavery *et al.* (2008a).

Mutation	Gene	Coding	Effect on Activity	Significant in CRD/ACRD?	Reference
83557A	*HSD11B1*	No	None	No	(Draper and Stewart, 2005)
83597T-G	*HSD11B1*	No	None	No	(Draper and Stewart, 2005)
Y316X	*H6PD*	Yes	Null	Yes	(Lavery *et al.*, 2008)
R109AfsX3	*H6PD*	Yes	Null	Yes	(Lavery *et al.*, 2008)
G359D	*H6PD*	Yes	Null	Yes	(Lavery *et al.*, 2008)
D620fsX3	*H6PD*	Yes	Null	Yes	(Lavery *et al.*, 2008)
R453Q	*H6PD*	Yes	None	No	(Mason *et al.*, 1999)

Table 1.3. Mutations which have been postulated to be involved with CRD and ACRD.

1.7. Short Chain Dehydrogenase/Reductases

The 11β-HSD1/11β-HSD2 enzymes are both members of the short chain dehydrogenase/reductase family of enzymes (SDRs). This class of enzymes was first discovered when functional differences were noted between sect-type and liver-type alcohol dehydrogenases, which correspond to the SDR and medium chain dehydrogenase/reductases (MDRs) families respectively (Jornvall *et al.*, 1981). One such difference was the binding of dinucleotide cofactor which, in contrast to pro-R' hydride transfer observed in MDRs, binds in an extended conformation which allowes pro-S' hydride transfer (Kavanagh *et al*., 2008). While SDRs primarily interconvert hydroxyl and carbonyl groups, SDR enzymes are also able to mediate dehydratase, isomerase, decarboxylation and sulphotransferase reactions and also catalyze the reduction of C=C and C=N double bonds (Figure 1.21) (Oppermann *et al.*, 2003). There are over 20,000 SDR depositions in sequence databases, with 71 distinct SDR enzymes reported in humans (Kavanagh *et al.*, 2008). The number of human SDRs doubles if variant enzymes are included due to differential splicing and related isoforms (Kavanagh *et al.*, 2008).

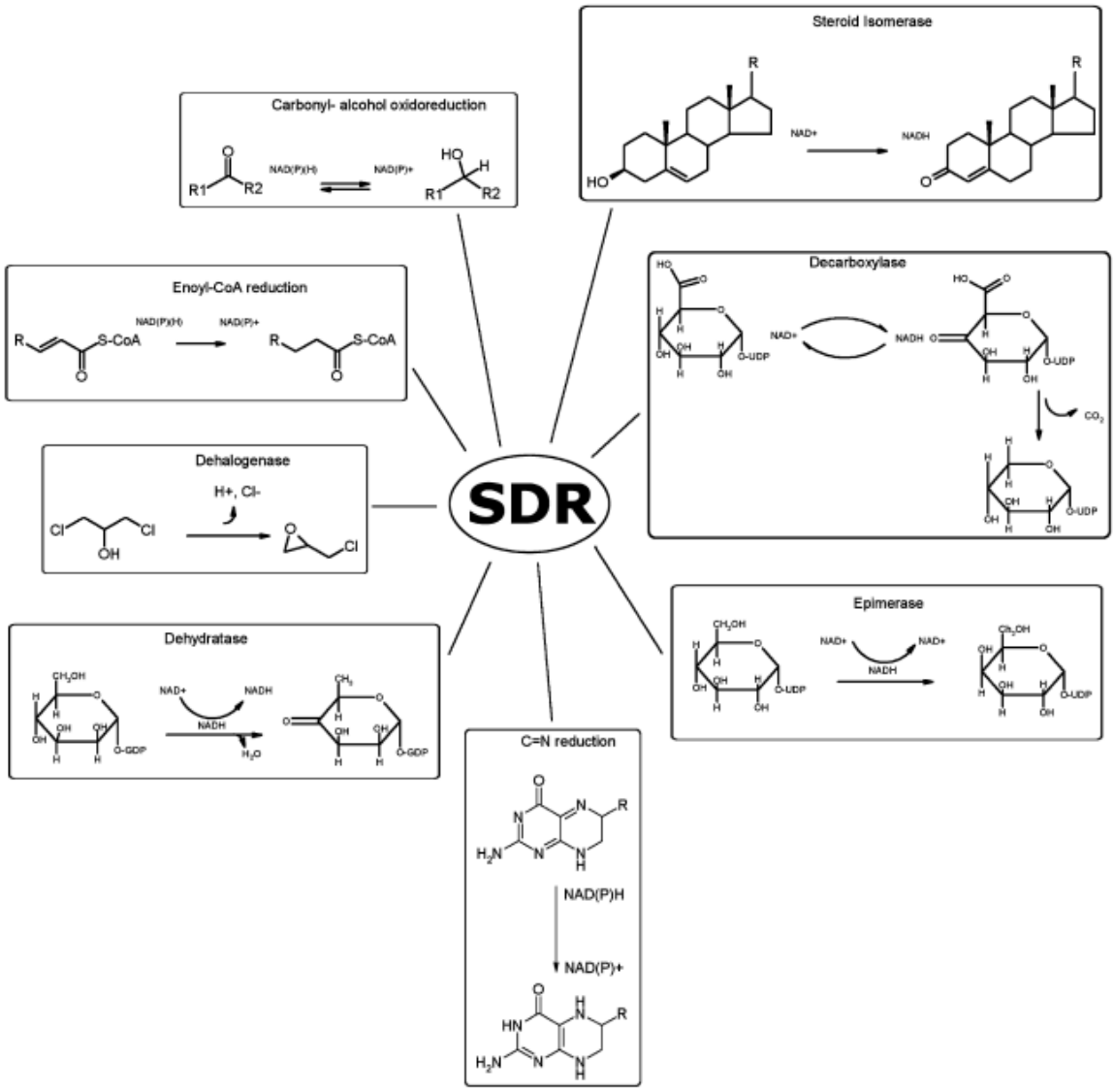

Figure 1.21. The various reactions catalyzed by SDR enzymes. Taken from Kavanagh *et al.* (2008).

The family of SDR enzymes are often not that closely related, with an amino acid homology of typically around 15-30%. However, all solved structures possess a Rossmann fold which consists of a central β-sheet flanked by α-helices which is common in the oxidoreductase class of enzyme (Jornvall *et al.*, 1995, Oppermann *et al.*, 2003) (Figure 1.22). The amino and carboxy termini of the SDRs are typically important for function with signal peptides or transmembrane domains sometimes associated with them (Jornvall *et al.*, 1995, Oppermann *et al.*, 2003).

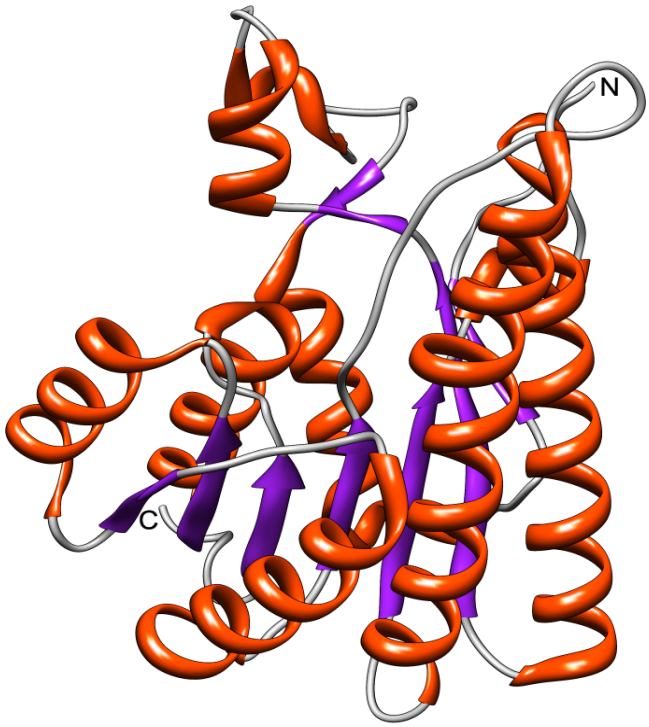

Figure 1.22. Ribbon diagram displaying the Rossmann fold of a monomer of 3α/17βHSD (PDB code 1xhx). All solved structures of the SDR family possess the Rossmann fold, which consists of a central β-sheet (blue) flanked by α-helices (red). N = N-terminus, C = C-terminus. Image produced using UCSF Chimera.

As with any protein family, SDRs have a number of sequence motifs which are conserved to different degrees. A well conserved N-terminal T-G-X-X-X-G-X-G motif constitutes the majority of the nucleotide binding region by forming a cleft in which the cofactor can bind (Figure 1.23) (Oppermann *et al.*, 2003). The motif is also involved with the maintenance of the central β-sheet (Oppermann *et al.*, 1997, Filling *et al.*, 2002). Another well conserved motif is the N-N-A-G motif which is also involved with maintenance of the central β-sheet (Oppermann *et al.*, 1997, Filling *et al.*, 2002). A P-G motif can also be involved in co-factor binding (Filling *et al.*, 2002). In addition, a relatively well conserved T residue is also involved in hydrogen bonding to the carboxamide of the nicotinamide ring of cofactor (Oppermann *et al.*, 1997).

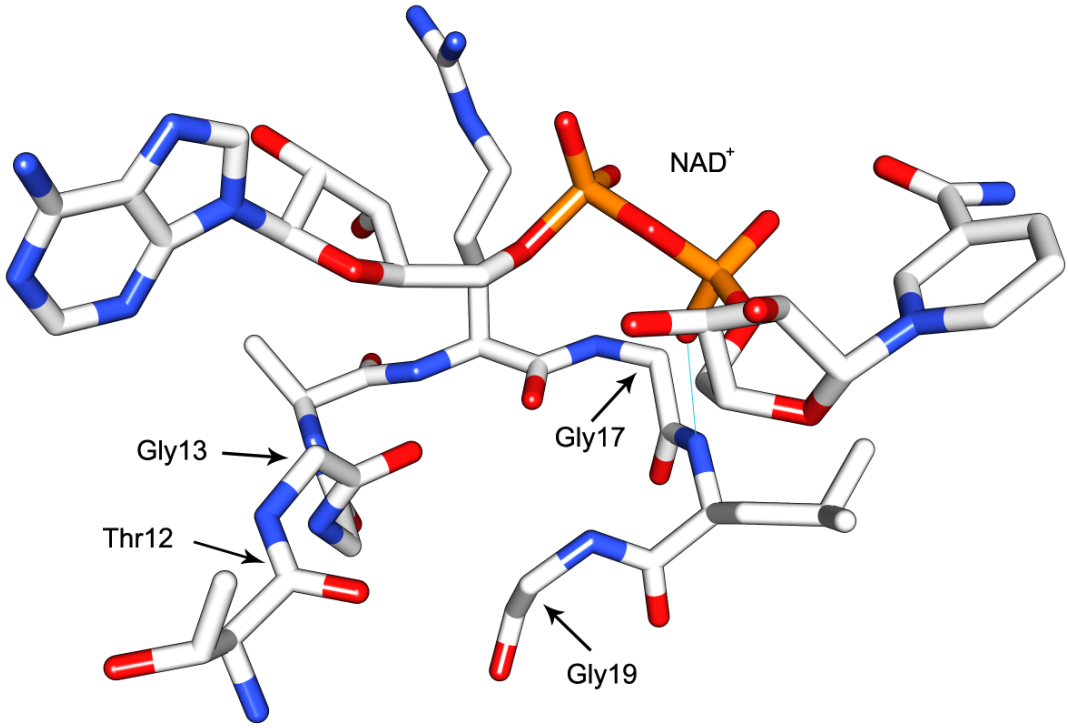

Figure 1.23. The N-terminal T-G-X-X-X-G-X-G motif involved with binding cofactor, in this case NAD^+, in the SDR family member 3α /20β-HSD (PDB code 2HSD). This motif is highly conserved across the SDR superfamily of proteins and is also involved with maintenance of the central β-sheet. Hydrogen bonds are indicated by the blue lines. Image produced using UCSF Chimera.

However, the most conserved of these motifs is the N-S-Y-K catalytic tetrad. It was originally thought that the catalytic mechanism of SDRs involved a catalytic triad of S-Y-K with the tyrosine working as the catalytic base, the serine stabilizing the substrate and lysine interacting with the nicotinamide ring of the ribose and lowering the pK_a of the Tyr-OH, promoting proton transfer (Jornvall *et al.*, 1995). This was similar to the mechanism observed in horse liver dehydrogenase (Liao *et al.*, 2001, Eklund *et al.*, 1982). However, inspection of the related *Drosophila* alcohol dehydrogenase structure suggested that an additional interaction existed between a conserved Asn residue, via a water molecule, with the active site Lys (Benach *et al.*, 1998). This was then subsequently shown in the 3β/17β-HSD structure and other SDR structures, which suggests this critical Asn has an analologous role in positioning the conserved water molecule in SDR catalysis (Figure 1.24) (Filling *et al.*,

2002). It is important to note here that some SDRs, instead of the critical Asn, have a Ser residue which acts in a similar way (Filling *et al.*, 2002). The completion of this proton relay system is critical in maintaining the position of the active site Lys.

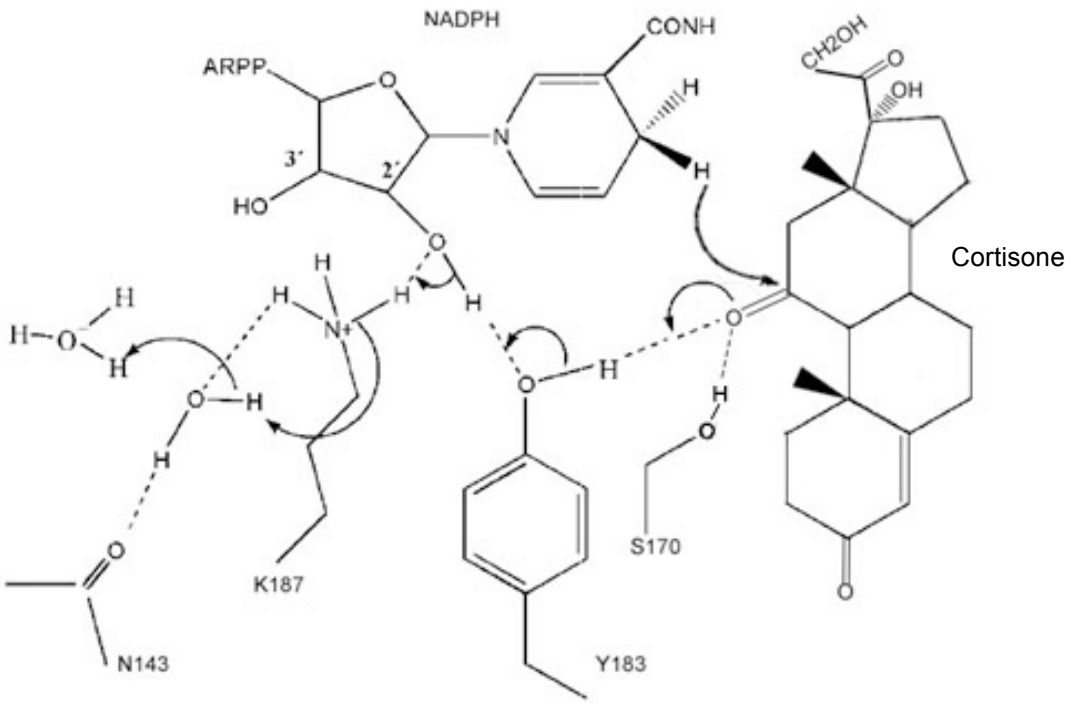

Figure 1.24. The catalytic mechanism of 11β-HSD1 and other "classical" SDRs. Catalysis is started by the transfer of a proton from Tyr-183 hydroxyl to the C-11 carbonyl group of cortisone. This is followed by hydride transfer to the C-11 of cortisone. A proton relay system involving the Tyr-183, 2'-OH of the nicotinamide ribose, a conserved Lys and a conserved water molecule is then formed. This conserved water molecule is positioned by the critical Asn residue. Residue numbering refers to the guinea pig enzyme. *ARPP*, the adenosine ribose pyrophosphate moiety. Adapted from Filling *et al.* (2003).

SDRs can vary in size, function and also in the motifs present. Using these differences, SDRs can be classified into five families 'classical', 'extended', 'intermediate', 'divergent' and 'complex' (Persson *et al.*, 2003). The motifs discussed above all refer to the 'classical' SDR family, to which 11β-HSD1 belongs. The 'classical' and 'extended' SDRs include similar motifs but differ in function and size, acting as either a ca 250 residue dehydrogenase or reductase ('classical') or a ca 350 residue isomerase, epimerase, dehydratase or lyase

('extended') (Persson *et al.*, 2003). The unusual activities of 'extended' SDRs are explained by the coupling of thsese activites to an initial reductive step on specific substrates. The NAD(P)(H) nucleotide cofactor dependence and conservation of active site residues when compared to 'classical' SDRs further emphasize the absence of any additional enzymatic steps in 'extended' SDRs. Examples of 'extended' SDRs include UDP-galactose epimerase, 3β-hydroxy-5ene-steroid isomerase and GDP-mannose dehydratase. The 'intermediate' family of SDRs are closely related in sequence to the 'classical' SDRs with the exception of a G/AxxGxxG/A nucleotide binding motif similar to that seen in extended SDRs (Table 1.4) (Persson *et al.*, 2003). Interestingly, in addition to changes to nucleotide binding regions, both 'divergent' and 'complex' SDRs have different active site motifs to the more common YxxxK observed in most SDRs i.e. YxxMxxxK in divergent SDRs and YxxxN in complex SDRs (Table 1.4) (Persson *et al.*, 2003). Despite this change, the Y and K side chains in 'divergent' enzymes are close in space and similarly spaced to those in 'classical' SDRs. However, due to the function of this class of enzymes (enoyl-thioester reductases involved in fatty acid metabolism) and the fact that proton is donated directly from solvent, not from the active site tyrosine residue, implies that different catalytic mechanisms are present in this class of SDRs. In contrast to the 'divergent' enzymes, if the three-dimensional structures of 'complex' SDRs are examined (e.g. the ACP-ketoacyl reductase domain of *Streptomyces* erythromycin synthase) all of the catalytic machinery i.e. the N, S, Y and K residues, while not close in sequence, are similarly spaced to those in 'classical' SDRs, implying they may function in a similar manner.

Subfamily	Cofactor binding	Active site
‘classical’	TGxxx[AG]xG	YxxxK
‘extended’	[ST]GxxGxxG	YxxxK
‘intermediate’	[GA]xxGxx[GA]	YxxxK
‘divergent’	GxxxxxSxA	YxxMxxxK
‘complex’	GGxGxxG	YxxxN

Table 1.4. Active site and cofactor binding site sequence motifs for the five SDR families. Takem from Kavanagh *et al,* (2008).

1.8. Structural studies of 11β-HSD1

For a protein whose substrate has such wide-reaching applications in medicine, only suprisingly recently have high resolution structures of 11β-HSD1 become available. This is primarily due to the fact that, in contrast to most other members of the SDR family, 11β-HSD1 is a glycosylated, membrane-bound protein making isolation of full length protein a difficult, although not impossible, task (Hult *et al.*, 2001, Nobel *et al.*, 2002). Since the crystallization of membrane-bound proteins has a low success rate (Newman, 1996), recombinant human 11β-HSD1 which has the N-terminal transmembrane domain removed has been engineered (Walker *et al.*, 2001a). Following expression of this construct in bacteria, 11β-HSD1 can be purified to a relatively high level of homogeneity and monodispersity, essential factors for crystallography (Walker *et al.*, 2001a). At the time of writing, 23 structures of recombinant N-terminally truncated 11β-HSD1 have been deposited in the PDB. The key features of these structures are listed in Table 1.5. A comparison of the guinea pig (1XSE), mouse (1Y5M) and human (2BEL) enzyme structures is shown in Figure 1.25. It can clearly be seen (Figure 1.25) that the mouse, guinea pig and human (2BEL) enzyme structures are very similar. Therefore, although the following description is for the human (1XU9) structure, solved to 1.55Å, most elements may be applied to the guinea pig and murine structures.

PDB Code	Species	Resolution (Å)	R	R_{free}	Ligand	Reference
2BEL	Human	2.11	0.190	0.246	CBX, $NADP^+$	(Wu *et al.*, 2007)
1XU7	Human	1.80	0.198	0.217	CPS, $NADP^+$	(Hosfield *et al.*, 2005)
1XU9	Human	1.55	0.158	0.181	CPS, $NADP^+$	(Hosfield *et al.*, 2005)
3CZR	Human	2.35	0.221	0.247	CPS, 3CZ $NADP^+$	(Sun *et al.*, 2008)
3BZU	Human	2.25	0.204	0.263	A21, $NADP^+$	(Hale *et al.*, 2008)
2ILT	Human	2.30	0.212	0.275	NN1, $NADP^+$	(Sorensen *et al.*, 2007)
2RBE	Human	1.90	0.219	0.264	ZMG, $NADP^+$	(Yuan *et al.*, 2007)
3BYZ	Human	2.69	0.222	0.293	H11, $NADP^+$	Johansson *et al*, to be published
3CH6	Human	2.35	0.188	0.230	311, $NADP^+$	(Wang *et al.*, 2008)
2IRW	Human	3.10	0.239	0.278	NN4, $NADP^+$	(Patel *et al.*, 2007)
3D5Q	Human	2.55	0.232	0.265	T30, $NADP^+$	(Tu *et al.*, 2008)
3D4N	Human	2.50	0.228	0.259	D4N, $NADP^+$	(Julian *et al.*, 2008)
3D3E	Human	2.60	0.230	0.283	D3E, $NADP^+$	(Julian *et al.*, 2008)
3FCO	Human	2.65	0.224	0.254	IIG, $NADP^+$	(McMinn *et al.*, 2009)
3H6K	Human	2.19	0.194	0.275	33T, $NADP^+$	(Wan *et al.*, 2009)
3HFG	Human	2.30	0.234	0.285	17R, $NADP^+$	(Wan *et al.*, 2009)
3FRJ	Human	2.30	0.210	0.243	A49,$NADP^+$	(Rew *et al.*, 2009)
3EY4	Human	3.00	0.219	0.319	352, $NADP^+$	Christopher *et al*, to be published
1Y5R	Mouse	3.00	0.210	0.247	Corticosterone $NADP^+$	(Zhang *et al.*, 2005)
1Y5M	Mouse	2.30	0.219	0.250	$NADP^+$	(Zhang *et al.*, 2005)

1XSE	Guinea Pig	2.50	0.196	0.267	$NADP^+$	(Ogg *et al.*, 2005)
3G49	Guinea Pig	2.50	0.191	0.225	3G4, $NADP^+$	(Siu *et al.*, 2009)
3DWF	Guinea Pig	2.20	0.200	0.255	$NADP^+$	(Lawson *et al.*, 2009)

Table 1.5. Comparison of the 23 11β-HSD1 structures in the pdb database. CBX = Carbenoxolone; CPS = 3-[(3-cholamidopropyl)dimethylammonio]-1-propanesulfonate (a steroidal detergent); NN1 = adamantane sulfone inhibitor; 3CZ, 17R, 3G4 = arylsulphonyl-piperazine inhibitors; H11, ZMG = 2-anilinothiazolone inhibitors; A21 = thiazolone inhibitor; 311 = pyridine amide inhibitor; T30 = triazole inhibitor; 352 = thialozone inhibitor; D4N = sulfonamide inhibitor; D3E, IIG, 33T, A49 = benzamide inhibitors.

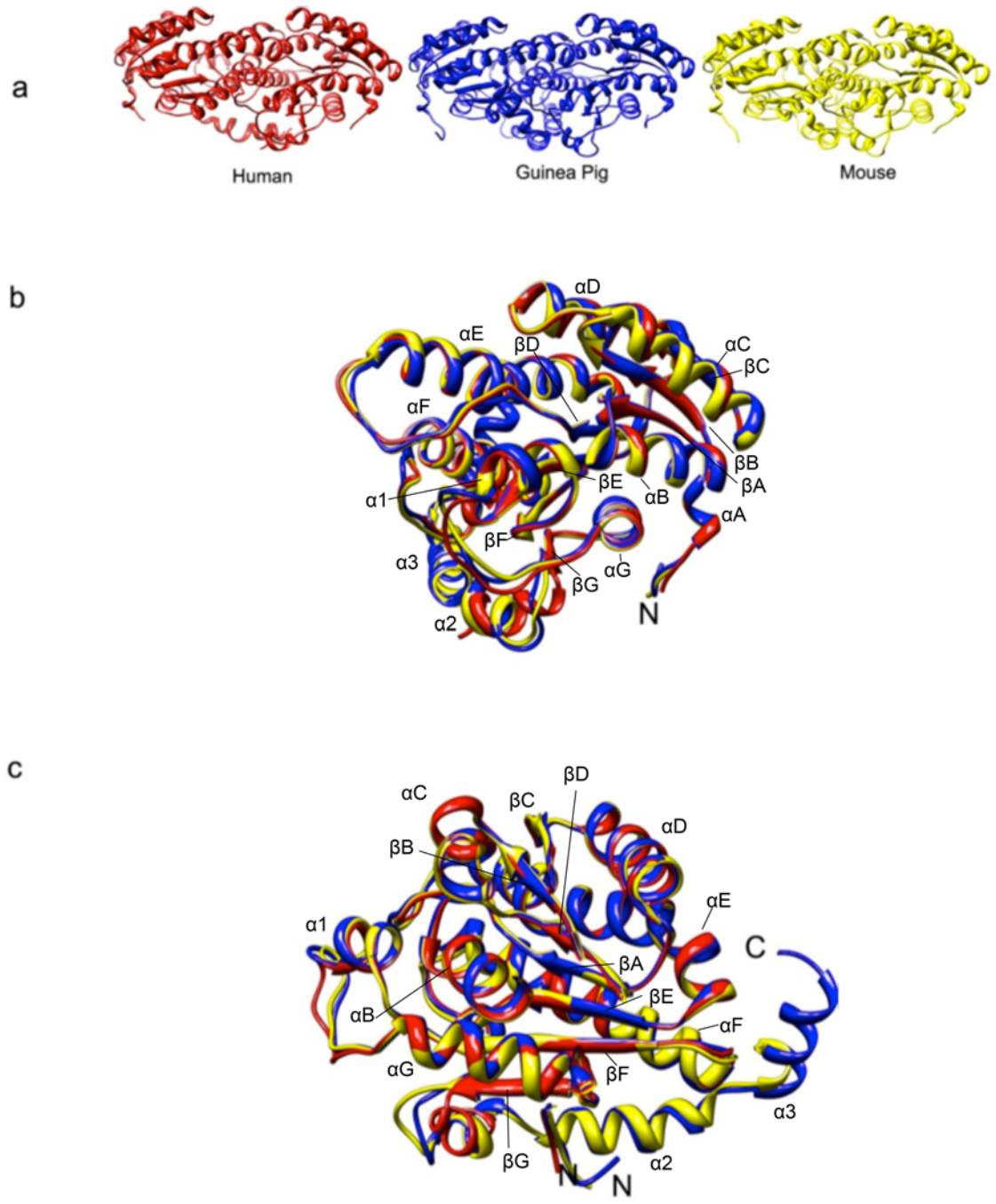

Figure 1.25. A comparison of the crystal structures of 11β-HSD1 from different species. **a** – Ribbon representation of human (2BEL), guinea pig (1XSE) and mouse (1Y5M) 11β-HSD1 dimers**. b** – Superimposition of human (red), guinea pig (blue) and mouse (yellow) monomers. **c** – The superimposition in b rotated 90^{o}. Note the varying lengths of the C-terminal helix in c, with the guinea pig helix longer than both the mouse and human. This extension (α2 & α3) is specific to 11β-HSD1 when compared to other SDRs. The dimerisation domain is made up of helices αE, αF, α2 and α3. N = N-terminus, C = C-terminus. Images produced using the UCSF Chimera package (Pettersen *et al.*, 2004).

The crystal structure of 11β-HSD1 confirmed that the protein existed as a homodimer with each monomer possessing a Rossmann fold, with the monomer described below. The central β- sheet which makes up the Rossmann fold, is made up from 7 β-strands (βA – βG) with 3 helices on each side (αB, αC, αG on one side and αD, αE, αF on the other) completing the fold (Figure 1.26). In addition, a double turn α-helix designated α-1, exists between βF and αG and forms a 'lid' over the substrate-binding pocket. Unsurprisingly, this central scaffold is highly similar (about 2Å RMSD) to most other SDRs such as porcine carbonyl reductase (1DOH), human estradiol 17β-hydroxysteroid dehydrogenase type I (1BHS) and *E.coli* 7α-hydroxysteroid dehydrogenase (1AHI). A topology diagram of the human 11β-HSD1 structure is shown in Figure 1.26. The annotated amino acid sequence is shown in Figure 1.27.

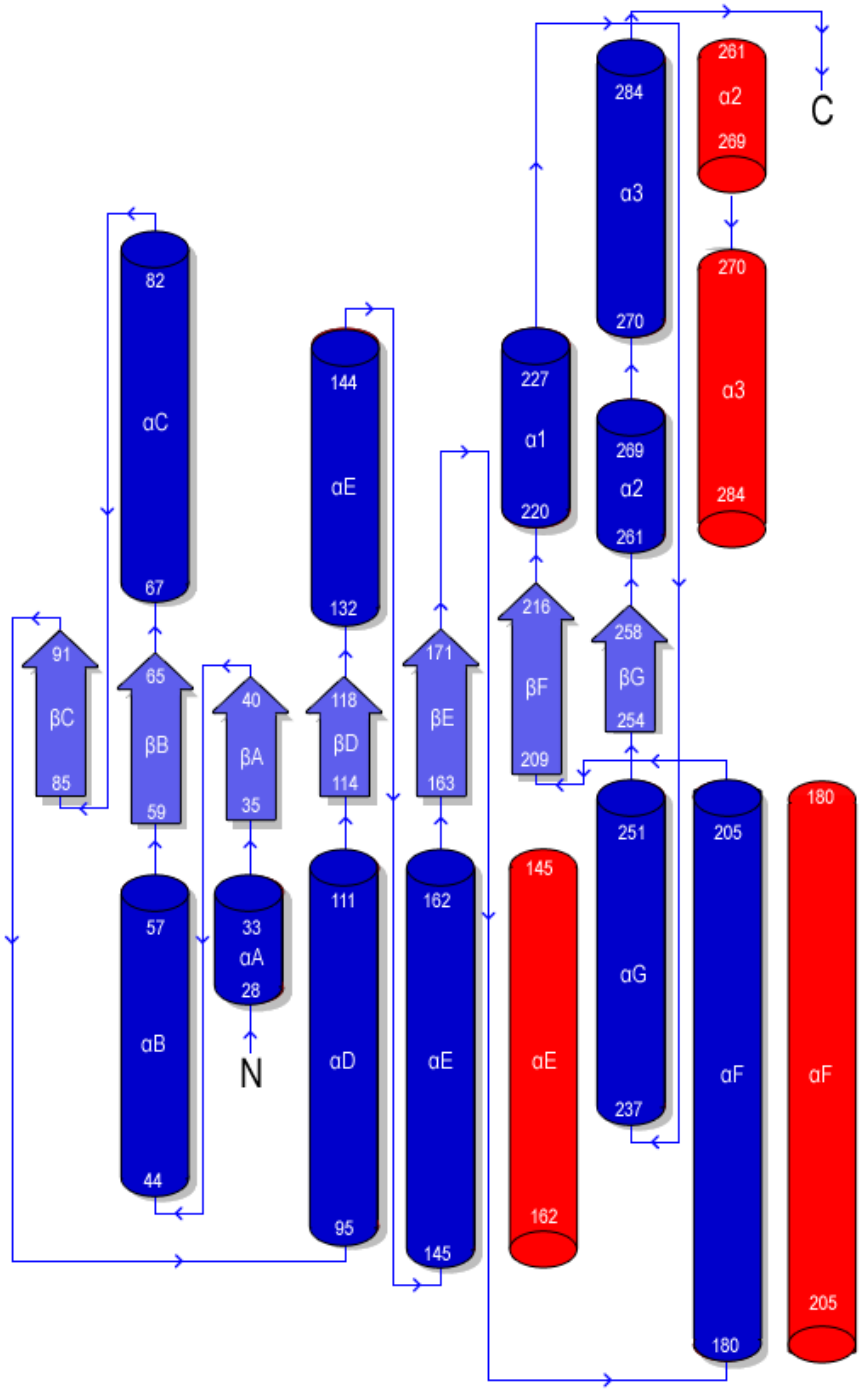

Figure 1.26. A topology diagram of human 11β-HSD1 (1XU9) coloured according to secondary structure. Dark blue cylinders = α helix, light blue arrows = β strand. The red cylinders represent helices from the corresponding monomer which make up the dimerisation domain. Image produced using PDBsum.

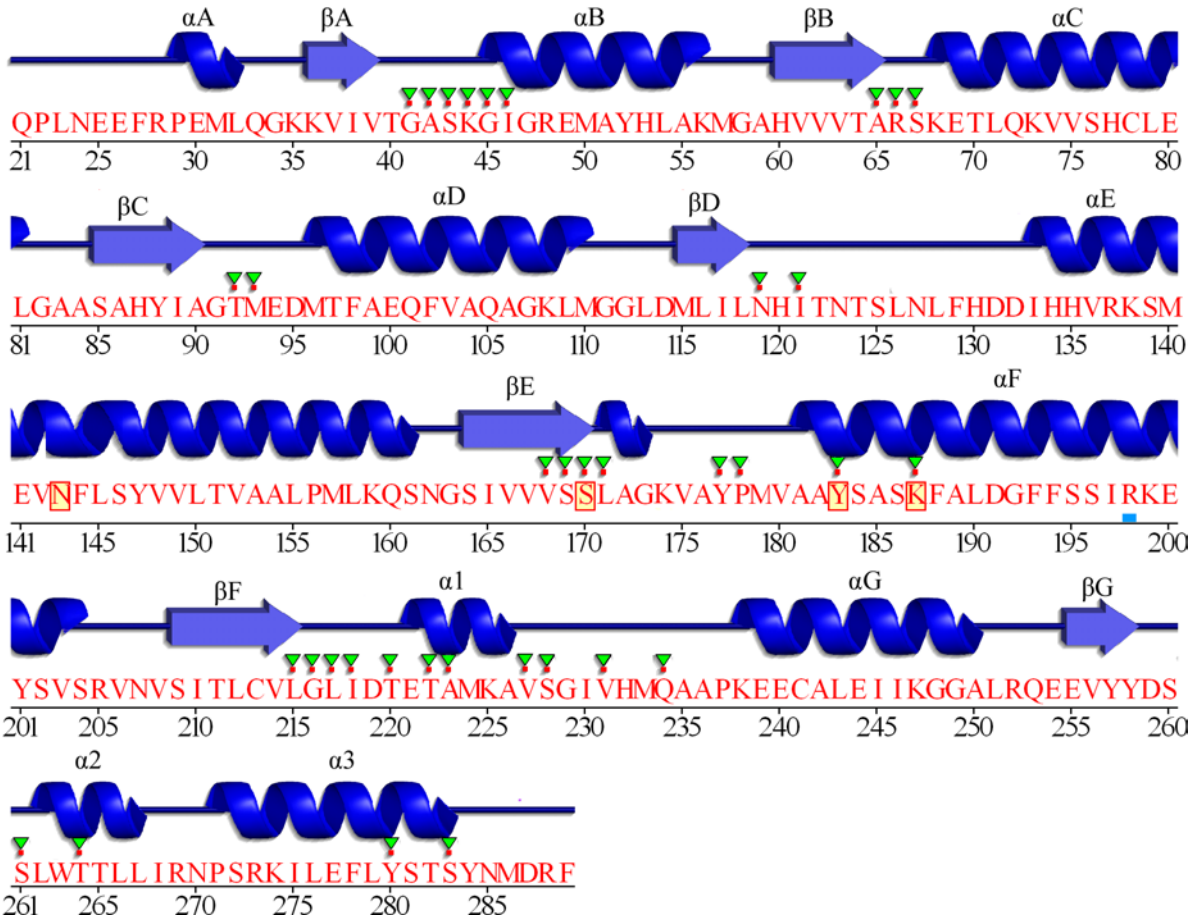

Figure 1.27. The amino acid sequence of human 11β-HSD1 aligned with secondary structure. α -helices are shown by the dark blue helical structure with β-strands shown by the light blue arrows. Catalytic residues are highlighted by a yellow box with residues which interact with co-factor shown by the green arrows and red dots. Image produced using PDBsum.

If the position of bound steroid and cofactor in the structure of human 11β-HSD1 is analysed (1XU9), it is clear that cofactor binds to residues towards the N-terminus (i.e. the 'top' of 11β-HSD1) while steroid will bind to the residues towards the C-terminus (i.e. the 'bottom' of 11β-HSD1) (Figure 1.28). The positioning of these binding sites could be important due to the position of 11β-HSD1 with respect to the ER membrane (discussed later). The central fold of 11β-HSD1 also contains many motifs and features associated with SDRs. The structure confirmed the presence of the N-S-Y-K catalytic tetrad (Figure 1.29), T-G-X-X-X-G-X-G motif (residues 40-45), an equivalent P-G motif (L-G, residues 215 & 216 in 11β-

HSD1) involved in cofactor binding and a N-K-V-N motif which is equivalent to the I-R-V-N motifs seen in other SDRs (Filling *et al.*, 2002, Ogg *et al.*, 2005).

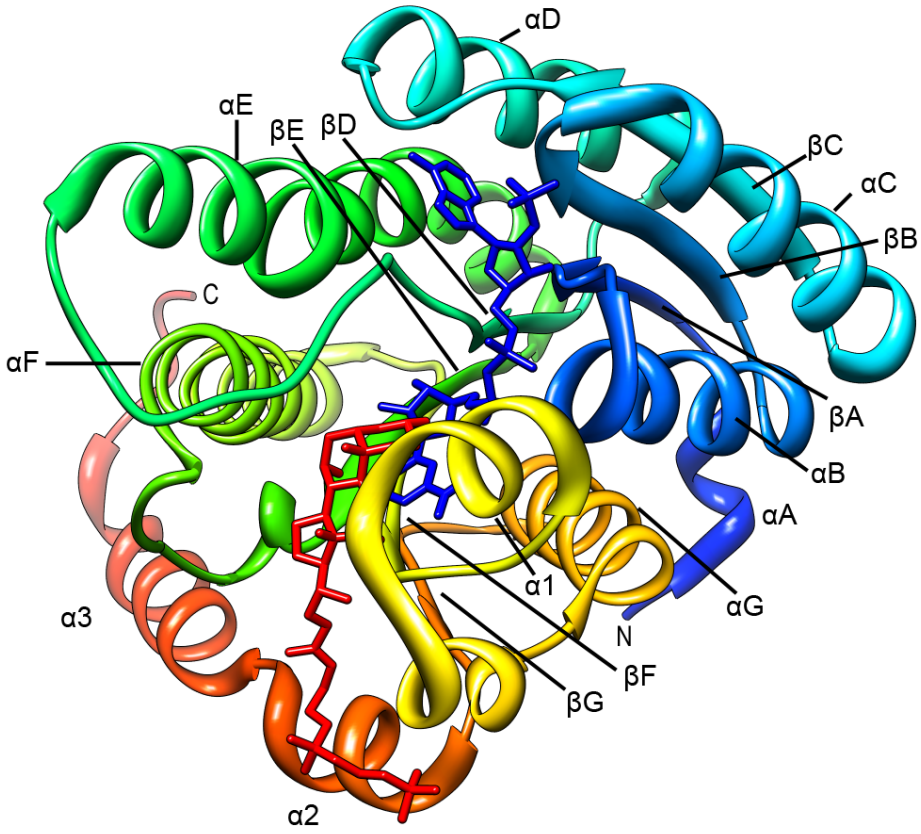

Figure 1.28. Ribbon representation of a monomer of human 11β-HSD1 (1XU9) using a colour gradient from blue (residues near the N-terminus) to red (residues near the C-terminus). The cofactor, NADP+, is coloured blue while the steroidal detergent, CHAPS, which is located in the active site in place of substrate, is coloured red. It can be seen that the cofactor and steroid are surrounded by blue/green and red/yellow residues respectively, illustrating the N-terminal location of the cofactor binding region and the C-terminal location of the substrate binding region. Image produced using UCSF Chimera.

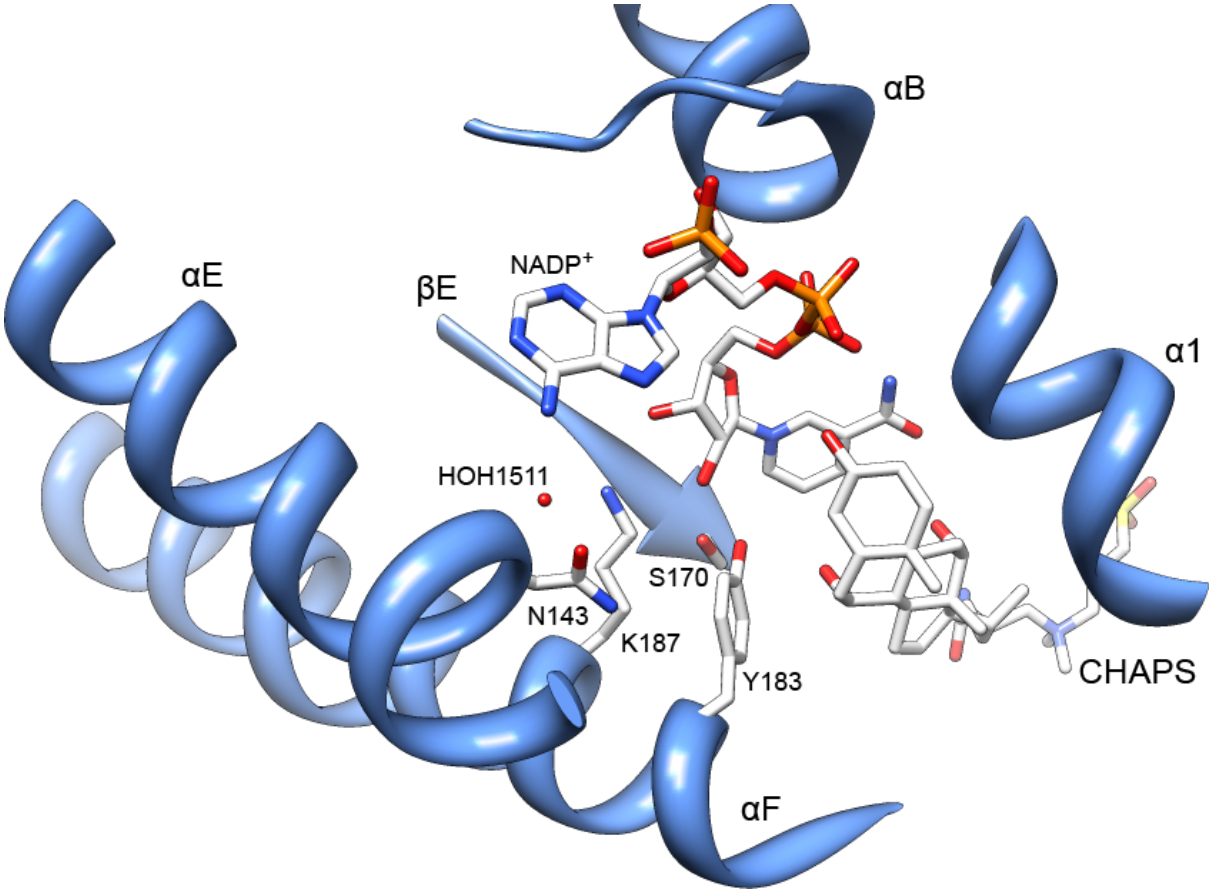

Figure 1.29. The N-S-Y-K active site of 11β-HSD1 (1XU9). The mechanism is a proton relay system involving the Tyr-OH, the 2'-OH of the nicotinamide ribose, a conserved Lys (K187) and a conserved water molecule. This conserved water molecule (HOH1511) is positioned by the critical Asn (N143) residue. Structure shows bound $NADP^+$ and the steroidal detergent, CHAPS. Image produced using UCSF Chimera.

However, 11β-HSD1 does show a striking difference to other SDR structures at the C-terminus. The last 2 helices (α2 and α3) protrude and form a long structure which packs against the C-terminus of the other subunit in an antiparallel conformation, extending the dimerization interface formed by helices αE and αF (Figure 1.30). This results in a total dimer interface of 2502.7 $Å^2$. This is unusual, as although some cases exist (Blankenfeldt *et al.*, 2002), most dimeric SDRs have a dimerization interface that involves only helices E and F (Powell *et al.*, 2000, Hoque *et al.*, 2008, Ghosh *et al.*, 1991, Tanaka *et al.*, 1996). Interestingly, a R137 residue, which is conserved across 11β-HSD1 proteins from different species, is present on helix αE of one subunit (A), positioned at the edge of the dimer

interface and forms a salt bridge with the highly conserved residue E141 on the other subunit (B). A corresponding interaction between R137 on the B subunit and E141 on the A subunit forms a second bridge. Salt bridges, particularly those involving arginine are known to have a prominent role in inter-subunit interactions in proteins (Musafia *et al.*, 1995) promoting correct orientation of the subunits during dimer formation in addition to stabilizing the final assembly (Vijayakumar *et al.*, 1998, Gabdoulline and Wade, 2001). The importance of this salt bridge is discussed in more detail in Chapter 3.

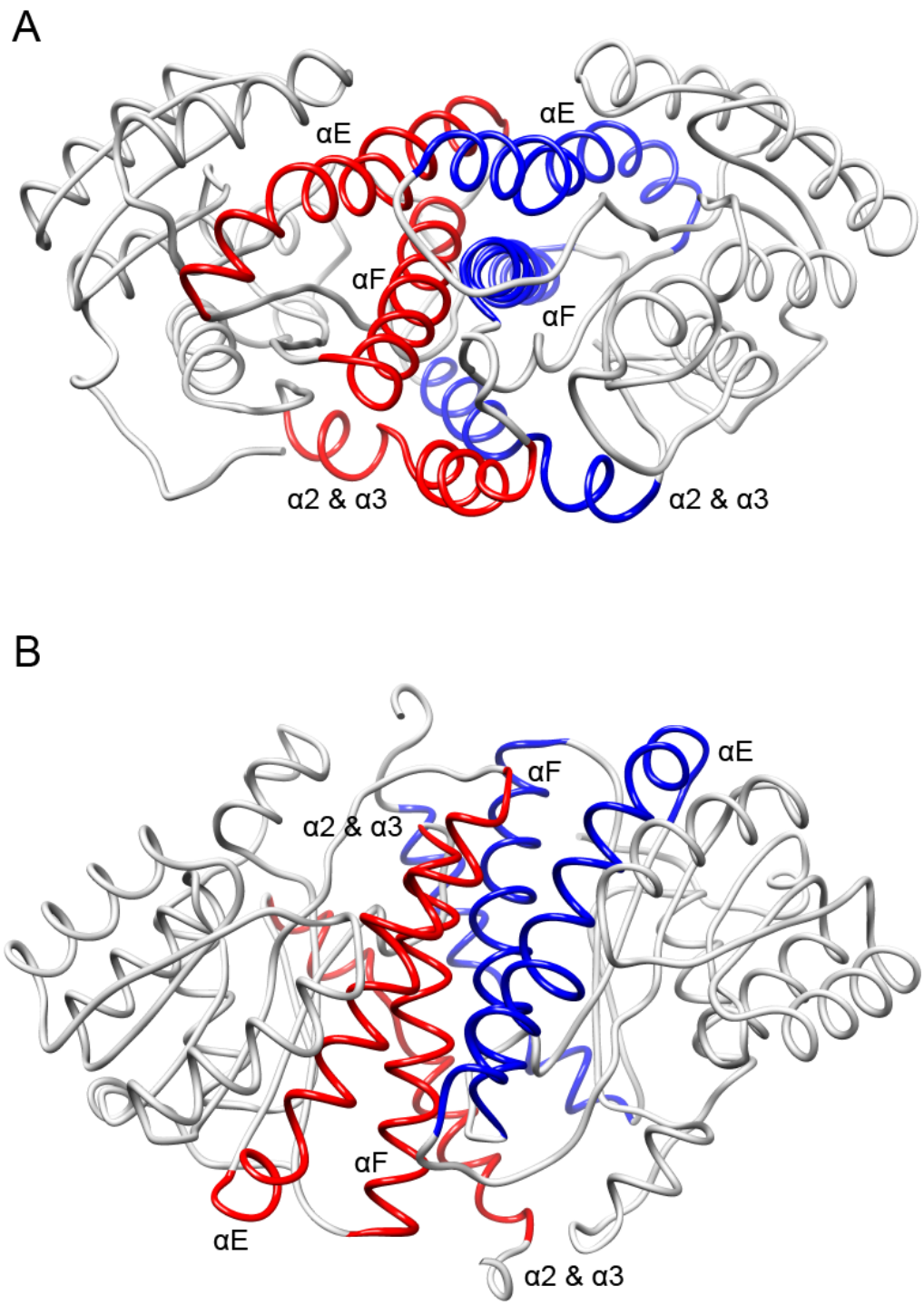

Figure 1.30. Ribbon representation of the dimerisation domain of human 11β-HSD1 (1XU9). A – side view of the 11β-HSD1 dimer. B – View of the 11β-HSD1 dimer from the top of the orientation shown in A. Helices which from the dimer interface (αE, αF, α1 & α2) are coloured red from one subunit and blue from the other.

In addition to the role in dimerization, the last helix in the C-terminus, α3, and the preceding loop of one subunit interact with the substrate-binding loop of the second subunit and form part of the substrate-binding pocket of that subunit (Figure 1.31). This 'domain swap' bears some resemblance to that seen in the *Drosophila* alcohol dehydrogenase (Benach *et al.*, 1998) (PDB code 1A4U) and is strikingly similar to some dimeric medium chain dehydrogenase/reductase (MDRs) (Eklund *et al.*, 1974).

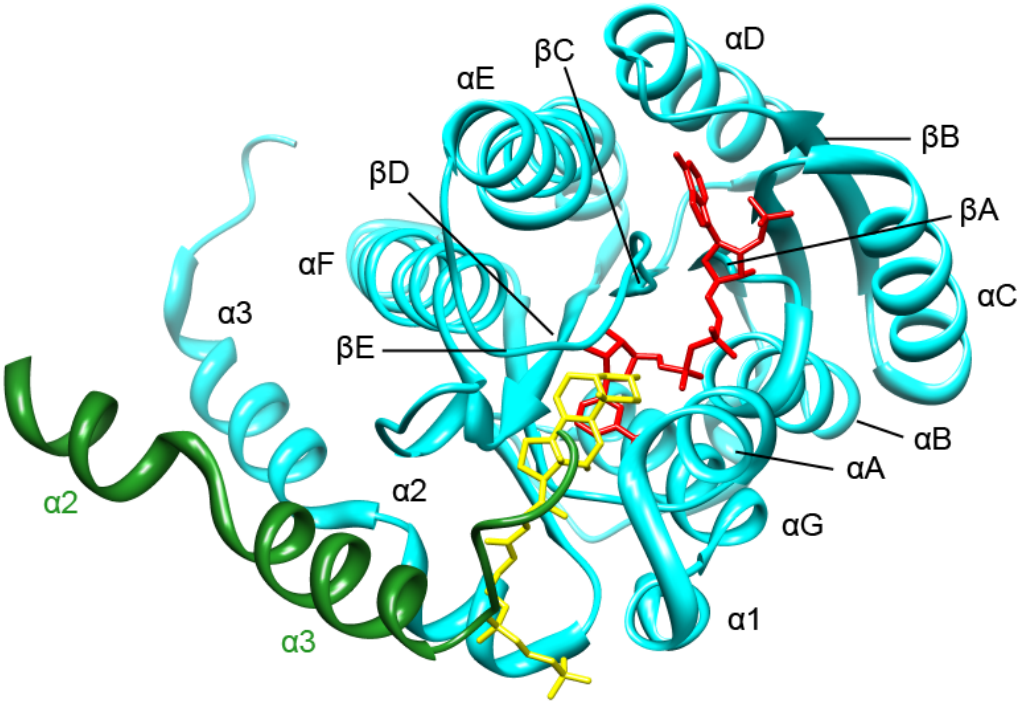

Figure 1.31. Showing the possible domain swap in 11β-HSD1 (1XU9). It can clearly be seen that the end of the C-terminal helix (α3) of subunit A (green) seems to complete the substrate binding pocket of subunit B (sky blue). Occupying the active site in place of substrate is the steroidal detergent, CHAPS (yellow), with NADP depicted in red. N = N-terminus of subunit B, C = C-terminus of subunit B. Image produced using UCSF Chimera.

Finally, if the overall surface charge distribution formed by the residues on these C-terminal helices are examined, it is clear that the region forms a non-polar plateau encircled by

positively charged residues (Ogg *et al.*, 2005), with hydrophobic residues in this region highlighted in Figure 1.32.

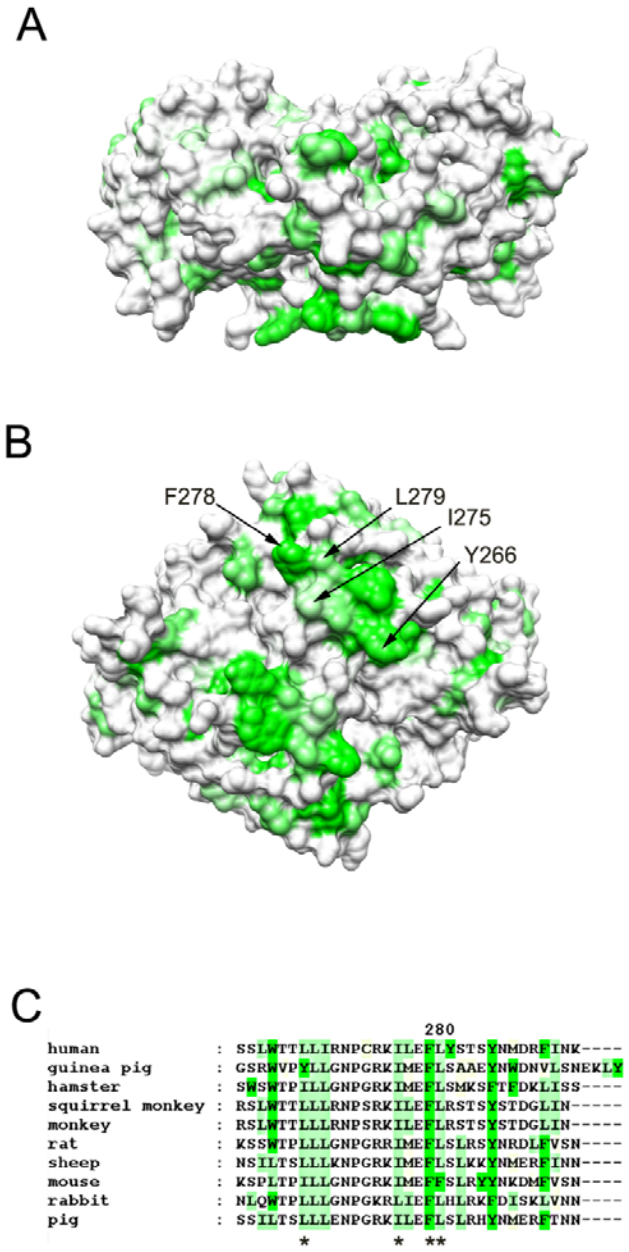

Figure 1.32. Putative membrane-dipping region of the guinea pig 11β-HSD1 structure (PDB code: 1XSE).Structures and sequences are coloured by the experimentally determined hydrophobicity scale for proteins at membrane surfaces (Wimley and White, 1996), with hydrophobicity shown as increasing green. A – Surface representation of a 'side' view of 11β-HSD1 with the putative membrane-associating region at the bottom of the structure, showing protrusion of the hydrophobic patch. B – 'Bottom' of the protein showing the hydrophobic surface region that might come into contact with the membrane. Hydrophobic residues contributing to this region are labelled for one of the two chains. C – Sequence alignment of the C-termini of mammalian 11β-HSD1 proteins, showing the conserved hydrophobicity. Structural images produced using UCSF Chimera.

Ogg *et al.* (2005) has suggested that *in vivo* the luminal domain of the 11β-HSD1 dimer, anchored to the ER membrane by the N-terminal transmembrane domains, will 'sit' on the luminal membrane surface with the amphipathic C-terminal helices free to interact with the membrane (Figure 1.33). If this orientation is to be believed, the plateau could exist in the non-polar centre of the membrane, with the charged residues forming salt bridges with the displaced phospholipid and sulpholipid head groups (Ogg *et al.*, 2005) (Figure 1.33). Due to the hydrophobic nature of the substrates of 11β-HSD1, this could constitute a potential 'membrane dipping' mechanism to funnel hydrophobic substrates from the membrane into the 11β-HSD1 active site (Ogg *et al.*, 2005) (Figure 1.33). Membrane dipping or 'substrate re-entry' loops are commonly found in polytopic membrane proteins. These loops can act as either selectivity filters as in the aquaglycerolporin family, or as gates of membrane pores as in the glutamate homologue transporter (Lasso *et al.*, 2006). However, studies on eukaryotic microsomal cytochrome P450s (CYP450s) have revealed that they too possess regions, in addition to the membrane spanning N-terminus, that associate with the membrane in a monofacial manner (Williams *et al.*, 2000). A report has detailed a program named TMLOOP which can predict the presence of membrane dipping loops (Lasso *et al.*, 2006). However, since this program is designed for polytopic membrane proteins it is unable to predict either the monofacial membrane attachment in CYP450 or the putative region in 11β-HSD1.

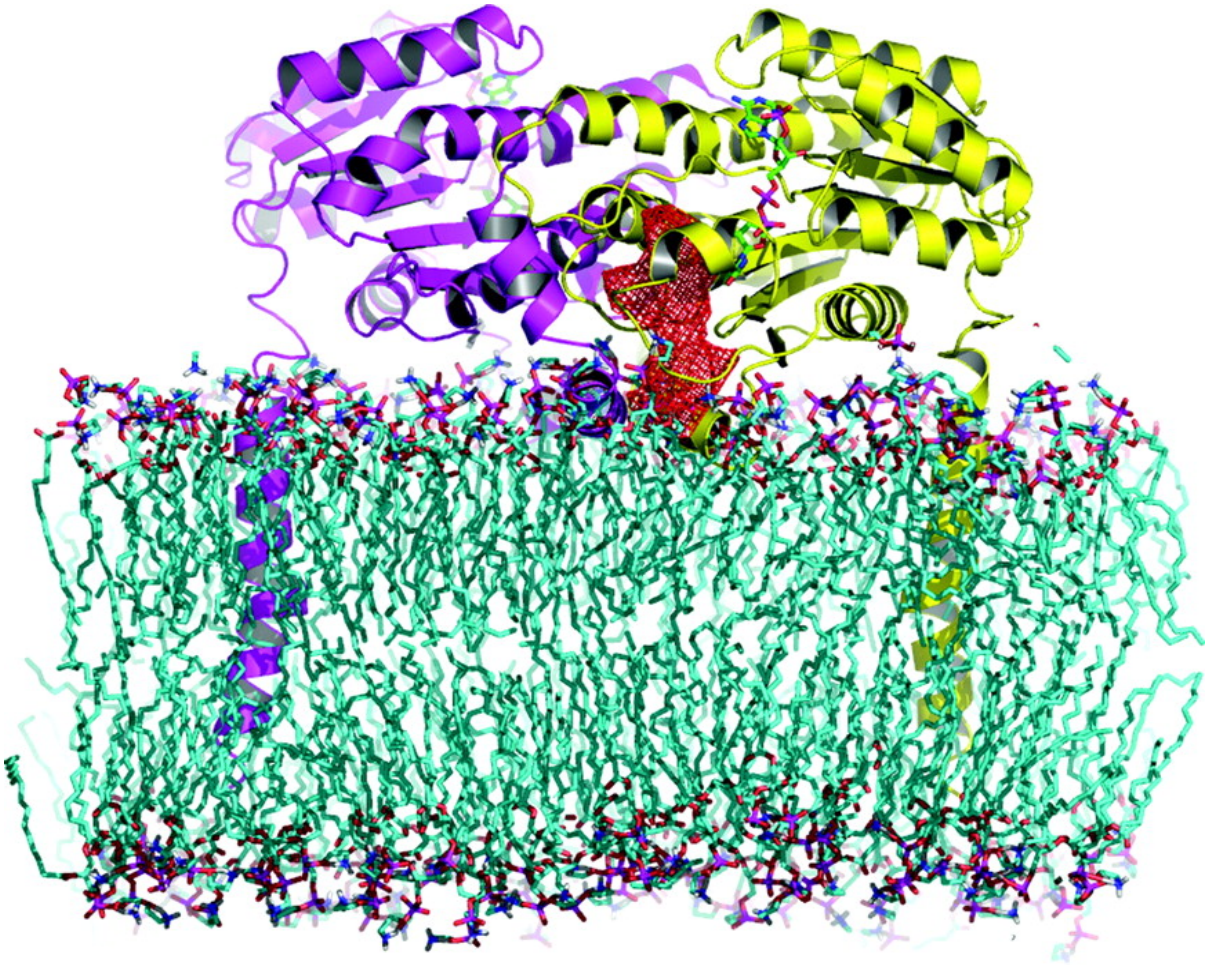

Figure 1.33. Diagrammatic representation of how the membrane dipping hypothesis would function *in vivo*. The hydrophobic plateau of 11β-HSD1 could exist in the non-polar centre of the membrane, with the charged residues forming salt bridges with the displaced phospholipid and sulpholipid head groups. The ER membrane is shown in *cyan* with the substrate binding site of one monomer shown in *red*. Taken from Ogg *et al* 2005.

Although the main structure of 11β-HSD1 is very similar in the guinea pig, human and mouse, differences do exist between them. Firstly, while the guinea pig and human enzymes contain a critical tyrosine at position 177, the equivalent position in the mouse enzyme is a glutamine. It has been postulated (Ogg *et al.*, 2005) that this substitution can account for the specificity of the mouse enzyme for its form of glucocorticoid substrate, 11-dehydrocorticosterone. Mutational studies of the human enzyme by Kim *et al.* (2006) have shown that Y177 is not a hydrogen bond donor in substrate binding, by virtue of unchanged

K_m values for cortisone when the tyrosine residue was replaced by its hydroxyl-lacking counterpart, phenylalanine (Kim *et al.*, 2006). These data, supported by increased K_m values for Y177A and Y177Q mutants, strongly suggest that in human 11β-HSD1, Y177 interacts with cortisone via its hydrophobic interactions. In addition, the study showed that Y177 does not confer substrate specificity between species as the three mutations had little effect on the binding of 11-deyhydrocorticosterone, the rodent substrate of 11β-HSD1 (Kim *et al.*, 2006).

The same group has also recently shown that Y177 together with Y280, a residue which was initially thought to be involved with substrate binding, are in fact involved with selective binding of the 11β-HSD1 inhibitor glycyrrhetinic acid (Kim *et al.*, 2006, Kim *et al.*, 2007). Interestingly, it would seem that neither residue is involved with binding of the 11β-HSD1 inhibitor carbenoxolone, suggesting that the involvement of these residues on inhibitor binding is highly dependent on the chemical structure of the inhibitor (Kim *et al.*, 2006, Kim *et al.*, 2007).

In addition to residue changes, the quaternary structure differs between the enzymes from different species. While the guinea pig, mouse and 2BEL human structures exist as dimers in the crystal structure (Ogg *et al.*, 2005, Zhang *et al.*, 2005), the human 1XU7/1XU9 structures are seen to exist as a tetramer (Hosfield *et al.*, 2005). This group crystallized two forms of 11β-HSD1 in what they call ‘open’ and ‘closed’ forms. Both conformations exist as a dimer of dimers, with the tetramerisation interface existing at the non-polar plateau at the C-terminus of all subunits. In the closed structure, hydrophobic interactions between the non-polar residues in the plateau occur to form the tetramer, while in the open structure this is mediated by steroids positioned in the cleft (Figure 1.34A) (Hosfield *et al.*, 2005). It is unclear whether this structure is physiologically relevant, or has occurred as a result of crystallisation. However, Hosfield *et al.* do propose a novel idea as to how this quaternary structure would function *in vivo* (Figure 1.34B). In the first proposed functional tetramer, the

four N-terminal transmembrane domains (*orange* in Figure 1.34B*a*) anchor the 11β-HSD1 protein (*blue*) in a single membrane in the ER lumen. The protein is in an orientation which allows the C-terminal helices (*black*) of each dimer to stack against each other forming the tetramerisation interface. This would create a hydrophobic channel in the interface open structure which would allow substrate to diffuse into the 11β-HSD1 active sites directly from the membrane. The second proposed functional tetramer (Figure 1.34B*b*) is similar in concept, although this time the interactions are possible due to two closely spaced membranes. This orientation may be relevant due to the highly invaginated structure of the ER membrane.

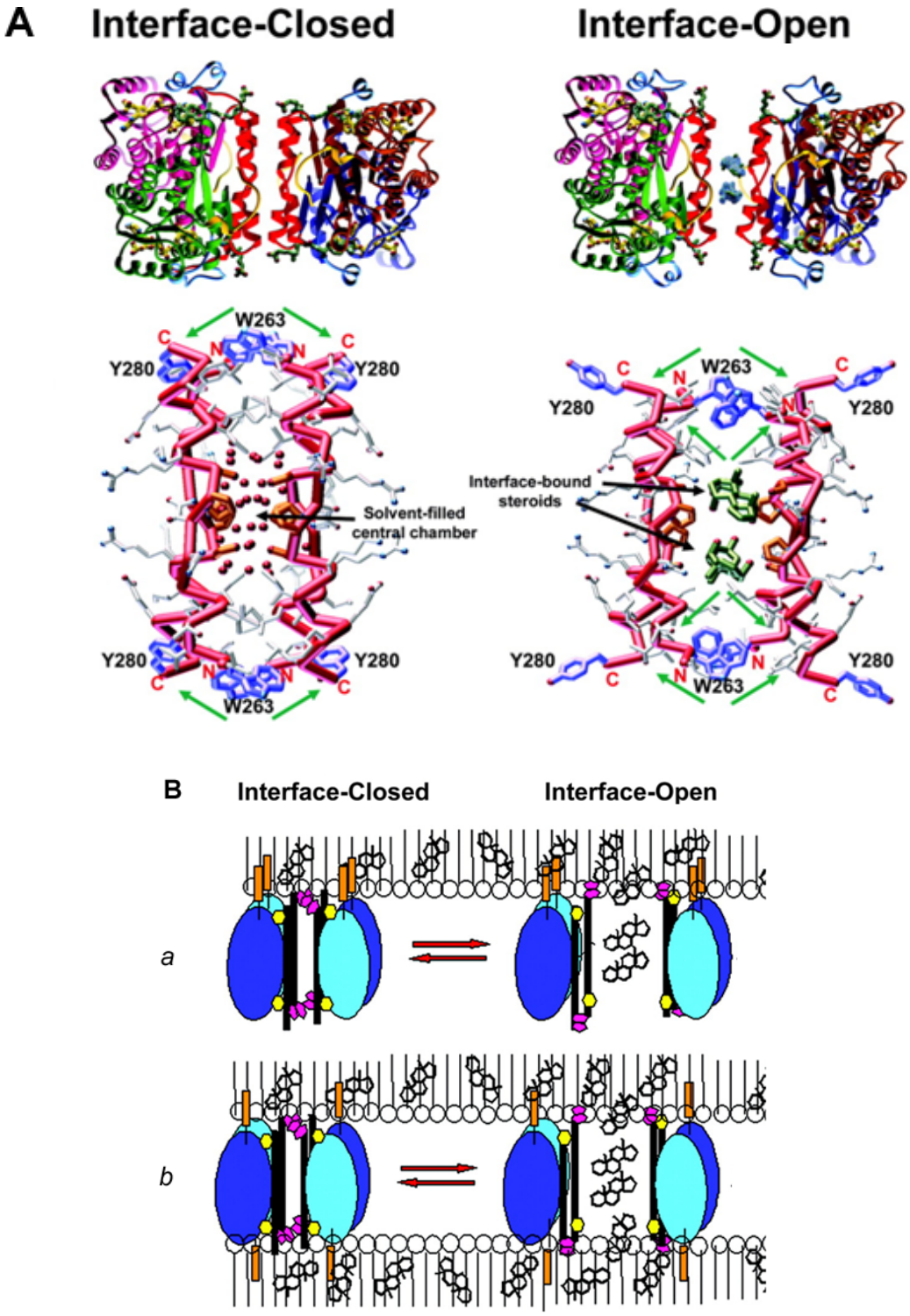

Figure 1.34. Possible tetrameric arrangement of human 11β-HSD1 (1XU7/1XU9). A - The open-closed hypothesis put forward for the structure of 11β-HSD1. NADP+ (*yellow*) and CHAPS (*green*) bind at two enzyme active sites located at the top and bottom of the enzyme tetramer. Each enzyme subunit is coloured differently except for the enzyme N and C termini, which are colored *yellow* and *red*, respectively. Conformationally variable loops between βF and α1 are colored *blue*. In the closed structure, hydrophobic interactions between the non-polar residues in the plateau between a pair of dimers interact to form the tetramer while in the open structure;

this is mediated by steroids positioned in the cleft between the dimer-of-dimers.. B – Two ideas as to how the tetrameric 11β-HSD1 would function *in vivo* with either one membrane *(a)* or two membranes *(b)*. 11β-HSD1 (*blue*), N-terminal transmembrane domain (*orange*), C terminus (*black*), Trp263 and Tyr280 (*yellow*). Taken from Hosfield *et al.* (2001)

1.9. Aims

The first aim of this research was the production of mutant 11β-HSD1 proteins in which key residues within the hydrophobic C-terminal region were replaced with the hydrophilic residue glutamate; this would be the first step towards analysing the biological significance of this region. These mutants would then be expressed in *E.coli* and analysed for any changes in solubility, monodispersity, activity or structure. This would hopefully reveal a mutant which was structurally and kinetically similar to WT but with disruption to the hydrophobicity of the C-terminal region. This would then allow comparison of the binding of WT and mutant 11β-HSD1 to microsomal membranes from either mouse liver or human cells, and also to artificially created liposomes, with the hope of determining whether this region is important in membrane association

The final aim was to develop a bacterial system that facilitates the purification of recombinant heterodimers (mutant/WT) of 11β-HSD1 which could then be used to analyse two recently-discovered, naturally-occurring mutations which are thought to cause CRD, both of which are found in the heterozygous state.

Chapter 2. Mutation of key hydrophobic C-terminal residues of 11β-hydroxysteroid dehydrogenase type 1

2.1. Introduction

11β-HSD1, as discussed earlier, is a protein expression of which has wide-reaching implications in health and medicine. In Section 1.4, the evidence that a dysregulation of cortisol at a tissue level, which would indicate abnormal 11β-HSD1 activity, may be the underlying pathology behind a range of conditions such as type 2 diabetes and the metabolic syndrome was discussed. This evidence included animal studies which have shown that 11β-HSD1 is an important regulator of hepatic glucose output and visceral adiposity with transgenic mice overexpressing 11β-HSD1 in liver and adipose tissue displaying features of the metabolic syndrome (Masuzaki *et al.*, 2001, Masuzaki *et al.*, 2003, Paterson *et al.*, 2004). In contrast, recombinant mice lacking 11β-HSD1 show improved glucose tolerance, enhanced insulin sensitivity, and reduced weight gain when given a high fat diet (Kotelevtsev *et al.*, 1997, Morton *et al.*, 2001). 11β-HSD1 has therefore emerged as a novel therapeutic target to treat patients with obesity and insulin resistance, with selective 11β-HSD1 inhibitors being tested in rodent (Alberts *et al.*, 2003) and mammalian models (Bhat *et al.*, 2007). Central to studies of this key enzyme has been the development of methods for providing sufficient amounts of pure protein.

2.1.1. Improvements in the expression and purification of 11β-HSD1

High resolution structures of 11β-HSD1 which allow the development of structure-based drug design for the treatment of type 2 diabetes and the metabolic syndrome have only recently become available. This is in part due to the problems inherent in heterologous protein production. Unless specific eukaryotic protein modifications are required, the first method of choice for the production of recombinant protein is usually overexpression of the

target gene in *E.coli*.. However, despite the extensive genetic knowledge of *E.coli*, widespread availability of vector systems and host strains, ease of use, the low cost and high expression levels which can be obtained, the current success rate to obtain soluble eukaryotic protein using *E.coli* is around 10% (Hozjan *et al.*, 2008). Common causes for the low success rate, such as gene product toxicity, biased codon usage and mRNA secondary structure and stability can usually be overcome by choosing the correct combination of vector/host strain together with modification or redesign of target genes. However, even when these problems are overcome and protein expression is high, the recombinant protein produced can often be insoluble, as was the case 11β-HSD1. This is particularly true for eukaryotic proteins, no doubt because the protein-folding environment in bacteria is different from that within eukaryotic cells. In the case of 11β-HSD1, this may be exacerbated by the fact that in contrast to most other members of the SDR family, 11β-HSD1 is a glycosylated, membrane-bound protein which normally folds within the lumen of the ER. These properties make expression and isolation of full-length 11β-HSD1 protein a difficult, although not impossible, task (Hult *et al.*, 2001, Nobel *et al.*, 2002). Since the crystallization of membrane-bound proteins has a low success rate (Newman, 1996), recombinant 11β-HSD1 which has the N-terminal transmembrane domain removed has been engineered (Walker *et al.*, 2001a). Following expression of this construct in bacteria, 11β-HSD1 can be purified to a relatively high level of homogeneity and monodispersity, essential factors for crystallography (Walker *et al.*, 2001a). Although the production of recombinant 11β-HSD1 outlined by Walker *et al.* (2001) reduced the temperature from 37 °C to 15 °C in the induction phase, a common technique for improving the yield of soluble protein, the final yield of the resulting soluble protein was low (~ 0.8 mg ml^{-1}). Improvements to this procedure have seen the co-expression of 11β-HSD1 with the chaperonins GroEL/GroES, enhancing the yield of soluble 11β-HSD1 around twofold (Elleby *et al.*, 2004, Hult *et al.*,

2006). The successful co-expression of target proteins with chaperonins has been known for over 10 years, with successes reported for human branched chain α-keto acid dehydrogenase complex, haloalkane dehalogenase and a recombinant IgG protein (Ailor and Betenbaugh, 1998, Wynn *et al.*, 2000, Widersten, 1998). In addition to co-expression with chaperonins, addition of an inhibitor of 11β-HSD1 during the induction phase has been shown to increase the yield of soluble human 11β-HSD1 significantly (Hozjan *et al.*, 2008, Hult *et al.*, 2006, Elleby *et al.*, 2004). Interestingly, a recent report has shown that addition of the inhibitor CBX during the production of 65 (non-11β-HSD1) SDRs can increase the yield of soluble protein two to threefold in 22 cases, with CBX supplementation seen to be a requirement for the production of soluble protein in 4 of the 65 SDRs analysed (Hozjan *et al.*, 2008).

2.1.2. Investigation into the solvent exposed hydrophobic region in 11β-HSD1 and other proteins

The presence of a solvent-exposed hydrophobic region in 11β-HSD1 which could potentially interact with the ER membrane is clear from the crystal structures (see Figure 1.31 and also Section 1.8). This may also explain the improved solubility of purified 11β-HSD1 on the addition of detergent (Elleby *et al.* 2004). In order to initiate investigations into the importance of this C-terminal hydrophobic region, the primary aim of this chapter was to determine the effect of replacing a series of key residues within the hydrophobic plateau, in both human and guinea pig 11β-HSD1, with the hydrophilic residue glutamate. Although such protein engineering studies include complications which may arise from the inability to control all effects of amino acid substitution on protein structure, this technique seemed the best approach to elucidate the importance of the hydrophobicity of this region of the protein. The principal residues which make up the hydrophobic plateau in the guinea pig protein are W263, Y266, I275, F278 and L279 (Figure 2.1); the human residues are identical apart from Leu at position 266. Hence these residues were chosen to be individually mutated to

glutamate. Although some previous studies into surface exposed hydrophobic residues have used milder amino acid substitutions to probe the role of specific residues on protein structure, e.g. a V213S mutation in cytosine-C5 methyltransferase protein (Daujotyte *et al.*, 2003), glutamate was chosen specifically not just for its strong hydrophilicity, but also because its negative charge might increase repulsion between this region of the protein and membrane phospholipid/sulpholipid head groups, and hence have a more deleterious effect on membrane association of the protein.

It was clearly important for the planned future studies that any mutation of solvent-exposed hydrophobic residues to charged residues such as glutamate should not adversely affect the activity or general structure of the protein. Hence the studies in this Chapter report the effects of these mutations on the solubility, monodispersity and activity of 11β-HSD1 expressed in *E.coli,* and on the crystal structure of one of the guinea pig enzyme mutants (F278E).

Prior to the work presented in this thesis, a bacterial expression construct containing DNA encoding residues 24-292 of the human 11β-HSD1 protein was generated in pET-28b(+) (Novagen) by PCR amplification from a previous construct (Walker *et al.*, 2001a). A guinea-pig expression construct containing DNA encoding residues 24-300 was a kind gift from Dr P Rejto (Pfizer, La Jolla, CA). Both constructs incorporated an N-terminal His_6-tag to aid purification. A series of single point mutations were made to hydrophobic residues at the C-terminus of both guinea pig and human 11β-HSD1 proteins. Target residues for mutation were chosen by analysis of the crystal structures for the human and guinea pig 11β-HSD1 (pdb 2BEL and 1XSE respectively). The positions of these hydrophobic residues are shown in Figure 1.32. The human enzyme mutants L266E, I275E, F278E and L279E and the guinea pig enzyme mutants Y266E, I275E, F278E and L279E were introduced into the bacterial expression construct and analyzed for their effect on protein expression. Analysis of bacterial

lysates by SDS-PAGE showed that the solubility of recombinant 11β-HSD1 was dramatically increased by the mutations I275E, F278E and L279E, in the guinea pig sequence and F278E in the human sequence (Figure 2.1). This was not simply due to an increase in total protein expression as there was not only an increase of protein in the soluble fraction, but also a concomitant decrease in the amount of protein in the insoluble fraction (data not shown). In this chapter, the expression of these mutants on a larger scale was explored.

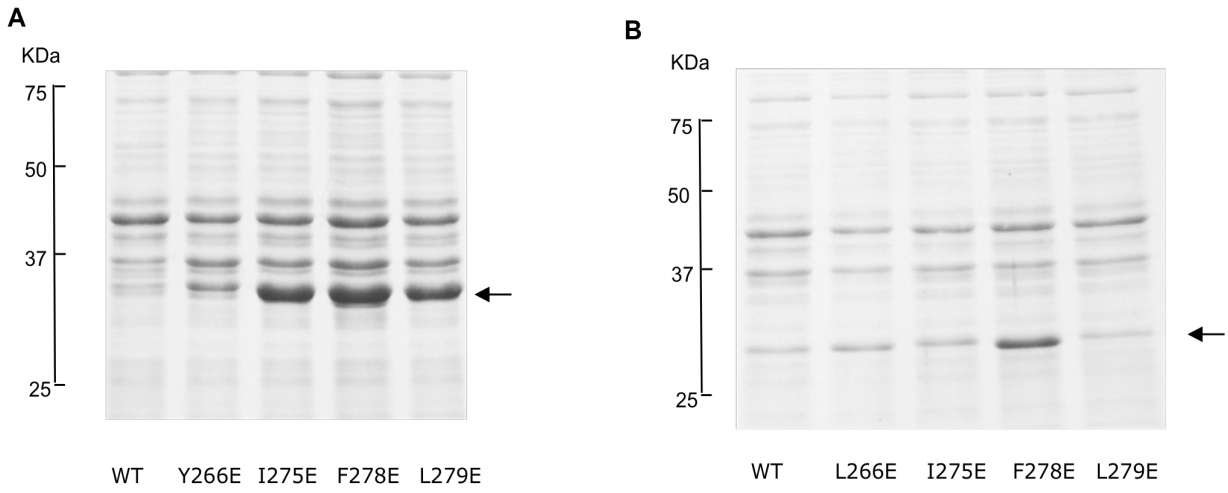

Figure 2.1. SDS-Page analysis of WT and mutant 11β-HSD1 recombinant proteins. Supernatant fractions from lysates of bacterial cultures expressing (A) guinea pig 11β-HSD1 proteins and (B) human 11β-HSD1 proteins indicate that the I275E, F278E and L279E point mutations dramatically increased the production of soluble 11β-HSD1. Arrows indicate positions of respective guinea pig and human recombinant proteins. (Images of gels used with kind permission of Dr E. A. Walker).

2.2. Materials and Methods

2.2.1. Cloning and Expression of Recombinant 11β-HSD1

Constructs containing 11β-HSD1 gene mutants cloned into pET-28b(+) were used to transform the BL21 (DE3) *E.coli* expression strain (Novagen). *E.coli* BL21(DE3) cells carrying the human gene were co-transformed using the pBAD-ESL plasmid (gift of Dr P Lund (Walker, 2000)), which contains the genes for the *E.coli* chaperonins GroEL/ES. For the expression of the guinea pig protein, cells were grown in LB broth supplemented with 30 μg/ml kanamycin with shaking (220 rpm) at 37 ^{o}C. Cells were induced with isopropyl-β-D-thiogalactoside (IPTG, 1 mM) when A_{600} had reached a value of 0.8-1. Cells were grown with shaking for a further 30 min at 37 ^{o}C, then transferred to 15 ^{o}C and grown with shaking overnight. For the expression of the human protein, cells were grown with shaking in LB broth supplemented with 30 μg/ml kanamycin and 50 μg/ml ampicillin at 37 ^{o}C. Arabinose (0.1% w/v) was added to the cultures at an A_{600} of 0.8-1, in order to induce the expression of the chaperonin proteins. Cells were grown with shaking for 1 h at 37 ^{o}C, before addition of 1 mM IPTG. The 11β-HSD inhibitor carbenoxolone (CBX, 0.1 mM) was also added at this stage. Following a further incubation of 30 min at 37 ^{o}C, cultures were transferred to 15 ^{o}C and grown with shaking for 16 h.

2.2.2. Purification of 11β-HSD1

Cells were pelleted (3000×*g*, 15 min) and then resuspended in Bugbuster reagent (Novagen) containing protease inhibitors (Mini-Complete EDTA free, Roche Molecular Biochemicals) and Benzonase DNase (Novagen). Cells were incubated with shaking at room temperature for 40 min and then cell debris was pelleted at 38,000×*g* for 30 min at 4˚C. Supernatant was loaded onto a His-Select (Sigma Aldrich) column and washed with buffer containing 25 mM sodium phosphate, 300 mM NaCl, 5% (v/v) glycerol, 2 mM TCEP and 0.005% (v/v) Anapoe

X-100 (Anatrace Inc), pH 8.0. Loosely bound protein was washed off with 3 column volumes of the same buffer containing 17.5 mM imidazole. Protein was then eluted with 3 volumes of buffer containing 175 mM imidazole. Fractions containing protein were separated by size-exclusion chromatography on a Superdex-200 HR10/30 column (Pharmacia) running at 0.4 ml min^{-1} in 25 mM sodium phosphate, 5% (v/v) glycerol, 0.005% (v/v) Anapoe X-100, pH 8.0. The amount of protein was measured using the absorbance of a given sample at 280 nm using a UV spectrophotometer.

2.2.3. Measurement of 11β-HSD1 activity

Dehydrogenase activity of 11β-HSD1 was assayed at 37 ^{o}C in 25 mM sodium phosphate, pH 8.0, with 200 μM $NADP^{+}$ and cortisol concentrations ranging from 0.5 μM to 32 μM, using a Perkin-Elmer LS-5 spectrofluorimeter. Excitation and emission wavelengths were 340nm and 456nm respectively. Amount of enzyme added was adjusted so that a linear rate of reaction was obtained for 5 min after cortisol addition. A calibration curve was constructed using 0-1μM NADPH. Reductase activity of 11β-HSD1 was assayed by measuring the cortisone to cortisol ratio by HPLC. In this reaction, an enzyme concentration which gave no more than 20% substrate conversion was incubated for 5 min at 37 ^{o}C in 25 mM sodium phosphate, pH 8.0, containing 200 μM NADPH and an NADPH-regenerating system (6 mM $MgCl_2$, 1 U/ml glucose-6-phosphate dehydrogenase (Sigma-Aldrich), 1 mM glucose-6-phosphate). Reactions were started by addition of 1-128 μM cortisone and incubated for 20 min. Reactions were terminated by addition of 3 ml dichloromethane. Samples were then centrifuged for 5 min at 1000×*g* and the aqueous layer removed. After evaporation of the dichloromethane, samples were redissolved in 60μl of 50% (v/v) aq. acetonitrile and loaded onto an RP-HPLC system consisting of a Prevail Select C-18, 5μm column (Grace), a GP50 gradient pump and a UVD170S detector (Dionex). Samples were eluted with a gradient of 54% to 69% (v/v) aq. methanol over a period of 15 min. Substrate and product were monitored by UV absorbance

at 242 nm with retention times of approximately 11 and 12 min respectively. An example of a typical HPLC trace is shown in Figure 2.2. Rates, as a function of substrate concentration, were fitted to a simple Michaelis Menten equation and analysed using non-linear regression by Visual Enzymics (Softzymics Inc.).

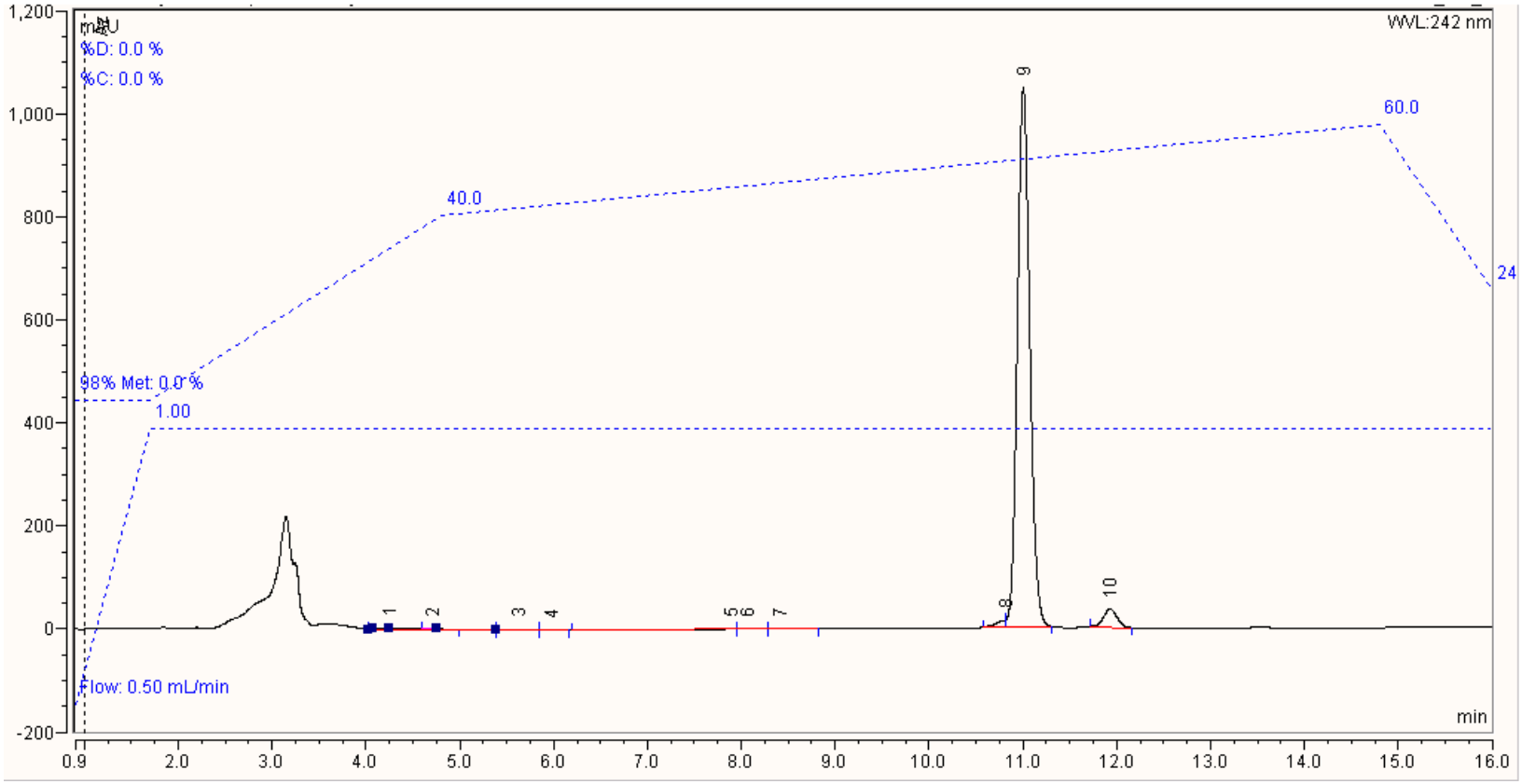

Figure 2.2. An example of a typical HPLC chromatogram to analyse the reductive activity of 11β-HSD1. Steroid samples were eluted using a gradient of 54% to 69% (v/v) aq. methanol over a period of 15 min, with this gradient represented by the blue line. Cortisone and cortisol were monitored by UV absorbance at 242nm with retention times of approximately 11 (peak 9) and 12 (peak 10) min respectively. Axis represent time (x) vs absorbance (y),

2.2.4. Measurement of turnover of enzyme-bound $NADP^+$

To estimate the proportion of protein molecules with bound $NADP^+$, human F27E or wild-type enzyme (1 μM) was incubated in 25 mM sodium phosphate pH 8.0 at 37^{o}C and the fluorescence of cofactor monitored as described above. An excess of cortisol was then swiftly added to a final concentration of 50 μM, and the single turnover of the $NADP^+$ in the enzyme preparation monitored. The fluorescence increased and reached a plateau from which the original concentration of $NADP^+$ could be estimated. The system was calibrated by subsequent addition of a known sub-stoichiometric amount of $NADP^+$ and monitoring the fluorescence increase. Control reactions with cortisone in place of cortisol showed no change in fluorescence.

2.2.5. Analytical Ultracentrifugation

Sedimentation velocity measurements were made using a Beckman XLI analytical ultracentrifuge. Samples at a concentration of 0.5 mg ml^{-1}, 0.25 mg ml^{-1} or 0.1 mg ml^{-1} were centrifuged at 40000 rpm in an X rotor at 4 ^{o}C for 8 hours in a buffer containing 25 mM sodium phosphate, 300 mM NaCl, 5% (v/v) glycerol, 2 mM TCEP and 0.005% (v/v) Anapoe X-100 (Anatrace Inc), pH 8.0. The concentration of protein within the cells was analysed by scanning each cell at 280 nm, a total 200 scans being made during each run. These data were then processed using the C(M) model implemented in SEDFIT (Schuck, 2000) using parameters for protein and buffer determined using SEDNTERP.

2.2.6. Structure determination of the F278E mutant

Crystals were grown using the sitting-drop vapour diffusion method with a 10 mg/ml protein stock solution in 25 mM sodium phosphate, 5% glycerol, 0.005% Anapoe X-100, pH 8.0, equilibrated against a reservoir containing 0.1 M Tris-HCl, 1.75 M ammonium sulphate and 5% (v/v) glycerol (pH 8.0). The sitting drop contained 2 μl of protein solution and 2 μl of

reservoir. No $NADP^+$ was added during purification or crystallization. Crystals of the F278E 11β-HSD1 were soaked for 10 minutes in each of a series of artificial mother liquor solutions containing glycerol in 5% increments. In the final solution containing 25% (v/v) glycerol, crystals were soaked for 45 minutes before being flash-cooled by plunging into liquid nitrogen. Data were collected at 100 K at the European Synchrotron Radiation Facility, Grenoble, France, using beam line ID14-1. All data were indexed, integrated and scaled using XDS (Kabsch, 1993). Data was collected by Dr Scott White and is reproduced here with his kind permission with full data collection statistics shown in Table 2.1. The structure was determined by molecular replacement using the program Phaser with 1XSE as the search molecule. After initial refinement, the model was improved using Arp/wArp (Perrakis *et al.*, 1999), then refined using phenix.refine (Afonine, 2005). The refinement statistics are listed in Table 2.1.

Data collection statistics[a]	
Cell parameters *a, b, c* (Å)	78.1, 85.9, 176.3
Space Group	$P2_12_12_1$
Resolution (Å)	2.2 (2.33-2.20)
Completeness (%)	99.2 (96.6)
Multiplicity	4.7
$I/\sigma I$	11.43 (2.8)
No. of observations	288,334 (39,957)
No. of unique observations	60,915 (9,432)
R_{sym}	9.5 (54.5)
Refinement statistics	
Average B factor	43.8
No. of non-hydrogen atoms/waters	9153/452
RMSD bond (Å)/angle (deg)	0.005/0.923
Ramachandran (%)[b]	90.1/9.0/0.7/0.2
R/R_{free}[c]	20.0/25.5
PDB code	3DWF

[a] Statistics as reported by XDS. [b] Percentage of non-glycine, non-proline residues in the core/allowed/generously allowed/disallowed regions of the Ramachandran plot. [c] 5% of reflections set aside for cross validation.

Table 2.1. X-ray data and refinement statistics. Data was collected by Dr Scott White and is reproduced here with his kind permission.

2.3. Results

2.3.1. Effect of Mutations on the Expression and Purification of Recombinant 11β-HSD1

The effect of the various mutations on the final yield of soluble protein when the protein was purified from large cultures (at least 400 ml) by IMAC and gel-filtration is shown in Figure 2.3. All the mutations increased the final yield of soluble protein, with the human F278E and guinea pig I275E mutants showing the most dramatic increases (approximately 8-fold and 23-fold increases compared to respective wild-type constructs).

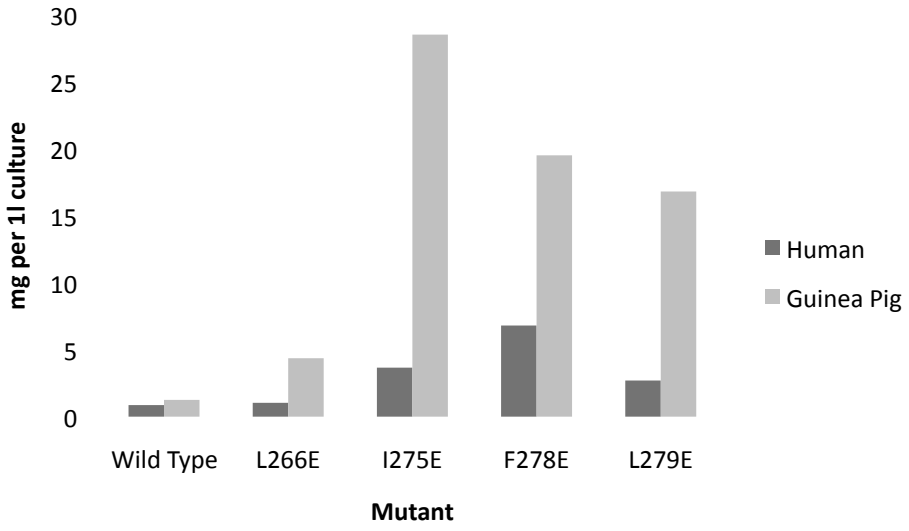

Figure 2.3. Relative yields of wild type and mutant human and guinea pig 11β-HSD1 proteins. Proteins were produced as per materials and methods. Levels of protein produced are shown in mg protein per litre LB broth with preparations performed in duplicate. Variation existed between protein preperations but since n = 2, reliable statistical analysis is not possible. Introduction of glutamate at position 275, 278 and 279 in the guinea-pig sequences and 278 in the human sequence, dramatically increased the yield of recombinant 11β-HSD1 protein.

2.3.2. Effect of Mutations on Enzyme Kinetics

The effect of the mutations on the k_{cat} and K_m for the steroid substrates of 11β-HSD1 was analyzed in both dehydrogenase and reductase directions (Tables 2.2 & 2.3). For the guinea

pig enzyme, the F278E mutant had virtually unchanged K_m and k_{cat} compared to wild type, in both dehydrogenase and reductase directions (Table 2.3). The Y266E and L279E mutants showed a slight decrease in turn-over rate but with little change in K_m. The only pronounced variation from wild type was seen with the I275E mutant, which showed a marked decrease in K_m for cortisol, and a dramatic increase in K_m for cortisone (Table 2.3). In the case of the human enzyme, the K_m for the F278E mutant was virtually unchanged compared to wild type in both directions, although the k_{cat} increased approximately 4-fold and 2-fold for the dehydrogenase and reductase reactions respectively (Table 2.2). The constants for the L266E mutant were virtually identical to the F278E mutant, except that there was a ~50% increase in K_m for cortisone. In contrast, both the L279E and I275E mutants showed an increase in K_m and k_{cat} for dehydrogenase and reductase reactions (Table 2.2). Kinetic measurements of the human enzyme mutant F278E with a higher concentration (500μM) of $NADP^+$/NADPH showed no change in K_m or k_{cat} for both the dehydrogenase and reductase reactions.

	Dehydrogenase		Reductase	
Protein	**K_m (Cortisol)**	**k_{cat}**	**K_m (Cortisone)**	**k_{cat}**
Wild Type	7.05±2.15	0.31±0.04	8.95±0.80	0.18±0.00
L266E	6.63±0.50	1.29±0.03	15.26±1.58	0.31±0.01
I275E	11.68±1.13	0.98±0.04	27.93±1.80	0.22±0.01
F278E	6.16±0.44	1.27±0.03	10.61±1.49	0.31±0.01
L279E	12.57±1.05	0.65± 0.00	18.93±2.26	0.14±0.01

Table 2.2. Kinetic analysis of human 11β-HSD1 wild type and mutant proteins. Assays were carried out as per materials and methods. K_m values are given in μM with k_{cat} values given in min^{-1} (mean ± SEM). Results were analyzed using non-linear regression by Visual Enzymics (Softzymics Inc.) and are based on the average of duplicate experiments. K_m and k_{cat} values for cortisone and cortisol are comparable to those reported by Shafqat *et al.,* (2003) (see Table 1.2).

	Dehydrogenase		Reductase	
Protein	**K_m (Cortisol)**	**k_{cat}**	**K_m (Cortisone)**	**k_{cat}**
Wild Type	4.59±0.49	1.02±0.04	4.09±0.35	0.57±0.01
Y266E	2.86±0.22	0.47±0.01	3.67±0.58	0.20±0.01
I275E	1.35±0.40	0.24±0.02	31.1±9.8	0.37±0.04
F278E	5.73±1.13	1.12±0.08	3.13±0.63	0.48±0.02
L279E	3.23±0.29	0.53±0.01	5.27±1.33	0.41±0.03

Table 2.3. Kinetic analysis of guinea pig 11β-HSD1 wild type and mutant proteins. Assays were carried out as per materials and methods. K_m values are given in μM with k_{cat} values given in min^{-1} (mean ± SEM). Results were analyzed using non-linear regression by Visual Enzymics (Softzymics Inc.) and are based on the average of duplicate experiments

Effect of Mutations on Aggregation State - Guinea pig and human F278E and WT proteins were analyzed by sedimentation analytical ultracentrifugation (AUC) to assess their aggregation state *in vitro* (Figure 2.4). Both the guinea pig and human wild type proteins exhibited a rather broad peak with a maximum at around 200 kDa. Since the 11β-HSD1 dimer has a size of 68 kDa and 64 kDa for the guinea pig and human enzymes respectively, these data suggest that the recombinant wild type proteins aggregate significantly in solution, with a size averaging around a hexamer. Interestingly, it was observed that the F278E mutation in the guinea pig enzyme converted the main species to a much narrower peak with a size indicative of a tetramer. This is shown by a peak at approximately 120-140 kDa. The human F278E mutant at 0.5 mg ml^{-1} also showed a main peak at 130 kDa, but in addition had a second major peak at 65 kDa, indicating the majority of protein existed as tetramer with a lesser amount as a dimeric protein. In order to probe the equilibrium between the dimeric and tetrameric forms, three different concentrations of guinea pig and human F278E were analyzed by AUC (Figure 2.4). Dilution of the guinea pig F278E protein did not affect its aggregation state, with all dilutions showing one peak at around 140 kDa, indicating a stable tetrameric form. The human F278E mutant, however, showed a significant increase in the ratio of dimer to tetramer as the concentration of protein was decreased, indicating a concentration-dependent equilibrium between dimeric and tetrameric forms.

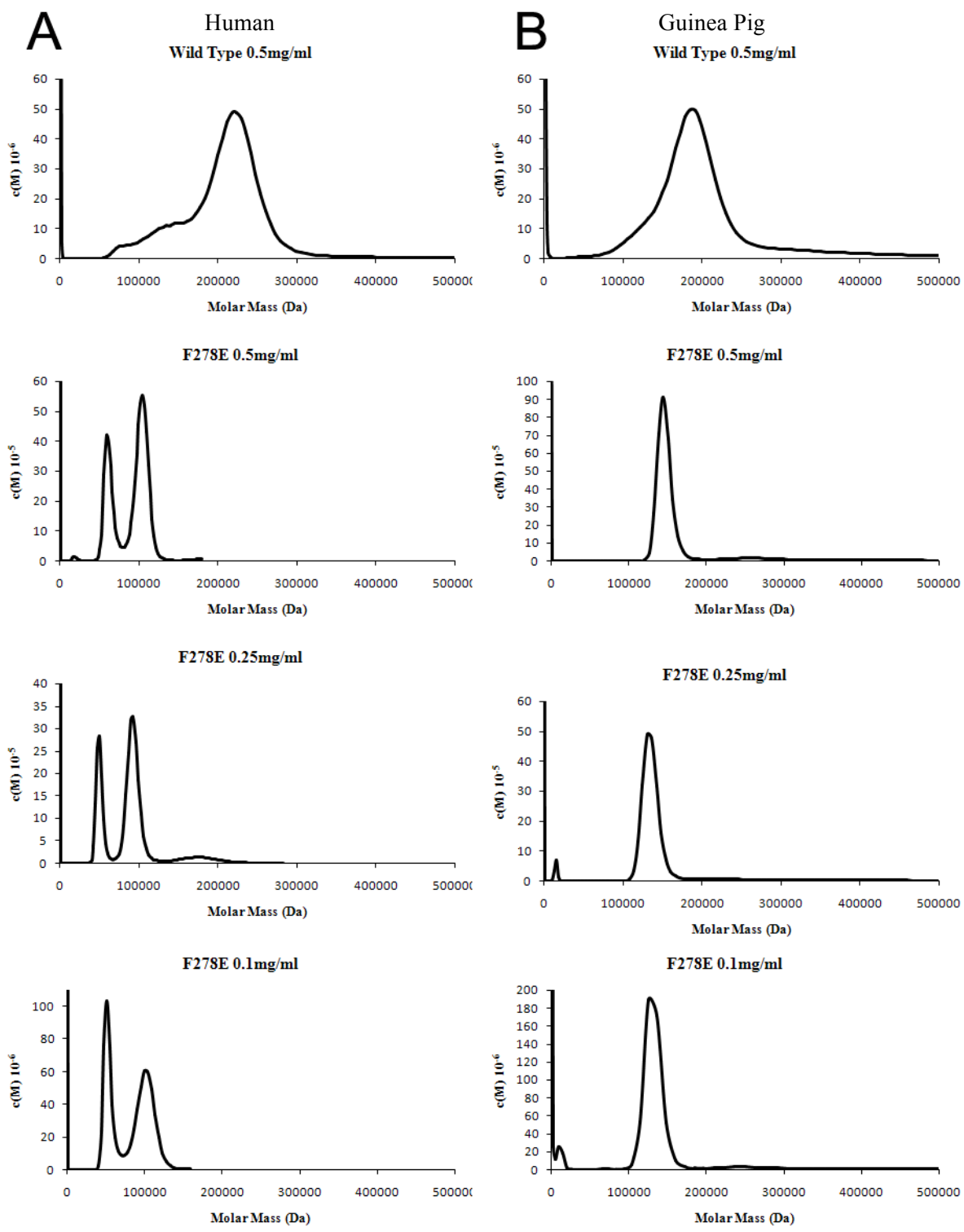

Figure 2.4. AUC analysis of the aggregation states of the human (A) and guinea pig (B) wild-type and F278E proteins. Also shown is the effect of dilution on the oligomerisation state of the human and guinea pig F278E enzymes. Images were produced using SedFit (Schuck 2000) with density, viscosity and v-bar measurements calculated by Sednterp. Human and guinea pig v-bar measurements were 0.7405 and 0.7391 respectively. The buffer had a density (P) value of 1.016 and viscosity (H) value of 1.18 E-2.

2.3.3. Crystal Structure of Guinea Pig F278E

Due to a large yield of protein, the crystallisation of guinea pig F278E mutant protein could be attempted to check for changes in structure. Crystals were grown as per Materials and Methods with the data collection and refinements statistics given in Table I. Each monomer in the guinea pig F278E structure had the same overall Rossmann fold as the other published 11β-HSD1 structures (Ogg *et al.*, 2005, Hosfield *et al.*, 2005, Zhang *et al.*, 2005) and had a quaternary assembly of a tetramer made up of a dimer-of-dimers (Figure 2.5a). Analysis using the PISA server (Krissinel and Henrick, 2007) suggested tetramer to be the most probable quaternary structure for the guinea pig F278E protein, while the previously published wild type structure (1XSE) (Ogg *et al.*, 2005) was suggested to exist as a dimer. The structure of the guinea pig F278E dimer is largely identical to 1XSE with the dimers superimposable with a root mean square displacement (RMSD) of 0.48 Å. Slight differences in the backbone exist in the loop region Glu221 to Pro234 and in the final helix from Leu267 to Ala291. One clear difference is evident between chains A and D and chains B and C in the guinea pig F278E protein structure (Figure 2.5b). In chains A and D, Tyr123 points towards the active site bound $NADP^+$, while in chains B and C, the Tyr123 points away from the active site. Both orientations have good electron density in both the 2fofc map and the omit map calculated by PHENIX. Interestingly, strong electron density can be seen for $NADP^+$ (Figure 2.5c) even though none was added at any point in the purification or crystallization process. Our structure also shows that the C-terminal residue, Trp299, in each chain has bound into a hydrophobic pocket consisting of residues Phe129, Val152, Met155, Leu197 and Phe201. The position of this Trp residue has not been reported in any other 11β-HSD1 structure.

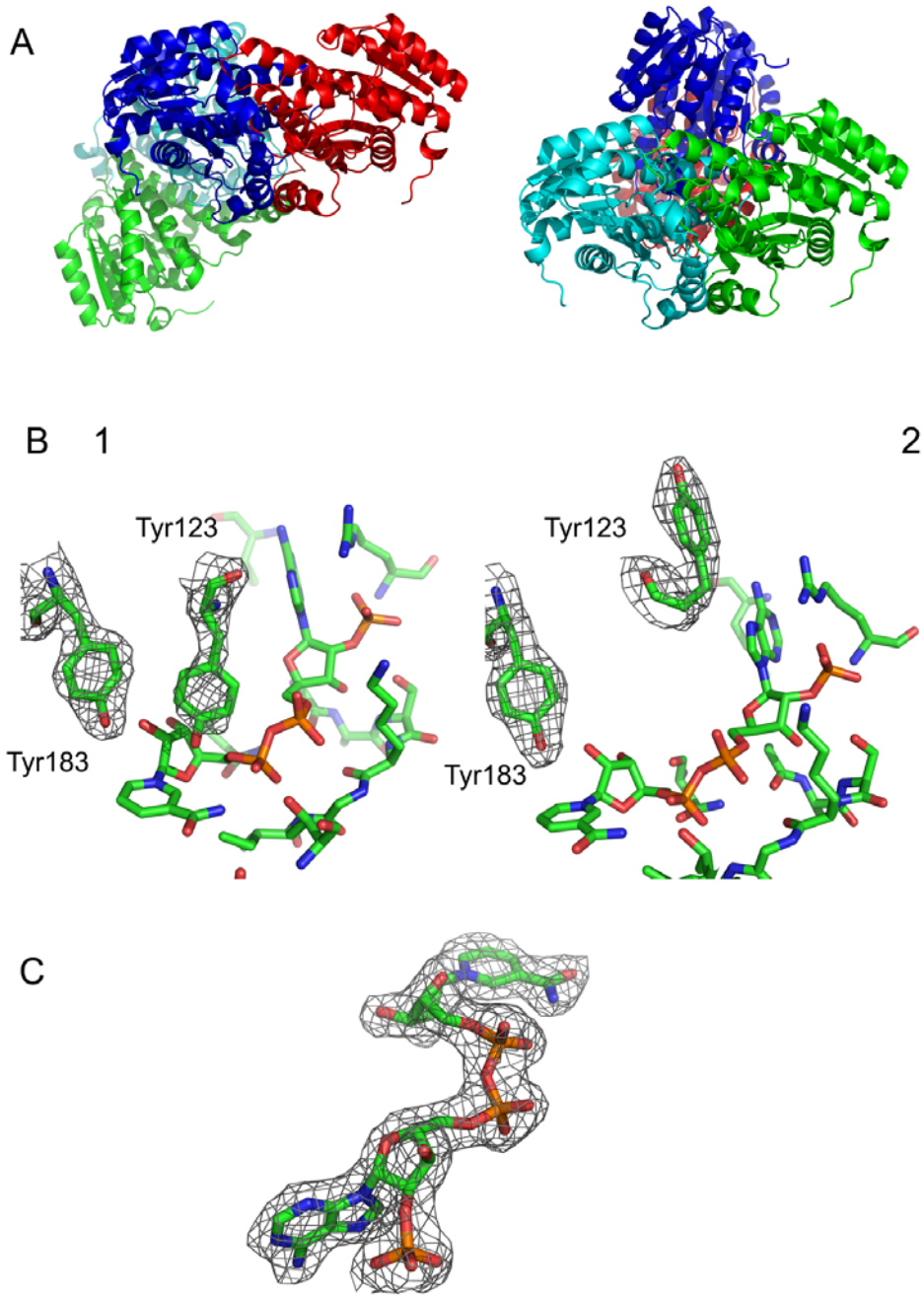

Figure 2.5. Crystal structure of the guinea pig F278E enzyme. The three dimensional structure can be superimposed on the previously published guinea pig structure to a value of 0.48Å RMSD (not shown). A - Tetrameric arrangement of the two guinea pig F278E 11β-HSD1 dimers. Two views are shown to illustrate the orientation of the two dimers. B – The two orientations of Tyr123 seen in the active site of the guinea pig F278E mutant. 1 shows the Tyr123 residue pointing towards the active site which would block substrate binding. 2 shows the Tyr123 residue pointing away from the active site towards bulk solvent, which would allow substrate to bind. C – The bound $NADP^+$ molecule seen in all monomers of the guinea pig F278E tetramer. Map shown in B and C is the 2fofc map produced by Refmac5 to a value of 1.0 sigma. Image produced using PyMOL (DeLano, 2002)

2.3.4. Estimation of proportion of active molecules in the human F278E and wild-type enzymes

Since the crystal structure indicated the guinea pig enzyme contained bound cofactor, we used fluorescence to monitor the single turnover of cofactor on addition of excess steroid to a known amount of protein, as a means to estimate the proportion of molecules which contained bound cofactor and were active. It was assumed that since $NADP^+$ binding is required for correct folding of 11β-HSD1 in the bacterial expression system used, any enzyme which had bound $NADP^+$ would be active. Addition of cortisol to enzyme resulted in a rapid rise in fluorescence due to conversion of endogenous $NADP^+$ to NADPH, which reached a plateau from which the original concentration of $NADP^+$ was estimated. By contrast, addition of cortisone resulted in no change in fluorescence, confirming that the cofactor was present in the enzyme in the oxidized form. Measurements on several preparations of the human F278E enzyme indicated that between 62 and 69% of the protein molecules contained $NADP^+$ and were active. In contrast, measurements on wild-type enzyme yielded values of 20-48%.

2.4. Discussion

It has been hypothesized (Ogg *et al.*, 2005) that due to the unusual charge distribution across the C-terminal helices in the 11β-HSD1 structures, this area could be involved in 'membrane dipping', with residues in this region forming a non-polar plateau encircled by positively charged residues (Figure 1.32). This plateau could exist in the non-polar centre of the membrane, with the charged residues forming salt bridges with the displaced phospholipid and sulpholipid head groups. This conformation might increase accessibility of the enzyme to membrane embedded steroid substrates. The way chosen to test this hypothesis was to mutate the non-polar residues in this region of 11β-HSD1 to the hydrophilic residue glutamic acid, and observe the effect on activity of full-length protein *in vivo*. Firstly, however, the effect of such mutations on enzyme activity and protein structure *in vitro*, in the absence of membranes, had to be established. For this purpose the mutations were introduced into an N-terminally truncated, His-tagged enzyme, produced in a previously developed and validated bacterial expression system (Walker *et al.*, 2001a). C-terminal mutations introduced into the human enzyme were L266E, I275E, F278E and L279E while the equivalent guinea pig enzyme mutants created were Y266E, I275E, F278E and L279E. On expression in *E.coli*, all mutations increased the yield of soluble 11β-HSD1, with human F278E and guinea pig I275E and F278E showing the most dramatic increases compared to wild-type protein (Figure 2.3). Presumably the pronounced surface hydrophobicity of the C-terminal region of the wild-type protein enhances the chance of misfolding and aggregation under the high-level expression conditions of the bacterial expression system. The lack of membrane association via the N-terminal anchor may also compound the problem. The mutations to glutamate introduced here not only decrease hydrophobicity, but also promote repulsion between these regions and thus aid correct folding and solubility. This was evidenced by a reduced formation of insoluble inclusion bodies in addition to an increase in soluble protein production. A similar

increase in solubility has been previously been engineered into several other proteins by mutation of surface hydrophobic residues (Sim and Sim, 1999, Daujotyte *et al.*, 2003, Mosavi and Peng, 2003), often by substitution with negatively charged amino acids (Dale *et al.*, 1994, Nieba *et al.*, 1997), indicating the general applicability of this approach to improving protein expression. Also of interest is that this study indicates that the wild type guinea pig enzyme is naturally more soluble than its human counterpart. This may also be related, at least in part, to surface hydrophobicity of the C-terminal region, in that the guinea pig enzyme has a number of residues with reduced hydrophobicity in this area when compared to the human protein (e.g. Y266 vs. L266, R262 vs. L262).

Sedimentation AUC analysis of purified wild-type and mutant proteins endorsed the concept that aggregation was reduced by the C-terminal mutations (Figure 2.4). Both human and guinea pig wild-type recombinant proteins existed in solution as a collection of aggregated species, with broad c(M) peaks averaging approximately 200 kDa. In contrast the F278E mutants showed a much lower degree of aggregation and a greater degree of monodispersity, with the guinea pig F278E protein appearing to be a stable monodisperse tetramer, and the human F278E protein existing as a concentration-dependent equilibrium of dimer and tetramer.

All the mutant proteins had similar kinetics (k_{cat} and K_m) for the steroid substrate as the wild-type, in both dehydrogenase and reductase directions– a prerequisite for the use of these proteins in the analysis of the membrane dipping hypothesis. The F278E mutants in particular, seem promising for future studies. The guinea-pig F278E protein showed unaltered substrate affinity or turnover rate in either reaction direction, whilst the human F278E protein also showed unaltered K_m values, although, in common with the other mutations to this enzyme, the apparent k_{cat} was significantly higher than wild-type. Since it had previously been shown that bacterially-expressed wild-type human 11β-HSD1 may have

only ~20% active enzyme molecules (Elleby *et al.*, 2004), it seemed likely that the increased specific activity seen with these mutations was due to an increased proportion of active molecules in these preparations. To get an estimate of the proportion of molecules which contained bound $NADP^+$, and therefore the number of active molecules in our enzyme preparations, fluorescence was used to monitor the single turnover of enzyme-bound $NADP^+$ to NADPH on addition of an excess of cortisol. This indicated that 62-69% of the human F278E protein molecules contained bound cofactor and were functional, whereas the proportion for the wild-type was lower at 20-48%. This supports the hypothesis that the increased observed k_{cat} of this mutant is at least in part due to an increased proportion of active molecules in the preparation. It is nevertheless possible that the decreased aggregation status of the mutant also contributes to the increase in turnover rates.

In order to investigate the effect of the C-terminal mutations on the structure of 11β-HSD1, the guinea pig F278E protein was crystallized. The structure of guinea pig F278E reported here is of a higher resolution with a lower R_{free} than that of the previously published wild-type guinea pig structure (PDB code: 1XSE (Ogg *et al.*, 2005)). Of importance, the conditions required to crystallize the guinea pig F278E protein were different from those used previously; in particular it was not necessary to include guanidinium hydrochloride to enhance monodispersity of the enzyme (Ogg *et al.*, 2005). The crystal structure we obtained indicated that the enzyme exists as a tetramer made up of a dimer-of-dimers (Figure 2.5a). This contrasts with the 1XSE structure, which is seen to exist as a single dimer. Analysis of the structure reported here using the PISA server (Krissinel and Henrick, 2007) showed that the interface for the two dimers is sufficient to make the tetramer the most likely quaternary assembly, which is in agreement with the AUC findings that the guinea pig F278E protein exists as a stable tetramer in solution. Apart from this quaternary difference, the structure of each of the guinea pig F278E dimers is largely identical to 1XSE. Interestingly, all monomers

of the F278E protein contained a well-defined $NADP^+$ molecule, even though none was added during any step of the purification or crystallization (Figure 2.5c). This supports previous suggestions that cofactor is required for correct protein folding and conformational stability (Elleby *et al.*, 2004).

The only significant difference that exists between the previously published 1XSE and the guinea pig F278E structure reported here is the orientation of the residue Tyr123. In the 1XSE structure, the Tyr123 in both chains A and B are pointed towards the bound $NADP^+$ molecule. This would not be expected since in the active site of the murine 11β-HSD1 structure (PDB code:1Y5R), the equivalent Gln123 residue is pointing away from the active site allowing the steroid substrate to bind (Filling *et al.*, 2002). If the 1XSE structure is superimposed on 1Y5R, it can be seen that the Tyr123 in this orientation would sterically prevent glucocorticoid binding. To explain this orientation, Ogg *et al.* (2005) hypothesized that a conformational change must be a prerequisite for substrate binding (Ogg *et al.*, 2005). In the structure reported here, two orientations of Tyr123 can be seen. In chains A and D, the Tyr123 is in the same orientation as the 1XSE structure, whilst in chains B and C, the Tyr123 is pointing away from the active site, towards bulk solvent (Figure 2.5b). These two conformations of Tyr123 have also been seen in an unpublished wild-type guinea pig 11β-HSD1 structure (Loh & Ding, pers. comm.). Each dimer therefore has one Tyr123 pointing into the active site and one Tyr123 pointing towards bulk solvent. If the binding of substrate to one subunit would alter the orientation of Tyr123 of the second subunit, thereby altering the affinity for binding of substrate, it could be argued that this conformation of Tyr123 is highly suggestive of cooperative kinetics for 11β-HSD1 (Maser *et al.*, 2002). However, the data from this study and others (Arampatzis *et al.*, 2005, Castro *et al.*, 2007, Shafqat *et al.*, 2003), does not support this concept. The fact that the protein is not in its physiological

environment could mean that the kinetics seen here and elsewhere are not indicative of the in-cell situation.

In summary, in this chapter it has been shown that mutations to the C-terminus of recombinant 11β-HSD1 can increase yield of soluble protein without adversely affecting activity. It has also been shown, using one of the mutants as an example (guinea pig F278E), that these mutations have no adverse effects on structure compared to wild type protein. Hence 11β-HSD1 mutants have been engineered that will be useful, not only for probing membrane interactions, but also for many other future biochemical and biophysical studies of the enzyme due to their increased solubility, monodispersity and in some cases, activity.

Chapter 3. Identification and functional impact of novel mutations in the gene encoding 11β-hydroxysteroid dehydrogenase type 1 in patients with hyperandrogenism

3.1. Introduction

Cortisone reductase deficiency (CRD) is a human disorder in which there is a failure to regenerate the active glucocorticoid cortisol (F) from cortisone (E) via 11β-HSD1 (Tomlinson *et al.*, 2004). A lack of cortisol regeneration stimulates ACTH-mediated adrenal hyperandrogenism, with males manifesting in adolescence with precocious pseudopuberty and females presenting in midlife with hirsuitism, oligoamenorrhoea, and infertility. Biochemically, CRD has been diagnosed through the assessment of urinary cortisol and cortisone metabolites, such as measuring the ratio of tetrahydrocortisol (THF) plus 5α-THF to tetrahydrocortisone (THE) (Figure 1.19). In CRD patients the ratio is typically lower than 0.1 (reference range 0.7–1.2) (Tomlinson *et al.*, 2004). Previous cases of CRD and ACRD were discussed in more detail in Section 1.6. Recent work in our group has highlighted two cases of hyperandrogenism which could potentially be caused by defective 11β-HSD1 activity.

3.1.1. Urinary steroid metabolite analysis

The two cases (A and B) presented with hyperandrogenism and premature pseudopuberty. Measurement of cortisone and cortisol metabolites in the urine of both case A and case B indicated abnormally low activity of 11β-HSD1 (Figure 3.1A & B). Thus a low (THF+5αTHF)/THE ratio was observed in case A (0.26) and B (0.16); both cases were lower than age- and sex-specific reference cohorts. The ratio of cortols to cortolones, which also reflects secondary metabolism of cortisol and cortisone respectively, was also low when compared to age- and sex-specific reference cohorts (Figure 3.1B). In addition, absolute

levels of the metabolites of cortisol and cortisone were analysed (μg/24 h). While the metabolites of cortisol were low to normal, the metabolites of cortisone were extremely elevated compared to age- and sex-specific reference cohorts (Figure 3.1B), again in keeping with a block in 11β-HSD1-mediated cortisone to cortisol conversion. Thus in both cases there were indications of a mild form of cortisone reductase deficiency (CRD), a syndrome previously associated with mutations in the gene encoding the cofactor-regenerating enzyme H6PDH. All urinary analyses were performed by Dr G.A Lavery and results reproduced here with his kind permission.

3.1.2. Molecular analysis of H6PD and HSD11B1 genes

No mutations were identified in *H6PD*. However, sequencing of *HSD11B1* revealed two novel sequence variants in cases A and B, one each in the heterozygous state, which were not detected in 120 control (i.e. normal) chromosomes. Case A was heterozygous for a maternally inherited c.409C>T mutation in exon 4 generating an arginine to cysteine missense mutation (R137C) (Figure 3.1C). Case B was heterozygous for a c.561G>T mutation in exon 5 generating a lysine to asparagine missense mutation (K187N) (Figure 3.1C). All molecular analysis was performed by Dr E.A Walker and results reproduced here with her kind permission.

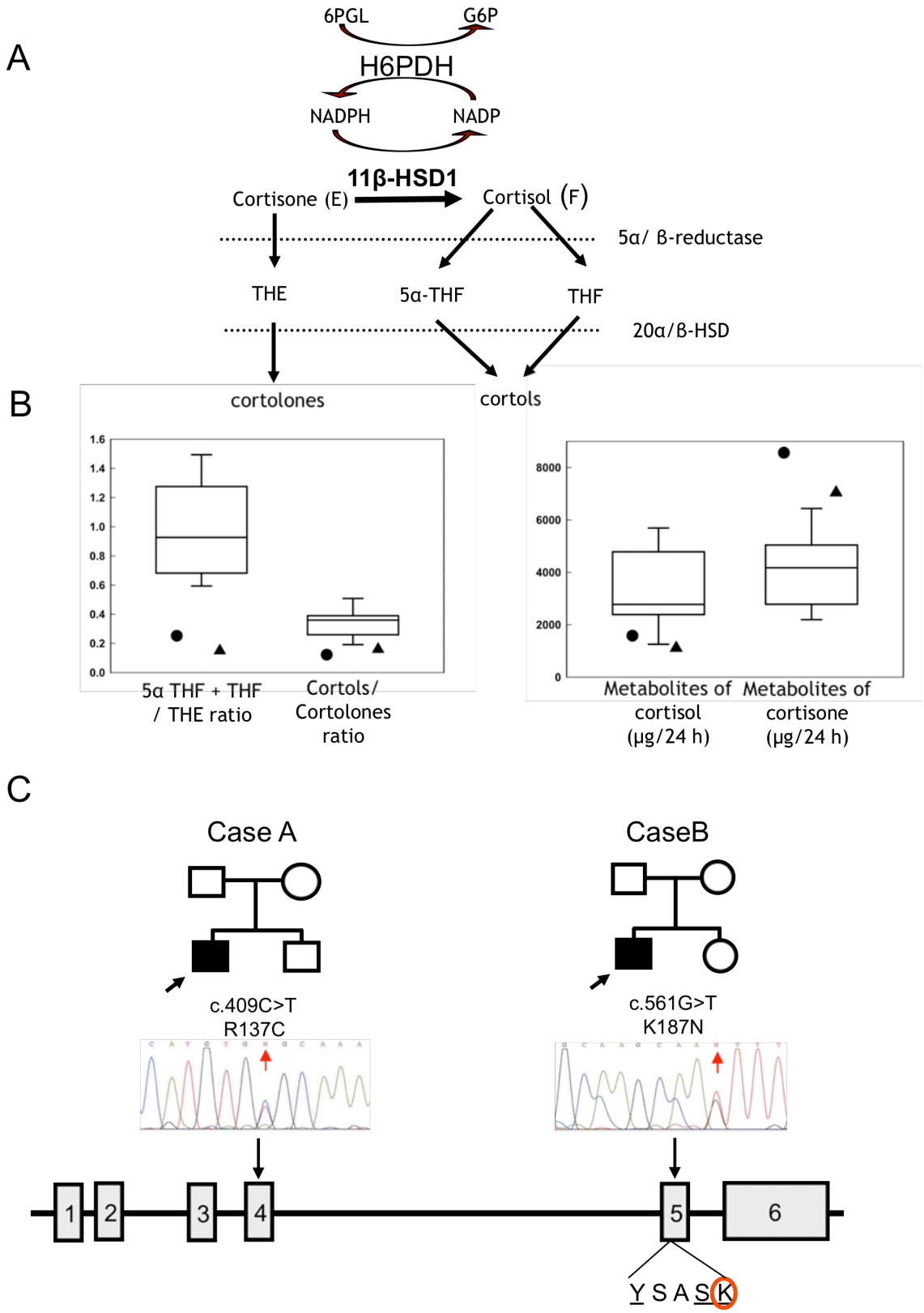

Figure 3.1. Urinary steroid analysis and molecular genetic assessments of cases A and B. A - Schematic representation of the interaction between 11β-HSD1 and H6PDH. H6PDH generates NADPH, enabling 11β-HSD1 ketoreductase activity to convert cortisone (E) to cortisol (F). Cortisone and cortisol are metabolized by 5α- and 5β- reductases to produce THE and 5α-THF and THF respectively. 20α- and 20β-HSDs further metabolize

these to cortolones and cortols. These metabolites are detectable in urine and serve as biomarkers of 11β-HSD1 activity. **B**- Normal ranges for urinary steroid analysis are depicted as box-and-whisker plots and were determined using sex and age specific normal cohorts, which for the purposes of this report are drawn from a cohort of males between the ages of 10 and 16 years of age. Box-and-whisker plots describe the smallest observation (bottom 'whisker'), lower quartile, median (middle line), upper quartile and largest observation (top 'whisker') of the cohort. It can clearly be seen that both case A (●) and case B (▲) have a low 5α-THF + THF/THE ratio, low cortols/cortolones ratio, low total cortisol metabolies and high total cortisone metabolites**.** All of which is indicitive of a block in 11β-HSD1 reductive activity. **C**- HSD11B1 gene mutations in CRD cases A and B. Pedigrees for each case are shown with the affected male being the filled square with unaffected parents and siblings shown by unfilled shapes. The gene structure for HSD11B1 is shown as filled boxes for exons and intervening lines as introns. A sequencing trace is shown indicating the affected nucleotide. The position and alteration at the nucleotide and protein levels are given above each trace. The heterozygous nature of the mutations are shown by the double peak underneath the red arrow. The position of the K187N missense mutation relative to the highly conserved YxxxK catalytic motif is shown below the gene schematic. (Images used with kind permission of Dr E. A. Walker.)

3.1.3. Functional analysis of HSD11B1 mutations

Sequence alignments indicate that R137 and K187 are strictly conserved within 11β-HSD1 proteins from different species (Figure 3.2A & B). K187 is strictly conserved within the short chain dehydrogenase/reductase (SDR) family as a whole, being part of the core catalytic tetrad of Asn, Ser, Tyr and Lys required for enzyme activity (Filling *et al.*, 2002).

Examination of the position of R137 in crystal structures of 11β-HSD1 (PDB entries 2BEL, 2IRW, 3FCO, 1XU7, and 1XU9) reveals a potentially vital role in dimerization of the enzyme via the formation of a salt bridge between R137 on one subunit with E141 on the opposing subunit, with the importance of this interaction discussed in Section 1.6. It seems reasonable to propose therefore that disruption of these strong interactions would hinder subunit-subunit binding and compromise dimer formation and stability.

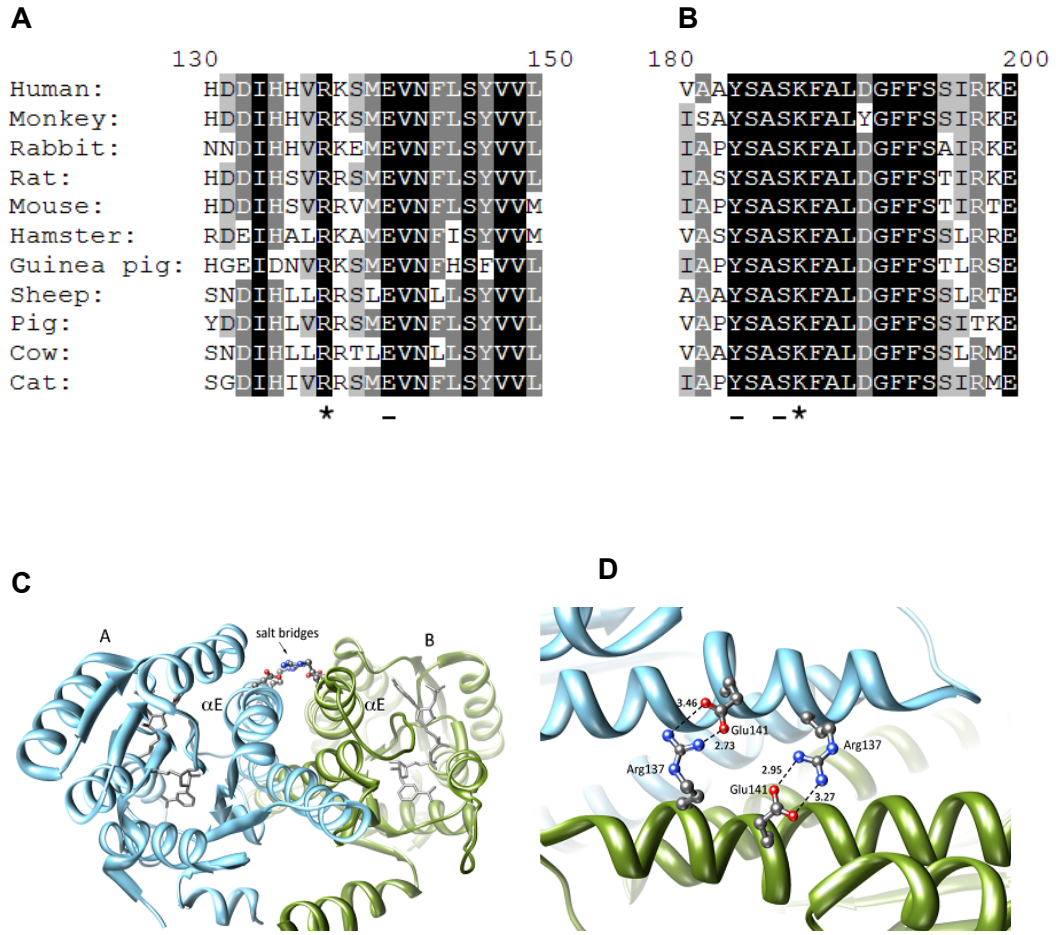

Figure 3.2. The structural importance of the 11β-HSD1 mutations R137C and K187N. **(A)** Alignment showing the strict conservation of R137 (marked with *) in 11β-HSD1 protein sequences from different species. R137 interacts to form a salt-bridge with conserved residue E141 (underlined on the alignment) on the opposing subunit. **(B)** Alignment showing the conservation of K187 (marked with *) across species. K187 forms part of the catalytic tetrad, which includes the adjacent residues Tyr183 and Ser170 (both underlined in the alignment). **(C)** A ribbons representation of the crystal structure of the 11β-HSD1 dimer (PDB code: 2bel, chains A and B) showing the salt bridges between R137 and E141 on the αE helices of opposing subunits. R137 and E141 are represented in ball-stick format coloured by heteroatom. **(D)** A closer view of the side-chain interactions between the two pairs of R137and E141 residues at the subunit interface of 11β-HSD1 (PDB code: 2bel, chains A and B), showing the close interaction (<4Å) between the heavy atoms. The salt-bridges are of the fork-fork class (Folch *et al.*, 2008) in this structure, although other 11β-HSD1 crystal structures show the fork-stick type. These interactions may promote correct orientation of the subunits during dimer formation in addition to stabilizing the final assembly. The position of K187 is shown in Figure 1.29. Structural images produced using UCSF Chimera from the Resource for Biocomputing, Visualization, and Informatics at the University of California, San Francisco (supported by NIH P41 RR-01081) (Pettersen *et al.*, 2004). Distances calculated between nitrogen and oxygen atoms are shown in Å.

3.1.4. Expression in mammalian cells

To further address the functional consequence of these mutations, the R137C and K187N mutants were stably expressed *in vitro* in HEK-293 cells and 11β-HSD1 enzyme activity measured by the conversion of cortisone to cortisol within the intact cells. HEK-293 cells mock-transfected with empty vector had no detectable activity (Figure 3.3A). Upon transfection with WT 11β-HSD1 robust activity was seen; however, when cells were transfected to similar levels (as evidenced by similar mRNA expression; Figure 3.4B) with the two mutant 11β-HSD1 constructs, approximately 5% of WT activity for R137C and no activity from the K187N mutant was detected (Figure 3.3A). Western blot analyses of total lysates from these cells indicated that, compared to WT, low levels of 11β-HSD1 protein accumulated from the R137C mutant (Figure 3.3C), whilst the K187N construct was capable of producing some 11β-HSD1 protein, although it was clearly inactive. All mammalian expression analysis was performed by Dr E.A Walker and results reproduced here with her kind permission

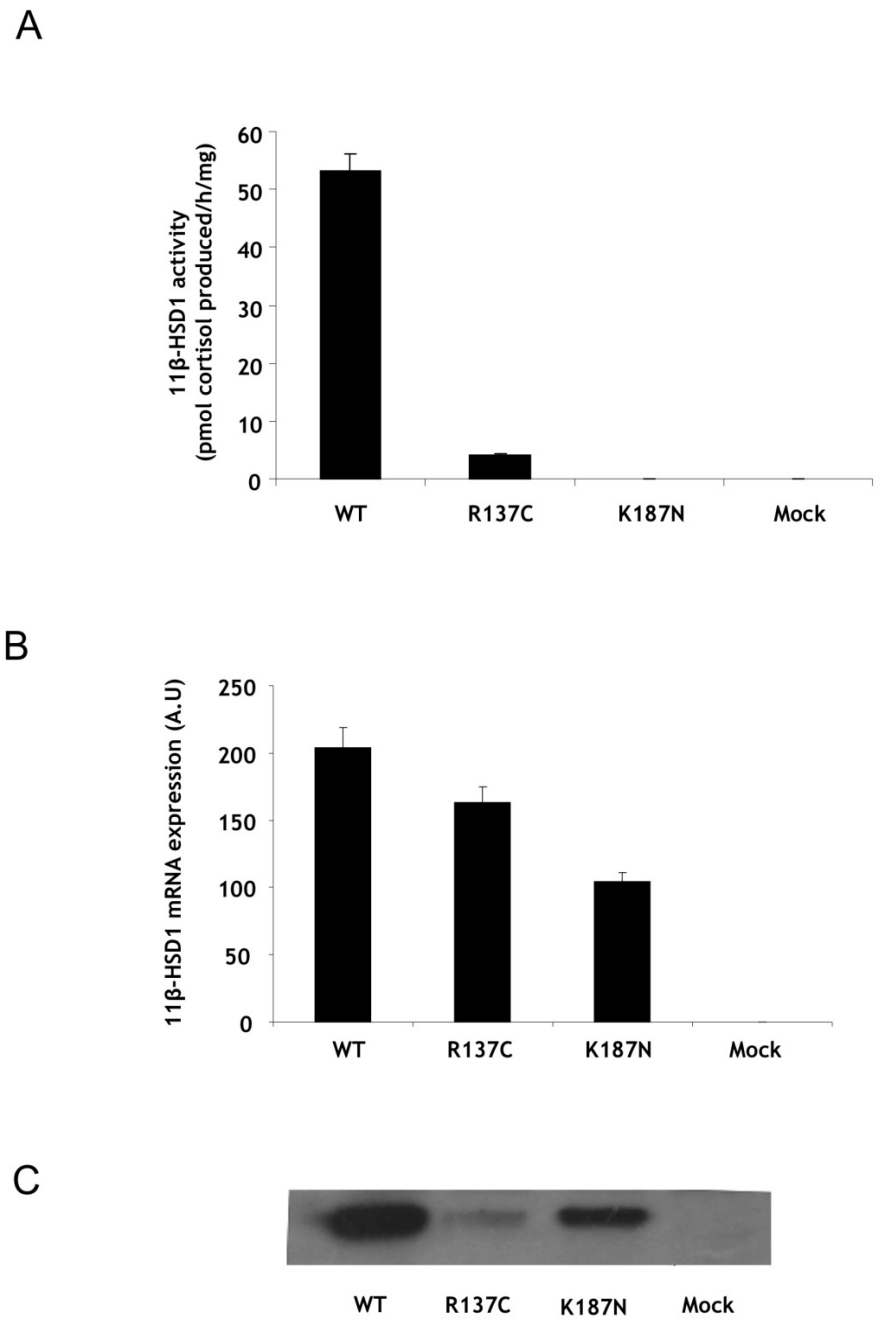

Figure 3.3. 11β-HSD1 ketoreductase activity, mRNA levels, and protein expression from homodimers expressed in stably transfected HEK293 cells (A) 11β-HSD1 enzyme activity assays in HEK 293 cells mock or stably transfected with the WT and mutant cDNA constructs expressed as pmol cortisol produced / mg of protein / h (mean ±SE). Mock treated cells had no 11β-HSD1 ketoreductase activity; Activity in cells transfected with WT 11β-HSD1 was 53.1±3.1 and 4.1±0.4 for the R137C mutant. No ketoreductase activity was detectable for the K187N mutant. (B) Real time- PCR assessment of HSD11B1 gene expression in stably transfected clones compared to mock transfected controls indicating over expression of HSD11B1 mRNA in transfected lines (expressed in arbitrary units, A.U.). (C) Western Blot analysis of whole cell extracts from HEK 293 transfected cells. High levels of WT protein was produced with significantly lower levels from the R137C and K187N mutants. (Images used with kind permission of Dr E. A. Walker).

3.1.5. Hybrid dimers

To complement the work performed on mammalian cells, this chapter will investigate the effect of the two novel 11β-HSD1 mutations (R137C and K187N) on both protein expression and enzyme activity using the recombinant bacterial expression system described in Chapter 2. However, both cases of CRD were in the heterozygous state. In order to investigate the heterozygous nature of the cases, the construction of a novel *in vitro* system which results in the purification of a recombinant 11β-HSD1 heterodimer has been developed. In this system, one monomer contains, in addition to the F278E mutation described in Chapter 2, either the R137C or K187N mutation. The other monomer will only contain the F278E mutation. This technique of creating *in vitro* hybrid dimers has been described previously for both the dimeric *E.coli* biotin carboxylase (Janiyani *et al.*, 2001) and caspase-7 (Denault *et al.*, 2006). Biotin carboxylase is a key enzyme involved in fatty acid synthesis and exists as a homodimer with each monomer containing a functional active site (Janiyani *et al.*, 2001). In order to elucidate how each subunit contributes to the overall function of biotin carboxylase Janiyani *et al.* (2001) created a heterodimeric protein in which one monomer contained a mutation known to significantly decrease enzyme activity, while the other monomer contained no mutation (WT). To aid purification, mutant monomers contained an N-terminal His_6-tag while WT monomers contained an N-terminal FLAG-tag. Expression of both proteins from a single plasmid, with subsequent purification using sequential chromatographic steps (immobilized nickel chelate followed by an anti-FLAG affinity matrix) yielded pure heterodimeric biotin carboxylase (Janiyani *et al.*, 2001). When assayed both *in vitro* and *in vivo*, the presence of mutant monomer in heterodimeric biotin carboxylase showed a dominant negative effect with a 285-fold decrease in activity (Janiyani *et al.*, 2001). This indicated that both subunits are required for activity and that the two subunits of biotin carboxylase must be in communication during enzyme function (Janiyani *et*

al., 2001). These findings have now been supported by a numerical simulation of the biotin carboxylase mechanism which has suggested that the two active sites of the enzyme alternate their catalytic cycles (de Queiroz and Waldrop, 2007). A similar system has been used to investigate the mechanism of dimerization in caspase-7. Caspase-7 is a cytosolic protease involved in apoptosis, with the protein consisting of one large and one small domain joined by a small region known as the interchain connector. In order for caspase-7 to be active, the protein is cleaved in the interchain connector region, which results in formation of the active homodimer (Figure 3.4) (Denault *et al.*, 2006). However, it was not known whether this dimerization was via simple association of C-terminal regions or via interdigitation (Figure 3.4). In order to investigate this, Denault *et al.* (2006) constructed a system in which C-terminal His_6-tagged proteins containing either WT, R233A or C186A/R233A mutations were coexpressed with C-terminal FLAG-tagged WT proteins with the resulting hybrid dimer purified and assayed for activity (Figure 3.4). Since caspase-7 activity is dependent on the presence of both Cys186 and Arg233, they should be able to complement each other if provided individually on the separate units of a dimer if the interdigitation model is correct (Figure 3.4). Since the activity results matched those expected from a direct dimerization, it was concluded that no interdigitation took place (Denault *et al.*, 2006).

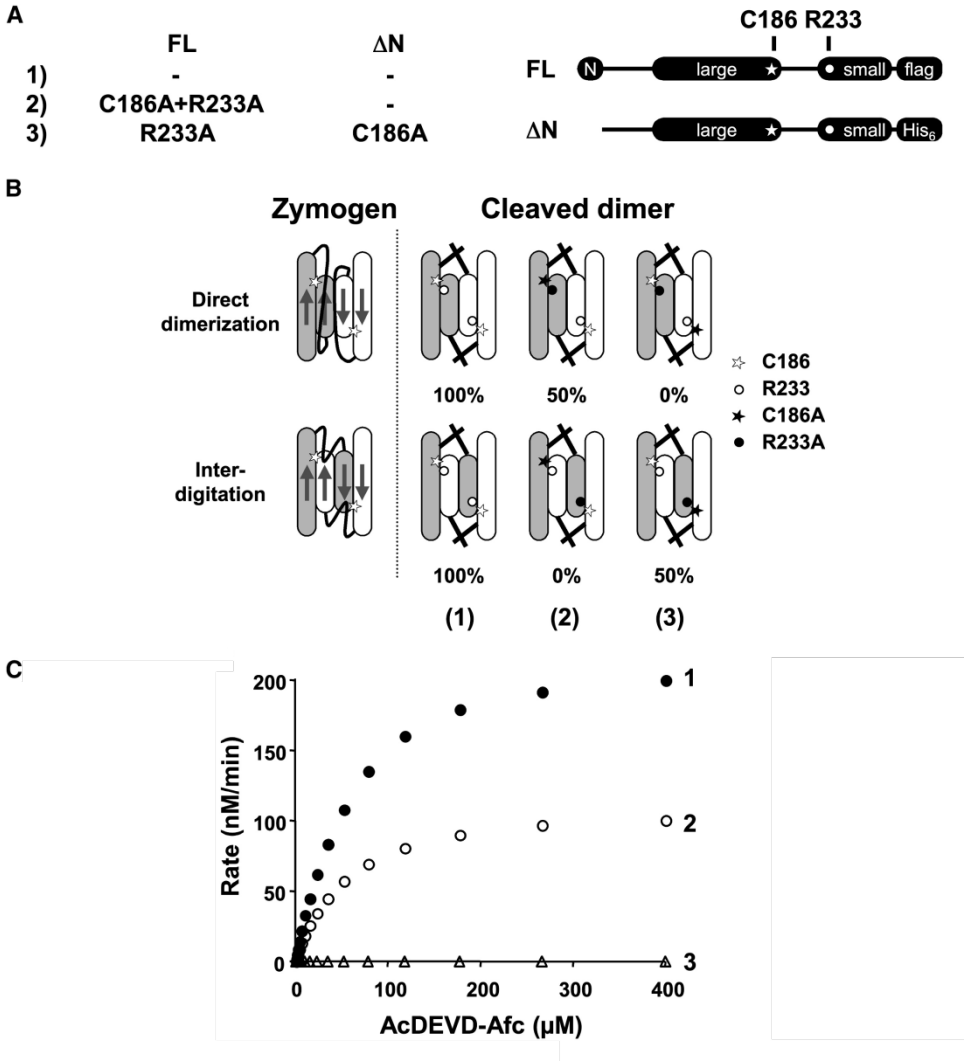

Figure 3.4. **The construction of hybrid dimers has shown that the active caspase-7 dimer does not form by interdigitation**. Caspase-7 consists of one large and one small domain joined by a small region known as the interchain connector. Cleavage of the protein in the interchain connector region results in formation of the active homodimer. A – Schematic representation of the different caspase-7 mutants. ΔN represents a N-terminally deleted caspase-7. This N-terminal deletion allowed the different protein constructs to be distinguished on the basis of size and therefore allowed Denult *et al.* to elucidate which large subunit came from which precusor (i.e. FL or ΔN). B – The possible heterodimers which will be formed. WT residues are shown in white, while mutant residues are shown in black. Enzyme is only active when two unmutated (white) residues come together. Theoretical activity is shown in percent. C – The activity of the purified heterodimers. Since the measured activity matches the theoretical activity of the direct dimerization model (B), it was concluded that this is the correct method of dimerization. Image taken from Denault *et al.* (2006).

In contrast to the studies described above, which labelled one monomer with a poly-His tag and the other with a FLAG tag, in this study one monomer of 11β-HSD1 has been labelled

with a poly-His tag but the other with a Strep-tag due to the high level of purification this system can achieve. Using this system the possible dominant negative effects of the CRD causing mutations R137C and K187N will be analysed.

3.2. Materials and Methods

3.2.1. Cloning and Expression of Recombinant 11β-HSD1

The R137C and K187N mutations were introduced into a bacterial expression construct of the human 11β-HSD1 protein encoding residues 24-292 with or without F278E mutation described previously (Chapter 2) using Quick-change site-directed mutagenesis (Stratagene, La Jolla, CA). The F278E human 11β-HSD1 construct was then cloned from the existing pET-28b(+) (Novagen) vector into pET-51b(+) (Novagen) using BamHI and HindIII. The pET-51b(+) plasmid encodes an N-terminal Strep tag to aid purification, a F1 ori and ampicillin resistance. Three different bacterial expression constructs of the human 11β-HSD1 protein encoding residues 24-292, the single mutant F278E and the double mutants F278E/R137C and F278E/K187N, were cloned from their respective existing pET-28b(+) (Novagen) vectors into separate pRSF-1b (Novagen) vectors using *Bam*HI and *Xho*I. The pRSF-1b plasmid encodes an N-terminal His_6-tag to aid purification, a RSF ori and kanamycin resistance. A summary of the different plasmids used throughout this text is shown in Table 3.1.

Plasmid	Promoter	Ori	Tag	Antibiotic Resistance	Copy Number
pET-28b(+)	T7	F1	Poly-Histidine	Kanamycin	~ 40
pET-51b(+)	T7	F1	Streptavidin	Ampicillin	~ 40
pRSF-1b	T7	RSF	Poly-Histidine	Kanamycin	> 100
pBAD-ESL	P_{BAD}	pBR322	-	Ampicillin	Low
pAJW-3	P_{BAD}	pBR322	-	Chloramphenicol	Low

Table 3.1. Plasmids used for the expression of 11β-HSD1 and chaperonins throughout this thesis. Copy number was estimated based on gel analysis (Sektas, 2002, Held, 2003). pAJW-3 was derived from pBAD18Cm (Guzman *et al.*, 1995).

After sequence verification, constructs were used individually or in combinations, to transform the BL21(DE3) *E.coli* expression strain (Novagen). Cells were co-transformed with the pAJW-3 plasmid (gift of Dr P Lund (Walker, 2000)), which contains the genes for the *E.coli* chaperonins GroEL/ES on the pBAD promoter and also for chloramphenicol resistance. For the expression of the 11β-HSD1 constructs, cells were grown with shaking (220rpm) in LB broth supplemented with either 30 μg ml^{-1} kanamycin (pRSF-1b and pET-28b(+)) or 50 μg ml^{-1} ampicillin (pET-51b(+)) in addition to 50 μg ml^{-1} chloramphenicol at 37 ^{o}C. Cells containing all 3 plasmids were grown on LB broth supplemented with 30 μg ml-1 kanamycin, 50 μg ml^{-1} ampicillin and 50 μg ml^{-1} chloramphenicol. Arabinose (0.02% w/v) was added to the cultures at an A_{600} of 0.8-1, in order to induce the expression of the chaperonin proteins.. Cells were grown with shaking for 1 h at 37 °C, before addition of isopropyl- β-D-thiogalactoside (IPTG, 1 mM). The 11β-HSD inhibitor carbenoxolone (CBX, 0.1 mM) was also added at this stage. Following a further incubation of 30 min at 37˚C, cultures were transferred to 15˚C and grown with shaking for 16 h.

3.2.2. Purification of HIS_6-tagged 11β-HSD1

Cells were pelleted (3000 × g, 15 min) and then resuspended in Bugbuster reagent (Novagen) containing protease inhibitors (Mini-Complete EDTA free, Roche Molecular Biochemicals) and Benzonase DNase (Novagen). Cells were incubated with shaking at room temperature for 40 min, then cell debris was pelleted at 38,000 × g for 30 min at 4˚C. Supernatant was loaded onto a His-Select (Sigma Aldrich) column and washed with buffer containing 25 mM sodium phosphate, 300 mM NaCl, 5% glycerol, 10 mM imidazole and 0.005% Anapoe X-100 (Anatrace Inc), pH 8.0. Protein was then eluted with 3 volumes of buffer containing 175 mM imidazole. Fractions containing protein were separated by size-exclusion chromatography on a Superdex-200 HR10/30 column (Pharmacia) running at 0.4ml min^{-1} in 25 mM sodium phosphate, 5% (v/v) glycerol, 0.005% (v/v) Anapoe X-100, pH 8.0.

3.2.3. Purification of Strep-tagged 11β-HSD1

Cells and cell debris were pelleted as per His_6-tagged protein (above). Supernatant from 38,000 × g spin was loaded onto a Strep-Tactin Superflow Column (Novagen) and washed with buffer containing 25 mM sodium phosphate, 300 mM NaCl, 5% glycerol, 10 mM Imidazole and 0.005% Anapoe X-100 (Anatrace Inc), pH 8.0. Protein was then eluted with 6 volumes of buffer containing 2.5 mM desthiobiotin, a reversibly binding analogue of biotin. Fractions containing protein were separated by size-exclusion chromatography as per His_6-tagged protein.

3.2.4. Estimation of protein concentration

Due to the presence of a high concentration of detergent in all samples in this chapter, the amount of protein in a given sample was measured using the enhanced BCA method (Pierce) (Smith *et al.*, 1985). In this method, a standard amount of sample (100 µl) was mixed with 2 ml of BCA working reagent (50:1, BCA Reagent A: Reagent B) in a test tube and incubated at 60 °C for 30 minutes. Tubes were then cooled to room temperature with the resulting absorbance read at 562 nm. Standard curves were constructed using known amounts of BSA.

3.2.5. Purification of 11β-HSD1 heterodimers

BL21(DE3) cells containing pET-51b(+):F278E, pAJW3 and either pRSF-1b:F278E, F278E/R137C or F278E/K187N were purified as per His_6-tagged 11β-HSD1. The protein concentration in samples was quantified and they were diluted to a final protein concentration of 0.04 mg ml^{-1} and left for 15 h at 15˚C in a buffer containing 25 mM sodium phosphate, 300 mM NaCl, 5% glycerol, 10 mM imidazole and 0.005% Anapoe X-100, pH 8.0. Sample was then loaded onto a His-Select column and eluted as per purification of HIS_6-tagged protein. The protein concentration in samples was once again quantified and samples diluted to a final protein concentration of 0.04 mg ml^{-1} and left for 15 h at 15˚C in the above buffer.

Sample was then loaded onto a Strep-Tactin Superflow Column (Novagen) and eluted as per Strep-tagged protein. Neither tagged construct bound to the heterologous affinity column, as long as 10 mM imidazole was included in the wash buffer.

3.2.6. Measurement of 11β-HSD1 activity

Activity of 11β-HSD1 was assayed as per section 2.2.3.

3.2.7. Western Blot Analysis

Western blots were prepared by electro-blotting 11% SDS-polyacrylamide gels onto Immobilon PVDF membranes (Millipore) at 100 V for 1 h, in a buffer containing 25 mM Tris, 200 mM glycine and 20% (v/v) methanol. SDS-PAGE was performed using the method of Laemmli (1970). Non-specific protein binding to membrane was blocked in PBS containing 0.1% (v/v) Tween-20 and 20% (w/v) skimmed milk powder, washed, and then incubated with either an anti-HIS, anti-STREP, or anti-11β-HSD1 polyclonal antibody (Binding Site) diluted 1/1000 in PBS containing 0.05% (v/v) Tween-20. Membrane was then washed and incubated with secondary antibody (peroxidase-conjugated goat anti-sheep antibody for 11β-HSD1 or peroxidase-conjugated goat anti-mouse antibody for HIS or STREP) diluted 1/25,000 in PBS containing 0.05% (v/v) Tween-20. Detection was by enhanced chemiluminescence (Amersham Biosciences, Bucks, UK) and band intensities were quantified using ImageMaster 1D (Amersham Biosciences). Standards with known amounts of 11β-HSD1 protein were included on each blot.

3.3. Results

3.3.1. Expression and purification of recombinant 11β-HSD1 homodimers using the pET-28b(+) vector

In order to obtain more accurate kinetic data for the CRD causing mutations when compared to expression in HEK-293 cells, the R137C and K187N mutations were introduced into the recombinant *E.coli* system outlined in Section 2.2.1. Expression of the R137C and K187N mutants in the wild type protein background did not yield any soluble protein in this system (Figure 3.5a). In Section 2.3, it was shown that a single point mutation, F278E, to the C-terminus of 11β-HSD1 could increase solubility of recombinant protein while not adversely affecting activity. Although expression of the active site mutant K187N in the human F278E background did not yield any soluble protein expression of the R137C mutation in the human F278E background did result in soluble protein, albeit with an 80% reduction in protein yield (Figure 3.5b). Kinetic analysis of the R137C/F278E mutant showed a pronounced reduction of the k_{cat} of the enzyme from 1.27 ± 0.03min^{-1} to 0.48 ± 0.02min^{-1} for the dehydrogenase reaction and 0.31 ± 0.01min^{-1} to 0.09 ± 0.01min^{-1} for the reductive reaction (compared to the F278E control). The R137C mutation had little effect on the K_m of the enzyme showing a small decrease in the dehydrogenase direction (6.16 ± 0.44μM to 4.82 ± 0.62μM) and a small increase in the reductive reaction (10.61 ± 1.49μM to 15.42 ± 5.93μM). Since soluble protein could only be obtained for the R137C mutant with the inclusion of the F278E mutation, this F278E background was therefore used for all experiments in this chapter.

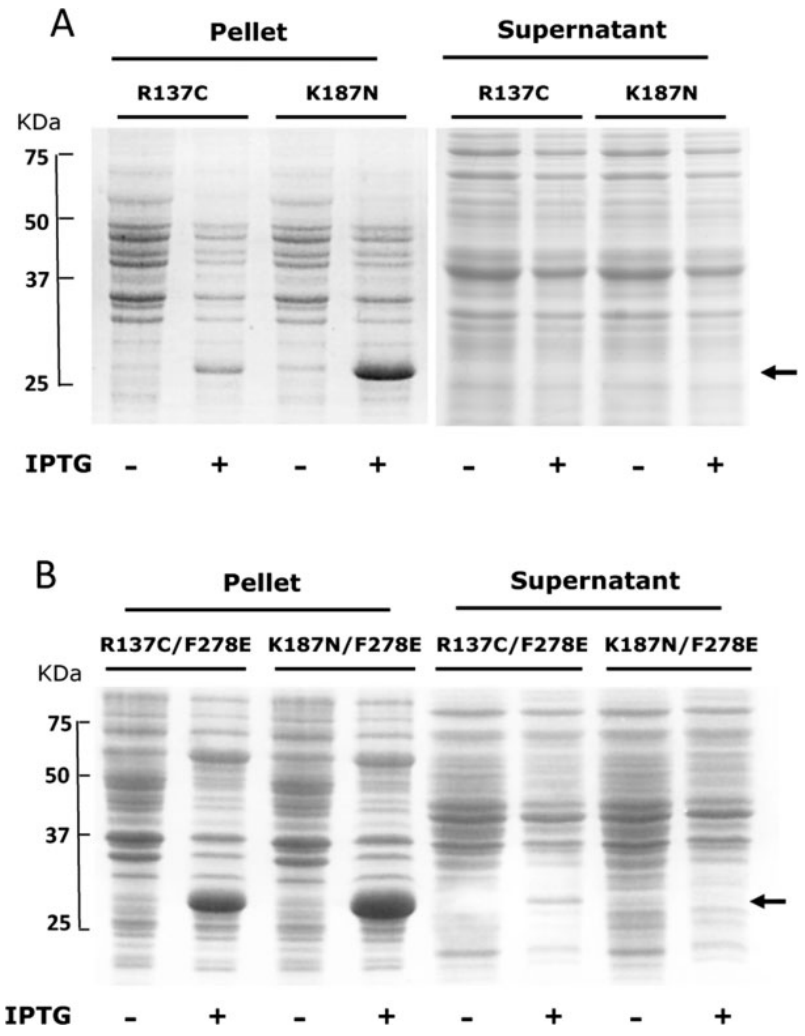

Figure 3.5. SDS-Page analysis of expression in *E.coli* of the human 11 β -HSD1 mutants (R137C and K187N) in both wild-type (A) and F278E (B) backgrounds. A - Insoluble (pellets) and soluble (supernatant) fractions from lysates of cultures expressing R137C and K187N mutants in the wild-type background. Expression levels of both recombinant proteins were low and neither mutant was expressed in a soluble form. B - Insoluble (pellets) and soluble (supernatant) fractions from lysates of cultures expressing the double mutants R137C/F278E and K187N/F278E. Arrows indicate position of the recombinant proteins. Although the protein produced was still largely insoluble, some soluble protein was evident in the supernatant for the F278E/R137C mutant.

3.3.2. Expression and purification of recombinant 11β-HSD1 homo-oligomers using pRSF-1b and pET-51b(+) vectors

In order to investigate the potential dominant negative effects of the CRD-causing mutations R137C and K187N on 11β-HSD1 activity, a recombinant system using two different

plasmids which express 11β-HSD1 was constructed. The previously used pET-28 plasmid could not be used as it was not suitable for dual expression analysis. Firstly, the human 11β-HSD1 F278E construct was cloned from the pET-28b(+) plasmid into a new plasmid, pET-51b(+), which encodes an N-terminal Strep tag, a F1 ori and ampicillin resistance. This plasmid was transformed into the BL21(DE3) *E.coli* expression strain along with the GroEL/GroES encoding plasmid, pAJW3. Protein was then purified as per Section 3.2.3. SDS-PAGE analysis of the Strep-Tactin Superflow chromatography is shown in Figure 3.6. After subsequent purification by gel filtration, the resulting human pET-51b(+) F278E homo-oligomer had the same k_{cat} and K_m for cortisol as the pET-28b(+) homo-oligomer construct described previously, although, it is worth noting that the yield of soluble protein was lower than with the pET28(+) construct.

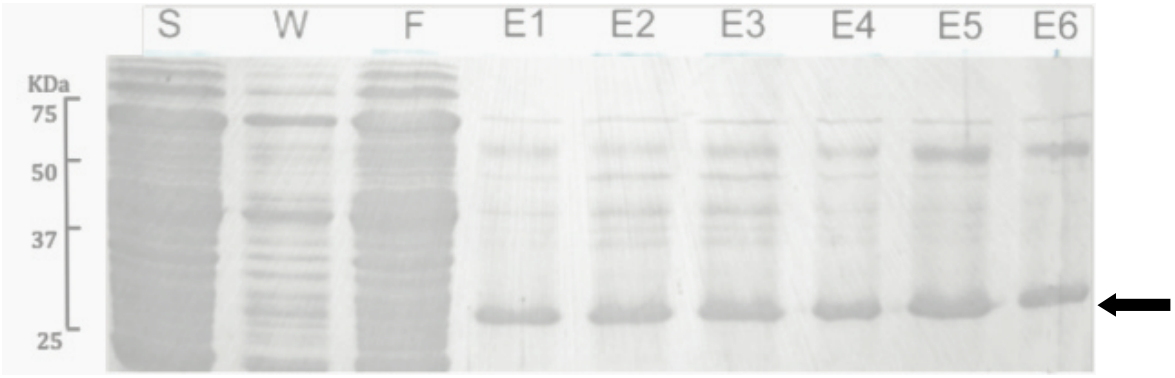

Figure 3.6. SDS-PAGE of the purification of the pET-51b(+) 11β-HSD1 F278E construct via the Strep-Tactin Superflow column. Fractions were eluted with 2.5 mM desthiobiotin. Eluted fractions containing protein were subsequently purified via gel filtration. S=supernatant applied to column; W=wash; F=flow-through; E=successive fractions (0.5 ml) eluted with desthiobiotin. The position of 11β-HSD1 is shown by the black arrow.

Three different bacterial expression constructs encoding the human 11β-HSD1 protein (containing residues 24-292), the single F278E mutant and the double mutants F278E/R137C and F278E/K187N, were cloned from their respective existing pET-28b(+) vectors into

separate pRSF-1b vectors which encode an N-terminal His_6-tag, a RSF ori and kanamycin resistance. These plasmids were transformed into the BL21(DE3) *E.coli* expression strain along with the GroEL/GroES encoding plasmid, pAJW3. Protein was then purified as per Section 3.2.2. Like the pET-51b(+) construct, after subsequent purification by gel filtration, the resulting human pRSF-1b F278E homo-oligomer had the same k_{cat} and K_m for cortisol as the pET-28b(+) homo-oligomer construct described previously. Interestingly, the yield of soluble protein for this construct was also lower than the pET28(+) construct.

Introduction of the gene for K187N into pRSF-1b resulted in a complete absence of any soluble protein, while the equivalent R137C/F278E construct yielded 6 times less soluble protein than F278E (Figure 3.7). The yield of total protein (soluble+insoluble) was not significantly affected by the mutations. Thus both mutations drastically affected either subunit folding or dimer assembly/stability in this expression system. The R137C mutant protein also showed a small decrease in turnover rate (k_{cat}), although there was no significant change in K_m (Figure 3.7). This is in agreement with the studies using pET-28 constructs and parallels the results obtained from the mammalian expression system (Figure 3.4). Using AUC, the R137C/F278E mutant protein was observed to exist in a similar dimer/tetramer equilibrium to the background F278E protein (Figure 3.8).

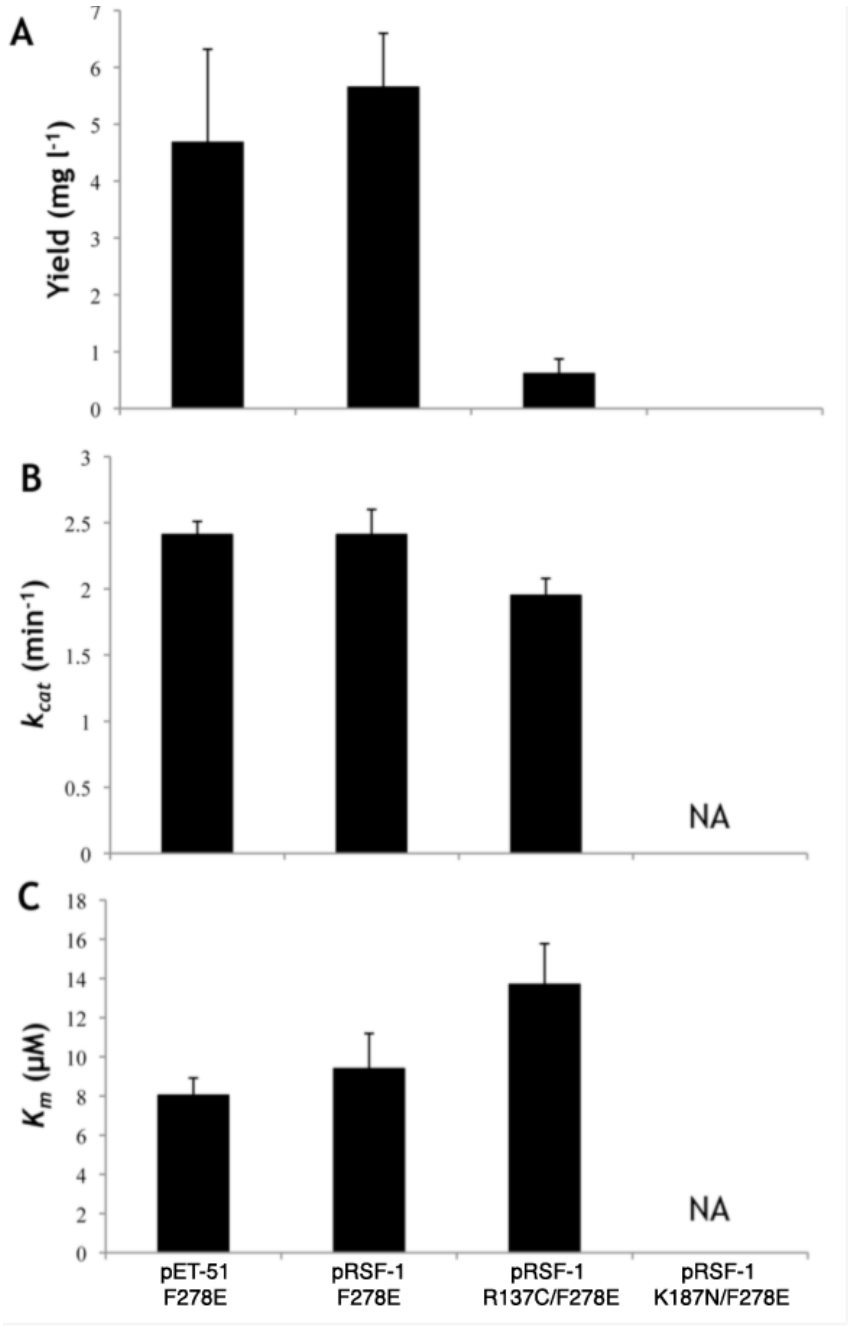

Figure 3.7. Yield of soluble protein and kinetic parameters of homo-oligomers of 11β-HSD1 in the bacterial expression system. (A) Yield of soluble, purified, 11β-HSD1 protein. Values are given in mg of protein purified per litre of LB broth. Bars represent SEM. (B) Turnover rates (k_{cat}) for the conversion of cortisol to cortisone. The decrease observed for the R137C/F278E mutant is statistically significant ($p<0.05$). No data are available for the K187N/F278E mutant, because no soluble protein was produced. (C) K_m values for cortisol for F278E and mutant proteins. The increase observed for the R137C/F278E mutant when compared to F278E is not statistically significant. No data are presented for the K187N/F278E mutant, because no soluble protein was produced. Bars represent SEM.

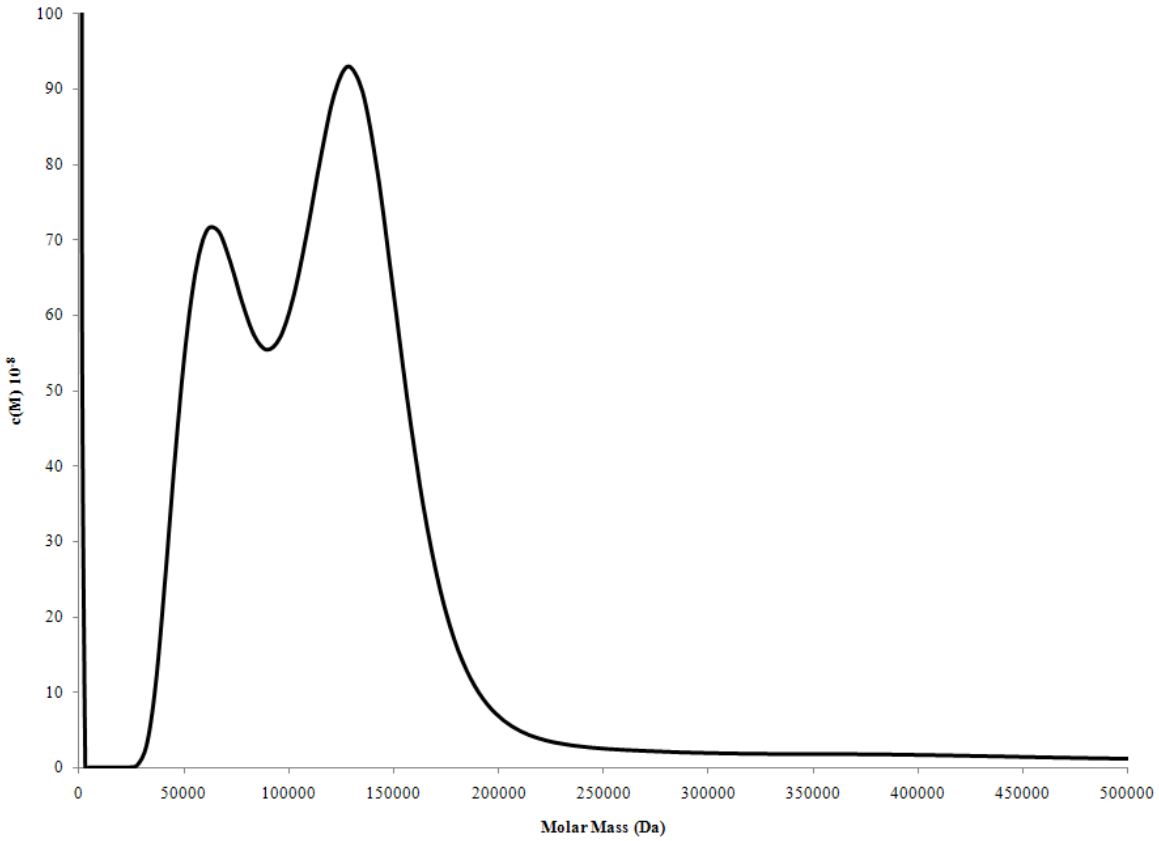

Figure 3.8. AUC analysis of the aggregation states of the R137C/F278E protein when expressed in the pRSF-1b vector. The mutant protein showed a main peak at 130kDa, in addition to a second major peak at 65kDa, indicating the majority of protein existed as tetramer with a lesser amount as a dimeric protein. This shows that the protein exists in a similar dimer/tetramer equilibrium to the background F278E protein illustrated previously (Figure 2.5). Images were produced using SedFit (Schuck 2000) with density, viscosity and v-bar measurements calculated by Sednterp. Human and guinea pig v-bar measurements were 0.7405 and 0.7391 respectively. The buffer had a density (P) value of 1.016 and viscosity (H) value of 1.18 E-2.

3.3.3. Analysis of 11β-HSD1 hetero-oligomers in cleared lysates of bacterial cells

In order to fully investigate the effects of the R137C & K187N mutations on heterodimer formation and activity, bacterial cells were simultaneously transformed with both the pRSF-1 and the pET-51 plasmids, with one vector containing F278E 11β-HSD1 and one containing the F278E Construct carrying either the R137C or K187N mutant. The effect of this dual expression of F278E and mutant (R137C/F278E or K187N/F278E) constructs was initially estimated by assaying total enzyme activity, and relative amounts of His/Strep tag, in cleared lysates of the bacterial cells (Figure 3.9). When both plasmids contained the F278E construct,

the pET-51 plasmid expressed more soluble protein than pRSF-1, as evidenced by a higher level of Strep-tagged than His-tagged protein when quantified by Western blotting (Figure 3.9B). This could be due to either greater promoter efficiency or higher copy number of pET-51. When the R137C or K187N mutations were present in the pRSF-1 F278E plasmid, a decrease in total enzyme activity of 40-50% was observed (Figure 3.9A). There was also a significant reduction (by 55-65%) in the amount of mutant polypeptide found in the soluble fraction, although the level of soluble F278E subunit (from pET-51) was much less affected (Figure 3.9B). A greater decrease in enzyme activity, of 85-95%, was observed in the reverse situation, when the mutants were present in the pET-51 plasmid with pRSF-1 expressing F278E protein (Figure 3.9A). This was accompanied by a substantial decrease in the amount of both F278E and mutant polypeptide in the soluble fraction (Figure 3.9B). This suggested that in this situation, due to the greater amount of mutant protein produced by the pET-51 plasmid, more F278E monomers were interacting with mutant monomers and forming unstable/insoluble heterodimers, or other complexes, and hence the reduction in enzyme activity.

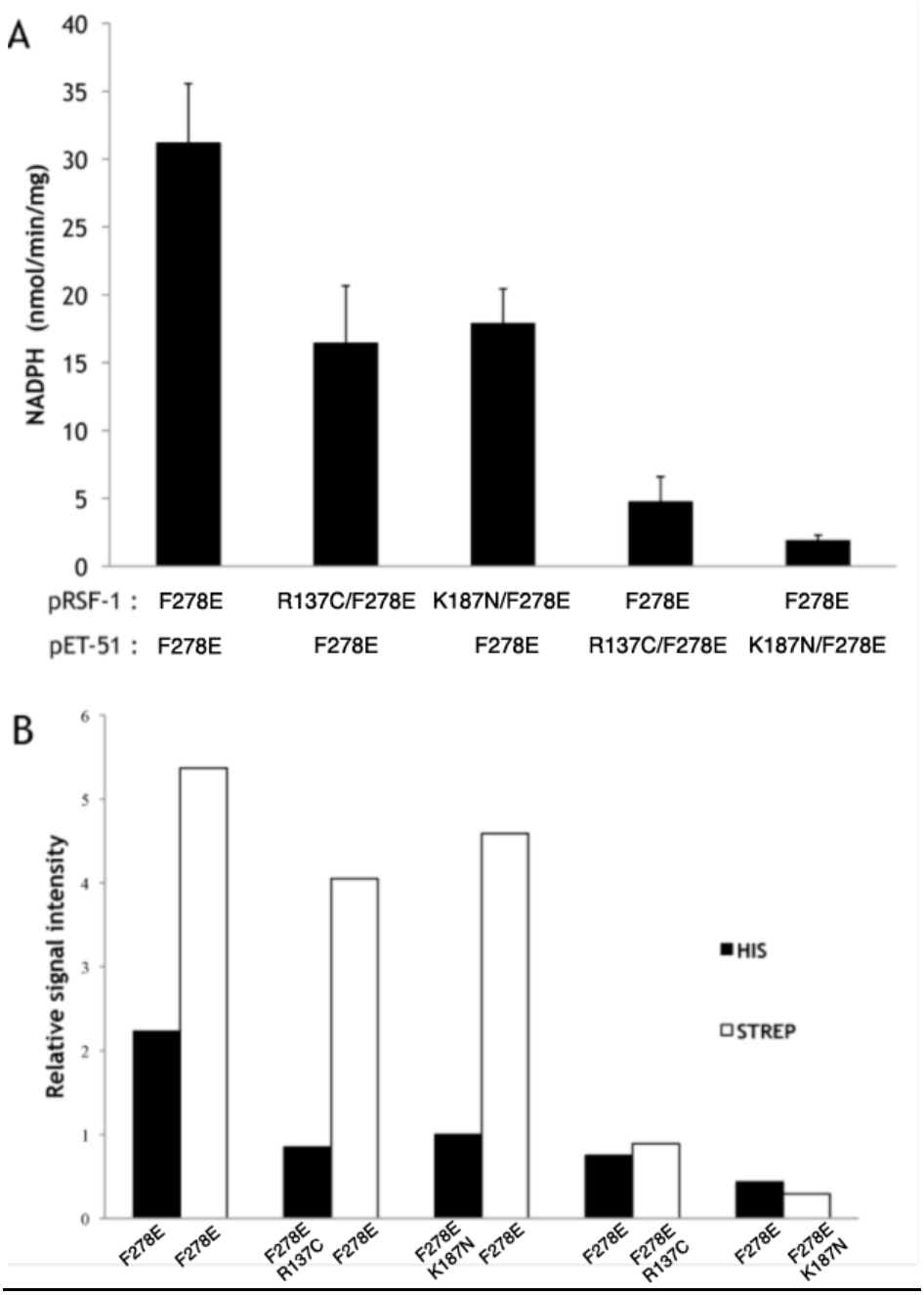

Figure 3.9. Effect of co-expression of mutant and F278E 11β-HSD1 constructs in *E.coli*.. **(A)** Specific enzyme activity of cleared lysates of bacteria transformed with two plasmids: - pET-51 encoding a Strep-tagged protein, and pRSF-1 encoding a His_6-tagged protein. Enzyme activity was measured in the dehydrogenase direction (conversion of cortisol to cortisone) at saturating (128 μM) substrate concentrations. NADP(H) concentration was 200 μM. Expression of the mutants (R137C or K187N) from the pRSF1 plasmid resulted in a decrease in enzyme activity, but the decrease was much greater when the mutants were in pET-51. **(B)** Western blot densitometry analysis of relative concentrations of His- and Strep-tags in cleared bacterial lysates. Expression of either mutant caused a reduction in both mutant and wild-type polypeptides found in soluble form, but the effect was greater when the mutants were in pET-51. Note the greater expression of Strep-tagged protein driven by pET-51, compared to His-tagged from pRSF-1, in the F278E/F278E control.

3.3.4. Purification and kinetic analysis of 11β-HSD1 heterodimers

In order to elucidate the true effect of both the R137C and K187N mutants on heterodimer formation and activity, a protocol was developed to purify mutant/WT heterodimers from the bacterial lysates. The procedure exploited the different N-terminal tags on the different constructs, which meant that addition of lysate to a His-column with eluted protein applied to a subsequent Strep-column would theoretically isolate pure hybrid dimeric protein. However, several problems exist in this idealised experimental procedure for the isolation of a hybrid dimer. Firstly, the experiment assumes that no exchange of monomeric subunits between dimers occurs during the experiment. Secondly, the concentration dependent equilibrium of the human 11β-HSD1 mutant F278E between dimeric and tetrameric species could lead to a mix of species which could influence correct binding (Figure 3.11A). Both of these problems were tested by a control experiment in which an equal amount of homodimeric His-tagged F278E (2 mg) and homodimeric Strep-tagged F278E (2 mg) were mixed, diluted to 0.04 mg $ml^{-1}$and left to equilibrate for 15 h at 15˚C. The mix of protein was then applied to a His-select column. Protein assay showed that 2mg of protein was present in the flow-through with 1.7 mg of protein bound to the His-resin. The 1.7 mg of eluted protein was then diluted, left to equilibrate (as per His-select column) and applied to the Strep-Tactin Superflow column. Protein assay showed that 0.03 mg of protein bound to the Strep-resin with 1.4 mg of protein present in the flow-through. SDS-PAGE analysis confirmed the only protein assayed was 11β-HSD1 (Figure 3.10). The correct stoichiometric binding of His-tagged protein to the HIS-Select column and subsequent lack of binding to the Strep-Tactin Superflow column indicates that, with the large dilution step, 11β-HSD1 is present as a dimeric species when applied to both columns. It can also be concluded that there was no exchange of monomeric subunits between dimers for the timescale of the experiment. The protocol for the purification of hybrid dimers is outlined in Figure 3.11. Following the procedure, the presence of true

heterodimers was additionally confirmed by analysis of the relative proportions of His and Strep tags by standardised Western blots. All purified preparations showed equal levels of the two tags (Figure 3.12), as expected for true heterodimers

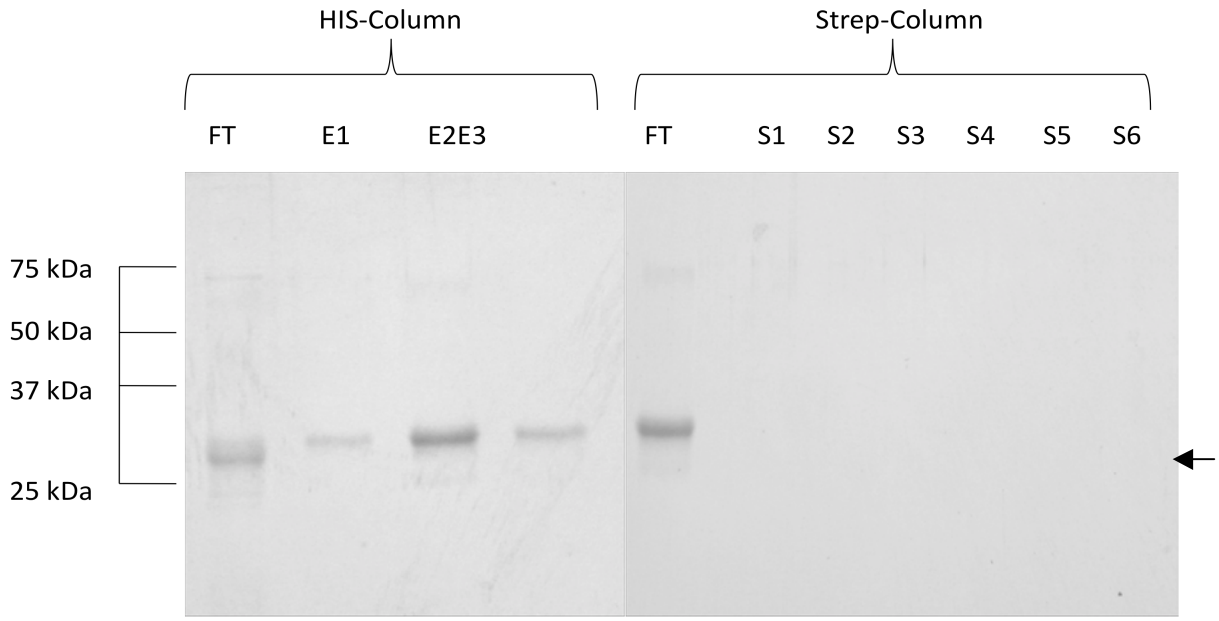

Figure 3.10. SDS-PAGE demonstrating that, with a dilution step, no aggregation of 11β-HSD1 dimers occurs. An equimolar mix of homodimeric His-tagged F278E and homodimeric Strep-tagged F278E were mixed, diluted, left to equilibrate and applied to a His-Select column. The gel shows that around half the protein applied bound to the resin. When this bound protein was eluted, diluted, left to equilibrate and applied to a Strep-Tactin Superflow column, no protein bound to the resin. The gel also shows that there was no exchange of monomeric subunits between dimers for the timescale of the experiment. FT=Flow through concentrated to 0.5ml. E=successive fractions eluted with imidazole. S=successive fractions eluted with desthiobiotin. An arrow indicates the position of 11β-HSD1.

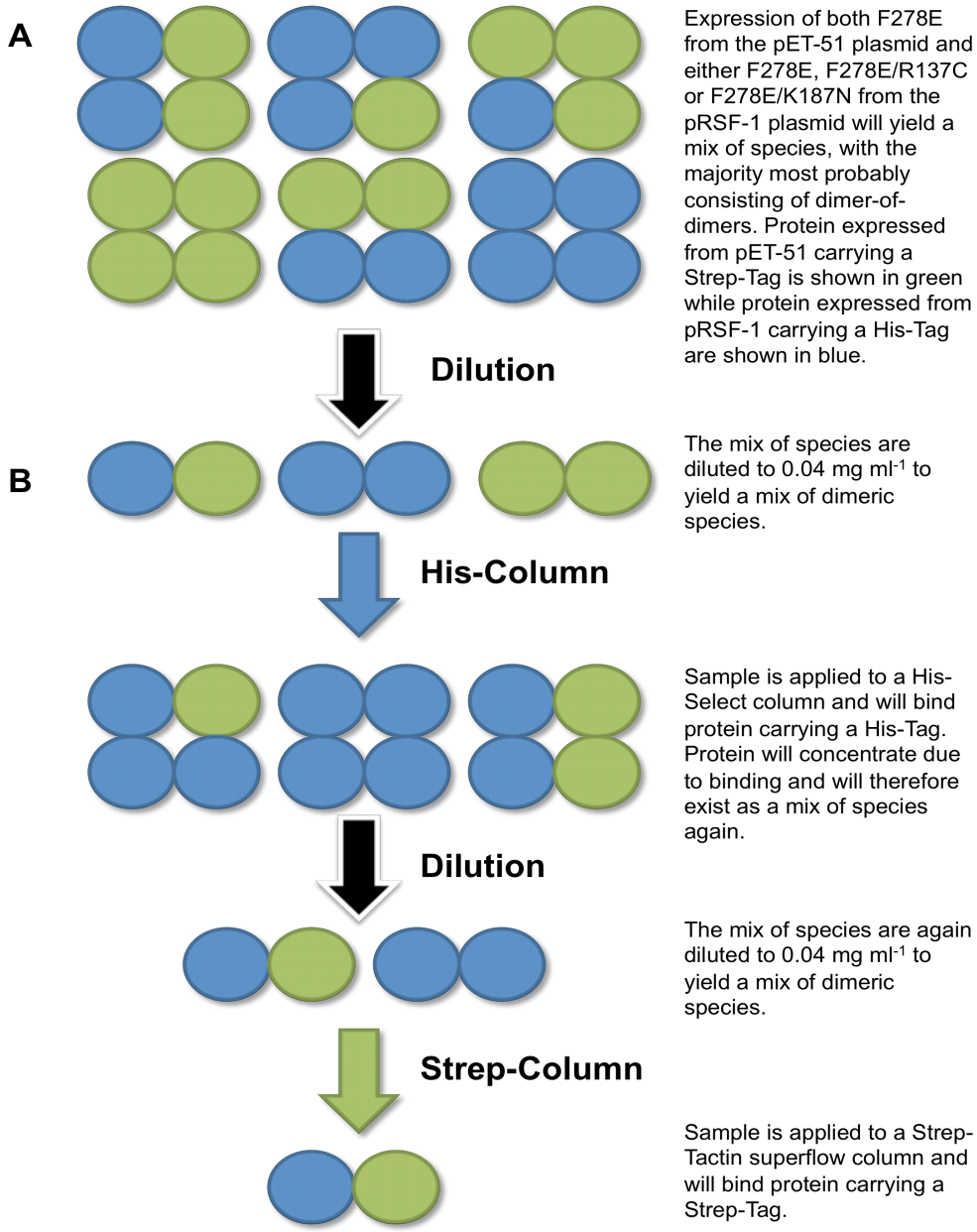

Figure 3.11. An illustration of the purification strategy for the production of hybrid dimer human 11β-HSD1. His_6-tagged proteins are shown in blue, with Strep-tagged proteins shown in green. *E.coli* is transformed with two plasmids which can express a combination of F278E-F278E homodimers, F278E-R137C/F278E heterodimers and R137C/F278E-R137C/F278E homodimers. After a dilution step, the initial purification, using a His-select column, will bind only WT-R137C heterodimers and R137C-R137C homodimers. The second purification using a Strep-Tactin Superflow column, once again after a dilution step, will bind only the WT-R137C heterodimers, as the R137C-R137C homodimers do not contain a Strep-tag. This process will also be used to purify the human 11β-HSD1 heterodimer WT-K187N. Western blot analysis of the samples assayed confirmed that the purification procedure detailed here yielded samples which contained an approximate 50:50 mix of His and Strep-Tags indicating hybrid dimers were the species assayed (Figure 3.12).

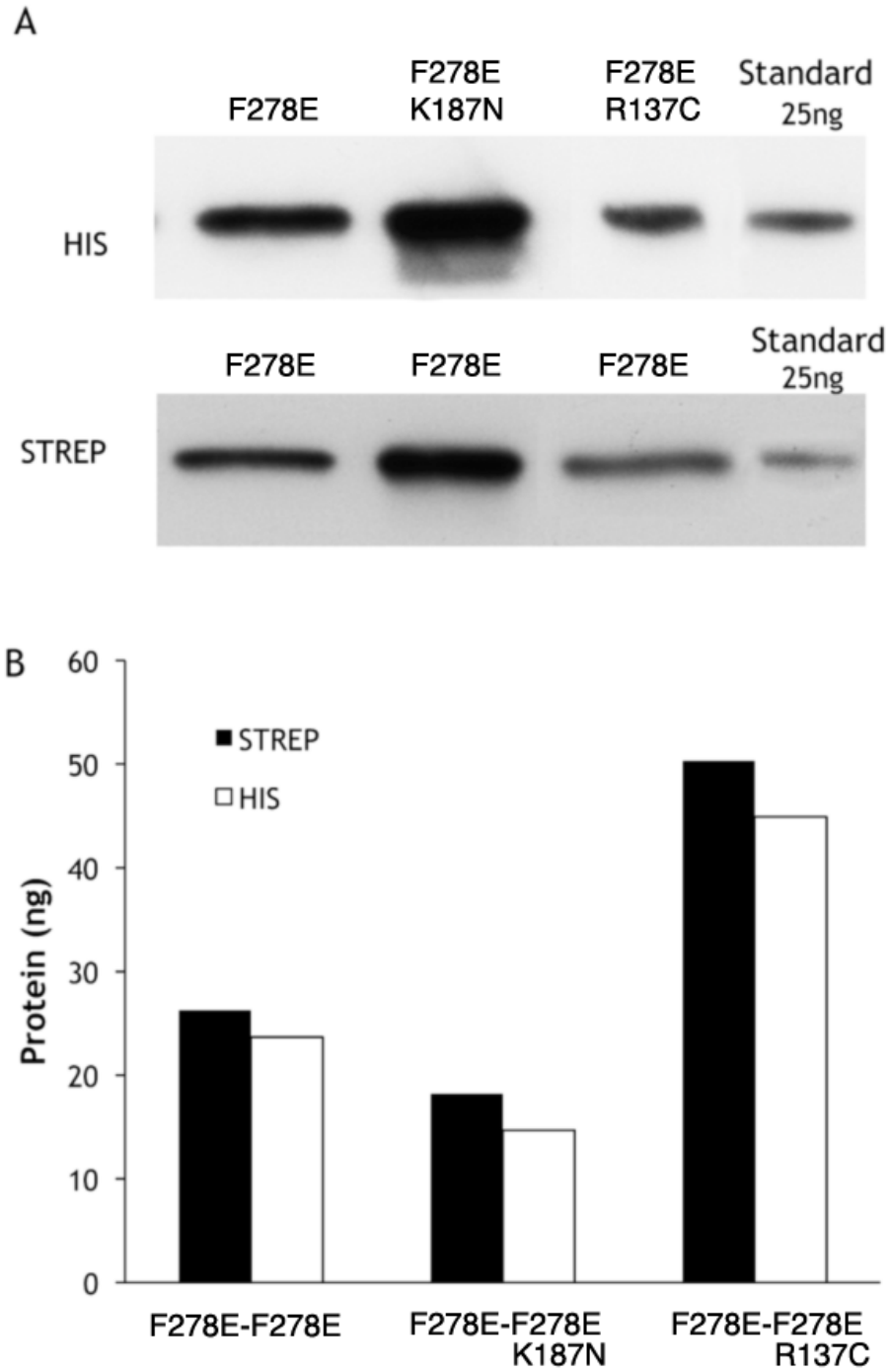

Figure 3.12. Western blot analysis of the hybrid dimers of 11β-HSD1 purified from the bacterial expression system. (A) Western blot of the samples analysed in Table 3.1. Anti-His and anti-Strep antibodies were used to detect the two different monomers in the purified heterodimers. **(B)** Densitometry estimation of concentrations of His- and Strep-tags in the purified heterodimers. The intensity of bands in (A) was analysed and used to calculate the protein amount (ng) present on the blots. The results confirmed that, for all samples, there was an equal amount of Strep and His tagged protein on the blot, in agreement with the production of hybrid dimers.

The F278E-F278E hybrid dimer had unchanged k_{cat} and K_m when compared to either the pET-51b or pRSF-1b F278E homo-oligomer (Figure 3.5 & Table 3.2). However, the yield of soluble protein has decreased significantly. This is perhaps not surprising as a certain amount of non-specific binding would be expected at each stage of the purification procedure shown in Figure 3.11. The F278E-R137C/F278E hybrid dimer showed a slight reduction in k_{cat} with a pronounced reduction in yield compared to the F278E-F278E hybrid dimer (Table 3.2). Interestingly, the 75% reduction in yield and 20% reduction in k_{cat} for the F278E-R137C/F278E hybrid dimer is highly similar to the 80% decrease in yield and 15% decrease in k_{cat} observed when homo-oligomeric pRSF-1b R137C/F278E is compared to pRSF-1b F278E homodimer (Figure 3.5). This is highly suggestive that the deleterious effects on subunit folding or dimer assembly/stability of the R137C mutation in one monomer, can affect the activity of other, fully active monomer. The F278E-K187N/F278E hybrid dimer showed a similar 75% decrease in yield compared to F278E-F278E; however the protein produced was inactive (Table 3.2). Once again, this suggests that the deleterious effects of the K187N mutation, in this case inactivity, will knock out activity of the active F278E monomer, leading to an inactive 11β-HSD1 protein.

Construct				
pRSF-1 (His tag)	**pET-51 (Strep tag)**	**Yield (mg l^{-1})**	**k_{cat} (min^{-1})**	**K_m (μM)**
F278E	F278E	0.047 ± 0.003	2.29 ± 0.17	7.62 ± 1.45
R137C/F278E	F278E	0.008 ± 0.001	1.73 ± 0.15	14.72 ± 2.81
K187N/F278E	F278E	0.008 ± 0.004	-	-

Table 3.2. Yield of soluble protein and kinetic parameters and for the various hybrid dimers of 11β-HSD1 purified from the bacterial expression system. The k_{cat} and K_m values for the F278E-His/F278E-Strep heterodimer construct are not significantly different from the previous homodimeric F278E constructs, although the yield of the heterodimer is lower. Heterodimeric R137C/F278E-F278E constructs have decreased k_{cat} values and increased K_m values; there is also a significant reduction in the yield of soluble protein compared to the F278E-F278E equivalent. Heterodimeric K187/F278E-F278E constructs have no detectable enzyme activity, in addition to a significant reduction in the yield of soluble protein. Yield values are given in mg of protein per litre of LB broth ± SEM. Yield data is based on duplicate protein preperations with kinetic measurements reported as an average of duplicate measurements on each preperation.

3.4. Discussion

Prior to this work, deficiency in the reduction of cortisone to cortisol had previously only been attributed to mutations in the gene encoding H6PDH, the enzyme that supplies NADPH to 11β-HSD1 (Lavery *et al.*, 2008), a condition subsequently termed Apparent Cortisone Reductase Deficiency (ACRD). However this study suggests that mutations in the coding region of the 11β-HSD1-encoding gene itself may also be responsible in some cases, even when present in a heterozygous state. The *HSD11B1* gene was examined in two cases presenting with hyperandrogenism and premature pseudopuberty, with biochemical features indicative of a milder form of CRD, in whom the *H6PD* gene was normal. Two novel mutations (R137C and K187N) in *HSD11B1* were identified. Although the cases were only heterozygous for the mutations rather than homozygous it was possible that because of the dimeric nature of 11β-HSD1, expression of mutant subunits could in some way interfere with the activity of the co-expressed WT subunits i.e. the mutations could have a dominant-negative character. The main purpose of this chapter was therefore to address this question using the previously developed bacterial expression system (Walker *et al.*, 2001a, Lawson *et al.*, 2009), together with a mammalian cell expression system.

Sequence alignment indicated that both R137 and K187 are strictly conserved within 11β-HSD1 proteins from different species (Fig. 3.2A & B). K187 forms part of the YxxxK motif that is strictly conserved within the short chain dehydrogenase/reductase (SDR) family, being part of the core catalytic tetrad of Asn, Ser, Tyr and Lys required for enzyme activity (Filling *et al.*, 2002). In most of the SDR enzymes characterized to date, the highly conserved Tyr residue functions as general acid/base catalyst, while the Lys facilitates catalysis, acting as part of a proton relay and interacting with the nicotinamide cofactor. Site-directed mutagenesis of this residue in rat 11β-HSD1 resulted in complete loss of enzyme activity

(Obeid and White, 1992). The importance of this residue to human 11β-HSD1 activity is confirmed in this study; no enzyme activity could be detected when the K187N/F278E mutant was expressed in either mammalian or bacterial cells. In the bacterial system, no soluble protein could be detected at all, indicating the probable additional importance of this residue to structural stability. K187 is known to ligate the 2- and 3-ribose hydroxyls of the nicotinamide cofactor in 11β-HSD1 (Hosfield *et al.*, 2005), and cofactor binding may be essential for correct folding/stability (Figure 1.29).

However, 11β-HSD1 is a dimeric enzyme and whilst a mutant K187N homodimer would be expected to be inactive the effect of heterodimer formation between wild-type and mutant subunits, (as could occur in heterozygous humans such as Case B), was uncertain. The two subunits of 11β-HSD1 are closely intertwined facilitating a close structural interplay between the monomers (Ogg *et al.*, 2005, Zhang *et al.*, 2005). It is therefore possible that the K187N mutation in one subunit could negatively affect the activity of an adjacent WT subunit. This type of effect has been reported for the enzyme biotin carboxylase where an inactivating mutation in the active site of one monomer of the protein had a dominant negative effect on the other monomer resulting in a 285-fold decrease in activity (Janiyani *et al.*, 2001). The experimental evidence from the hybrid F278E-K187N/F278E dimer constructed in this study suggests that this is indeed the case for 11β-HSD1. The purified heterodimer had no detectable enzyme activity. However, the simultaneous expression of the K187N/F278E mutant had a second unexpected effect on the co-expressed F278E 11β-HSD1, in that it substantially reduced the yield of soluble F278E polypeptide. It seems probable therefore that the mutant subunit is capable of interacting with F278E subunits to cause unstable and ultimately insoluble aggregates, i.e. the mutation exerts a dominant negative effect on protein yield as well as activity.

With respect to the second mutation, R137C, expression of this mutant as a homodimer in either mammalian or bacterial cells also resulted in a dramatic decrease in the yield of functional, soluble protein, coupled this time with a more minor effect on the k_{cat} of the purified enzyme. An explanation for this effect can be found in the potentially vital role of R137 in dimerization of the enzyme. This conserved residue forms two interfacial salt bridges with the similarly conserved E141 between each pair of subunits (Figure 3.2). Salt bridges, particularly those involving arginine, can play a prominent role in protein stability (Vijayakumar and Zhou, 2001, Strickler *et al.*, 2006, Kumar and Nussinov, 2002), including stabilizing inter-subunit interactions (Musafia *et al.*, 1995). In addition to this thermodynamic role in stabilizing protein structure it has been well established that interfacial salt bridges, by the long-range nature of their strong electrostatic interactions, can also have a kinetic effect by enhancing the diffusional encounter between two subunits, thus speeding up the association process and guiding the proteins to the correct docked arrangement (Vijayakumar *et al.*, 1998, Gabdoulline and Wade, 2001). R137 may thus promote correct orientation of the subunits during dimer formation, in addition to stabilizing the final assembly. It seems reasonable to propose therefore that disruption of these strong interactions would hinder correct subunit-subunit binding and hence compromise dimer formation and/or stability. Of relevance here is that an Arg-Asp salt bridge at the dimeric interface of another SDR, 3α-hydroxysteroid dehydrogenase/carbonyl reductase, has recently been shown to be essential for conformational stability, oligomeric integrity and enzymatic activity (Hwang *et al.*, 2009). Salt bridges may therefore be a common way in which dimer formation is promoted, and dimer integrity maintained, in the SDR family.

As with the K187N mutant, co-expression of the R137C/F278E mutant with F278E 11β-HSD1 resulted in a marked suppression of the yield of soluble protein, including F278E strands. Interestingly, on purifying the F278E-R137C/F278E hybrid dimer from this system it

showed a similar reduction in yield (ca 80%) and reduction in k_{cat} (ca 20%) to that observed when homodimeric R137C/F278E was compared to homodimeric F278E (Figure 3.7). This implies that the deleterious effects of the R137C mutation can extend across the dimer interface to influence the activity of other, non-mutant, monomer.

Once again this suggests that in the natural heterozygous situation, the negative effects of both the K187N and R137C mutations can extend to the normally-active 'WT' partner, leading to a marked suppression of 11β-HSD1 activity. Although further examples of the association of these mutations with disease would help establish causality beyond doubt, these dominant-negative effects help explain the condition of patients who are heterozygous for these mutations. True "Cortisone Reductase Deficiency" due to mutations in *HSD11B1* may thus be a further monogenic cause of hyperandrogenism/premature pseudopuberty.

Chapter 4. Membrane binding properties of 11β-hydroxysteroid dehydrogenase type 1

4.1. Techniques to examine the potential association of proteins with biological membranes

In Section 2.3, it was shown that mutations to the surface hydrophobic residues at the C-terminus of recombinant, N-terminally truncated 11β-HSD1 can increase yield of soluble protein without adversely affecting activity. It was also shown, using one of the mutants as an example (guinea pig F278E), that these mutations are unlikely to have any major adverse effects on structure compared to wild type protein. In this chapter the ability of N-terminally truncated human 11β-HSD1 to bind to membranes will be examined. The effect of one of these mutations (F278E) on membrane binding will then be assessed. Numerous techniques have previously been used to examine the potential association of proteins with biological membranes with relevant examples discussed below.

4.1.1. Fluorescence

One of the most common techniques utilizes a fluorophore, which can either be intrinsic (i.e. a Trp residue) or artificially engineered into the protein, whose emission spectra will change dependent on the relative hydrophobicity of the local environment of the fluorescent species. For example, the removal of a Trp residue from the hydrophobic interior of the protein via thermal denaturation will lead to a red shifted emission spectrum (i.e. an increase in emission maximum wavelength) (Ostrovsky *et al.*, 1988) while addition of detergent or membrane to a solvent exposed Trp will lead to a blue shifted emission spectrum (i.e. a decrease in emission maximum wavelength) (Neves *et al.*, 2009) provided that the Trp residue becomes embedded in the hydrophobic interior of the detergent micelle or biological membrane. Due to the presence of a single Trp at position 263 in 11β-HSD1, which conveniently faces the exterior

of the C-terminal hydrophobic plateau thought to associate with membrane, it was hoped that decreases in the emission maximum wavelength of this residue would follow any kind of membrane association in this region. If both WT and F278E proteins are able to associate with the biological membrane, but to different amounts, any difference in the resulting spectrum could be interpreted as a change in the membrane binding properties of 11β-HSD1. A related approach to detecting membrane association and monitoring any difference in binding between proteins is through the use of molecules which are able to decrease the emission intensity of the fluorophore. These are known as quenchers.

4.1.2. Quenching

The differing accessibilities of quenchers to fluorophores have been used to study a wide range of proteins. Recently it has been used to investigate quinolone antibiotic resistance in the bacterial protein OmpF (Neves *et al.*, 2009). The technique has also been used to investigate the membrane bound topology of helices 1 and 2 in the channel domain of the pore forming toxin, colicin E1 (White *et al.*, 2006, Musse *et al.*, 2006). In these colicin studies, residues which constituted two amphipathic helices thought to lie on the membrane surface were mutated, one by one, to cysteine. These single cysteine mutants were then labelled using a bimane fluorophore. The effect of either membrane-embedded (e.g.10-DN) or aqueous (e.g. KI) quenchers on bimane fluorescence were then compared in order to create a model for the membrane bound topology of these helices (Musse *et al.*, 2006, White *et al.*, 2006). In order to elucidate the level of membrane association of 11β-HSD1 (WT or F278E), the differing accessibilities of a quencher, in this case acrylamide, to the naturally occurring fluorophore W263 will be used. Therefore any disruption of membrane association brought about by the introduction of the F278E mutation should be observed by a relatively higher degree of quenching compared to WT protein.

4.1.3. Western Blotting

Although there were many possible approaches of detecting physical association of 11β-HSD1 with membrane fractions (e.g. radiolabelling the protein, or monitoring enzyme activity), the availability of a reliable, specific and sensitive anti-11β-HSD1 polyclonal antibody (Section 3.3.3) made western blotting the method of first choice. This antibody had been successfully used many times before within the group (Walker *et al.*, 2001a, Bujalska *et al.*, 2008, Ricketts *et al.*, 1998, Onyimba *et al.*, 2006). In addition western blotting had previously been used to measure the sequestration of other proteins into biological membranes, e.g. the binding of the signal transduction protein GlnK into the plasma membrane (Coutts *et al.*, 2002, Tremblay *et al.*, 2007). In this study the aim was to incubate purified recombinant 11β-HSD1 (WT or F278E) with a suspension of biological membranes. The membrane and soluble fractions would then be separated by ultracentrifugation and the amount of protein in the membrane fraction estimated by quantification of western blots. Therefore any disruption of membrane association brought about by the introduction of the F278E mutation should hopefully be evident by a decrease in intensity of the 11β-HSD1 signal on the blots when compared to WT.

4.1.4. Substrate association with membranes.

Finally, the notion that two steroid substrates of 11β-HSD1, cortisone and 7-ketocholesterol, are able to be sequestered into biological membranes will be analysed. In Section 2.2.3 it was shown that cortisone can be detected using HPLC, with previous studies showing that 7-ketocholesterol could be measured in the same way (Hult *et al.*, 2004). Therefore in order to estimate the partitioning of the steroids into biological membranes, the aim was to incubate either cortisone or 7-ketocholesterol with a suspension of biological membranes. The membrane and soluble fractions will then be separated by ultracentrifugation, with the amount of steroid in the membrane fraction measured by HPLC. Although radioactive

cortisone could be used with subsequent separation by thin layer chromatography (TLC) as shown by Arampatzis *et al.* (2005), for ease of use the already established HPLC method was used for the steroid analysis. It is also for this reason that the gas chromatography-mass spectrometry (GC-MS) technique for measuring 7-ketocholesterol outlined by Arampatzis *et al.* (2005) was not used.

4.1.5. Choice of membrane

In order to use the above techniques to probe the potential interaction of human 11β-HSD1 with membrane, a suitable model for the physiologically relevant human ER membrane must be used. To get the clearest idea of this potential interaction, microsomes from human liver tissue could be utilized, but due to practical and ethical constraints experiments presented here will use microsomes purified from both mouse livers and human embryonic kidney (HEK)-293 cells. The purification of mouse liver microsomes is well documented and the process was in regular use in the laboratory (Lavery *et al.*, 2006a). Due to the presence of native 11β-HSD1 in the mouse liver microsomes it is reasonable to assume that the composition of the ER membrane will be similar to human liver ER, and that our recombinant human 11β-HSD1 should be able to associate with them if possible. The presence of murine 11β-HSD1 in these microsomes should hopefully not be a problem due to the difference in size and charge between the full-length mouse protein which will be present in the microsomes, and the recombinant human protein which will be added. The purification of microsomes from HEK-293 cells was also in regular use within the laboratory (Lavery *et al.*, 2008) and while the microsomes may perhaps not have the physiologically relevant composition as those from mouse livers, the absence of 11β-HSD1 in these cells may make interpretation of results clearer. The cell line also have the advantage of derived from human cells, which could perhaps lead to greater association with the human 11β-HSD1 used in this chapter. Both were therefore be used throughout this chapter. However, due to the presence

of a generally large amount of protein in microsomes from both mouse livers and HEK-293 cells which could interfere with 11β-HSD1 fluorescence, artificial liposomes were created for fluorescence quenching experiments. Liposomes were created using the anionic lipid 1,2-dimyristoyl-sn-glycero-3-phosphoglycerol (DMPG) as when in the form of a liposome, the lipid should have a structure relatively similar to the physiologically relevant phospholipid bilayer (Neves *et al.*, 2009).

4.2. Materials and Methods

4.2.1. Expression and purification of 11β-HSD1

Expression and purification of both human wild-type and F278E 11β-HSD1 was carried out as per Section 2.2.2.

4.2.2. Preparation of microsomes

Mouse liver or HEK-293 cells were resuspended in a buffer containing 250 mM sucrose, protease inhibitors (Mini-Complete EDTA free, Roche Molecular Biochemicals) and 20 mM HEPES pH 7.2. Samples were homogenized using a glass homogenizer then centrifuged at 1,000 × g for 10 min at 4˚C to remove large cell debris. The resulting pellet was discarded and supernatant was centrifuged at 12,000 × g for 10 min at 4˚C. Pellet was discarded and supernatant spun at 100,000 × g for 1 h at 4˚C. The resulting microsomal pellet was then twice washed with MOPS buffer (100 mM KCl, 20 mM NaCl, 20 mM MOPS and 1 mM $MgCl_2$ pH 7.2) and recentrifuged (100,000 × g, 1 h, 4˚C). The clean pellet was then resuspended in MOPS buffer and flash frozen in liquid nitrogen as 50 µl aliquots. The amount of protein in the microsomes was estimated using the Bradford method (Bradford, 1976) using the commercial kit from Biorad.

4.2.3. Binding of 11β-HSD1 to microsomes

Purified 11β-HSD1 was transferred to MOPS buffer by washing with 3 x 20 ml MOPS buffer using a Vivaspin 20 centrifugal concentrator. Any detergent remaining from the purification procedure was then removed using Extraci-Gel D (Pierce). A standard amount of 11β-HSD1 protein (10 µg) was added to 7 ml of MOPS buffer containing either mouse liver microsomes or HEK-293 microsomes equivalent to around 200 µg of protein. Samples were left to

equilibrate with shaking (200 rpm) at room temperature for 1 h, then spun at 100,000 × g for 1 h at 15˚C. Pellets were then resuspended in 250 µl H_2O.

4.2.4. Western blot analysis of membrane bound protein

Resuspended pellets were mixed with 250 µl of double strength SDS-PAGE sample buffer (60 mM Tris-HCl pH 6.8, 4% (w/v) SDS, 10% (v/v) β-mercaptoethanol, 20% (v/v) glycerol, 0.002% (w/v) bromophenol blue) with a volume corresponding to 6 µg of protein then resolved on a 12.5% acrylamide gel. Western blots were performed as per Section 3.2.7. Standards with known amounts of 11β-HSD1 protein were included on each blot.

4.2.5. Binding of steroids to microsomes

A standard amount (20 nmol) of either cortisone or 7-ketocholesterol was incubated in 7 ml of MOPS buffer (100 mM KCl, 20 mM NaCl, 20 mM MOPS and 1mM $MgCl_2$ pH 7.2) containing mouse liver microsomes equivalent to around 200 µg of protein. This gave a steroid conentration of 2.86 µM. Samples were left to equilibrate with shaking at room temperature for 1 h, then centrifuged at 100,000 × g for 1 h at 15˚C. Pellets were resuspended in 250 µl H_2O. Steroids were partitioned into 3 ml of dichloromethane. Samples were then centrifuged for 5 min at 1000 × g and the aqueous layer discarded. After evaporation of the dichloromethane, samples were redissolved in 60 µl of 50% (v/v) aq. acetonitrile and loaded onto an RP-HPLC system consisting of a Prevail Select C-18, 5 µm column (Grace), a GP50 gradient pump and a UVD170S detector (Dionex). Cortisone was eluted with a gradient of 54% to 69% aq. methanol over a period of 15 min while 7-ketocholesterol was eluted using a gradient of 0% to 98% aq. methanol over 22 min. Both substrates were monitored by UV absorbance at 242 nm. Examples of the HPLC traces can be seen in Figure 4.6. Amount of steroid bound to membrane was quantified by comparison with a series of standards.

4.2.6. Preparation of DMPG liposomes

A lipid solution of 1,2-dimyristoyl-sn-glycero-3-phosphoglycerol (DMPG) (~ 5.7 μmol) in a 1:1 mixture of chloroform/methanol was evaporated to dryness under a stream of helium in order to create a lipid film. The film was then dried under vacuum for 3 h. The lipid film was then dispersed using sonication for 3 min with a 3ml of 50 mM sodium phosphate pH 7.2 at 37˚C.

4.2.7. Quenching of 11β-HSD1 fluorescence by acrylamide

Studies on fluorescence quenching were carried out by the successive additions of a constant volume (10 μl) of acrylamide (4.22 M) to a cuvette containing a constant amount of 11β-HSD1 (~0.2 μM) in a solution of 3 ml 50 mM sodium phosphate pH 7.2 with or without DPMG liposomes. After each addition, the fluorescence spectrum was recorded using an excitation wavelength 278 nm, with any changes to the emission at wavelength 326nm documented. An example of the fluorescence spectrum is shown in Figure 4.1. All experiments were performed using a Hitachi F-7000 spectrofluorimeter at 37˚C. Data was analysed by the Stern-Volmer equation for collisional quenching (Lakowicz, 1999):

$$F_0 / F = 1 + K_{sv}[Q] \qquad (2)$$

where F and F_0 are the fluorescence intensities in the presence and absence of quencher, Q is the concentration of quencher, in this case acrylamide, and K_{sv} is the Stern-Volmer constant.

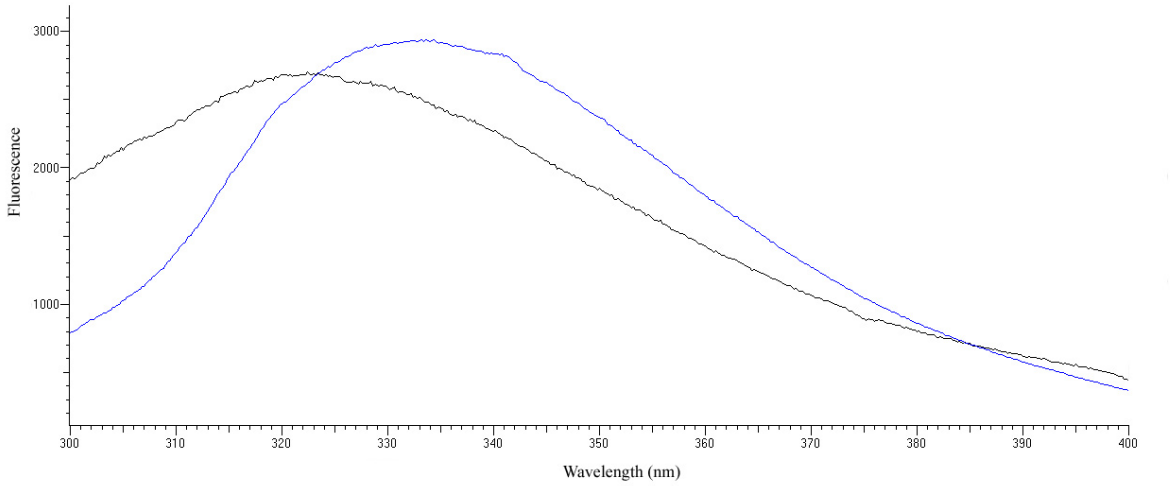

Figure 4.1. Fluorescence emission spectrum of 11β-HSD1 either in buffer (blue line) or in a liposome suspension (black line) using an excitation wavelength of 278 nm. Note the characteristic blue shift in the spectrum when 11β-HSD1 is incubated with liposomes.

4.3. Results

4.3.1. Binding of human 11β-HSD1 to microsomes

The ability of recombinant, N-terminally truncated human 11β-HSD1 (either WT or F278E) to associate with membranes was analysed using microsomes from either mouse liver or HEK-293 cells, as models for the physiologically relevant ER membrane. A standard amount of 11β-HSD1 protein was added to a suspension containing buffer together with either mouse liver microsomes or HEK-293 microsomes. Samples were left to equilibrate, then pelleted by centrifugation. Amount of 11β-HSD1 in the microsomal pellet was then analysed by western blotting. A control experiment in which no recombinant human 11β-HSD1 was added to mouse liver microsomes showed bands at 35KDa and 60KDa, which presumably correspond to monomeric and dimeric full-length murine 11β-HSD1 (Figure 4.2). Importantly, no human 11β-HSD1 band or equivalent was present in empty microsome. The same experiment using microsomes derived from HEK-293 cells showed no bands.

Using mouse liver microsomes, approximately 25% of WT 11β-HSD1 incubated with the microsomal suspension associated with the microsomal membranes (Figure 4.3). However, an approximate 50% decrease in the amount of 11β-HSD1 bound was observed when the protein carried the F278E mutation i.e. around 12.5% protein was bound (Figure 4.3). The difference in the amount of membrane association between the WT and F278E proteins was statistically significant when analysed using an unpaired *t*-test (p-value = 0.006). When microsomes from HEK-293 cells were used, a smaller decrease in membrane association of 20% were observed when the F278E mutant was introduced. This difference in binding, however, was not significant (p-value = 0.226) (Figure 4.3).

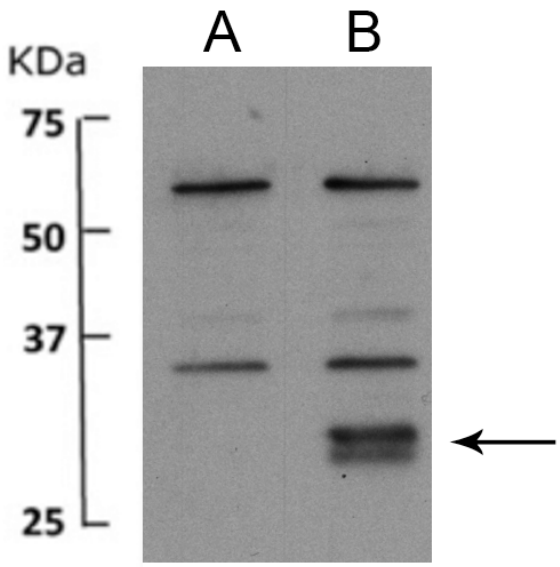

Figure 4.2. Western blot of mouse liver microsomes with (B) or without (A) human 11β-HSD1. The additional bands at 35KDa and 60KDa correspond to monomeric and dimeric full-length murine 11β-HSD1. The position of human 11β-HSD1 on the western blots is indicated by the arrow.

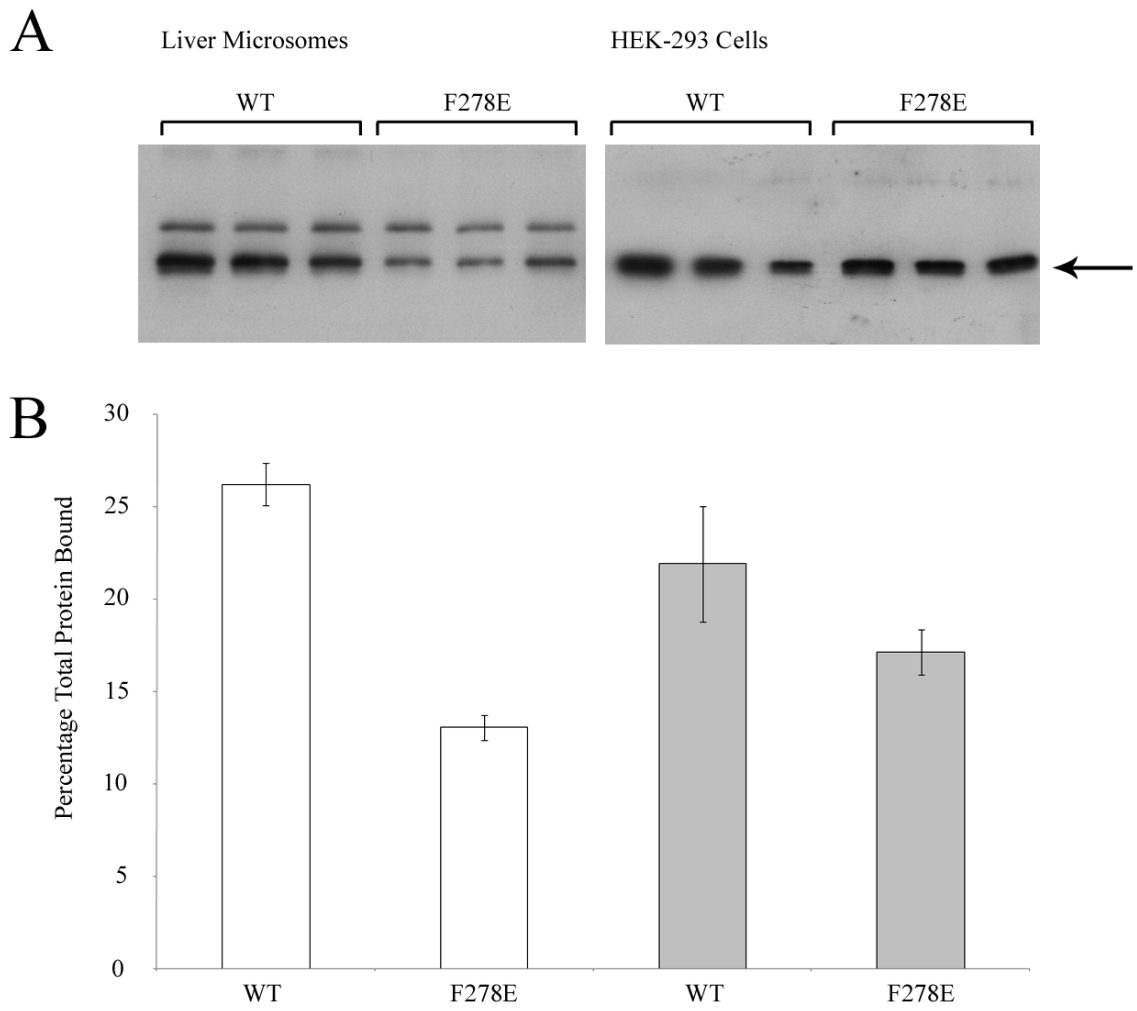

Figure 4.3. Binding of human 11β-HSD1 to microsomes from both mouse liver (left) and HEK-293 cells (right). Western blots (A) showing triplicates of bound 11β-HSD1 to membrane. Comparison to known standards of 11β-HSD1 were used to quantify the amount of protein which was bound to the microsomes (B). The position of 11β-HSD1 on the western blots is indicated by the arrow. The difference in binding between WT and F278E was significant when a microsomal preparation from mouse livers was used (p-value = 0.006) but not when the microsomes were sourced from HEK-293 cells (p-value = 0.2255). Bars represent SEM.

4.3.2. Effect of salt on the binding of human 11β-HSD1 to microsomes

Figure 4.3 clearly shows that the F278E mutant retained some affinity for microsomes, despite the partial disruption of the hydrophobic plateau. This suggested that the binding of 11β-HSD1 might possibly be more complicated than a simple hydrophobic interaction. To investigate the involvement of any electrostatic interaction which may occur between protein and membrane by virtue of the positively charged residues which surround the hydrophobic plateau, WT 11β-HSD1 was incubated with a solution of mouse liver microsomes in buffer

containing 20 mM MOPS together with either 500 mM, 100 mM or no NaCl. No other additives were present in this buffer system. The microsomes were then pelleted with bound 11β-HSD1 and analysed via western blots as described in the methods (Section 4.2.4). Visual examination, and densitometric analysis, of the blots appeared to show that the amount of 11β-HSD1 bound to microsomes decreased with increasing concentrations of salt, with an approximate 40% decrease in binding between 0 and 500 mM NaCl (Figure 4.4). One way ANOVA with a post-hoc Tukey test indicated a significant difference ($p = 0.009$) between the 0 and 500 mM NaCl treatments, but no difference was observed between 0 and 100 mM NaCl or 100 mM and 500 mM NaCl.

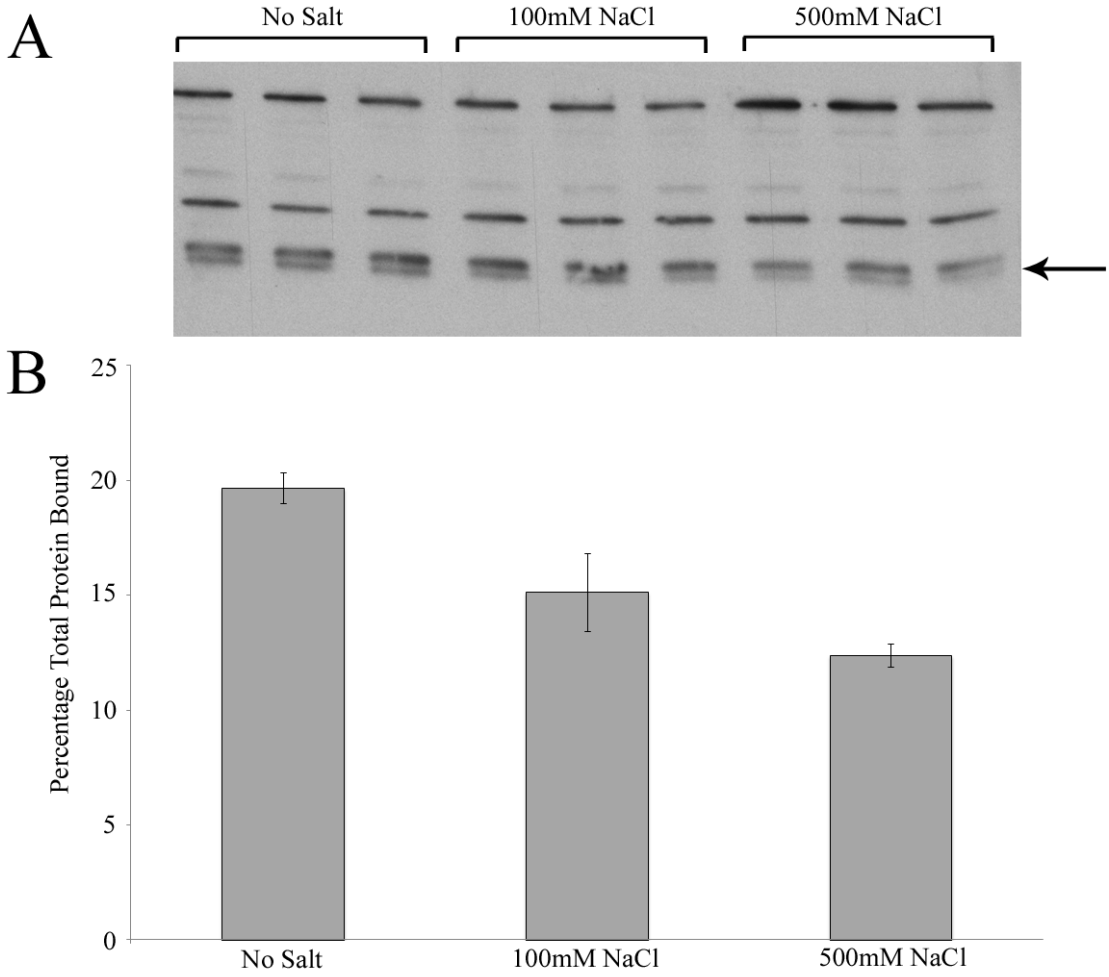

Figure 4.4. The effect of salt on the binding of human 11β-HSD1 to microsomes from mouse livers. Western blots (A) showing triplicates of bound 11β-HSD1 to membrane. Comparison to known standards of 11β-HSD1 were used to quantify the amount of protein which was bound to the microsomes (B).The position of human 11β-HSD1 on the western blots is indicated by the arrow. The amount of 11β-HSD1 bound to microsomes was seen to decrease with increasing salt concentrations. One way ANOVA showed that a significant difference existed ($p = 0.009$) between the 3 groups with a post-hoc Tukey test showing that the difference was between no salt and 500 mM NaCl. The position of human 11β-HSD1 on the western blots is indicated by the arrow. Bars represent SEM.

4.3.3. Binding of steroid substrates of 11β-HSD1 to microsomes

In order to ascertain whether the substrates of 11β-HSD1 are able to associate with biological membranes, a standard amount (20 nmol) of either cortisone or 7-ketocholesterol was incubated with a suspension of mouse liver microsomes. After centrifugation, the amount of steroid which associated with the membrane pellet was analysed via HPLC, with examples of

traces shown in Figure 4.5. Quantitative analysis of peak areas revealed that relatively small proportions of both cortisone and 7-ketocholesterol, around 1% and 2% respectively, associated with the membrane (Figure 4.6). Since there was a possibility that these figures could represent simply steroid that was trapped within the liquid of the pellet, rather than true membrane-bound steroid, an attempt was made to estimate the magnitude of the effect that entrapment would produce. The microsomal pellets analysed had an estimated volume of approximately 23 µl, which assuming a composition of entirely of water, could contain no more than 0.33% of the steroid added to the microsome suspension. Although microsomal pellets are composed of a great deal more than just water, this represented a useful hypothetical control value of the maximum amount of steroid which could be present without any association with the microsomal membranes. Therefore, since this value was considerably lower than the 1-2% observed in the experiment, it was concluded that the steroid binding observed was predominantly due to a genuine interaction with the biological membrane present in the mouse liver microsomes.

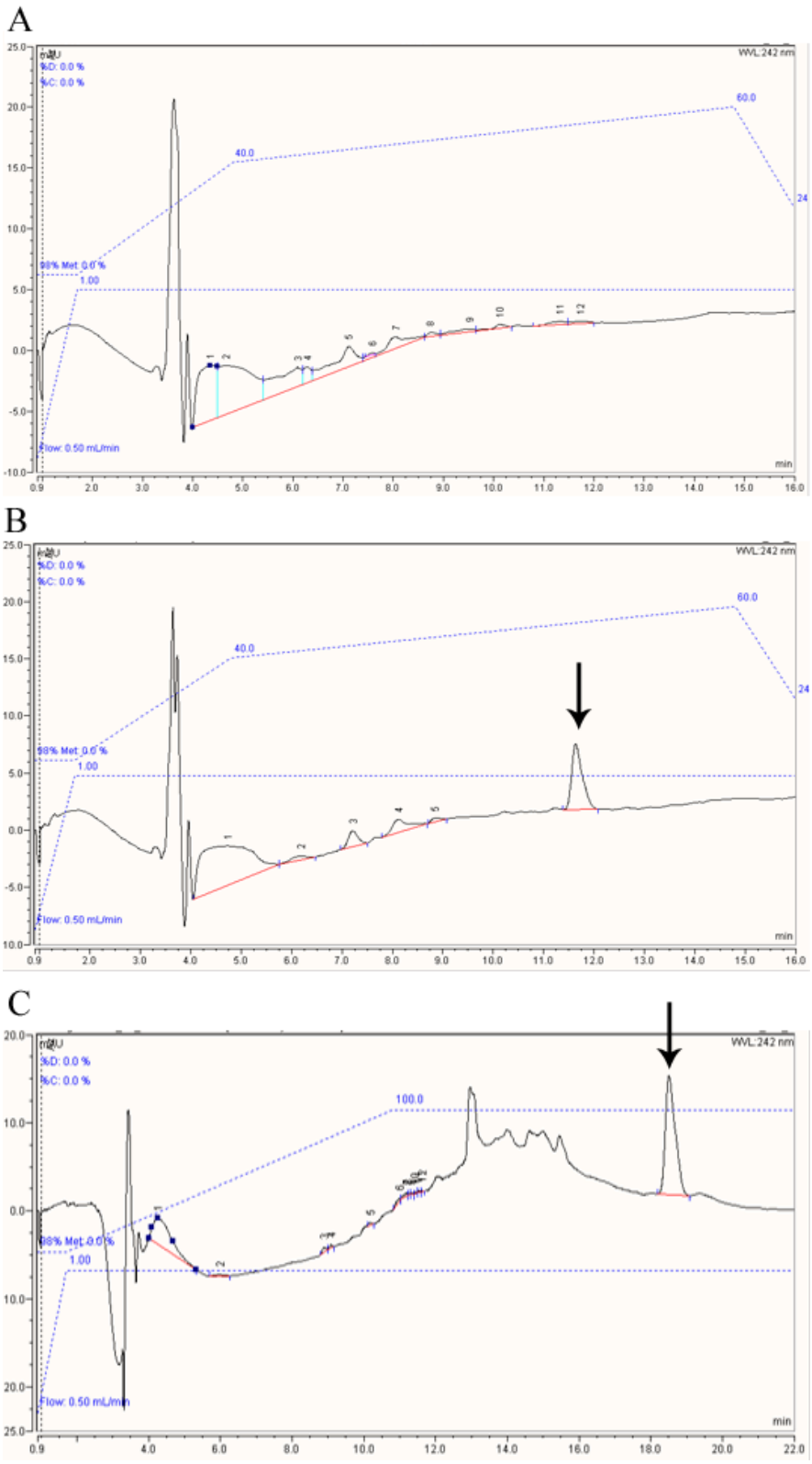

Figure 4.5. HPLC traces showing the binding of cortisone (B) and 7-ketocholesterol (C) to mouse liver microsomes. HPLC of microsome with no steroid added is shown by A. The positions of the substrates are shown by the black arrows. Axes represent absorbance (y) vs. time (x). Absorbance of steroid was recorded at 242 nm.

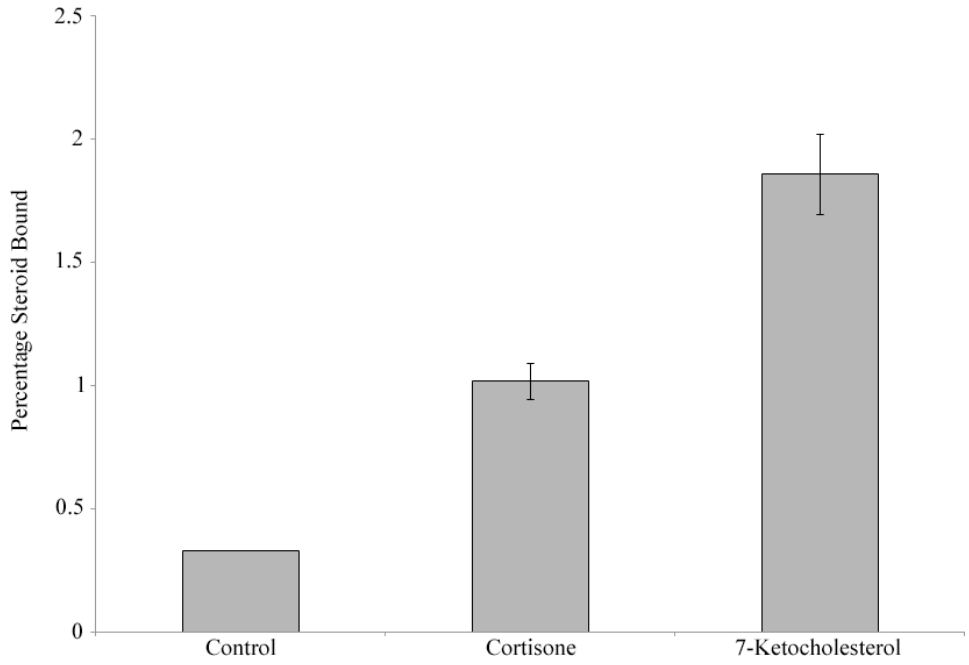

Figure 4.6. The binding of steroid substrates of 11β-HSD1 to mouse liver microsomes. The "control" represents the hypothetical percentage of total steroid which could be present in the microsomal pellet if the pellet is assumed to be composed entirely of water, and if there is no association of steroid and membranes. A significantly larger amount of both cortisone and 7-ketocholesterol are seen to associate with the membrane than in the control. Bars represent SEM.

4.3.4. Fluorescence quenching studies on human 11β-HSD1

Quenching studies were performed using human 11β-HSD1, WT or F278E, either free in solution or inserted into liposomes of the anionic lipid DPMG. The lipid was chosen as when in the form of a liposome, it should have a structure relatively similar to the physiologically relevant phospholipid bilayer (Neves *et al.*, 2009). The single Trp residue of human 11β-HSD1, W263, was used as the fluorophore. Acrylamide, a small polar molecule, is able to quench fluorophores free in solution, but unable to quench those imbedded in membranes (Lakowicz, 1999). Since W263 is positioned on the hydrophobic plateau, it was hoped that any association of the protein with the membranes of the liposomes which involved this region, would result in a decrease in the ability of acrylamide to quench the enzyme

fluorescence. The introduction of the F278E mutation would also be expected to reduce this difference in quenching if it countered the membrane association.

Quenching of both WT and F278E, either in solution or in micelles, by acrylamide gave rise to a linear plot of F/F_0 against [Q] with an intercept of 1 indicating a similar accessibility of all tryptophans to quencher (Figure 4.7). However, when inserted into DPMG liposomes, a decrease in the gradient of the line was observed reflecting a decrease in the quenching of W263 by acrylamide. This is shown clearly by a 64% decrease in the quenching constant, K_{sv}, for the WT protein and a smaller, 47% decrease for F278E (Table 4.1). This implies that while both WT and F278E proteins are able to associate with DMPG liposomes, the charge introduced by the F278E mutation has disrupted the hydrophobic plateau, indicated by the higher K_{sv} (Table 4.1).

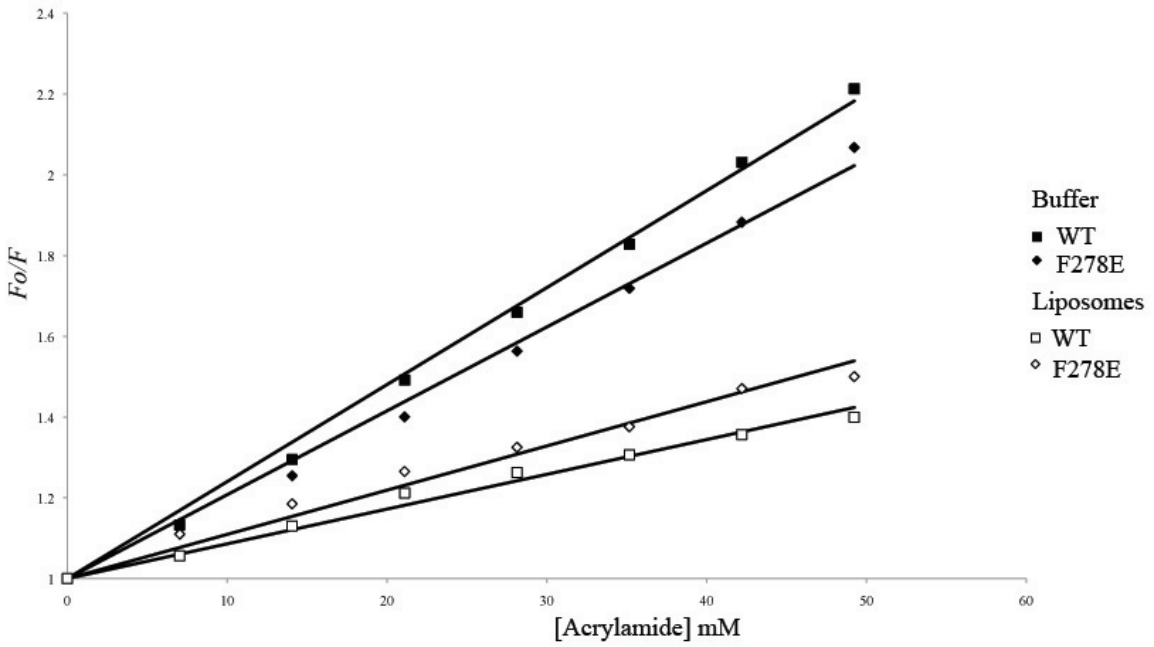

Figure 4.7. Stern-Volmer plots of acrylamide quenching of 11β-HSD1 (WT or F278E) either in buffer (top two lines) or inserted into DPMG liposomes (bottom two lines). Fitted lines were generated by Enzfitter (Biosoft) using the Stern-Volmer equation (Lakowicz, 1999).

	Buffer		Liposomes	
	K_{sv} (mM^{-1})	S.E	K_{sv} (mM^{-1})	S.E
Wild Type	0.0240	0.0003	0.0086	0.0002
F278E	0.0208	0.0004	0.0110	0.0003

Table 4.1. Stern-Volmer constants (mean ± SEM) of acrylamide quenching of 11β-HSD1 (WT or F278E) either in buffer or inserted into DPMG liposomes. Experiments were performed in triplicate using the same preperation of enzyme (either WT or F278E).

4.4. Discussion

Since the publication of the crystal structure of guinea pig 11β-HSD1 in 2004, the physiological role of the C-terminal hydrophobic plateau (Ogg *et al.*, 2005) has not been fully elucidated. The hydrophobic residues which form this region are encircled by positively charged residues, suggesting that the plateau could exist in the non-polar centre of the membrane, with the charged residues forming salt bridges with the displaced phospholipid and sulpholipid head groups (Ogg *et al.*, 2005). Substrates of 11β-HSD1, by virtue of both general structure and partition coeffecient ($logP_{oct/water}$) values, can be considered to be relatively hydrophobic and therefore could be present in the hydrophobic core of the lipid bilayer. The residues which form the protruding C-terminal hydrophobic plateau of 11β-HSD1 could conceivably dip into the ER membrane funnelling substrate into the active site.

Intriguingly, this proposed membrane dipping of the protein could perhaps explain the discrepancy between the different experimentally observed K_m values for 11β-HSD1. When assayed in intact cells, either transfected or from primary culture, 11β-HSD1 displays apparent K_m values between 100 and 400 nM (Jamieson *et al.*, 1999, Shafqat *et al.*, 2003, Davani *et al.*, 2000, Leckie *et al.*, 1998, Jamieson *et al.*, 1995, Bujalska *et al.*, 1999b). This is consistent with the physiologically relevant nanomolar circulating glucocorticoid concentrations. However, 11β-HSD1 derived from either homogenates or recombinant sources, this work included (see Section 2.3.2 & 3.3.6), displays K_m values in the low micromolar range (Hult *et al.*, 1998, Pu and Yang, 2000, Blum *et al.*, 2000, Maser *et al.*, 2002, Quinkler *et al.*, 1997, Stewart *et al.*, 1987, Arampatzis *et al.*, 2005, Shafqat *et al.*, 2003, Lawson *et al.*, 2009). Although cooperative kinetics has been proposed as an explanation for this discrepancy (Maser *et al.*, 2002), this has been disproven by a number of groups (Jamieson *et al.*, 1999, Shafqat *et al.*, 2003, Davani *et al.*, 2000, Leckie *et al.*, 1998, Jamieson

et al., 1995, Bujalska *et al.*, 1999b). A more likely explanation is that the presence of steroid substrate in the ER membrane allows for a local increase in substrate concentration from the circulating nanomolar levels to a local micromolar level, allowing for efficient 11β-HSD1 activity. However, before this study no experimental evidence had been presented to prove that either the hydrophobic plateau of 11β-HSD1, or any of its steroid substrates, interacts with the ER membrane.

In Section 2.3 it was shown that mutations to the C-terminus of recombinant, N-terminally truncated 11β-HSD1 which disrupt the hydrophobic plateau, can increase yield of soluble protein without adversely affecting activity. Therefore one of these mutants, F278E, was used to probe the effect that disruption of the hydrophobic plateau has on the binding of human 11β-HSD1 to membranes. Microsomes from either mouse liver or HEK-293 cells were used as models for the physiologically relevant human ER membrane, with binding of 11β-HSD1 to these model membranes assessed using western blot analysis. Figure 4.3 clearly shows that when mouse liver microsomes were used, approximately 25% of WT 11β-HSD1 associated with the microsomal membranes, with the F278E mutation causing a significant decrease in binding of around 50%. A slightly reduced proportion of WT 11β-HSD1 (20%) was seen to associate with microsomes from HEK-293 cells, with a smaller, and indeed statistically insignificant, 20% decrease in membrane association observed when the F278E mutation is introduced (Figure 4.3). While the exact organelle composition of each of these types of cell is not known, the microsomes prepared from mouse liver will almost certainly have a higher proportion of both rough and smooth ER, due to the considerable protein and lipid synthesis performed by hepatocytes. It would also appear that ER membranes are biochemically distinct from other membranes, being made up of a high percentage of phosphatidylcholine (van Meer *et al.*, 2008). Therefore, due to the expression of 11β-HSD1 in hepatic tissues (Lakshmi and Monder, 1988), the difference in binding observed between microsomes

derived from HEK-293 cells or mouse livers could be down to the preference for 11β-HSD1 to interact with the larger proportion of physiologically relevant ER membranes present in the microsomes derived from mouse livers.

Interestingly, the F278E mutant retains some affinity for microsomes, despite the significant disruption the mutation might be expected to make to the hydrophobicity of the plateau. This could suggest that the binding of 11β-HSD1 is more complicated than a simple hydrophobic interaction. As discussed previously, hydrophobic residues which form the putative membrane dipping region of 11β-HSD1 are encircled by positively charged residues which could form salt bridges with the displaced phospholipid and sulpholipid head groups. A similar combination of hydrophobic and charged interactions are observed in the membrane dipping regions of both prostaglandin H2 synthase-1 and squalene cyclase (Picot *et al.*, 1994, Wendt *et al.*, 1997). To ascertain the involvement these charged residues on the interaction between 11β-HSD1 and membrane, WT 11β-HSD1 was incubated with a suspension of mouse liver microsomes which contained 20 mM MOPS together with either 0 mM, 100 mM or 500 mM NaCl. Salt was included in the buffer to shield any potential electrostatic interactions between residues in 11β-HSD1 and phospholipid and sulpholipid head groups of the membrane. Increasing salt concentration is also known to increase the binding of proteins to hydrophobic matrices, a property exploited in hydrophobic interaction chromatography (Tsumoto *et al.*, 2007). Thus an increase in binding of 11β-HSD1 to membranes on addition of salt would indicate a greater importance of hydrophobic interactions, whereas a decrease in binding would signal a greater electrostatic contribution. In the experiments reported here, a modest decrease in binding was observed with increasing salt concentration, although this was only significant at relatively high (500 mM) concentrations. This suggests that positively charged residues, most probably Arg269 and Lys274, are contributing to the binding of 11β-HSD1 to membranes. These important electrostatic interactions also perhaps explain the

retention of some membrane binding affinity of the F278E mutant in the previous experiment (see Section 4.3.1). These data, taken together with the decrease in binding observed with the introduction of the F278E mutation, indicate that a combination of hydrophobic and electrostatic interactions are required for optimum binding of 11β-HSD1 to microsomal membranes.

Despite the physiological relevance of glucocorticoids, the molecular mechanism governing the entrance of these steroids into cells is poorly understood. In addition, knowledge of their intracellular distribution and concentration in cellular compartments is also scarce (Odermatt *et al.*, 2006). In order for the membrane dipping to function, substrates of 11β-HSD1 would have to be concentrated in the biological membrane. It is currently unclear whether free glucocorticoid enters target cells either by endocytotic uptake or insertion into the membrane, although, due to thr lipid-soluble structure of glucocorticoids, it is most probably the latter (Laycock, 1996). A comparison of full length 11β-HSD1 facing the ER lumen with a K5S:K6S cytoplasmic-facing mutant showed comparable catalytic activities, indicating glucocorticoids may accumulate in certain regions of the ER membrane (Odermatt *et al.*, 1999). Indeed, by comparing physical measures of bilayer order and polarity, formation of detergent resistant domains, phase separation and membrane microsolubilization by apolipoprotein A-I, the 11β-HSD1 substrate 7-ketocholesterol is known to localize in model membranes both in a similar location (e.g. in phospholipids with a small interfacial surface area such as sphingomyelin and saturated phosphatidylcholines) and also a location distinct (e.g. bilayers of unsaturated phospholipids and those above their midpoint temperature of gel to liquid crystalline phase transition, T_M) from cholesterol (Massey and Pownall, 2005).

The studies reported here show that when a standard amount (20 nmol) of either cortisone or 7-ketocholesterol is added to a suspension of mouse liver microsomes a small amount of both, around 1% and 2% respectively, associates with the membrane (Figure 4.6). Knowing

the approximate volume of the microsomal pellet, and assuming the steroids are evenly distributed within the pellet, it can be calculated that the concentrations of cortisone and 7-ketocholesterol in the pellet are approximately 7 μM and 13 μM respectively. This compares with a supernatant value of 2.26 μM and 2.28 μM for 7-ketocholesterol and cortisone respectively. Using the previously experimentally derived $\log P_{oct/water}$ value for cortisone of 1.47 (Hansch, 1995), the concentration of cortisone in the organic phase of an octanol/water mixture should be around 30 times greater than in water. In the system reported here, the concentration of cortisone in the microsomal fraction is only twice that in the supernatant. Although the preference of the steroids for the microsomal pellet is not that great, these values could still perhaps account for the discrepancies in K_m values observed between *in vivo* and *in vitro* studies. This is due to the fact that microsomes are not purely lipid; in particular, a significant amount of water will be sedimented within the microsomal vesicles. Hence the concentration of steroid within the lipid centre of the membrane may be significantly higher than observed here, in which case it would certainly affect 11β-HSD1 activity if the protein was able to dip into the membrane to utilize the associated steroid.

Also, since the human 11β-HSD1 substrates are not physiologically relevant to the mouse liver microsomes used in these experiments, it is possible that the different types of lipids or proteins which constitute these cells may interact with 11β-HSD1 substrates differently when compared to human liver microsomes. Other factors, such as the presence of lipid rafts and associated proteins, may also affect substrate binding into the membrane. The buffer used to incubate microsomes and proteins in these experiments is also probably a poor mimic of contents of either the cytosol or the ER lumen; in particular the high amounts of solutes inside the cell would result in a higher ionic strength, resulting in an increased preference of the steroid for the membrane. Interestingly, evidence seems to suggest that the stabilization of lysosomal membranes, therefore preventing proteolytic enzyme release, by cortisol is

particularly important (Laycock, 1996). Finally, since no ATP was added at any point during the experiment, it can also be concluded that no active transport took place, inferring that the steroid substrates were either associated with a protein in the microsomal pellet, or more likely, were sequestered into the membrane bilayer in a similar way to that observed with cholesterol (Brown and Jessup, 1999).

The differing accessibilities of quenchers to fluorophores have been used to study a wide range of proteins. Recently this technique has been used to investigate quinolone antibiotic resistance in the bacterial protein OmpF (Neves *et al.*, 2009). The technique has also been used to investigate the membrane bound topology of helices 1 and 2 in the channel domain of the pore forming toxin, colicin E1 (White *et al.*, 2006, Musse *et al.*, 2006). In contrast to the colicin E1 study in which an artificial fluorophore was used, with 11β-HSD1 the naturally occurring fluorophore W263 which faces the exterior of the C-terminal hydrophobic plateau thought to associate with membrane was utilized. Since this is the only Trp residue in human 11β-HSD1, we were confident that any fluorescence observed was due to this residue. Indeed, when 11β-HSD1 (both WT and F278E) was incubated with DPMG liposomes, a blue-shift in the emission spectrum was observed (Figure 4.1), indicating the normally solvent exposed Trp residue had become buried in the DPMG liposome. This implies that any interaction between 11β-HSD1 and membrane occurs in the region surrounding W263.

Acrylamide was able to quench WT and F278E 11β-HSD1 fluorescence both in buffer and in a solution of DPMG liposomes (Figure 4.7). Incubation with liposomes was accompanied by a decrease in quenching efficiency of acrylamide for both WT and F278E proteins, indicated by a decrease in the K_{sv} value, once again suggesting insertion of the W263 residue into the membrane. However, the greater decrease in K_{sv} observed for WT (64%) compared to F278E (47%) when incubated with liposomes indicates that, although W263 is able to interact with membrane in both proteins, the F278E mutation appears to at least partially disrupted the

hydrophobic plateau leading to a decrease in association between 11β-HSD1 and membrane. These data once again suggest of the importance of the C-terminal hydrophobic plateau on the interaction of 11β-HSD1 and membrane.

Chapter 5. General Discussion

For some time it has been known that dysregulation of cortisol at a tissue level, which would indicate abnormal 11β-HSD1 activity, may be the underlying pathology behind a range of conditions such as obesity, type 2 diabetes, ACRD, various neurodegenerative diseases and glaucoma. However, surprisingly for a protein which has such wide-reaching involvement in the pathology of disease, the high resolution structures which would allow the development of structure-based drug design for the treatment of these diseases have only become available in the last 5-6 years. This is can in part be attributed to the fact that, in contrast to most other members of the SDR family, 11β-HSD1 is a glycosylated, membrane-bound, ER luminal protein which has made production and purification of full length protein difficult (Hult *et al.,* 2001, Nobel *et al.,* 2002). The development of recombinant 11β-HSD1 which has the N-terminal transmembrane domain removed has allowed the protein to be expressed in *E.coli* (Walker *et al.,* 2001a), which, together with co-expression of 11β-HSD1 with the chaperonins GroEL/GroES and the addition of an inhibitor of 11β-HSD1 during the induction phase (Hozjan *et al.,* 2008, Hult *et al.,* 2006, Elleby *et al*., 2004), has allowed purification of sufficient quantities of 11β-HSD1 to a relatively high level of homogeneity and monodispersity.

The crystal structure of 11β-HSD1 confirmed that the protein existed as a homodimer, with a highly similar central scaffold to most other SDRs. However, 11β-HSD1 does show a striking difference to other SDR structures at the C-terminus with the last 2 helices (α2 and α3) which are seen to protrude and form a long structure which packs against the C-terminus of the other subunit in an antiparallel conformation. The residues on the surface of these C-terminal helices are in the form of a non-polar plateau encircled by positively charged residues (Ogg *et al.*, 2005). This plateau is thought to exist in the non-polar centre of the ER membrane, with

the charged residues forming salt bridges with the displaced phospholipid and sulpholipid head groups. Due to the hydrophobic nature of the substrates of 11β-HSD1, this could constitute a potential 'membrane dipping' mechanism to funnel hydrophobic substrates from the membrane into the 11β-HSD1 active site (Ogg *et al.,* 2005).

To initiate investigations in the importance of this C-terminus of 11β-HSD1, the four residues which make up the hydrophobic plateau in both the human and guinea pig 11β-HSD1, were each mutated to the charged amino acid glutamic acid. The aim was to create a membrane truncated, recombinant 11β-HSD1 mutant with unchanged kinetics and structure, but altered membrane association properties which could subsequently be used to probe the membrane dipping hypothesis. On expression in *E.coli*, all mutations increased the yield of soluble 11β-HSD1, with the F278E mutant in both human and guinea pig showing the most dramatic increases compared to wild-type protein. The increased solubility of these mutants was due to a decrease in protein aggregation, as shown by sedimentation AUC analysis. All the mutant proteins had similar kinetics (k_{cat} and K_m) for the steroid substrate to the wild-type, in both dehydrogenase and reductase directions, with the guinea pig F278E mutant enzyme showing an overall structure largely identical to the previously published wild-type guinea pig structure (PDB code: 1XSE) (Ogg *et al.,* 2005).

Due to the increased solubility, monodispersity and activity of the human 11β-HSD1 F278E mutant, this protein was used to as a background to investigate two novel mutations in 11β-HSD1 which result in cortisone reductase deficiency (CRD). CRD is a human disorder in which there is a failure to regenerate the cortisol from cortisone via the activity of 11β-HSD1 (Tomlinson *et al.,* 2004) which results ACTH-mediated adrenal hyperandrogenism. The two cases reported here were diagnosed via urinary steroid metabolite analysis, with molecular analysis of the HSD11B1 gene indicating two novel mutations (R137C and K187N) which were both in the heterozygous state. R137 and K187 are strictly conserved within 11β-HSD1

proteins, R137 forming a salt bridge vital for dimerization (together with E141) and K187 being a key residue in the active site of 11β-HSD1.When K187N was expressed in *E.coli* in the F278E background, no soluble protein could be detected at all, indicating the additional importance of this residue to structural stability. Since K187 is known to ligate the 2- and 3-ribose hydroxyls of the nicotinamide cofactor in 11β-HSD1 (Hosfield *et al.,* 2005), cofactor binding may be essential for correct folding/stability. For R137C, expression in *E.coli* in the F278E background also resulted in a dramatic decrease in the yield of functional, soluble protein, coupled this time with a minor effect on the kcat of the purified enzyme. These decreases are presumably due to the R137C mutation interfering with correct subunit-subunit binding and hence compromising dimer formation and/or stability.

However, 11β-HSD1 is a dimeric enzyme and since both cases described here were in the heterozygous state, the effect of heterodimer formation between wild-type and mutant subunits was uncertain. The data from construction of a novel system to purify hybrid dimers (e.g. one monomer containing R137C/F278E and the other F278E) suggests that a mutation in one subunit could negatively affect the activity of an adjacent WT subunit. Each mutation exerted a dominant negative effect on protein yield as well as on activity, with the K187N mutant showing more marked suppression of both. Although further examples of the association of these mutations with disease would help establish causality beyond doubt, these dominant-negative effects help explain the condition of patients who are heterozygous for these mutations.

The human 11β-HSD1 F278E mutant was an ideal protein to probe the effect of disruption of the hydrophobic plateau on the binding of human 11β-HSD1 to membranes. Western blot analysis showed that when purified, recombinant 11β-HSD1 is incubated with mouse liver microsomes, approximately 25% of WT 11β-HSD1 associated with the microsomal membranes, with the F278E mutation causing a significant decrease in binding giving only.

12.5% association. Inclusion of NaCl in the incubation of WT 11β-HSD1 with a solution of mouse liver microsomes in a buffer containing 20 mM MOPS showed a modest decrease in binding with increasing salt concentration, although this was only significant at relatively high (500 mM) concentrations. These data indicate that a combination of hydrophobic and electrostatic interactions (potential salt bridges between phospholipid/sulpholipid head groups and R269 and/or K274 on 11β-HSD1) are required for optimum binding of 11β-HSD1 to microsomal membranes. Further experiments, in which the differing accessibility of acrylamide to W263, in either WT or F278E, supported this observation. Although acrylamide was able to quench the fluorescence of WT and F278E 11β-HSD1 both in buffer and in a solution of DPMG liposomes, the F278E mutation once again partially disrupted the hydrophobic plateau, as evidenced by a greater decrease in acrylamide quenching observed for WT 11β-HSD1 compared to F278E 11β-HSD1when inserted into liposomes.

In order for the membrane-dipping hypothesis to function, substrates of 11β-HSD1 would have to be concentrated in the biological membrane. The studies reported here show that when a standard amount of either cortisone or 7-ketocholesterol are added to a suspension of mouse liver microsomes a small amount of both, around 1% and 2% respectively, associate with the membrane. This corresponds to a concentration of 7 μM and 13 μM in the microsomal pellet for cortisone and 7-ketocholesterol respectively. This indicates that there is two to four times the concentration of steroid in the pellet compared to the supernatant. Although this is not quite as great as the partition expected from the $\log P_{oct/water}$ value of cortisone, the fact that 11β-HSD1 substrates are able to associate with microsomes used here may account for the discrepancies in K_m values observed between in vivo studies in biological cells and in vitro studies in solution. The microsomes used in this study are not purely lipid due to a significant amount of water which will have sedimented within the microsomal vesicles. Therefore, the concentration of steroid within the lipid centre of the

membrane may be significantly higher than observed here, in which case it would certainly affect 11β-HSD1 activity if the protein was able to dip into the membrane to utilize the associated steroid.

Further work to fully elucidate the binding of steroid substrates of 11β-HSD1 to membrane could include the use of small angle x-ray diffraction to compare the membrane interaction of cortisone to the interaction of both 7-ketocholesterol and cholesterol to membrane which have been previously characterised using this technique (Phillips *et al.,* 2001). In this x-ray diffraction method, cholesterol, which has a known x-ray diffraction pattern in lipid vesicles, was replaced with 7-ketocholesterol which produced distinct changes in membrane structure as evidenced from the change in x-ray diffraction. For example, there was an increase in electron density associated with the upper acyl chain region corresponding to the bilayer location of the steroid nucleus of 7-ketocholesterol (Phillips *et al.,* 2001). Methods which have been used to further characterise the interaction of 7-ketocholesterol and cholesterol to membrane by Massey *et al.* (2005) could potentially be extended to cortisone. These methods include comparing physical measures of bilayer order and polarity, formation of detergent resistant domains, phase separation and membrane microsolubilization by apolipoprotein A-I (Massey and Pownall, 2005).

Future work to investigate the nature of the binding of 11β-HSD1 to membranes could include mutation of the charged residues R269 and K274, which would further probe the electrostatic contribution of these residues to the association of the protein to microsomal membranes. In addition, more drastic alterations to the plateau via a greater number of simultaneous mutations of hydrophobic residues would also help further elucidate the respective roles of hydrophobicity and electrostatics on the binding. Finally, improvements to the procedure to further mirror the in vivo environment (e.g. ionic strength and pH of buffer, composition of model membranes) may also be beneficial in providing a clearer picture of

how 11β-HSD1 may behave in the cell. However, it is worth noting that the findings presented here use purified, recombinant 11β-HSD1. Therefore, it would be interesting to express full-length 11β-HSD1 in mammalian cells and observe the effect of the F278E mutation. Although the effect of the hydrophobic plateau on physical association with the membrane could not be measured, since the N-terminal anchor would preserve this, observation of changes in apparent K_m might be revealing, although it is by no means easy to get accurate K_m values from transfected cell systems. An alternative approach might be to engineer a cleavage site at the end of the current signal anchor, to create a signal peptide. If this worked it would deliver N-terminally truncated enzyme into the lumen of the ER when expressed in mammalian cell lines. It might then be possible to monitor membrane association of the WT and mutant proteins, and the importance of the hydrophobic plateau, in a more natural situation.

In summary, in this thesis I have described the construction of a series of mutants in which hydrophobic residues in the C-terminal helices of human and guinea pig 11β-HSD1 were mutated to glutamic acid. One of these mutants, F278E, displayed increased solubility, monodispersity and activity with an unchanged crystal structure. Human F278E was then used as a background to construct a novel hybrid dimer system to analyse the CRD causing mutations in 11β-HSD1 (R137C and K187N). Analysis of the resulting heterodimers revealed that the negative effects of both the K187N and R137C mutations can extend to the normally-active WT partner, leading to a marked suppression of 11β-HSD1 activity which could account for the phenotype observed in patients presenting with CRD. Finally, a comparison of human WT and F278E was used to probe the membrane association of 11β-HSD1. A combination of western blot analysis and fluorescence quenching experiments revealed that the binding of 11β-HSD1 to mouse liver microsomes is via a combination of hydrophobic and electrostatic interactions.

References

AFONINE, P. V., GROSSE-KUNSTLEVE, R. W. & ADAMS, P. D (2005) the phenix refinement framework. *CCP4 Newsletter,* 42.

AGARWAL, A. K. & AUCHUS, R. J. (2005) Minireview: cellular redox state regulates hydroxysteroid dehydrogenase activity and intracellular hormone potency. *Endocrinology,* 146**,** 2531-8.

AGARWAL, A. K., MUNE, T., MONDER, C. & WHITE, P. C. (1994) NAD(+)-dependent isoform of 11 beta-hydroxysteroid dehydrogenase. Cloning and characterization of cDNA from sheep kidney. *J Biol Chem,* 269**,** 25959-62.

AGARWAL, A. K., TUSIELUNA, M. T., MONDER, C. & WHITE, P. C. (1990) Expression of 11-Beta-Hydroxysteroid Dehydrogenase Using Recombinant Vaccinia Virus. *Molecular Endocrinology,* 4**,** 1827-1832.

AILOR, E. & BETENBAUGH, M. J. (1998) Overexpression of a cytosolic chaperone to improve solubility and secretion of a recombinant IgG protein in insect cells. *Biotechnol Bioeng,* 58**,** 196-203.

AJILORE, O. A. & SAPOLSKY, R. M. (1999) In vivo characterization of 11beta-hydroxysteroid dehydrogenase in rat hippocampus using glucocorticoid neuroendangerment as an endpoint. *Neuroendocrinology,* 69**,** 138-44.

AL BAKIR, M., BUTT, A. N. & SWAMINATHAN, R. (2008) Circulating 11beta-hydroxysteroid dehydrogenase type 1 mRNA and cardiovascular risk factors. *Ann N Y Acad Sci,* 1137**,** 283-9.

ALBERTI, L., GIROLA, A., GILARDINI, L., CONTI, A., CATTALDO, S., MICHELETTO, G. & INVITTI, C. (2007) Type 2 diabetes and metabolic syndrome are associated with increased expression of 11beta-hydroxysteroid dehydrogenase 1 in obese subjects. *Int J Obes (Lond),* 31**,** 1826-31.

ALBERTS, P., ENGBLOM, L., EDLING, N., FORSGREN, M., KLINGSTROM, G., LARSSON, C., RONQUIST-NII, Y., OHMAN, B. & ABRAHMSEN, L. (2002) Selective inhibition of 11beta-hydroxysteroid dehydrogenase type 1 decreases blood glucose concentrations in hyperglycaemic mice. *Diabetologia,* 45**,** 1528-32.

ALBERTS, P., NILSSON, C., SELEN, G., ENGBLOM, L. O., EDLING, N. H., NORLING, S., KLINGSTROM, G., LARSSON, C., FORSGREN, M., ASHKZARI, M., NILSSON, C. E., FIEDLER, M., BERGQVIST, E., OHMAN, B., BJORKSTRAND, E. & ABRAHMSEN, L. B. (2003) Selective inhibition of 11 beta-hydroxysteroid dehydrogenase type 1 improves hepatic insulin sensitivity in hyperglycemic mice strains. *Endocrinology,* 144**,** 4755-62.

ALBISTON, A. L., OBEYESEKERE, V. R., SMITH, R. E. & KROZOWSKI, Z. S. (1994) Cloning and tissue distribution of the human 11 beta-hydroxysteroid dehydrogenase type 2 enzyme. *Mol Cell Endocrinol,* 105**,** R11-7.

AMOR-MAHJOUB, M., SUPPINI, J. P., GOMEZ-VRIELYUNCK, N. & LADJIMI, M. (2006) The effect of the hexahistidine-tag in the oligomerization of HSC70 constructs. *J Chromatogr B Analyt Technol Biomed Life Sci,* 844**,** 328-34.

ANDERSEN, J. M. & DIETSCHY, J. M. (1978) Relative importance of high and low density lipoproteins in the regulation of cholesterol synthesis in the adrenal gland, ovary, and testis of the rat. *J Biol Chem,* 253**,** 9024-32.

ANDREW, R., PHILLIPS, D. I. & WALKER, B. R. (1998) Obesity and gender influence cortisol secretion and metabolism in man. *J Clin Endocrinol Metab,* 83**,** 1806-9.

ANDREWS, R. C., HERLIHY, O., LIVINGSTONE, D. E., ANDREW, R. & WALKER, B. R. (2002) Abnormal cortisol metabolism and tissue sensitivity to cortisol in patients with glucose intolerance. *J Clin Endocrinol Metab,* 87**,** 5587-93.

ANDREWS, R. C., ROOYACKERS, O. & WALKER, B. R. (2003) Effects of the 11 beta-hydroxysteroid dehydrogenase inhibitor carbenoxolone on insulin sensitivity in men with type 2 diabetes. *J Clin Endocrinol Metab,* 88**,** 285-91.

AOYAGI, A., ITO-KOBAYASHI, M., ONO, Y., FURUKAWA, Y., TAKAHASHI, M., MURAMATSU, Y., UMETANI, M. & TAKATSU, T. (2008) Colletoic acid, a novel 11beta-hydroxysteroid dehydrogenase type 1 inhibitor from Colletotrichum gloeosporioides SANK 21404. *J Antibiot (Tokyo),* 61**,** 136-41.

ARAMPATZIS, S., KADEREIT, B., SCHUSTER, D., BALAZS, Z., SCHWEIZER, R. A., FREY, F. J., LANGER, T. & ODERMATT, A. (2005) Comparative enzymology of 11beta-hydroxysteroid dehydrogenase type 1 from six species. *J Mol Endocrinol,* 35**,** 89-101.

ARANDA, A., MARTINEZ-IGLESIAS, O., RUIZ-LLORENTE, L., GARCIA-CARPIZO, V. & ZAMBRANO, A. (2009) Thyroid receptor: roles in cancer. *Trends Endocrinol Metab,* 20**,** 318-24.

ARION, W. J., LANGE, A. J. & WALLS, H. E. (1980a) Glucose-6-Phosphate Transport and Microsomal Glucose-6-Phosphatase .5. Microsomal Membrane Integrity and the Interactions of Phlorizin with the Glucose-6-Phosphatase System. *Journal of Biological Chemistry,* 255**,** 387-395.

ARION, W. J., LANGE, A. J., WALLS, H. E. & BALLAS, L. M. (1980b) Glucose-6-Phosphate Transport and Microsomal Glucose-6-Phosphatase .6. Evidence for the Participation of Independent Translocases for Phosphate and Glucose-6-Phosphate in the Microsomal Glucose-6-Phosphatase System - Interactions of the System with Ortho-Phosphate, Inorganic Pyrophosphate, and Carbamyl-Phosphatee. *Journal of Biological Chemistry,* 255**,** 396-406.

ARNALDI, G., ANGELI, A., ATKINSON, A. B., BERTAGNA, X., CAVAGNINI, F., CHROUSOS, G. P., FAVA, G. A., FINDLING, J. W., GAILLARD, R. C., GROSSMAN, A. B., KOLA, B., LACROIX, A., MANCINI, T., MANTERO, F., NEWELL-PRICE, J., NIEMAN, L. K., SONINO, N., VANCE, M. L., GIUSTINA, A. & BOSCARO, M. (2003) Diagnosis and complications of Cushing's syndrome: a consensus statement. *J Clin Endocrinol Metab,* 88**,** 5593-602.

ARRIZA, J. L., SIMERLY, R. B., SWANSON, L. W. & EVANS, R. M. (1988) The neuronal mineralocorticoid receptor as a mediator of glucocorticoid response. *Neuron,* 1**,** 887-900.

ATANASOV, A. G., DZYAKANCHUK, A. A., SCHWEIZER, R. A., NASHEV, L. G., MAURER, E. M. & ODERMATT, A. (2006) Coffee inhibits the reactivation of glucocorticoids by 11beta-hydroxysteroid dehydrogenase type 1: a glucocorticoid connection in the anti-diabetic action of coffee? *FEBS Lett,* 580**,** 4081-5.

ATANASOV, A. G., NASHEV, L. G., GELMAN, L., LEGEZA, B., SACK, R., PORTMANN, R. & ODERMATT, A. (2008) Direct protein-protein interaction of 11beta-hydroxysteroid dehydrogenase type 1 and hexose-6-phosphate dehydrogenase in the endoplasmic reticulum lumen. *Biochim Biophys Acta,* 1783**,** 1536-43.

ATANASOV, A. G., NASHEV, L. G., SCHWEIZER, R. A., FRICK, C. & ODERMATT, A. (2004) Hexose-6-phosphate dehydrogenase determines the reaction direction of 11beta-hydroxysteroid dehydrogenase type 1 as an oxoreductase. *FEBS Lett,* 571**,** 129-33.

BARF, T., VALLGARDA, J., EMOND, R., HAGGSTROM, C., KURZ, G., NYGREN, A., LARWOOD, V., MOSIALOU, E., AXELSSON, K., OLSSON, R., ENGBLOM, L.,

EDLING, N., RONQUIST-NII, Y., OHMAN, B., ALBERTS, P. & ABRAHMSEN, L. (2002) Arylsulfonamidothiazoles as a new class of potential antidiabetic drugs. Discovery of potent and selective inhibitors of the 11beta-hydroxysteroid dehydrogenase type 1. *J Med Chem,* 45**,** 3813-5.

BENACH, J., ATRIAN, S., GONZALEZ-DUARTE, R. & LADENSTEIN, R. (1998) The refined crystal structure of Drosophila lebanonensis alcohol dehydrogenase at 1.9 A resolution. *J Mol Biol,* 282**,** 383-99.

BENDTSEN, J. D., NIELSEN, H., VON HEIJNE, G. & BRUNAK, S. (2004) Improved prediction of signal peptides: SignalP 3.0. *J Mol Biol,* 340**,** 783-95.

BENEDIKTSSON, R., LINDSAY, R. S., NOBLE, J., SECKL, J. R. & EDWARDS, C. R. (1993) Glucocorticoid exposure in utero: new model for adult hypertension. *Lancet,* 341**,** 339-41.

BEUTLER, E. & MORRISON, M. (1967) Localization and Characteristics of Hexose 6-Phosphate Dehydrogenase (Glucose Dehydrogenase). *Journal of Biological Chemistry,* 242**,** 5289-&.

BHAT, B. G., HOSEA, N., FANJUL, A., HERRERA, J., CHAPMAN, J., THALACKER, F., STEWART, P. M. & REJTO, P. (2007) Demonstration of Proof of Mechanism and Pharmacokinetics and Pharmacodynamic Relationship with PF-915275, an Inhibitor of 11{beta}HSD1, in Cynomolgus Monkeys. *J Pharmacol Exp Ther,* 5**,** 5.

BILLAUDEL, B. & SUTTER, B. C. (1979) Direct effect of corticosterone upon insulin secretion studied by three different techniques. *Horm Metab Res,* 11**,** 555-60.

BLANKENFELDT, W., KERR, I. D., GIRAUD, M. F., MCMIKEN, H. J., LEONARD, G., WHITFIELD, C., MESSNER, P., GRANINGER, M. & NAISMITH, J. H. (2002) Variation on a theme of SDR. dTDP-6-deoxy-L- lyxo-4-hexulose reductase (RmlD) shows a new Mg2+-dependent dimerization mode. *Structure,* 10**,** 773-86.

BLUM, A., MARTIN, H. J. & MASER, E. (2000) Human 11beta-hydroxysteroid dehydrogenase type 1 is enzymatically active in its nonglycosylated form. *Biochem Biophys Res Commun,* 276**,** 428-34.

BRAAKMAN, I., HELENIUS, J. & HELENIUS, A. (1992) Manipulating disulfide bond formation and protein folding in the endoplasmic reticulum. *Embo J,* 11**,** 1717-22.

BRADFORD, M. M. (1976) A rapid and sensitive method for the quantitation of microgram quantities of protein utilizing the principle of protein-dye binding. *Anal Biochem,* 72**,** 248-54.

BRANDS, R., SNIDER, M. D., HINO, Y., PARK, S. S., GELBOIN, H. V. & ROTHMAN, J. E. (1985) Retention of Membrane-Proteins by the Endoplasmic-Reticulum. *Journal of Cell Biology,* 101**,** 1724-1732.

BRONNEGARD, M., ARNER, P., HELLSTROM, L., AKNER, G. & GUSTAFSSON, J. A. (1990) Glucocorticoid receptor messenger ribonucleic acid in different regions of human adipose tissue. *Endocrinology,* 127**,** 1689-96.

BROWN, A. J. & JESSUP, W. (1999) Oxysterols and atherosclerosis. *Atherosclerosis,* 142**,** 1-28.

BROWN, R. W., CHAPMAN, K. E., EDWARDS, C. R. & SECKL, J. R. (1993) Human placental 11 beta-hydroxysteroid dehydrogenase: evidence for and partial purification of a distinct NAD-dependent isoform. *Endocrinology,* 132**,** 2614-21.

BUJALSKA, I. J., DRAPER, N., MICHAILIDOU, Z., TOMLINSON, J. W., WHITE, P. C., CHAPMAN, K. E., WALKER, E. A. & STEWART, P. M. (2005) Hexose-6-phosphate dehydrogenase confers oxo-reductase activity upon 11 beta-hydroxysteroid dehydrogenase type 1. *J Mol Endocrinol,* 34**,** 675-84.

BUJALSKA, I. J., HEWITT, K. N., HAUTON, D., LAVERY, G. G., TOMLINSON, J. W., WALKER, E. A. & STEWART, P. M. (2008) Lack of hexose-6-phosphate

dehydrogenase impairs lipid mobilization from mouse adipose tissue. *Endocrinology,* 149**,** 2584-91.

BUJALSKA, I. J., KUMAR, S., HEWISON, M. & STEWART, P. M. (1999a) Differentiation of adipose stromal cells: The roles of glucocorticoids and 11 beta-hydroxysteroid dehydrogenase. *Endocrinology,* 140**,** 3188-3196.

BUJALSKA, I. J., KUMAR, S., HEWISON, M. & STEWART, P. M. (1999b) Differentiation of adipose stromal cells: the roles of glucocorticoids and 11beta-hydroxysteroid dehydrogenase. *Endocrinology,* 140**,** 3188-96.

BUJALSKA, I. J., KUMAR, S. & STEWART, P. M. (1997) Does central obesity reflect "Cushing's disease of the omentum"? *Lancet,* 349**,** 1210-3.

BUJALSKA, I. J., QUINKLER, M., TOMLINSON, J. W., MONTAGUE, C. T., SMITH, D. M. & STEWART, P. M. (2006) Expression profiling of 11beta-hydroxysteroid dehydrogenase type-1 and glucocorticoid-target genes in subcutaneous and omental human preadipocytes. *J Mol Endocrinol,* 37**,** 327-40.

BUJALSKA, I. J., WALKER, E. A., HEWISON, M. & STEWART, P. M. (2002) A switch in dehydrogenase to reductase activity of 11 beta-hydroxysteroid dehydrogenase type 1 upon differentiation of human omental adipose stromal cells. *J Clin Endocrinol Metab,* 87**,** 1205-10.

BUREIK, M., LISUREK, M. & BERNHARDT, R. (2002) The human steroid hydroxylases CYP1B1 and CYP11B2. *Biol Chem,* 383**,** 1537-51.

CAILLE, S., CUI, S., HWANG, T. L., WANG, X. & FAUL, M. M. (2009) Two asymmetric syntheses of AMG 221, an inhibitor of 11beta-hydroxysteroid dehydrogenase type 1. *J Org Chem,* 74**,** 3833-42.

CASTRO, A., ZHU, J. X., ALTON, G. R., REJTO, P. & ERMOLIEFF, J. (2007) Assay optimization and kinetic profile of the human and the rabbit isoforms of 11beta-HSD1. *Biochem Biophys Res Commun,* 357**,** 561-6.

CHEN, R., LEWIS, K. A., PERRIN, M. H. & VALE, W. W. (1993) Expression cloning of a human corticotropin-releasing-factor receptor. *Proc Natl Acad Sci U S A,* 90**,** 8967-71.

CHIANG, J. Y. (2002) Bile acid regulation of gene expression: roles of nuclear hormone receptors. *Endocr Rev,* 23**,** 443-63.

CHUNG, B. C., MATTESON, K. J., VOUTILAINEN, R., MOHANDAS, T. K. & MILLER, W. L. (1986) Human cholesterol side-chain cleavage enzyme, P450scc: cDNA cloning, assignment of the gene to chromosome 15, and expression in the placenta. *Proc Natl Acad Sci U S A,* 83**,** 8962-6.

CLARK, A. G., GLANOWSKI, S., NIELSEN, R., THOMAS, P. D., KEJARIWAL, A., TODD, M. A., TANENBAUM, D. M., CIVELLO, D., LU, F., MURPHY, B., FERRIERA, S., WANG, G., ZHENG, X., WHITE, T. J., SNINSKY, J. J., ADAMS, M. D. & CARGILL, M. (2003) Inferring nonneutral evolution from human-chimp-mouse orthologous gene trios. *Science,* 302**,** 1960-3.

CLARKE, J. L. & MASON, P. J. (2003) Murine hexose-6-phosphate dehydrogenase: a bifunctional enzyme with broad substrate specificity and 6-phosphogluconolactonase activity. *Archives of Biochemistry and Biophysics,* 415**,** 229-234.

CLASSEN-HOUBEN, D., SCHUSTER, D., DA CUNHA, T., ODERMATT, A., WOLBER, G., JORDIS, U. & KUEENBURG, B. (2009) Selective inhibition of 11beta-hydroxysteroid dehydrogenase 1 by 18alpha-glycyrrhetinic acid but not 18beta-glycyrrhetinic acid. *J Steroid Biochem Mol Biol,* 113**,** 248-52.

COLLARD, F., COLLET, J. F., GERIN, I., VEIGA-DA-CUNHA, M. & VAN SCHAFTINGEN, E. (1999) Identification of the cDNA en coding human 6-

phosphogluconolactonase, the enzyme catalyzing the second step of the pentose phosphate pathway. *Febs Letters,* 459**,** 223-226.
CONDON, J., RICKETTS, M. L., WHORWOOD, C. B. & STEWART, P. M. (1997) Ontogeny and sexual dimorphic expression of mouse type 2 11beta-hydroxysteroid dehydrogenase. *Mol Cell Endocrinol,* 127**,** 121-8.
COPE, C. L. & BLACK, E. (1958) The production rate of cortisol in man. *Br Med J,* 1**,** 1020-4.
COUTTS, G., THOMAS, G., BLAKEY, D. & MERRICK, M. (2002) Membrane sequestration of the signal transduction protein GlnK by the ammonium transporter AmtB. *Embo J,* 21**,** 536-45.
CRYER, A., VAN, R.L.R (1985) *New Perspectives In Adipose Tissue. Structure, Function and Development*, Butterworths.
CUTLER, G. B., JR., GLENN, M., BUSH, M., HODGEN, G. D., GRAHAM, C. E. & LORIAUX, D. L. (1978) Adrenarche: a survey of rodents, domestic animals, and primates. *Endocrinology,* 103**,** 2112-8.
DAHLMAN-WRIGHT, K., SILTALA-ROOS, H., CARLSTEDT-DUKE, J. & GUSTAFSSON, J. A. (1990) Protein-protein interactions facilitate DNA binding by the glucocorticoid receptor DNA-binding domain. *J Biol Chem,* 265**,** 14030-5.
DAHLMAN-WRIGHT, K., WRIGHT, A., CARLSTEDT-DUKE, J. & GUSTAFSSON, J. A. (1992) DNA-binding by the glucocorticoid receptor: a structural and functional analysis. *J Steroid Biochem Mol Biol,* 41**,** 249-72.
DAHLMAN-WRIGHT, K., WRIGHT, A., GUSTAFSSON, J. A. & CARLSTEDT-DUKE, J. (1991) Interaction of the glucocorticoid receptor DNA-binding domain with DNA as a dimer is mediated by a short segment of five amino acids. *J Biol Chem,* 266**,** 3107-12.
DALE, G. E., BROGER, C., LANGEN, H., DARCY, A. & STUBER, D. (1994) Improving Protein Solubility through Rationally Designed Amino-Acid Replacements - Solubilization of the Trimethoprim-Resistant Type S1 Dihydrofolate-Reductase. *Protein Engineering,* 7**,** 933-939.
DAUJOTYTE, D., VILKAITIS, G., MANELYTE, L., SKALICKY, J., SZYPERSKI, T. & KLIMASAUSKAS, S. (2003) Solubility engineering of the HhaI methyltransferase. *Protein Engineering,* 16**,** 295-301.
DAVANI, B., KHAN, A., HULT, M., MARTENSSON, E., OKRET, S., EFENDIC, S., JORNVALL, H. & OPPERMANN, U. C. (2000) Type 1 11beta -hydroxysteroid dehydrogenase mediates glucocorticoid activation and insulin release in pancreatic islets. *J Biol Chem,* 275**,** 34841-4.
DE QUEIROZ, M. S. & WALDROP, G. L. (2007) Modeling and numerical simulation of biotin carboxylase kinetics: implications for half-sites reactivity. *J Theor Biol,* 246**,** 167-75.
DELANO, W. L. (2002) The PyMOL Molecular Graphics System. *DeLano Scientific, Palo Alto, CA, USA.*
DENAULT, J. B., BEKES, M., SCOTT, F. L., SEXTON, K. M., BOGYO, M. & SALVESEN, G. S. (2006) Engineered hybrid dimers: tracking the activation pathway of caspase-7. *Mol Cell,* 23**,** 523-33.
DESBRIERE, R., VUAROQUEAUX, V., ACHARD, V., BOULLU-CIOCCA, S., LABUHN, M., DUTOUR, A. & GRINO, M. (2006) 11beta-hydroxysteroid dehydrogenase type 1 mRNA is increased in both visceral and subcutaneous adipose tissue of obese patients. *Obesity (Silver Spring),* 14**,** 794-8.
DESPRES, J. P., MOORJANI, S., FERLAND, M., TREMBLAY, A., LUPIEN, P. J., NADEAU, A., PINAULT, S., THERIAULT, G. & BOUCHARD, C. (1989) Adipose

tissue distribution and plasma lipoprotein levels in obese women. Importance of intra-abdominal fat. *Arteriosclerosis,* 9**,** 203-10.

DHINGRA, D., PARLE, M. & KULKARNI, S. K. (2004) Memory enhancing activity of Glycyrrhiza glabra in mice. *J Ethnopharmacol,* 91**,** 361-5.

DIEDERICH, S., HANKE, B., OELKERS, W. & BAHR, V. (1997) Metabolism of dexamethasone in the human kidney: nicotinamide adenine dinucleotide-dependent 11beta-reduction. *J Clin Endocrinol Metab,* 82**,** 1598-602.

DRAPER, N., POWELL, B. L., FRANKS, S., CONWAY, G. S., STEWART, P. M. & MCCARTHY, M. I. (2006) Variants implicated in cortisone reductase deficiency do not contribute to susceptibility to common forms of polycystic ovary syndrome. *Clin Endocrinol (Oxf),* 65**,** 64-70.

DRAPER, N. & STEWART, P. M. (2005) 11beta-hydroxysteroid dehydrogenase and the pre-receptor regulation of corticosteroid hormone action. *J Endocrinol,* 186**,** 251-71.

DRAPER, N., WALKER, E. A., BUJALSKA, I. J., TOMLINSON, J. W., CHALDER, S. M., ARLT, W., LAVERY, G. G., BEDENDO, O., RAY, D. W., LAING, I., MALUNOWICZ, E., WHITE, P. C., HEWISON, M., MASON, P. J., CONNELL, J. M., SHACKLETON, C. H. & STEWART, P. M. (2003) Mutations in the genes encoding 11beta-hydroxysteroid dehydrogenase type 1 and hexose-6-phosphate dehydrogenase interact to cause cortisone reductase deficiency. *Nat Genet,* 34**,** 434-9.

DUNKELMAN, S. S., FAIRHURST, B., PLAGER, J. & WATERHOUSE, C. (1964) Cortisol Metabolism in Obesity. *J Clin Endocrinol Metab,* 24**,** 832-41.

DZYAKANCHUK, A. A., BALAZS, Z., NASHEV, L. G., AMREIN, K. E. & ODERMATT, A. (2009) 11beta-Hydroxysteroid dehydrogenase 1 reductase activity is dependent on a high ratio of NADPH/NADP(+) and is stimulated by extracellular glucose. *Mol Cell Endocrinol,* 301**,** 137-41.

ECKEL, R. H., GRUNDY, S. M. & ZIMMET, P. Z. (2005) The metabolic syndrome. *Lancet,* 365**,** 1415-28.

EHRHART-BORNSTEIN, M., HINSON, J. P., BORNSTEIN, S. R., SCHERBAUM, W. A. & VINSON, G. P. (1998) Intraadrenal interactions in the regulation of adrenocortical steroidogenesis. *Endocr Rev,* 19**,** 101-43.

EKLUND, H., NORDSTROM, B., ZEPPEZAUER, E., SODERLUND, G., OHLSSON, I., BOIWE, T. & BRANDEN, C. I. (1974) The structure of horse liver alcohol dehydrogenase. *FEBS Lett,* 44**,** 200-4.

EKLUND, H., PLAPP, B. V., SAMAMA, J. P. & BRANDEN, C. I. (1982) Binding of Substrate in a Ternary Complex of Horse Liver Alcohol-Dehydrogenase. *Journal of Biological Chemistry,* 257**,** 4349-4358.

ELLEBY, B., SVENSSON, S., WU, X., STEFANSSON, K., NILSSON, J., HALLEN, D., OPPERMANN, U. & ABRAHMSEN, L. (2004) High-level production and optimization of monodispersity of 11beta-hydroxysteroid dehydrogenase type 1. *Biochim Biophys Acta,* 1700**,** 199-207.

ENGELI, S., BOHNKE, J., FELDPAUSCH, M., GORZELNIAK, K., HEINTZE, U., JANKE, J., LUFT, F. C. & SHARMA, A. M. (2004) Regulation of 11beta-HSD genes in human adipose tissue: influence of central obesity and weight loss. *Obes Res,* 12**,** 9-17.

ERDMANN, B., DENNER, K., GERST, H., LENZ, D. & BERNHARDT, R. (1995a) Human adrenal CYP11B1: localization by in situ-hybridization and functional expression in cell cultures. *Endocr Res,* 21**,** 425-35.

ERDMANN, B., GERST, H., BULOW, H., LENZ, D., BAHR, V. & BERNHARDT, R. (1995b) Zone-specific localization of cytochrome P45011B1 in human adrenal tissue by PCR-derived riboprobes. *Histochem Cell Biol,* 104**,** 301-7.

FERGUSON, S. E., PALLIKAROS, Z., MICHAEL, A. E. & COOKE, B. A. (1999) The effects of different culture media, glucose, pyridine nucleotides and adenosine on the activity of 11 beta-hydroxysteroid dehydrogenase in rat Leydig cells. *Molecular and Cellular Endocrinology,* 158**,** 37-44.

FILLING, C., BERNDT, K. D., BENACH, J., KNAPP, S., PROZOROVSKI, T., NORDLING, E., LADENSTEIN, R., JORNVALL, H. & OPPERMANN, U. (2002) Critical residues for structure and catalysis in short-chain dehydrogenases/reductases. *J Biol Chem,* 277**,** 25677-84.

FILLING, C., NORDLING, E., BENACH, J., BERNDT, K. D., LADENSTEIN, R., JORNVALL, H. & OPPERMANN, U. (2001) Structural role of conserved Asn179 in the short-chain dehydrogenase/reductase scaffold. *Biochem Biophys Res Commun,* 289**,** 712-7.

FOLCH, B., ROOMAN, M. & DEHOUCK, Y. (2008) Thermostability of salt bridges versus hydrophobic interactions in proteins probed by statistical potentials. *Journal of Chemical Information and Modeling,* 48**,** 119-127.

FOSTER, J. D., PEDERSON, B. A. & NORDLIE, R. C. (1997) Glucose-6-phosphatase structure regulation, and function: An update. *Proceedings of the Society for Experimental Biology and Medicine,* 215**,** 314-332.

FOTSCH, C., BARTBERGER, M. D., BERCOT, E. A., CHEN, M., CUPPLES, R., EMERY, M., FRETLAND, J., GURAM, A., HALE, C., HAN, N., HICKMAN, D., HUNGATE, R. W., HAYASHI, M., KOMOROWSKI, R., LIU, Q., MATSUMOTO, G., ST JEAN, D. J., JR., URSU, S., VENIANT, M., XU, G., YE, Q., YUAN, C., ZHANG, J., ZHANG, X., TU, H. & WANG, M. (2008) Further studies with the 2-amino-1,3-thiazol-4(5H)-one class of 11beta-hydroxysteroid dehydrogenase type 1 inhibitors: reducing pregnane X receptor activity and exploring activity in a monkey pharmacodynamic model. *J Med Chem,* 51**,** 7953-67.

FRASER, R., INGRAM, M. C., ANDERSON, N. H., MORRISON, C., DAVIES, E. & CONNELL, J. M. (1999) Cortisol effects on body mass, blood pressure, and cholesterol in the general population. *Hypertension,* 33**,** 1364-8.

FUJIOKA, S., MATSUZAWA, Y., TOKUNAGA, K. & TARUI, S. (1987) Contribution of intra-abdominal fat accumulation to the impairment of glucose and lipid metabolism in human obesity. *Metabolism,* 36**,** 54-9.

GABDOULLINE, R. R. & WADE, R. C. (2001) Protein-protein association: Investigation of factors influencing association rates by Brownian dynamics simulations. *Journal of Molecular Biology,* 306**,** 1139-1155.

GE, R. S., HARDY, D. O., CATTERALL, J. F. & HARDY, M. P. (1997) Developmental changes in glucocorticoid receptor and 11 beta-hydroxysteroid dehydrogenase oxidative and reductive activities in rat Leydig cells. *Endocrinology,* 138**,** 5089-5095.

GHAYEE, H. K. & AUCHUS, R. J. (2007) Basic concepts and recent developments in human steroid hormone biosynthesis. *Rev Endocr Metab Disord,* 8**,** 289-300.

GHOSH, D., WEEKS, C. M., GROCHULSKI, P., DUAX, W. L., ERMAN, M., RIMSAY, R. L. & ORR, J. C. (1991) Three-dimensional structure of holo 3 alpha,20 beta-hydroxysteroid dehydrogenase: a member of a short-chain dehydrogenase family. *Proc Natl Acad Sci U S A,* 88**,** 10064-8.

GLASS, A. R., BURMAN, K. D., DAHMS, W. T. & BOEHM, T. M. (1981) Endocrine function in human obesity. *Metabolism,* 30**,** 89-104.

GOEDECKE, J. H., WAKE, D. J., LEVITT, N. S., LAMBERT, E. V., COLLINS, M. R., MORTON, N. M., ANDREW, R., SECKL, J. R. & WALKER, B. R. (2006) Glucocorticoid metabolism within superficial subcutaneous rather than visceral

adipose tissue is associated with features of the metabolic syndrome in South African women. *Clin Endocrinol (Oxf),* 65**,** 81-7.

GOMEZ-SANCHEZ, E. P., GANJAM, V., CHEN, Y. J., LIU, Y., CLARK, S. A. & GOMEZ-SANCHEZ, C. E. (2001) The 11beta hydroxysteroid dehydrogenase 2 exists as an inactive dimer. *Steroids,* 66**,** 845-8.

GOMEZ-SANCHEZ, E. P., GOMEZ-SANCHEZ, M. T., DE RODRIGUEZ, A. F., ROMERO, D. G., WARDEN, M. P., PLONCZYNSKI, M. W. & GOMEZ-SANCHEZ, C. E. (2009) Immunohistochemical demonstration of the mineralocorticoid receptor, 11beta-hydroxysteroid dehydrogenase-1 and -2, and hexose-6-phosphate dehydrogenase in rat ovary. *J Histochem Cytochem,* 57**,** 633-41.

GROMADA, J., DING, W. G., BARG, S., RENSTROM, E. & RORSMAN, P. (1997) Multisite regulation of insulin secretion by cAMP-increasing agonists: evidence that glucagon-like peptide 1 and glucagon act via distinct receptors. *Pflugers Arch,* 434**,** 515-24.

GUILLEMIN, R. & ROSENBERG, B. (1955) Humoral hypothalamic control of anterior pituitary: a study with combined tissue cultures. *Endocrinology,* 57**,** 599-607.

GUMY, C., THURNBICHLER, C., AUBRY, E. M., BALAZS, Z., PFISTERER, P., BAUMGARTNER, L., STUPPNER, H., ODERMATT, A. & ROLLINGER, J. M. (2009) Inhibition of 11beta-hydroxysteroid dehydrogenase type 1 by plant extracts used as traditional antidiabetic medicines. *Fitoterapia,* 23**,** 23.

GUZMAN, L. M., BELIN, D., CARSON, M. J. & BECKWITH, J. (1995) Tight regulation, modulation, and high-level expression by vectors containing the arabinose PBAD promoter. *J Bacteriol,* 177**,** 4121-30.

HALE, C., VENIANT, M., WANG, Z., CHEN, M., MCCORMICK, J., CUPPLES, R., HICKMAN, D., MIN, X., SUDOM, A., XU, H., MATSUMOTO, G., FOTSCH, C., ST JEAN, D. J., JR. & WANG, M. (2008) Structural characterization and pharmacodynamic effects of an orally active 11beta-hydroxysteroid dehydrogenase type 1 inhibitor. *Chem Biol Drug Des,* 71**,** 36-44.

HANSCH, C. L., A (1995) *Exploring QSAR, Fundamentals and Applications in Chemistry and Biology*, American Chemical Society.

HAUNER, H., SCHMID, P. & PFEIFFER, E. F. (1987) Glucocorticoids and insulin promote the differentiation of human adipocyte precursor cells into fat cells. *J Clin Endocrinol Metab,* 64**,** 832-5.

HAUTANEN, A. & ADLERCREUTZ, H. (1993) Altered adrenocorticotropin and cortisol secretion in abdominal obesity: implications for the insulin resistance syndrome. *J Intern Med,* 234**,** 461-9.

HAYASHI, R., WADA, H., ITO, K. & ADCOCK, I. M. (2004) Effects of glucocorticoids on gene transcription. *Eur J Pharmacol,* 500**,** 51-62.

HELD, D., YAEGER, K., AND NOVY, R. (2003) *inNovations***,** 3.

HENNEBERT, O., MONTES, M., FAVRE-REGUILLON, A., CHERMETTE, H., FERROUD, C. & MORFIN, R. (2009) Epimerase activity of the human 11beta-hydroxysteroid dehydrogenase type 1 on 7-hydroxylated C19-steroids. *J Steroid Biochem Mol Biol,* 114**,** 57-63.

HEWITT, K. N., WALKER, E. A. & STEWART, P. M. (2005) Minireview: Hexose-6-phosphate dehydrogenase and redox control of 11 beta-hydroxysteroid dehydrogenase type 1 activity. *Endocrinology,* 146**,** 2539-2543.

HOLLENBERG, S. M., WEINBERGER, C., ONG, E. S., CERELLI, G., ORO, A., LEBO, R., THOMPSON, E. B., ROSENFELD, M. G. & EVANS, R. M. (1985) Primary structure and expression of a functional human glucocorticoid receptor cDNA. *Nature,* 318**,** 635-41.

HOLMES, M. C., CARTER, R. N., NOBLE, J., CHITNIS, S., DUTIA, A., PATERSON, J. M., MULLINS, J. J., SECKL, J. R. & YAU, J. L. (2010) 11beta-hydroxysteroid dehydrogenase type 1 expression is increased in the aged mouse hippocampus and parietal cortex and causes memory impairments. *J Neurosci,* 30**,** 6916-20.

HOLT, R. G. & HANLEY, N. A. (2007) *Essential Endocrinology and Diabetes*, Blackwell Publishing.

HOQUE, M. M., SHIMIZU, S., HOSSAIN, M. T., YAMAMOTO, T., IMAMURA, S., SUZUKI, K., TSUNODA, M., AMANO, H., SEKIGUCHI, T. & TAKENAKA, A. (2008) The structures of Alcaligenes faecalis D-3-hydroxybutyrate dehydrogenase before and after NAD+ and acetate binding suggest a dynamical reaction mechanism as a member of the SDR family. *Acta Crystallogr D Biol Crystallogr,* 64**,** 496-505.

HOSFIELD, D. J., WU, Y., SKENE, R. J., HILGERS, M., JENNINGS, A., SNELL, G. P. & AERTGEERTS, K. (2005) Conformational flexibility in crystal structures of human 11beta-hydroxysteroid dehydrogenase type I provide insights into glucocorticoid interconversion and enzyme regulation. *J Biol Chem,* 280**,** 4639-48.

HOZJAN, V., GUO, K., WU, X. & OPPERMANN, U. (2008) Ligand supplementation as a method to increase soluble heterologous protein production. *Expert Rev Proteomics,* 5**,** 137-43.

HUANG, Y. W., PINEAU, I., CHANG, H. J., AZZI, A., BELLEMARE, V., LABERGE, S. & LIN, S. X. (2001) Critical residues for the specificity of cofactors and substrates in human estrogenic 17beta-hydroxysteroid dehydrogenase 1: variants designed from the three-dimensional structure of the enzyme. *Mol Endocrinol,* 15**,** 2010-20.

HULT, M., ELLEBY, B., SHAFQAT, N., SVENSSON, S., RANE, A., JORNVALL, H., ABRAHMSEN, L. & OPPERMANN, U. (2004) Human and rodent type 1 11beta-hydroxysteroid dehydrogenases are 7beta-hydroxycholesterol dehydrogenases involved in oxysterol metabolism. *Cell Mol Life Sci,* 61**,** 992-9.

HULT, M., JORNVALL, H. & OPPERMANN, U. C. (1998) Selective inhibition of human type 1 11beta-hydroxysteroid dehydrogenase by synthetic steroids and xenobiotics. *FEBS Lett,* 441**,** 25-8.

HULT, M., NOBEL, C. S., ABRAHMSEN, L., NICOLL-GRIFFITH, D. A., JORNVALL, H. & OPPERMANN, U. C. (2001) Novel enzymological profiles of human 11beta-hydroxysteroid dehydrogenase type 1. *Chem Biol Interact,* 130-132**,** 805-14.

HULT, M., ORTSATER, H., SCHUSTER, G., GRAEDLER, F., BECKERS, J., ADAMSKI, J., PLONER, A., JORNVALL, H., BERGSTEN, P. & OPPERMANN, U. (2009) Short-term glucocorticoid treatment increases insulin secretion in islets derived from lean mice through multiple pathways and mechanisms. *Mol Cell Endocrinol,* 301**,** 109-16.

HULT, M., SHAFQAT, N., ELLEBY, B., MITSCHKE, D., SVENSSON, S., FORSGREN, M., BARF, T., VALLGARDA, J., ABRAHMSEN, L. & OPPERMANN, U. (2006) Active site variability of type 1 11beta-hydroxysteroid dehydrogenase revealed by selective inhibitors and cross-species comparisons. *Mol Cell Endocrinol,* 248**,** 26-33.

HWANG, C. C., HSU, C. N., HUANG, T. J., CHIOU, S. J. & HONG, Y. R. (2009) Interactions across the interface contribute the stability of homodimeric 3 alpha-hydroxysteroid dehydrogenase/carbonyl reductase. *Archives of Biochemistry and Biophysics,* 490**,** 36-41.

ITO-KOBAYASHI, M., AOYAGI, A., TANAKA, I., MURAMATSU, Y., UMETANI, M. & TAKATSU, T. (2008) Sterenin A, B, C and D, novel 11beta-hydroxysteroid dehydrogenase type 1 inhibitors from Stereum sp. SANK 21205. *J Antibiot (Tokyo),* 61**,** 128-35.

JACOBS, M. N. & LEWIS, D. F. (2002) Steroid hormone receptors and dietary ligands: a selected review. *Proc Nutr Soc,* 61**,** 105-22.

JAMIESON, A., WALLACE, A. M., ANDREW, R., NUNEZ, B. S., WALKER, B. R., FRASER, R., WHITE, P. C. & CONNELL, J. M. (1999) Apparent cortisone reductase deficiency: a functional defect in 11beta-hydroxysteroid dehydrogenase type 1. *J Clin Endocrinol Metab,* 84**,** 3570-4.

JAMIESON, P. M., CHAPMAN, K. E., EDWARDS, C. R. & SECKL, J. R. (1995) 11 beta-hydroxysteroid dehydrogenase is an exclusive 11 beta- reductase in primary cultures of rat hepatocytes: effect of physicochemical and hormonal manipulations. *Endocrinology,* 136**,** 4754-61.

JANIYANI, K., BORDELON, T., WALDROP, G. L. & CRONAN, J. E., JR. (2001) Function of Escherichia coli biotin carboxylase requires catalytic activity of both subunits of the homodimer. *J Biol Chem,* 276**,** 29864-70.

JEAN, D. J., JR., YUAN, C., BERCOT, E. A., CUPPLES, R., CHEN, M., FRETLAND, J., HALE, C., HUNGATE, R. W., KOMOROWSKI, R., VENIANT, M., WANG, M., ZHANG, X. & FOTSCH, C. (2007) 2-(S)-phenethylaminothiazolones as potent, orally efficacious inhibitors of 11beta-hydroxysteriod dehydrogenase type 1. *J Med Chem,* 50**,** 429-32.

JORNVALL, H., PERSSON, B., KROOK, M., ATRIAN, S., GONZALEZ-DUARTE, R., JEFFERY, J. & GHOSH, D. (1995) Short-chain dehydrogenases/reductases (SDR). *Biochemistry,* 34**,** 6003-13.

JORNVALL, H., PERSSON, M. & JEFFERY, J. (1981) Alcohol and Polyol Dehydrogenases Are Both Divided into 2 Protein Types, and Structural-Properties Cross-Relate the Different Enzyme-Activities within Each Type. *Proceedings of the National Academy of Sciences of the United States of America-Biological Sciences,* 78**,** 4226-4230.

JULIAN, L. D., WANG, Z., BOSTICK, T., CAILLE, S., CHOI, R., DEGRAFFENREID, M., DI, Y., HE, X., HUNGATE, R. W., JAEN, J. C., LIU, J., MONSHOUWER, M., MCMINN, D., REW, Y., SUDOM, A., SUN, D., TU, H., URSU, S., WALKER, N., YAN, X., YE, Q. & POWERS, J. P. (2008) Discovery of novel, potent benzamide inhibitors of 11beta-hydroxysteroid dehydrogenase type 1 (11beta-HSD1) exhibiting oral activity in an enzyme inhibition ex vivo model. *J Med Chem,* 51**,** 3953-60.

KABSCH, W. (1993) Automatic processing of rotation diffraction data from crystals of initially unknown symmetry and cell constants. *Journal of Applied Crystallography,* 26**,** 795-800.

KANNISTO, K., PIETILAINEN, K. H., EHRENBORG, E., RISSANEN, A., KAPRIO, J., HAMSTEN, A. & YKI-JARVINEN, H. (2004) Overexpression of 11beta-hydroxysteroid dehydrogenase-1 in adipose tissue is associated with acquired obesity and features of insulin resistance: studies in young adult monozygotic twins. *J Clin Endocrinol Metab,* 89**,** 4414-21.

KAVANAGH, K. L., JORNVALL, H., PERSSON, B. & OPPERMANN, U. (2008) Medium- and short-chain dehydrogenase/reductase gene and protein families : the SDR superfamily: functional and structural diversity within a family of metabolic and regulatory enzymes. *Cell Mol Life Sci,* 65**,** 3895-906.

KENOUCH, S., LOMBES, M., DELAHAYE, F., EUGENE, E., BONVALET, J. P. & FARMAN, N. (1994) Human skin as target for aldosterone: coexpression of mineralocorticoid receptors and 11 beta-hydroxysteroid dehydrogenase. *J Clin Endocrinol Metab,* 79**,** 1334-41.

KERSTENS, M. N., RIEMENS, S. C., SLUITER, W. J., PRATT, J. J., WOLTHERS, B. G. & DULLAART, R. P. (2000) Lack of relationship between 11beta-hydroxysteroid dehydrogenase setpoint and insulin sensitivity in the basal state and after 24h of

insulin infusion in healthy subjects and type 2 diabetic patients. *Clin Endocrinol (Oxf),* 52**,** 403-11.

KHAN, N., SHARMA, K. K., ANDERSSON, S. & AUCHUS, R. J. (2004) Human 17beta-hydroxysteroid dehydrogenases types 1, 2, and 3 catalyze bi-directional equilibrium reactions, rather than unidirectional metabolism, in HEK-293 cells. *Arch Biochem Biophys,* 429**,** 50-9.

KIM, K. W., WANG, Z., BUSBY, J., TSURUDA, T., CHEN, M., HALE, C., CASTRO, V. M., SVENSSON, S., NYBO, R., XIONG, F. & WANG, M. (2006) The role of tyrosine 177 in human 11beta-hydroxysteroid dehydrogenase type 1 in substrate and inhibitor binding: an unlikely hydrogen bond donor for the substrate. *Biochim Biophys Acta,* 1764**,** 824-30.

KIM, K. W., WANG, Z., BUSBY, J., TSURUDA, T., CHEN, M., HALE, C., CASTRO, V. M., SVENSSON, S., NYBO, R., XIONG, F. & WANG, M. (2007) The selectivity of tyrosine 280 of human 11beta-hydroxysteroid dehydrogenase type 1 in inhibitor binding. *FEBS Lett,* 581**,** 995-9.

KLEMCKE, H. G., SAMPATH KUMAR, R., YANG, K., VALLET, J. L. & CHRISTENSON, R. K. (2003) 11beta-hydroxysteroid dehydrogenase and glucocorticoid receptor messenger RNA expression in porcine placentae: effects of stage of gestation, breed, and uterine environment. *Biol Reprod,* 69**,** 1945-50.

KONOPELSKA, S., KIENITZ, T., HUGHES, B., PIRLICH, M., BAUDITZ, J., LOCHS, H., STRASBURGER, C. J., STEWART, P. M. & QUINKLER, M. (2009) Hepatic 11beta-HSD1 mRNA expression in fatty liver and nonalcoholic steatohepatitis. *Clin Endocrinol (Oxf),* 70**,** 554-60.

KOTELEVTSEV, Y., HOLMES, M. C., BURCHELL, A., HOUSTON, P. M., SCHMOLL, D., JAMIESON, P., BEST, R., BROWN, R., EDWARDS, C. R., SECKL, J. R. & MULLINS, J. J. (1997) 11beta-hydroxysteroid dehydrogenase type 1 knockout mice show attenuated glucocorticoid-inducible responses and resist hyperglycemia on obesity or stress. *Proc Natl Acad Sci U S A,* 94**,** 14924-9.

KRISSINEL, E. & HENRICK, K. (2007) Inference of macromolecular assemblies from crystalline state. *J Mol Biol,* 372**,** 774-97.

KROGH, A., LARSSON, B., VON HEIJNE, G. & SONNHAMMER, E. L. (2001) Predicting transmembrane protein topology with a hidden Markov model: application to complete genomes. *J Mol Biol,* 305**,** 567-80.

KROZOWSKI, Z., STUCHBERY, S., WHITE, P., MONDER, C. & FUNDER, J. W. (1990) Characterization of 11 beta-hydroxysteroid dehydrogenase gene expression: identification of multiple unique forms of messenger ribonucleic acid in the rat kidney. *Endocrinology,* 127**,** 3009-13.

KROZOWSKI, Z. S. & FUNDER, J. W. (1983) Renal mineralocorticoid receptors and hippocampal corticosterone-binding species have identical intrinsic steroid specificity. *Proc Natl Acad Sci U S A,* 80**,** 6056-60.

KULKARNI, A. P. & HODGSON, E. (1982) Mouse-Liver Microsomal Hexose-6-Phosphate Dehydrogenase - Nadph Generation and Utilization in Monooxygenation Reactions. *Biochemical Pharmacology,* 31**,** 1131-1137.

KUMAR, S. & NUSSINOV, R. (2002) Close-range electrostatic interactions in proteins. *Chembiochem,* 3**,** 604-617.

LAKOWICZ, J. R. (1999) *Principles of Fluorescence Spectroscopy,* New York, Penum Press.

LAKSHMI, V. & MONDER, C. (1988) Purification and characterization of the corticosteroid 11 beta-dehydrogenase component of the rat liver 11 beta-hydroxysteroid dehydrogenase complex. *Endocrinology,* 123**,** 2390-8.

LAKSHMI, V., NATH, N. & MUNEYYIRCI-DELALE, O. (1993) Characterization of 11 beta-hydroxysteroid dehydrogenase of human placenta: evidence for the existence of two species of 11 beta-hydroxysteroid dehydrogenase. *J Steroid Biochem Mol Biol,* 45**,** 391-7.

LAMBILLOTTE, C., GILON, P. & HENQUIN, J. C. (1997) Direct glucocorticoid inhibition of insulin secretion. An in vitro study of dexamethasone effects in mouse islets. *J Clin Invest,* 99**,** 414-23.

LANDFIELD, P. W., BASKIN, R. K. & PITLER, T. A. (1981) Brain aging correlates: retardation by hormonal-pharmacological treatments. *Science,* 214**,** 581-4.

LANDFIELD, P. W., WAYMIRE, J. C. & LYNCH, G. (1978) Hippocampal aging and adrenocorticoids: quantitative correlations. *Science,* 202**,** 1098-102.

LANGE, A. J., ARION, W. J. & BEAUDET, A. L. (1980) Type-Ib Glycogen-Storage Disease Is Caused by a Defect in the Glucose-6-Phosphate Translocase of the Microsomal Glucose-6-Phosphatase System. *Journal of Biological Chemistry,* 255**,** 8381-8384.

LARSON, J. R., COON, M. J. & PORTER, T. D. (1991) Alcohol-inducible cytochrome P-450IIE1 lacking the hydrophobic NH2-terminal segment retains catalytic activity and is membrane-bound when expressed in Escherichia coli. *J Biol Chem,* 266**,** 7321-4.

LASSO, G., ANTONIW, J. F. & MULLINS, J. G. (2006) A combinatorial pattern discovery approach for the prediction of membrane dipping (re-entrant) loops. *Bioinformatics,* 22**,** e290-7.

LAVERY, G. G., WALKER, E. A., DRAPER, N., JEYASURIA, P., MARCOS, J., SHACKLETON, C. H., PARKER, K. L., WHITE, P. C. & STEWART, P. M. (2006a) Hexose-6-phosphate dehydrogenase knock-out mice lack 11 beta-hydroxysteroid dehydrogenase type 1-mediated glucocorticoid generation. *J Biol Chem,* 281**,** 6546-51.

LAVERY, G. G., WALKER, E. A., DRAPER, N., JEYASURIA, P., MARCOS, J., SHACKLETON, C. H. L., PARKER, K. L., WHITE, P. C. & STEWART, P. M. (2006b) Hexose-6-phosphate dehydrogenase knock-out mice lack 11 beta-hydroxysteroid dehydrogenase type 1-mediated glucocorticoid generation. *Journal of Biological Chemistry,* 281**,** 6546-6551.

LAVERY, G. G., WALKER, E. A., TIGANESCU, A., RIDE, J. P., SHACKLETON, C. H., TOMLINSON, J. W., CONNELL, J. M., RAY, D. W., BIASON-LAUBER, A., MALUNOWICZ, E. M., ARLT, W. & STEWART, P. M. (2008) Steroid biomarkers and genetic studies reveal inactivating mutations in hexose-6-phosphate dehydrogenase in patients with cortisone reductase deficiency. *J Clin Endocrinol Metab,* 93**,** 3827-32.

LAWSON, A. J., WALKER, E. A., WHITE, S. A., DAFFORN, T. R., STEWART, P. M. & RIDE, J. P. (2009) Mutations of key hydrophobic surface residues of 11 beta-hydroxysteroid dehydrogenase type 1 increase solubility and monodispersity in a bacterial expression system. *Protein Sci,* 18**,** 1552-63.

LAYCOCK, J. F., LEE J, WISE P.H (1996) *Essential Endocrinology*, Oxford Medical Publications.

LECKIE, C. M., WELBERG, L. A. & SECKL, J. R. (1998) 11beta-hydroxysteroid dehydrogenase is a predominant reductase in intact rat Leydig cells. *J Endocrinol,* 159**,** 233-8.

LEPIFRE, F., CHRISTMANN-FRANCK, S., ROCHE, D., LERICHE, C., CARNIATO, D., CHARON, C., BOZEC, S., DOARE, L., SCHMIDLIN, F., LECOMTE, M. & VALEUR, E. (2009) Discovery and structure-guided drug design of inhibitors of

11beta-hydroxysteroid-dehydrogenase type I based on a spiro-carboxamide scaffold. *Bioorg Med Chem Lett,* 19**,** 3682-5.

LI, K. X., SMITH, R. E., FERRARI, P., FUNDER, J. W. & KROZOWSKI, Z. S. (1996) Rat 11 beta-hydroxysteroid dehydrogenase type 2 enzyme is expressed at low levels in the placenta and is modulated by adrenal steroids in the kidney. *Mol Cell Endocrinol,* 120**,** 67-75.

LIAO, D. I., THOMPSON, J. E., FAHNESTOCK, S., VALENT, B. & JORDAN, D. B. (2001) A structural account of substrate and inhibitor specificity differences between two naphthol reductases. *Biochemistry,* 40**,** 8696-8704.

LINDSAY, R. S., WAKE, D. J., NAIR, S., BUNT, J., LIVINGSTONE, D. E., PERMANA, P. A., TATARANNI, P. A. & WALKER, B. R. (2003) Subcutaneous adipose 11 beta-hydroxysteroid dehydrogenase type 1 activity and messenger ribonucleic acid levels are associated with adiposity and insulinemia in Pima Indians and Caucasians. *J Clin Endocrinol Metab,* 88**,** 2738-44.

LIU, Y., MLADINOV, D., PIETRUSZ, J. L., USA, K. & LIANG, M. (2009) Glucocorticoid response elements and 11 beta-hydroxysteroid dehydrogenases in the regulation of endothelial nitric oxide synthase expression. *Cardiovasc Res,* 81**,** 140-7.

LIU, Y., NAKAGAWA, Y., WANG, Y., LI, R., LI, X., OHZEKI, T. & FRIEDMAN, T. C. (2003) Leptin activation of corticosterone production in hepatocytes may contribute to the reversal of obesity and hyperglycemia in leptin-deficient ob/ob mice. *Diabetes,* 52**,** 1409-16.

LIVINGSTONE, D. E., JONES, G. C., SMITH, K., JAMIESON, P. M., ANDREW, R., KENYON, C. J. & WALKER, B. R. (2000) Understanding the role of glucocorticoids in obesity: tissue-specific alterations of corticosterone metabolism in obese Zucker rats. *Endocrinology,* 141**,** 560-3.

LONDON, E., LALA, G., BERGER, R., PANZENBECK, A., KOHLI, A. A., RENNER, M., JACKSON, A., RAYNOR, T., LOYA, K. & CASTONGUAY, T. W. (2007) Sucrose access differentially modifies 11beta-hydroxysteroid dehydrogenase-1 and hexose-6-phosphate dehydrogenase message in liver and adipose tissue in rats. *J Nutr,* 137**,** 2616-21.

LOSEL, R. M., FALKENSTEIN, E., FEURING, M., SCHULTZ, A., TILLMANN, H. C., ROSSOL-HASEROTH, K. & WEHLING, M. (2003) Nongenomic steroid action: controversies, questions, and answers. *Physiol Rev,* 83**,** 965-1016.

MAGNESS, C. L., FELLIN, P. C., THOMAS, M. J., KORTH, M. J., AGY, M. B., PROLL, S. C., FITZGIBBON, M., SCHERER, C. A., MINER, D. G., KATZE, M. G. & IADONATO, S. P. (2005) Analysis of the Macaca mulatta transcriptome and the sequence divergence between Macaca and human. *Genome Biol,* 6**,** R60.

MARCOLONGO, P., SENESI, S., GAVA, B., FULCERI, R., SORRENTINO, V., MARGITTAI, E., LIZAK, B., CSALA, M., BANHEGYI, G. & BENEDETTI, A. (2008) Metyrapone prevents cortisone-induced preadipocyte differentiation by depleting luminal NADPH of the endoplasmic reticulum. *Biochem Pharmacol,* 76**,** 382-90.

MARGITTAI, E. & BANHEGYI, G. (2008) Isocitrate dehydrogenase: A NADPH-generating enzyme in the lumen of the endoplasmic reticulum. *Arch Biochem Biophys,* 471**,** 184-90.

MASER, E., VOLKER, B. & FRIEBERTSHAUSER, J. (2002) 11 Beta-hydroxysteroid dehydrogenase type 1 from human liver: dimerization and enzyme cooperativity support its postulated role as glucocorticoid reductase. *Biochemistry,* 41**,** 2459-65.

MASON, P. J., STEVENS, D., DIEZ, A., KNIGHT, S. W., SCOPES, D. A. & VULLIAMY, T. J. (1999) Human hexose-6-phosphate dehydrogenase (Glucose 1-dehydrogenase)

encoded at 1p36: Coding sequence and expression. *Blood Cells Molecules and Diseases,* 25**,** 30-37.
MASSEY, J. B. & POWNALL, H. J. (2005) The polar nature of 7-ketocholesterol determines its location within membrane domains and the kinetics of membrane microsolubilization by apolipoprotein A-I. *Biochemistry,* 44**,** 10423-33.
MASUZAKI, H., PATERSON, J., SHINYAMA, H., MORTON, N. M., MULLINS, J. J., SECKL, J. R. & FLIER, J. S. (2001) A transgenic model of visceral obesity and the metabolic syndrome. *Science,* 294**,** 2166-70.
MASUZAKI, H., YAMAMOTO, H., KENYON, C. J., ELMQUIST, J. K., MORTON, N. M., PATERSON, J. M., SHINYAMA, H., SHARP, M. G., FLEMING, S., MULLINS, J. J., SECKL, J. R. & FLIER, J. S. (2003) Transgenic amplification of glucocorticoid action in adipose tissue causes high blood pressure in mice. *J Clin Invest,* 112**,** 83-90.
MATTERI, R. (1995) *Hormones, Anterior Pituitary Hormones*, John Wiley & Sons, Inc.
MCMINN, D. L., REW, Y., SUDOM, A., CAILLE, S., DEGRAFFENREID, M., HE, X., HUNGATE, R., JIANG, B., JAEN, J., JULIAN, L. D., KAIZERMAN, J., NOVAK, P., SUN, D., TU, H., URSU, S., WALKER, N. P., YAN, X., YE, Q., WANG, Z. & POWERS, J. P. (2009) Optimization of novel di-substituted cyclohexylbenzamide derivatives as potent 11 beta-HSD1 inhibitors. *Bioorg Med Chem Lett,* 19**,** 1446-50.
MEANEY, M. J., AITKEN, D. H., VAN BERKEL, C., BHATNAGAR, S. & SAPOLSKY, R. M. (1988) Effect of neonatal handling on age-related impairments associated with the hippocampus. *Science,* 239**,** 766-8.
MEANEY, M. J., O'DONNELL, D., ROWE, W., TANNENBAUM, B., STEVERMAN, A., WALKER, M., NAIR, N. P. & LUPIEN, S. (1995) Individual differences in hypothalamic-pituitary-adrenal activity in later life and hippocampal aging. *Exp Gerontol,* 30**,** 229-51.
MIGEON, C. J., GREEN, O. C. & ECKERT, J. P. (1963) Study of Adrenocortical Function in Obesity. *Metabolism,* 12**,** 718-39.
MILLAN, M. A., SAMRA, A. B., WYNN, P. C., CATT, K. J. & AGUILERA, G. (1987) Receptors and actions of corticotropin-releasing hormone in the primate pituitary gland. *J Clin Endocrinol Metab,* 64**,** 1036-41.
MILLER, W. L. (1988) Molecular biology of steroid hormone synthesis. *Endocr Rev,* 9**,** 295-318.
MILLER, W. L. & MOREL, Y. (1989) The molecular genetics of 21-hydroxylase deficiency. *Annu Rev Genet,* 23**,** 371-93.
MILLER, W. L., TYRELL, J.B., (1995) *The adrenal cortex*, McGraw-Hill Press, New York, USA.
MOISAN, M. P., SECKL, J. R. & EDWARDS, C. R. (1990) 11 beta-hydroxysteroid dehydrogenase bioactivity and messenger RNA expression in rat forebrain: localization in hypothalamus, hippocampus, and cortex. *Endocrinology,* 127**,** 1450-5.
MONDER, C. & BRADLOW, H. L. (1980) Cortoic acids: explorations at the frontier of corticosteroid metabolism. *Recent Prog Horm Res,* 36**,** 345-400.
MOORE, C. C., MELLON, S. H., MURAI, J., SIITERI, P. K. & MILLER, W. L. (1993) Structure and function of the hepatic form of 11 beta-hydroxysteroid dehydrogenase in the squirrel monkey, an animal model of glucocorticoid resistance. *Endocrinology,* 133**,** 368-75.
MORENO-DIAZ, H., VILLALOBOS-MOLINA, R., ORTIZ-ANDRADE, R., DIAZ-COUTINO, D., MEDINA-FRANCO, J. L., WEBSTER, S. P., BINNIE, M., ESTRADA-SOTO, S., IBARRA-BARAJAS, M., LEON-RIVERA, I. &

NAVARRETE-VAZQUEZ, G. (2008) Antidiabetic activity of N-(6-substituted-1,3-benzothiazol-2-yl)benzenesulfonamides. *Bioorg Med Chem Lett,* 18**,** 2871-7.

MORTON, N. M., HOLMES, M. C., FIEVET, C., STAELS, B., TAILLEUX, A., MULLINS, J. J. & SECKL, J. R. (2001) Improved lipid and lipoprotein profile, hepatic insulin sensitivity, and glucose tolerance in 11beta-hydroxysteroid dehydrogenase type 1 null mice. *J Biol Chem,* 276**,** 41293-300.

MOSAVI, L. K. & PENG, Z. Y. (2003) Structure-based substitutions for increased solubility of a designed protein. *Protein Engineering,* 16**,** 739-745.

MULLER, C., POMPON, D., URBAN, P. & MORFIN, R. (2006) Inter-conversion of 7alpha- and 7beta-hydroxy-dehydroepiandrosterone by the human 11beta-hydroxysteroid dehydrogenase type 1. *J Steroid Biochem Mol Biol,* 99**,** 215-22.

MUNCK, A., GUYRE, P. M. & HOLBROOK, N. J. (1984) Physiological functions of glucocorticoids in stress and their relation to pharmacological actions. *Endocr Rev,* 5**,** 25-44.

MUSAFIA, B., BUCHNER, V. & ARAD, D. (1995) Complex Salt Bridges in Proteins - Statistical-Analysis of Structure and Function. *Journal of Molecular Biology,* 254**,** 761-770.

MUSSE, A. A., WANG, J., DELEON, G. P., PRENTICE, G. A., LONDON, E. & MERRILL, A. R. (2006) Scanning the membrane-bound conformation of helix 1 in the colicin E1 channel domain by site-directed fluorescence labeling. *J Biol Chem,* 281**,** 885-95.

MUSSIG, K., REMER, T., HAUPT, A., GALLWITZ, B., FRITSCHE, A., HARING, H. U. & MASER-GLUTH, C. (2008) 11beta-hydroxysteroid dehydrogenase 2 activity is elevated in severe obesity and negatively associated with insulin sensitivity. *Obesity (Silver Spring),* 16**,** 1256-60.

MZIAUT, H., KORZA, G., HAND, A. R., GERARD, C. & OZOLS, J. (1999) Targeting proteins to the lumen of endoplasmic reticulum using N-terminal domains of 11beta-hydroxysteroid dehydrogenase and the 50-kDa esterase. *J Biol Chem,* 274**,** 14122-9.

NAKAJIN, S., SHINODA, M., HANIU, M., SHIVELY, J. E. & HALL, P. F. (1984) C21 steroid side chain cleavage enzyme from porcine adrenal microsomes. Purification and characterization of the 17 alpha-hydroxylase/C17,20-lyase cytochrome P-450. *J Biol Chem,* 259**,** 3971-6.

NARAY-FEJES-TOTH, A. & FEJES-TOTH, G. (1995) Expression cloning of the aldosterone target cell-specific 11 beta-hydroxysteroid dehydrogenase from rabbit collecting duct cells. *Endocrinology,* 136**,** 2579-86.

NASHEV, L. G., CHANDSAWANGBHUWANA, C., BALAZS, Z., ATANASOV, A. G., DICK, B., FREY, F. J., BAKER, M. E. & ODERMATT, A. (2007) Hexose-6-phosphate dehydrogenase modulates 11beta-hydroxysteroid dehydrogenase type 1-dependent metabolism of 7-keto- and 7beta-hydroxy-neurosteroids. *PLoS ONE,* 2**,** e561.

NEELAMKAVIL, S. F., BOYLE, C. D., CHACKALAMANNIL, S., GREENLEE, W. J., ZHANG, L. & TERRACINA, G. (2009) The discovery of azepane sulfonamides as potent 11beta-HSD1 inhibitors. *Bioorg Med Chem Lett,* 19**,** 4563-5.

NEVES, P., SOUSA, I., WINTERHALTER, M. & GAMEIRO, P. (2009) Fluorescence quenching as a tool to investigate quinolone antibiotic interactions with bacterial protein OmpF. *J Membr Biol,* 227**,** 133-40.

NEWMAN, R. (1996) Crystallization and structure analysis of membrane proteins. *Methods Mol Biol,* 56**,** 365-87.

NICOLAIDES, N. C., GALATA, Z., KINO, T., CHROUSOS, G. P. & CHARMANDARI, E. (2009) The human glucocorticoid receptor: molecular basis of biologic function. *Steroids,* 75**,** 1-12.

NIEBA, L., HONEGGER, A., KREBBER, C. & PLUCKTHUN, A. (1997) Disrupting the hydrophobic patches at the antibody variable/constant domain interface: Improved in vivo folding and physical characterization of an engineered scFv fragment. *Protein Engineering,* 10**,** 435-444.

NIKKILA, H., TANNIN, G. M., NEW, M. I., TAYLOR, N. F., KALAITZOGLOU, G., MONDER, C. & WHITE, P. C. (1993) Defects in the HSD11 gene encoding 11 beta-hydroxysteroid dehydrogenase are not found in patients with apparent mineralocorticoid excess or 11-oxoreductase deficiency. *J Clin Endocrinol Metab,* 77**,** 687-91.

NOBEL, C. S., DUNAS, F. & ABRAHMSEN, L. B. (2002) Purification of full-length recombinant human and rat type 1 11beta-hydroxysteroid dehydrogenases with retained oxidoreductase activities. *Protein Expr Purif,* 26**,** 349-56.

NORDENSTROM, A., MARCUS, C., AXELSON, M., WEDELL, A. & RITZEN, E. M. (1999) Failure of cortisone acetate treatment in congenital adrenal hyperplasia because of defective 11beta-hydroxysteroid dehydrogenase reductase activity. *J Clin Endocrinol Metab,* 84**,** 1210-3.

NUOTIO-ANTAR, A. M., HACHEY, D. L. & HASTY, A. H. (2007) Carbenoxolone treatment attenuates symptoms of metabolic syndrome and atherogenesis in obese, hyperlipidemic mice. *Am J Physiol Endocrinol Metab,* 293**,** E1517-28.

OAKLEY, R. H., JEWELL, C. M., YUDT, M. R., BOFETIADO, D. M. & CIDLOWSKI, J. A. (1999) The dominant negative activity of the human glucocorticoid receptor beta isoform. Specificity and mechanisms of action. *J Biol Chem,* 274**,** 27857-66.

OBEID, J. & WHITE, P. C. (1992) Tyr-179 and Lys-183 Are Essential for Enzymatic-Activity of 11-Beta-Hydroxysteroid Dehydrogenase. *Biochemical and Biophysical Research Communications,* 188**,** 222-227.

OBEYESEKERE, V. R., LI, K. X., FERRARI, P. & KROZOWSKI, Z. (1997) Truncation of the N- and C-terminal regions of the human 11beta-hydroxysteroid dehydrogenase type 2 enzyme and effects on solubility and bidirectional enzyme activity. *Mol Cell Endocrinol,* 131**,** 173-82.

ODERMATT, A., ARNOLD, P., STAUFFER, A., FREY, B. M. & FREY, F. J. (1999) The N-terminal anchor sequences of 11beta-hydroxysteroid dehydrogenases determine their orientation in the endoplasmic reticulum membrane. *J Biol Chem,* 274**,** 28762-70.

ODERMATT, A., ATANASOV, A. G., BALAZS, Z., SCHWEIZER, R. A., NASHEV, L. G., SCHUSTER, D. & LANGER, T. (2006) Why is 11beta-hydroxysteroid dehydrogenase type 1 facing the endoplasmic reticulum lumen? Physiological relevance of the membrane topology of 11beta-HSD1. *Mol Cell Endocrinol,* 248**,** 15-23.

OGG, D., ELLEBY, B., NORSTROM, C., STEFANSSON, K., ABRAHMSEN, L., OPPERMANN, U. & SVENSSON, S. (2005) The crystal structure of guinea pig 11beta-hydroxysteroid dehydrogenase type 1 provides a model for enzyme-lipid bilayer interactions. *J Biol Chem,* 280**,** 3789-94.

OLSON, S., ASTER, S. D., BROWN, K., CARBIN, L., GRAHAM, D. W., HERMANOWSKI-VOSATKA, A., LEGRAND, C. B., MUNDT, S. S., ROBBINS, M. A., SCHAEFFER, J. M., SLOSSBERG, L. H., SZYMONIFKA, M. J., THIERINGER, R., WRIGHT, S. D. & BALKOVEC, J. M. (2005) Adamantyl

triazoles as selective inhibitors of 11beta-hydroxysteroid dehydrogenase type 1. *Bioorg Med Chem Lett,* 15**,** 4359-62.

ONYIMBA, C. U., VIJAPURAPU, N., CURNOW, S. J., KHOSLA, P., STEWART, P. M., MURRAY, P. I., WALKER, E. A. & RAUZ, S. (2006) Characterisation of the prereceptor regulation of glucocorticoids in the anterior segment of the rabbit eye. *J Endocrinol,* 190**,** 483-93.

OPPERMANN, U. (2007) Carbonyl reductases: the complex relationships of mammalian carbonyl- and quinone-reducing enzymes and their role in physiology. *Annu Rev Pharmacol Toxicol,* 47**,** 293-322.

OPPERMANN, U., FILLING, C., HULT, M., SHAFQAT, N., WU, X., LINDH, M., SHAFQAT, J., NORDLING, E., KALLBERG, Y., PERSSON, B. & JORNVALL, H. (2003) Short-chain dehydrogenases/reductases (SDR): the 2002 update. *Chem Biol Interact,* 143-144**,** 247-53.

OPPERMANN, U. C., NETTER, K. J. & MASER, E. (1995) Cloning and primary structure of murine 11 beta-hydroxysteroid dehydrogenase/microsomal carbonyl reductase. *Eur J Biochem,* 227**,** 202-8.

OPPERMANN, U. C. T., FILLING, C., BERNDT, K. D., PERSSON, B., BENACH, J., LADENSTEIN, R. & JORNVALL, H. (1997) Active site directed mutagenesis of 3 beta/17 beta-hydroxysteroid dehydrogenase establishes differential effects on short-chain dehydrogenase/reductase reactions. *Biochemistry,* 36**,** 34-40.

ORTIZ DE MONTELLANO, P. R. (1995) *Cytochrome P450: Structure, Mechanism, and Biochemsitry*.

ORTSATER, H., ALBERTS, P., WARPMAN, U., ENGBLOM, L. O., ABRAHMSEN, L. & BERGSTEN, P. (2005) Regulation of 11beta-hydroxysteroid dehydrogenase type 1 and glucose-stimulated insulin secretion in pancreatic islets of Langerhans. *Diabetes Metab Res Rev,* 21**,** 359-66.

OSTROVSKY, A. V., KALINICHENKO, L. P., EMELYANENKO, V. I., KLIMANOV, A. V. & PERMYAKOV, E. A. (1988) Environment of tryptophan residues in various conformational states of alpha-lactalbumin studied by time-resolved and steady-state fluorescence spectroscopy. *Biophys Chem,* 30**,** 105-12.

OZOLS, J. (1993) Isolation and the complete amino acid sequence of lumenal endoplasmic reticulum glucose-6-phosphate dehydrogenase. *Proc Natl Acad Sci U S A,* 90**,** 5302-6.

OZOLS, J. (1995) Lumenal orientation and post-translational modifications of the liver microsomal 11 beta-hydroxysteroid dehydrogenase. *J Biol Chem,* 270**,** 10360.

PATEL, J. R., SHUAI, Q., DINGES, J., WINN, M., PLIUSHCHEV, M., FUNG, S., MONZON, K., CHIOU, W., WANG, J., PAN, L., WAGAW, S., ENGSTROM, K., KERDESKY, F. A., LONGENECKER, K., JUDGE, R., QIN, W., IMADE, H. M., STOLARIK, D., BENO, D. W., BRUNE, M., CHOVAN, L. E., SHAM, H. L., JACOBSON, P. & LINK, J. T. (2007) Discovery of adamantane ethers as inhibitors of 11beta-HSD-1: Synthesis and biological evaluation. *Bioorg Med Chem Lett,* 17**,** 750-5.

PATERSON, J. M., MORTON, N. M., FIEVET, C., KENYON, C. J., HOLMES, M. C., STAELS, B., SECKL, J. R. & MULLINS, J. J. (2004) Metabolic syndrome without obesity: Hepatic overexpression of 11beta-hydroxysteroid dehydrogenase type 1 in transgenic mice. *Proc Natl Acad Sci U S A,* 101**,** 7088-93.

PAULMYER-LACROIX, O., BOULLU, S., OLIVER, C., ALESSI, M. C. & GRINO, M. (2002) Expression of the mRNA coding for 11beta-hydroxysteroid dehydrogenase type 1 in adipose tissue from obese patients: an in situ hybridization study. *J Clin Endocrinol Metab,* 87**,** 2701-5.

PAULSEN, S. K., PEDERSEN, S. B., FISKER, S. & RICHELSEN, B. (2007) 11Beta-HSD type 1 expression in human adipose tissue: impact of gender, obesity, and fat localization. *Obesity (Silver Spring),* 15**,** 1954-60.

PEEKE, P. M. & CHROUSOS, G. P. (1995) Hypercortisolism and obesity. *Ann N Y Acad Sci,* 771**,** 665-76.

PEPE, G. J., BURCH, M. G. & ALBRECHT, E. D. (2001) Localization and developmental regulation of 11beta-hydroxysteroid dehydrogenase-1 and -2 in the baboon syncytiotrophoblast. *Endocrinology,* 142**,** 68-80.

PERRAKIS, A., MORRIS, R. & LAMZIN, V. S. (1999) Automated protein model building combined with iterative structure refinement. *Nat Struct Biol,* 6**,** 458-63.

PERSSON, B., KALLBERG, Y., OPPERMANN, U. & JORNVALL, H. (2003) Coenzyme-based functional assignments of short-chain dehydrogenases/reductases (SDRs). *Chem Biol Interact,* 143-144**,** 271-8.

PETTERSEN, E. F., GODDARD, T. D., HUANG, C. C., COUCH, G. S., GREENBLATT, D. M., MENG, E. C. & FERRIN, T. E. (2004) UCSF Chimera--a visualization system for exploratory research and analysis. *J Comput Chem,* 25**,** 1605-12.

PHILLIPOV, G., PALERMO, M. & SHACKLETON, C. H. (1996) Apparent cortisone reductase deficiency: a unique form of hypercortisolism. *J Clin Endocrinol Metab,* 81**,** 3855-60.

PHILLIPS, J. E., GENG, Y. J. & MASON, R. P. (2001) 7-Ketocholesterol forms crystalline domains in model membranes and murine aortic smooth muscle cells. *Atherosclerosis,* 159**,** 125-35.

PICOT, D., LOLL, P. J. & GARAVITO, R. M. (1994) The X-ray crystal structure of the membrane protein prostaglandin H2 synthase-1. *Nature,* 367**,** 243-9.

PIERLUISSI, J., NAVAS, F. O. & ASHCROFT, S. J. (1986) Effect of adrenal steroids on insulin release from cultured rat islets of Langerhans. *Diabetologia,* 29**,** 119-21.

POWELL, A. J., READ, J. A., BANFIELD, M. J., GUNN-MOORE, F., YAN, S. D., LUSTBADER, J., STERN, A. R., STERN, D. M. & BRADY, R. L. (2000) Recognition of structurally diverse substrates by type II 3-hydroxyacyl-CoA dehydrogenase (HADH II)/amyloid-beta binding alcohol dehydrogenase (ABAD). *J Mol Biol,* 303**,** 311-27.

PRATT, W. B. (1993) The role of heat shock proteins in regulating the function, folding, and trafficking of the glucocorticoid receptor. *J Biol Chem,* 268**,** 21455-8.

PU, X. & YANG, K. (2000) Guinea pig 11beta-hydroxysteroid dehydrogenase type 1: primary structure and catalytic properties. *Steroids,* 65**,** 148-56.

QUINKLER, M., KOSMALE, B., BAHR, V., OELKERS, W. & DIEDERICH, S. (1997) Evidence for isoforms of 11 beta-hydroxysteroid dehydrogenase in the liver and kidney of the guinea pig. *J Endocrinol,* 153**,** 291-8.

RAJAN, V., CHAPMAN, K. E., LYONS, V., JAMIESON, P., MULLINS, J. J., EDWARDS, C. R. & SECKL, J. R. (1995) Cloning, sequencing and tissue-distribution of mouse 11 beta-hydroxysteroid dehydrogenase-1 cDNA. *J Steroid Biochem Mol Biol,* 52**,** 141-7.

RAJAN, V., EDWARDS, C. R. & SECKL, J. R. (1996) 11 beta-Hydroxysteroid dehydrogenase in cultured hippocampal cells reactivates inert 11-dehydrocorticosterone, potentiating neurotoxicity. *J Neurosci,* 16**,** 65-70.

RASK, E., OLSSON, T., SODERBERG, S., ANDREW, R., LIVINGSTONE, D. E., JOHNSON, O. & WALKER, B. R. (2001) Tissue-specific dysregulation of cortisol metabolism in human obesity. *J Clin Endocrinol Metab,* 86**,** 1418-21.

RASK, E., WALKER, B. R., SODERBERG, S., LIVINGSTONE, D. E., ELIASSON, M., JOHNSON, O., ANDREW, R. & OLSSON, T. (2002) Tissue-specific changes in

peripheral cortisol metabolism in obese women: increased adipose 11beta-hydroxysteroid dehydrogenase type 1 activity. *J Clin Endocrinol Metab,* 87**,** 3330-6.

RAUZ, S., CHEUNG, C. M., WOOD, P. J., COCA-PRADOS, M., WALKER, E. A., MURRAY, P. I. & STEWART, P. M. (2003) Inhibition of 11beta-hydroxysteroid dehydrogenase type 1 lowers intraocular pressure in patients with ocular hypertension. *Qjm,* 96**,** 481-90.

RAUZ, S., WALKER, E. A., SHACKLETON, C. H., HEWISON, M., MURRAY, P. I. & STEWART, P. M. (2001) Expression and putative role of 11 beta-hydroxysteroid dehydrogenase isozymes within the human eye. *Invest Ophthalmol Vis Sci,* 42**,** 2037-42.

REAVEN, G. M. (1988) Banting lecture 1988. Role of insulin resistance in human disease. *Diabetes,* 37**,** 1595-607.

REW, Y., MCMINN, D. L., WANG, Z., HE, X., HUNGATE, R. W., JAEN, J. C., SUDOM, A., SUN, D., TU, H., URSU, S., VILLEMURE, E., WALKER, N. P., YAN, X., YE, Q. & POWERS, J. P. (2009) Discovery and optimization of piperidyl benzamide derivatives as a novel class of 11beta-HSD1 inhibitors. *Bioorg Med Chem Lett,* 19**,** 1797-801.

RICKETTS, M. L., VERHAEG, J. M., BUJALSKA, I., HOWIE, A. J., RAINEY, W. E. & STEWART, P. M. (1998) Immunohistochemical localization of type 1 11beta-hydroxysteroid dehydrogenase in human tissues. *J Clin Endocrinol Metab,* 83**,** 1325-35.

RIMBACH, G., MOEHRING, J., HUEBBE, P. & LODGE, J. K. (2010) Gene-regulatory activity of alpha-tocopherol. *Molecules,* 15**,** 1746-61.

ROHDE, J. J., PLIUSHCHEV, M. A., SORENSEN, B. K., WODKA, D., SHUAI, Q., WANG, J., FUNG, S., MONZON, K. M., CHIOU, W. J., PAN, L., DENG, X., CHOVAN, L. E., RAMAIYA, A., MULLALLY, M., HENRY, R. F., STOLARIK, D. F., IMADE, H. M., MARSH, K. C., BENO, D. W., FEY, T. A., DROZ, B. A., BRUNE, M. E., CAMP, H. S., SHAM, H. L., FREVERT, E. U., JACOBSON, P. B. & LINK, J. T. (2007) Discovery and metabolic stabilization of potent and selective 2-amino-N-(adamant-2-yl) acetamide 11beta-hydroxysteroid dehydrogenase type 1 inhibitors. *J Med Chem,* 50**,** 149-64.

ROLAND, B. L. & FUNDER, J. W. (1996) Localization of 11beta-hydroxysteroid dehydrogenase type 2 in rat tissues: in situ studies. *Endocrinology,* 137**,** 1123-8.

ROMANELLI, A., STDENIS, J. F., VIDAL, H., TCHU, S. & VANDEWERVE, G. (1994) Absence of Glucose-Uptake by Liver-Microsomes - an Explanation for the Complete Latency of Glucose-Dehydrogenase. *Biochemical and Biophysical Research Communications,* 200**,** 1491-1497.

RUSSELL, R. B. & EGGLESTON, D. S. (2000) New roles for structure in biology and drug discovery. *Nat Struct Biol,* 7 Suppl**,** 928-30.

SAN MILLAN, J. L., BOTELLA-CARRETERO, J. I., ALVAREZ-BLASCO, F., LUQUE-RAMIREZ, M., SANCHO, J., MOGHETTI, P. & ESCOBAR-MORREALE, H. F. (2005) A study of the hexose-6-phosphate dehydrogenase gene R453Q and 11beta-hydroxysteroid dehydrogenase type 1 gene 83557insA polymorphisms in the polycystic ovary syndrome. *J Clin Endocrinol Metab,* 90**,** 4157-62.

SANDEEP, T. C., ANDREW, R., HOMER, N. Z., ANDREWS, R. C., SMITH, K. & WALKER, B. R. (2005) Increased in vivo regeneration of cortisol in adipose tissue in human obesity and effects of the 11beta-hydroxysteroid dehydrogenase type 1 inhibitor carbenoxolone. *Diabetes,* 54**,** 872-9.

SANDEEP, T. C., YAU, J. L., MACLULLICH, A. M., NOBLE, J., DEARY, I. J., WALKER, B. R. & SECKL, J. R. (2004) 11Beta-hydroxysteroid dehydrogenase

inhibition improves cognitive function in healthy elderly men and type 2 diabetics. *Proc Natl Acad Sci U S A,* 101**,** 6734-9.

SAVAGE, M. W. (1991) Increased metabolic clearance of cortisol in corticosteroid 11-reductase deficiency. *Journal of Endocrinology,* 129S**,** 1.

SCHIPPER, L., SPEE, B., ROTHUIZEN, J., WOUTERSEN-VAN NIJNANTEN, F. & FINK-GREMMELS, J. (2004) Characterisation of 11 beta-hydroxysteroid dehydrogenases in feline kidney and liver. *Biochim Biophys Acta,* 1688**,** 68-77.

SCHUCK, P. (2000) Size-distribution analysis of macromolecules by sedimentation velocity ultracentrifugation and lamm equation modeling. *Biophys J,* 78**,** 1606-19.

SCHWEIZER, R. A., ZURCHER, M., BALAZS, Z., DICK, B. & ODERMATT, A. (2004) Rapid hepatic metabolism of 7-ketocholesterol by 11beta-hydroxysteroid dehydrogenase type 1: species-specific differences between the rat, human, and hamster enzyme. *J Biol Chem,* 279**,** 18415-24.

SECKL, J. R. (1997) 11beta-Hydroxysteroid dehydrogenase in the brain: a novel regulator of glucocorticoid action? *Front Neuroendocrinol,* 18**,** 49-99.

SEKTAS, M. A. S., W (2002) *inNovations***,** 3.

SHACKLETON, C. H. (1993) Mass spectrometry in the diagnosis of steroid-related disorders and in hypertension research. *J Steroid Biochem Mol Biol,* 45**,** 127-40.

SHAFQAT, N., ELLEBY, B., SVENSSON, S., SHAFQAT, J., JORNVALL, H., ABRAHMSEN, L. & OPPERMANN, U. (2003) Comparative enzymology of 11 beta -hydroxysteroid dehydrogenase type 1 from glucocorticoid resistant (Guinea pig) versus sensitive (human) species. *J Biol Chem,* 278**,** 2030-5.

SHERBET, D. P., PAPARI-ZAREEI, M., KHAN, N., SHARMA, K. K., BRANDMAIER, A., RAMBALLY, S., CHATTOPADHYAY, A., ANDERSSON, S., AGARWAL, A. K. & AUCHUS, R. J. (2007) Cofactors, redox state, and directional preferences of hydroxysteroid dehydrogenases. *Mol Cell Endocrinol,* 265-266**,** 83-8.

SHMUELI, O., HORN-SABAN, S., CHALIFA-CASPI, V., SHMOISH, M., OPHIR, R., BENJAMIN-RODRIG, H., SAFRAN, M., DOMANY, E. & LANCET, D. (2003) GeneNote: whole genome expression profiles in normal human tissues. *C R Biol,* 326**,** 1067-72.

SIM, J. & SIM, T. S. (1999) Amino acid substitutions affecting protein solubility: high level expression of Streptomyces clavuligerus isopenicillin N synthase in Escherichia coli. *Journal of Molecular Catalysis B-Enzymatic,* 6**,** 133-143.

SIU, M., JOHNSON, T. O., WANG, Y., NAIR, S. K., TAYLOR, W. D., CRIPPS, S. J., MATTHEWS, J. J., EDWARDS, M. P., PAULY, T. A., ERMOLIEFF, J., CASTRO, A., HOSEA, N. A., LAPAGLIA, A., FANJUL, A. N. & VOGEL, J. E. (2009) N-(Pyridin-2-yl) arylsulfonamide inhibitors of 11beta-hydroxysteroid dehydrogenase type 1: Discovery of PF-915275. *Bioorg Med Chem Lett,* 19**,** 3493-7.

SMIT, P., DEKKER, M. J., DE JONG, F. J., VAN DEN BELD, A. W., KOPER, J. W., POLS, H. A., BRINKMANN, A. O., DE JONG, F. H., BRETELER, M. M. & LAMBERTS, S. W. (2006) Lack of Association of the 11{beta}-Hydroxysteroid Dehydrogenase Type 1 Gene 83,557insA and Hexose-6-Phosphate Dehydrogenase Gene R453Q Polymorphisms with Body Composition, Adrenal Androgen Production, Blood Pressure, Glucose Metabolism and Dementia. *J Clin Endocrinol Metab,* 24**,** 24.

SMITH, P. K., KROHN, R. I., HERMANSON, G. T., MALLIA, A. K., GARTNER, F. H., PROVENZANO, M. D., FUJIMOTO, E. K., GOEKE, N. M., OLSON, B. J. & KLENK, D. C. (1985) Measurement of protein using bicinchoninic acid. *Anal Biochem,* 150**,** 76-85.

SMITH, R. E., LI, K. X., ANDREWS, R. K. & KROZOWSKI, Z. (1997) Immunohistochemical and molecular characterization of the rat 11 beta-hydroxysteroid dehydrogenase type II enzyme. *Endocrinology,* 138**,** 540-7.

SORENSEN, B., WINN, M., ROHDE, J., SHUAI, Q., WANG, J., FUNG, S., MONZON, K., CHIOU, W., STOLARIK, D., IMADE, H., PAN, L., DENG, X., CHOVAN, L., LONGENECKER, K., JUDGE, R., QIN, W., BRUNE, M., CAMP, H., FREVERT, E. U., JACOBSON, P. & LINK, J. T. (2007) Adamantane sulfone and sulfonamide 11-beta-HSD1 Inhibitors. *Bioorg Med Chem Lett,* 17**,** 527-32.

SORENSEN, H., WINZELL, M. S., BRAND, C. L., FOSGERAU, K., GELLING, R. W., NISHIMURA, E. & AHREN, B. (2006) Glucagon receptor knockout mice display increased insulin sensitivity and impaired beta-cell function. *Diabetes,* 55**,** 3463-9.

STEWART, P. M. (2005) Tissue-specific Cushing's syndrome uncovers a new target in treating the metabolic syndrome - 11 beta-hydroxysteroid dehydrogenase type 1. *Clinical Medicine,* 5**,** 142-146.

STEWART, P. M., BOULTON, A., KUMAR, S., CLARK, P. M. & SHACKLETON, C. H. (1999) Cortisol metabolism in human obesity: impaired cortisone-->cortisol conversion in subjects with central adiposity. *J Clin Endocrinol Metab,* 84**,** 1022-7.

STEWART, P. M., CORRIE, J. E., SHACKLETON, C. H. & EDWARDS, C. R. (1988) Syndrome of apparent mineralocorticoid excess. A defect in the cortisol-cortisone shuttle. *J Clin Invest,* 82**,** 340-9.

STEWART, P. M., MURRY, B. A. & MASON, J. I. (1994) Human kidney 11 beta-hydroxysteroid dehydrogenase is a high affinity nicotinamide adenine dinucleotide-dependent enzyme and differs from the cloned type I isoform. *J Clin Endocrinol Metab,* 79**,** 480-4.

STEWART, P. M., WALLACE, A. M., VALENTINO, R., BURT, D., SHACKLETON, C. H. & EDWARDS, C. R. (1987) Mineralocorticoid activity of liquorice: 11-beta-hydroxysteroid dehydrogenase deficiency comes of age. *Lancet,* 2**,** 821-4.

STOKES, J., NOBLE, J., BRETT, L., PHILLIPS, C., SECKL, J. R., O'BRIEN, C. & ANDREW, R. (2000) Distribution of glucocorticoid and mineralocorticoid receptors and 11beta-hydroxysteroid dehydrogenases in human and rat ocular tissues. *Invest Ophthalmol Vis Sci,* 41**,** 1629-38.

STRAUSS, J. F. (1991) Steroid Hormones: Synthesis, Metabolism, and Action in Health and Disease. *Endocrinology and Metabolism Clinics of North America,* 20**,** 681-925.

STREETEN, D. H. (1993) Is hypothalamic-pituitary-adrenal hyperactivity important in the pathogenesis of excessive abdominal fat distribution? *J Clin Endocrinol Metab,* 77**,** 339-40.

STRICKLER, S. S., GRIBENKO, A. V., GRIBENKO, A. V., KEIFFER, T. R., TOMLINSON, J., REIHLE, T., LOLADZE, V. V. & MAKHATADZE, G. I. (2006) Protein stability and surface electrostatics: A charged relationship. *Biochemistry,* 45**,** 2761-2766.

STRYER, L., BERG J.M, TYMOCZKO J.L (2002) *Biochemistry*.

SU, X., VICKER, N., TRUSSELLE, M., HALEM, H., CULLER, M. D. & POTTER, B. V. (2009) Discovery of novel inhibitors of human 11beta-hydroxysteroid dehydrogenase type 1. *Mol Cell Endocrinol,* 301**,** 169-73.

SUN, D., WANG, Z., CARDOZO, M., CHOI, R., DEGRAFFENREID, M., DI, Y., HE, X., JAEN, J. C., LABELLE, M., LIU, J., MA, J., MIAO, S., SUDOM, A., TANG, L., TU, H., URSU, S., WALKER, N., YAN, X., YE, Q. & POWERS, J. P. (2009) Synthesis and optimization of arylsulfonylpiperazines as a novel class of inhibitors of 11beta-hydroxysteroid dehydrogenase type 1 (11beta-HSD1). *Bioorg Med Chem Lett,* 19**,** 1522-7.

SUN, D., WANG, Z., DI, Y., JAEN, J. C., LABELLE, M., MA, J., MIAO, S., SUDOM, A., TANG, L., TOMOOKA, C. S., TU, H., URSU, S., WALKER, N., YAN, X., YE, Q. & POWERS, J. P. (2008) Discovery and initial SAR of arylsulfonylpiperazine inhibitors of 11beta-hydroxysteroid dehydrogenase type 1 (11beta-HSD1). *Bioorg Med Chem Lett,* 18**,** 3513-6.

SWAAB, D. F., BAO, A. M. & LUCASSEN, P. J. (2005) The stress system in the human brain in depression and neurodegeneration. *Ageing Res Rev,* 4**,** 141-94.

SWALI, A., WALKER, E. A., LAVERY, G. G., TOMLINSON, J. W. & STEWART, P. M. (2008) 11beta-Hydroxysteroid dehydrogenase type 1 regulates insulin and glucagon secretion in pancreatic islets. *Diabetologia,* 51**,** 2003-11.

SWIFT, C. B., HAYS, J. L. & PETTY, W. J. (2008) Distinct functions of retinoic acid receptor beta isoforms: implications for targeted therapy. *Endocr Metab Immune Disord Drug Targets,* 8**,** 47-50.

SZYMANSKI, E. S. & FURFINE, C. S. (1977) 20beta-Hydroxysteroid oxidoreductase. Kinetics and binding of corticosteroids and corticosteroid-21-aldehydes. *J Biol Chem,* 252**,** 205-11.

TAMBURINI, P. P. & GIBSON, G. G. (1983) Thermodynamic studies of the protein-protein interactions between cytochrome P-450 and cytochrome b5. Evidence for a central role of the cytochrome P-450 spin state in the coupling of substrate and cytochrome b5 binding to the terminal hemoprotein. *J Biol Chem,* 258**,** 13444-52.

TANAKA, N., NONAKA, T., NAKANISHI, M., DEYASHIKI, Y., HARA, A. & MITSUI, Y. (1996) Crystal structure of the ternary complex of mouse lung carbonyl reductase at 1.8 A resolution: the structural origin of coenzyme specificity in the short-chain dehydrogenase/reductase family. *Structure,* 4**,** 33-45.

TANNIN, G. M., AGARWAL, A. K., MONDER, C., NEW, M. I. & WHITE, P. C. (1991) The human gene for 11 beta-hydroxysteroid dehydrogenase. Structure, tissue distribution, and chromosomal localization. *J Biol Chem,* 266**,** 16653-8.

TAYLOR, N. F., BARTLETT, W. A. & DAWSON, D. J. (1984) Cortisone reductase deficiency: evidence for a new inborn error in metabolism of adrenal steroids. *Journal of Endocrinology,* 102S**,** 1.

TETSUKA, M., YAMAMOTO, S., HAYASHIDA, N., HAYASHI, K. G., HAYASHI, M., ACOSTA, T. J. & MIYAMOTO, A. (2003) Expression of 11beta-hydroxysteroid dehydrogenases in bovine follicle and corpus luteum. *J Endocrinol,* 177**,** 445-52.

THOMAS, J. L., DUAX, W. L., ADDLAGATTA, A., BRANDT, S., FULLER, R. R. & NORRIS, W. (2003) Structure/function relationships responsible for coenzyme specificity and the isomerase activity of human type 1 3 beta-hydroxysteroid dehydrogenase/isomerase. *J Biol Chem,* 278**,** 35483-90.

TOMLINSON, J. W., SINHA, B., BUJALSKA, I., HEWISON, M. & STEWART, P. M. (2002) Expression of 11beta-hydroxysteroid dehydrogenase type 1 in adipose tissue is not increased in human obesity. *J Clin Endocrinol Metab,* 87**,** 5630-5.

TOMLINSON, J. W. & STEWART, P. M. (2001) Cortisol metabolism and the role of 11beta-hydroxysteroid dehydrogenase. *Best Pract Res Clin Endocrinol Metab,* 15**,** 61-78.

TOMLINSON, J. W. & STEWART, P. M. (2005) Mechanisms of disease: Selective inhibition of 11beta-hydroxysteroid dehydrogenase type 1 as a novel treatment for the metabolic syndrome. *Nat Clin Pract Endocrinol Metab,* 1**,** 92-9.

TOMLINSON, J. W., WALKER, E. A., BUJALSKA, I. J., DRAPER, N., LAVERY, G. G., COOPER, M. S., HEWISON, M. & STEWART, P. M. (2004) 11beta-hydroxysteroid dehydrogenase type 1: a tissue-specific regulator of glucocorticoid response. *Endocr Rev,* 25**,** 831-66.

TREMBLAY, P. L., DREPPER, T., MASEPOHL, B. & HALLENBECK, P. C. (2007) Membrane sequestration of PII proteins and nitrogenase regulation in the photosynthetic bacterium Rhodobacter capsulatus. *J Bacteriol,* 189**,** 5850-9.

TSUMOTO, K., EJIMA, D., SENCZUK, A. M., KITA, Y. & ARAKAWA, T. (2007) Effects of salts on protein-surface interactions: applications for column chromatography. *J Pharm Sci,* 96**,** 1677-90.

TU, H., POWERS, J. P., LIU, J., URSU, S., SUDOM, A., YAN, X., XU, H., MEININGER, D., DEGRAFFENREID, M., HE, X., JAEN, J. C., SUN, D., LABELLE, M., YAMAMOTO, H., SHAN, B., WALKER, N. P. & WANG, Z. (2008) Distinctive molecular inhibition mechanisms for selective inhibitors of human 11beta-hydroxysteroid dehydrogenase type 1. *Bioorg Med Chem,* 16**,** 8922-31.

UCKAYA, G., KARADURMUS, N., KUTLU, O., CORAKCI, A., KIZILDAG, S., URAL, A. U., GUL, D. & KUTLU, M. (2008) Adipose tissue 11-beta-Hydroxysteroid Dehydrogenase Type 1 and Hexose-6-Phosphate Dehydrogenase gene expressions are increased in patients with type 2 diabetes mellitus. *Diabetes Res Clin Pract,* 82 Suppl 2**,** S135-40.

UNWIN, N. (2006) The metabolic syndrome. *J R Soc Med,* 99**,** 457-62.

VALE, W., SPIESS, J., RIVIER, C. & RIVIER, J. (1981) Characterization of a 41-residue ovine hypothalamic peptide that stimulates secretion of corticotropin and beta-endorphin. *Science,* 213**,** 1394-7.

VALSAMAKIS, G., ANWAR, A., TOMLINSON, J. W., SHACKLETON, C. H., MCTERNAN, P. G., CHETTY, R., WOOD, P. J., BANERJEE, A. K., HOLDER, G., BARNETT, A. H., STEWART, P. M. & KUMAR, S. (2004) 11beta-hydroxysteroid dehydrogenase type 1 activity in lean and obese males with type 2 diabetes mellitus. *J Clin Endocrinol Metab,* 89**,** 4755-61.

VAN MEER, G., VOELKER, D. R. & FEIGENSON, G. W. (2008) Membrane lipids: where they are and how they behave. *Nat Rev Mol Cell Biol,* 9**,** 112-24.

VIJAYAKUMAR, M., WONG, K. Y., SCHREIBER, G., FERSHT, A. R., SZABO, A. & ZHOU, H. X. (1998) Electrostatic enhancement of diffusion-controlled protein-protein association: Comparison of theory and experiment on barnase and barstar. *Journal of Molecular Biology,* 278**,** 1015-1024.

VIJAYAKUMAR, M. & ZHOU, H. X. (2001) Salt bridges stabilize the folded structure of barnase. *Journal of Physical Chemistry B,* 105**,** 7334-7340.

WAKE, D. J., RASK, E., LIVINGSTONE, D. E., SODERBERG, S., OLSSON, T. & WALKER, B. R. (2003) Local and systemic impact of transcriptional up-regulation of 11beta-hydroxysteroid dehydrogenase type 1 in adipose tissue in human obesity. *J Clin Endocrinol Metab,* 88**,** 3983-8.

WALKER, A. (2000) In vivo functions and applications of molecular chaperones. *PhD Thesis, University of Birmingham*.

WALKER, B. R., CONNACHER, A. A., LINDSAY, R. M., WEBB, D. J. & EDWARDS, C. R. (1995) Carbenoxolone increases hepatic insulin sensitivity in man: a novel role for 11-oxosteroid reductase in enhancing glucocorticoid receptor activation. *J Clin Endocrinol Metab,* 80**,** 3155-9.

WALKER, E. A., AHMED, A., LAVERY, G. G., TOMLINSON, J. W., KIM, S. Y., COOPER, M. S., RIDE, J. P., HUGHES, B. A., SHACKLETON, C. H., MCKIERNAN, P., ELIAS, E., CHOU, J. Y. & STEWART, P. M. (2007) 11beta-Hydroxysteroid Dehydrogenase Type 1 Regulation by Intracellular Glucose 6-Phosphate Provides Evidence for a Novel Link between Glucose Metabolism and Hypothalamo-Pituitary-Adrenal Axis Function. *J Biol Chem,* 282**,** 27030-6.

WALKER, E. A., CLARK, A. M., HEWISON, M., RIDE, J. P. & STEWART, P. M. (2001a) Functional expression, characterization, and purification of the catalytic domain of human 11-beta -hydroxysteroid dehydrogenase type 1. *J Biol Chem,* 276**,** 21343-50.

WALKER, E. A., CLARK, A. M., HEWISON, M., RIDE, J. P. & STEWART, P. M. (2001b) Functional expression, characterization, and purification of the catalytic domain of human 11-beta-hydroxysteroid dehydrogenase type 1. *Journal of Biological Chemistry,* 276**,** 21343-21350.

WALLIN, E. & VON HEIJNE, G. (1998) Genome-wide analysis of integral membrane proteins from eubacterial, archaean, and eukaryotic organisms. *Protein Sci,* 7**,** 1029-38.

WAMIL, M. & SECKL, J. R. (2007) Inhibition of 11beta-hydroxysteroid dehydrogenase type 1 as a promising therapeutic target. *Drug Discov Today,* 12**,** 504-20.

WAN, Z. K., CHENAIL, E., XIANG, J., LI, H. Q., IPEK, M., BARD, J., SVENSON, K., MANSOUR, T. S., XU, X., TIAN, X., SURI, V., HAHM, S., XING, Y., JOHNSON, C. E., LI, X., QADRI, A., PANZA, D., PERREAULT, M., TOBIN, J. F. & SAIAH, E. (2009) Efficacious 11beta-hydroxysteroid dehydrogenase type I inhibitors in the diet-induced obesity mouse model. *J Med Chem,* 52**,** 5449-61.

WANG, H., RUAN, Z., LI, J. J., SIMPKINS, L. M., SMIRK, R. A., WU, S. C., HUTCHINS, R. D., NIRSCHL, D. S., VAN KIRK, K., COOPER, C. B., SUTTON, J. C., MA, Z., GOLLA, R., SEETHALA, R., SALYAN, M. E., NAYEEM, A., KRYSTEK, S. R., JR., SHERIFF, S., CAMAC, D. M., MORIN, P. E., CARPENTER, B., ROBL, J. A., ZAHLER, R., GORDON, D. A. & HAMANN, L. G. (2008) Pyridine amides as potent and selective inhibitors of 11beta-hydroxysteroid dehydrogenase type 1. *Bioorg Med Chem Lett,* 18**,** 3168-72.

WENDT, K. U., PORALLA, K. & SCHULZ, G. E. (1997) Structure and function of a squalene cyclase. *Science,* 277**,** 1811-5.

WESTERBACKA, J., YKI-JARVINEN, H., VEHKAVAARA, S., HAKKINEN, A. M., ANDREW, R., WAKE, D. J., SECKL, J. R. & WALKER, B. R. (2003) Body fat distribution and cortisol metabolism in healthy men: enhanced 5beta-reductase and lower cortisol/cortisone metabolite ratios in men with fatty liver. *J Clin Endocrinol Metab,* 88**,** 4924-31.

WHITE, D., MUSSE, A. A., WANG, J., LONDON, E. & MERRILL, A. R. (2006) Toward elucidating the membrane topology of helix two of the colicin E1 channel domain. *J Biol Chem,* 281**,** 32375-84.

WHITWORTH, J. A., WILLIAMSON, P. M., MANGOS, G. & KELLY, J. J. (2005) Cardiovascular consequences of cortisol excess. *Vasc Health Risk Manag,* 1**,** 291-9.

WHORWOOD, C. B., RICKETTS, M. L. & STEWART, P. M. (1994) Epithelial cell localization of type 2 11 beta-hydroxysteroid dehydrogenase in rat and human colon. *Endocrinology,* 135**,** 2533-41.

WIDERSTEN, M. (1998) Heterologous expression in Escherichia coli of soluble active-site random mutants of haloalkane dehalogenase from Xanthobacter autotrophicus GJ10 by coexpression of molecular chaperonins GroEL/ES. *Protein Expr Purif,* 13**,** 389-95.

WIEGAND, S., RICHARDT, A., REMER, T., WUDY, S. A., TOMLINSON, J. W., HUGHES, B., GRUTERS, A., STEWART, P. M., STRASBURGER, C. J. & QUINKLER, M. (2007) Reduced 11beta-hydroxysteroid dehydrogenase type 1 activity in obese boys. *Eur J Endocrinol,* 157**,** 319-24.

WILLIAMS, P. A., COSME, J., SRIDHAR, V., JOHNSON, E. F. & MCREE, D. E. (2000) Mammalian microsomal cytochrome P450 monooxygenase: structural adaptations for membrane binding and functional diversity. *Mol Cell,* 5**,** 121-31.

WIMLEY, W. C. & WHITE, S. H. (1996) Experimentally determined hydrophobicity scale for proteins at membrane interfaces. *Nat Struct Biol,* 3**,** 842-8.

WOOLLEY, C. S., GOULD, E. & MCEWEN, B. S. (1990) Exposure to excess glucocorticoids alters dendritic morphology of adult hippocampal pyramidal neurons. *Brain Res,* 531**,** 225-31.

WU, X., LUKACIK, P., KAVANAGH, K. L. & OPPERMANN, U. (2007) SDR-type human hydroxysteroid dehydrogenases involved in steroid hormone activation. *Mol Cell Endocrinol,* 265-266**,** 71-6.

WYNN, R. M., DAVIE, J. R., SONG, J. L., CHUANG, J. L. & CHUANG, D. T. (2000) Expression of E1 component of human branched-chain alpha-keto acid dehydrogenase complex in Escherichia coli by cotransformation with chaperonins GroEL and GroES. *Methods Enzymol,* 324**,** 179-91.

XIANG, J., WAN, Z. K., LI, H. Q., IPEK, M., BINNUN, E., NUNEZ, J., CHEN, L., MCKEW, J. C., MANSOUR, T. S., XU, X., SURI, V., TAM, M., XING, Y., LI, X., HAHM, S., TOBIN, J. & SAIAH, E. (2008) Piperazine sulfonamides as potent, selective, and orally available 11beta-hydroxysteroid dehydrogenase type 1 inhibitors with efficacy in the rat cortisone-induced hyperinsulinemia model. *J Med Chem,* 51**,** 4068-71.

YANG, K., SMITH, C. L., DALES, D., HAMMOND, G. L. & CHALLIS, J. R. (1992) Cloning of an ovine 11 beta-hydroxysteroid dehydrogenase complementary deoxyribonucleic acid: tissue and temporal distribution of its messenger ribonucleic acid during fetal and neonatal development. *Endocrinology,* 131**,** 2120-6.

YAU, J. L., NOBLE, J., KENYON, C. J., HIBBERD, C., KOTELEVTSEV, Y., MULLINS, J. J. & SECKL, J. R. (2001) Lack of tissue glucocorticoid reactivation in 11beta - hydroxysteroid dehydrogenase type 1 knockout mice ameliorates age-related learning impairments. *Proc Natl Acad Sci U S A,* 98**,** 4716-21.

YAU, J. L., OLSSON, T., MORRIS, R. G., MEANEY, M. J. & SECKL, J. R. (1995) Glucocorticoids, hippocampal corticosteroid receptor gene expression and antidepressant treatment: relationship with spatial learning in young and aged rats. *Neuroscience,* 66**,** 571-81.

YUAN, C., ST JEAN, D. J., JR., LIU, Q., CAI, L., LI, A., HAN, N., MONIZ, G., ASKEW, B., HUNGATE, R. W., JOHANSSON, L., TEDENBORG, L., PYRING, D., WILLIAMS, M., HALE, C., CHEN, M., CUPPLES, R., ZHANG, J., JORDAN, S., BARTBERGER, M. D., SUN, Y., EMERY, M., WANG, M. & FOTSCH, C. (2007) The discovery of 2-anilinothiazolones as 11beta-HSD1 inhibitors. *Bioorg Med Chem Lett,* 17**,** 6056-61.

ZHANG, J., OSSLUND, T. D., PLANT, M. H., CLOGSTON, C. L., NYBO, R. E., XIONG, F., DELANEY, J. M. & JORDAN, S. R. (2005) Crystal structure of murine 11 beta-hydroxysteroid dehydrogenase 1: an important therapeutic target for diabetes. *Biochemistry,* 44**,** 6948-57.

ZHANG, X., ZHOU, Z., YANG, H., CHEN, J., FENG, Y., DU, L., LENG, Y. & SHEN, J. (2009a) 4-(Phenylsulfonamidomethyl)benzamides as potent and selective inhibitors of the 11beta-hydroxysteroid dehydrogenase type 1 with efficacy in diabetic ob/ob mice. *Bioorg Med Chem Lett,* 19**,** 4455-8.

ZHANG, Y. L., ZHONG, X., GJOKA, Z., LI, Y., STOCHAJ, W., STAHL, M., KRIZ, R., TOBIN, J. F., ERBE, D. & SURI, V. (2009b) H6PDH interacts directly with 11beta-HSD1: implications for determining the directionality of glucocorticoid catalysis. *Arch Biochem Biophys,* 483**,** 45-54.

ZHOU, J. & CIDLOWSKI, J. A. (2005) The human glucocorticoid receptor: one gene, multiple proteins and diverse responses. *Steroids,* 70**,** 407-17.

ZHOU, M. Y., GOMEZ-SANCHEZ, E. P., COX, D. L., COSBY, D. & GOMEZ-SANCHEZ, C. E. (1995) Cloning, expression, and tissue distribution of the rat nicotinamide adenine dinucleotide-dependent 11 beta-hydroxysteroid dehydrogenase. *Endocrinology,* 136**,** 3729-34.

ZHU, Y., OLSON, S. H., GRAHAM, D., PATEL, G., HERMANOWSKI-VOSATKA, A., MUNDT, S., SHAH, K., SPRINGER, M., THIERINGER, R., WRIGHT, S., XIAO, J., ZOKIAN, H., DRAGOVIC, J. & BALKOVEC, J. M. (2008a) Phenylcyclobutyl triazoles as selective inhibitors of 11beta-hydroxysteroid dehydrogenase type I. *Bioorg Med Chem Lett,* 18**,** 3412-6.

ZHU, Y., OLSON, S. H., HERMANOWSKI-VOSATKA, A., MUNDT, S., SHAH, K., SPRINGER, M., THIERINGER, R., WRIGHT, S., XIAO, J., ZOKIAN, H. & BALKOVEC, J. M. (2008b) 4-Methyl-5-phenyl triazoles as selective inhibitors of 11beta-hydroxysteroid dehydrogenase type I. *Bioorg Med Chem Lett,* 18**,** 3405-11.

Appendix One – Published Work

Protein Science. **18**(7): 1552-63.

Mutations of key hydrophobic surface residues of 11 beta-hydroxysteroid dehydrogenase type 1 increase solubility and monodispersity in a bacterial expression system.